

# **MicroRNA-Mediated Regulation of Stomatal Development in Arabidopsis**

**INAUGURALDISSERTATION**

zur  
Erlangung der Würde eines Doktors der Philosophie  
vorgelegt der  
Philosophisch-Naturwissenschaftlichen Fakultät  
der Universität Basel

von  
Claudia Kutter

aus  
Deutschland

Friedrich-Miescher-Institut  
Basel, September 2007

Genehmigt von der Philosophisch-Naturwissenschaftlichen Fakultät  
auf Antrag von Prof. Dr. Frederick Meins Jr. and PD Dr. Ortrun Mittelsten Scheid  
Basel, den 18. September 2007

Prof. Dr. Hans-Peter Hauri  
Dekan

## Danksagung

Die vorliegende Arbeit entstand am Friedrich-Miescher-Institut in Basel in der Arbeitsgruppe von Prof. Frederick Meins. Prof. Frederick Meins gilt an erster Stelle mein besonderer Dank für die Bereitstellung des interessanten Themas, die geduldige Betreuung, stetige Diskussionsbereitschaft und wunderbaren Ideen, die meine Arbeit in eine faszinierende Richtung leiteten.

Weiterhin möchte ich mich bei PD Ortrun Mittelsten-Scheid und Prof. Witold Filipowicz dafür bedanken, dass sie als Betreuer und Gutachter meiner Doktorarbeit zur Verfügung standen, für ihr stetiges Interesse am Fortgang dieser Arbeit, und ihren vielen hilfreichen Ratschlägen - mehr als ich erwarten konnte.

Ein ausgesprochen grosser Dank gilt Dr. Azeddine Si-Ammour, der die Doktorarbeit betreute und dessen großartigen Leistungen und Enthusiasmus von grosser Wichtigkeit für mich und meine Arbeit waren. Ich weiss seine experimentellen Anleitungen, die Zusammenarbeit und seinen endlosen Optimismus sehr zu schätzen.

Ich möchte mich auch bei der gesamten Meinsgruppe bedanken: Estelle Arn, Franck Vazquez, Jerome Alias, Todd Blevins und Yang Ping Lee für die ausgesprochen freundliche und gute Arbeitsatmosphäre, für die wissenschaftlichen und nichtwissenschaftlichen Diskussionen und all die geteilten Kilogramm Schokolade.

Ebenso danke ich den ehemaligen Mitgliedern des Labors Elzbieta Kowalska, Heike Schley, Konstantina Boutsika, Magali Perret, Monique Thomas, Razel Arpagaus, Sina Henrichs, Simona Bieri, Dominik Ziegler, Martin Regenass und Quanan Hu. Ich habe die Zeit mit ihnen sehr genossen.

Weiterhin bin ich vielen Mitarbeitern des FMIs zu Dank verpflichtet, für deren professionelle Hilfe und das überaus angenehme Arbeitsklima.

Von ganzem Herzen danke ich meinen Eltern, meiner Schwester und ihrer Familie, ohne deren uneingeschränkte Unterstützung mein Studium und diese Arbeit nicht möglich gewesen wären. Von unschätzbarem Wert ist für mich die familiäre Freundschaft zu Andrea und Luca und ihrem erfrischenden Humor, der so vieles vereinfachte.

Und schließlich danke ich Toni, für die unglaublich verlässliche und liebevolle Person, die er ist und natürlich auch an alle ungenannten guten Freunde: Dankeschön!

## Summary

MicroRNAs have important functions in the development of eukaryotes. In plants, highly conserved miRNA families have been shown to regulate morphogenesis and organ identity, primarily by targeting cleavage of mRNAs encoding transcription factors. Cloning identified a 21 nt Arabidopsis miRNA, miR824, conserved in *Brassica* species, but not in more distantly related species. miR824 is encoded at a single genetic locus as a polyadenylated, primary miRNA that is spliced and then processed via a precursor miRNA intermediate. miR824 mediates cleavage of the *AGAMOUS-LIKE 16 (AGL16)* mRNA. AGL16 is a member of the MADS-box protein family. The plant-specific MADS-box protein family has many established functions in regulating growth and development. Impairing the miR824-mediated repression of *AGL16* leads to leaf abnormalities and growth defects raising the possibility that AGL16 has pleiotropic function in leaf developmental programs. This study shows that the density and development of stomatal complexes on the epidermis of Arabidopsis leaves depend, in part, on microRNA-mediated regulation of *AGL16* assigning a novel function for the MADS-box protein family. Mutants deficient in *AGL16* and transgenics overexpressing miR824 show decrease in stomatal density and developed only primary stomatal complexes. Ectopic expression of a miR824-resistant *AGL16* mRNA, but not of the wild-type *AGL16* mRNA in transgenic plants, increases the stomatal density and the incidence of higher-order stomatal complexes. These results and the localization of *AGL16* mRNA and miR824 in mature stomata and satellite meristemoids, respectively, leads to the conclusion that miR824/*AGL16* pathway functions in stomatal development. The miR824-*AGL16* regulatory pathway is restricted to *Brassica* and might account for some Brassicaceae-specific taxonomic features of stomatal organization.

## Zusammenfassung

MicroRNAs haben wichtige Funktionen in Entwicklungsprozessen von Eukaryonten. Im pflanzlichen Organismus regulieren die evolutionär konservierten miRNA Familien Gestalt- und Formbildung, indem sie an komplementäre Sequenzen ihrer Ziel-mRNA, die meist für Transkriptionsfaktoren kodieren, binden und spalten. Eine 21 Nukleotid lange miRNA, miR824, wurde aus *Arabidopsis* kloniert. Diese miRNA ist in *Brassica* Arten vorhanden, jedoch nicht in entfernteren verwandten Arten. miR824 ist auf einem einzelnen genetischen Locus kodiert. Die primäre miRNA liegt polyadenyliert vor, wird gespleißt und zu einer Vorläufer miRNA prozessiert. miR824 spaltet *AGAMOUS-LIKE 16 (AGL16)* mRNA. AGL16 gehört zur Familie der MADS-box Proteine. Pflanzliche MADS-box Proteine regulieren Wachstums- und Entwicklungsprozesse. Wird die durch miR824 vermittelte Unterdrückung von AGL16 beeinträchtigt, führt dies zu Blattmissbildung und Wachstumsdefekten, die eine pleiotrope Funktion von AGL16 in Blattentwicklungsprogrammen nahe legen. Die vorliegende Arbeit zeigt, dass die Dichte und Entwicklung von Spaltöffnungskomplexen auf der Epidermis von *Arabidopsis* Blättern zum Teil von der miRNA vermittelten Regulation von *AGL16* abhängt. Dies stellt eine bislang unbekannte Funktion der MADS-box Proteinfamilie dar. Mutanten die *AGL16* in unzureichendem Masse bilden und transgene Pflanze, die die miR824 verstärkt bilden, zeigen eine verminderte Dichte an Spaltöffnungen und entwickeln hauptsächlich einfache Spaltöffnungskomplexe. Die ektopische Expression einer miRNA resistenten Form der *AGL16* mRNA, jedoch nicht der Wildtypform, führt in transgenen Pflanzen zu einer erhöhten Spaltöffnungsdichte und einem verstärkten Auftreten von multimeren Spaltöffnungskomplexen. Dieses Ergebnis sowie die Lokalisierung der *AGL16* mRNA und der miR824 in ausgeformten Spaltöffnungen bzw. Satellitenmeristemoiden führt zur Schlussfolgerung, dass die miR824-*AGL16* Wechselwirkung die Entwicklung des Spaltöffnungsapparates reguliert. Dieser Regulierungsprozess beschränkt sich auf die Gattung der *Brassica* und kann die Ausbildung von einigen Brassicaceae spezifischen taxonomischen Merkmalen der Spaltöffnungsanordnung bedingen.

---

## Contents

Contents . . . . .	I
List of Figures . . . . .	IV
List of Tables . . . . .	VI
Acronyms . . . . .	VII
I. Introduction . . . . .	1
1. Introduction . . . . .	2
1.1. Small RNA pathways . . . . .	2
1.1.1. Classes of smRNAs . . . . .	2
1.1.2. smRNA biogenesis and smRNA-mediated gene regulation . . . . .	4
1.1.3. Evolution of miRNA genes in plants . . . . .	9
1.1.4. miRNA function in Arabidopsis - a developmental view . . . . .	9
1.2. The MADS-box gene family . . . . .	16
1.2.1. The modular structure of plant MADS-box proteins . . . . .	17
1.2.2. Functions of MADS-box genes in Arabidopsis . . . . .	18
1.2.3. Evolutionary complexity of MADS-box gene family members . . . . .	22
1.3. Stomatal development and patterning . . . . .	23
1.3.1. Evolution and function of epidermal structures . . . . .	23
1.3.2. Anatomy of stomata . . . . .	24
1.3.3. Environmental factors affecting stomatal development . . . . .	26
1.4. Aim of the dissertation . . . . .	29
II. Materials and Methods . . . . .	30
2. Materials and Methods . . . . .	31
1. Materials . . . . .	31
1.1. Chemicals and enzymes . . . . .	31
1.2. Plasmids . . . . .	31
1.3. Bacterial strains . . . . .	32
1.4. Plant materials and condition of culture . . . . .	32
2. Methods . . . . .	32
2.1. Cloning and construction of the plasmids . . . . .	32
2.2. Transformation and agroinfiltration . . . . .	33
2.3. Characterization of T-DNA insertion . . . . .	34

---

2.4.	Isolation of plant nucleic acids . . . . .	34
2.5.	Southern analysis . . . . .	34
2.6.	RNA blot hybridization . . . . .	35
2.7.	RNA ligation mediated rapid amplification of cDNA ends (RLM-RACE)	35
2.8.	RT-PCR and quantitative RT-PCR (RT-qPCR) . . . . .	35
2.9.	Microarray analysis . . . . .	36
2.10.	In situ hybridization (ISH) . . . . .	36
2.11.	Physiological experiments . . . . .	36
2.12.	Staining for $\beta$ -glucuronidase (GUS) activity . . . . .	36
2.13.	Analysis of luciferase (LUC) activity . . . . .	37
2.14.	Electro mobility shift assays (EMSA) . . . . .	37
2.15.	Imaging experiments . . . . .	37
2.16.	Dental resin imprinting technique . . . . .	37
III. Results		39
3.	Establishing a Collection of RNA Silencing Mutants	40
1.	Elucidation of RNA silencing pathways using deficiency mutants . . . . .	41
2.	Partial Characterization of T-DNA Insertion mutants . . . . .	41
4.	Identification and characterization of the <i>miR824/AGL16</i> regulatory pathway	44
1.	Characterization of the miR824 locus . . . . .	45
1.1.	Identification of miR824 and its precursor . . . . .	45
1.2.	Characterization of the <i>MIR824</i> locus . . . . .	46
1.3.	Promoter analysis of <i>MIR824</i> . . . . .	53
1.4.	Characterization of <i>MIR824</i> T-DNA insertion alleles . . . . .	53
2.	miR824 target gene prediction and validation . . . . .	54
2.1.	Identification of <i>AGL16</i> as the unique target gene . . . . .	56
2.2.	<i>AGL16</i> expression in RNA silencing and <i>MIR824</i> locus mutants . . .	58
2.3.	miRNA-mediated regulation of other Arabidopsis MADS-box genes . .	58
2.4.	Analysis of <i>AGL16</i> expression . . . . .	61
2.5.	Promoter regulation of <i>AGL16</i> . . . . .	62
3.	Role of miR824 and <i>AGL16</i> upon abiotic stress and hormonal treatment . . .	63
4.	Evolutionary conservation of miR824 and <i>AGL16</i> . . . . .	66
5.	The biological function of the miR824/ <i>AGL16</i> pathway	67
1.	Molecular characterization of transgenic lines altered in <i>AGL16</i> expression .	68

2.	Phenotypical characterization of transgenic lines altered in <i>AGL16</i> expression	69
2.1.	Leaf abnormalities . . . . .	69
2.2.	Alteration in stomatal density . . . . .	71
2.3.	Alterations in the density of higher-order stomatal complexes . . . . .	77
2.4.	Localization studies of miR824 and <i>AGL16</i> mRNA in stomatal complexes	80
6.	The molecular basis for <i>AGL16</i> function	81
1.	Specific effects of ectopic expression of <i>AGL16</i> on the plant transcriptome . .	82
1.1.	Ectopic expression of <i>AGL16</i> regulates genes with diverse functions .	82
1.2.	Identification and analysis of promoter motifs of the candidate genes .	84
IV.	Discussion	87
7.	General Discussion	88
1.	Evolutionary relevance of miR824 in its biological function . . . . .	88
2.	<i>AGL16</i> is a novel player in stomatal development . . . . .	89
3.	Pleiotropic effects of <i>AGL16</i> in gene transcription . . . . .	90
4.	Evolution of species specific miRNA regulation . . . . .	91
5.	<i>AGL16</i> might be regulated by both miR824 and miR824* . . . . .	92
6.	Role of AGO1 in miR824 processing . . . . .	93
V.	Bibliography	i
VI.	Appendices	A
A.	Supplemental Data	B
A.	Arabidopsis microRNA families and their target genes . . . . .	B
B.	Applied primers . . . . .	E
C.	Vector maps . . . . .	G
D.	Characterization of mutant lines . . . . .	T
E.	Publications . . . . .	AA
F.	Eidesstattliche Erklärung . . . . .	AB
G.	Curriculum vitae . . . . .	AC



## List of Figures

1.1. Generalized core RNA silencing pathways . . . . .	4
1.2. The miRNA pathway in Arabidopsis . . . . .	5
1.3. Inverted gene duplication model for evolution of <i>MIRNA</i> genes. . . . .	10
1.4. Phenotypical consequences of Arabidopsis plants impaired in miRNA and target gene expression . . . . .	11
1.5. The Arabidopsis MIKC-type of MADS box protein interaction map . . . . .	19
1.6. The “ABCDE” and “quartet model” in Arabidopsis . . . . .	22
1.7. Lineage-based mechanism for the patterning and determination of stomata in Arabidopsis . . . . .	27
3.1. Phenotypes of Arabidopsis mutants impaired in smRNA biogenesis . . . . .	42
4.1. Expression of miR824 in leaves of Arabidopsis miRNA mutants and other plant species . . . . .	47
4.2. Genomic locations of smRNA sequences of the miR824 precursor . . . . .	48
4.3. Fold back structure of miR824 precursor . . . . .	48
4.4. Genomic organization of the <i>MIR824</i> locus . . . . .	49
4.5. Expression of miR824 in leaves of Col-0 and independent transgenic lines expressing <i>Pro</i> <sub>2x35S</sub> : <i>MIR824</i> Δ <i>E1E2</i> (+) . . . . .	50
4.6. Genomic organization of the <i>MIR824</i> locus and the annotated gene At4g24410 . . . . .	51
4.7. Expression of <i>MIR824</i> , <i>AGL16</i> , and <i>ACTIN2</i> in leaves of miRNA mutants and corresponding wild-type backgrounds . . . . .	52
4.8. Expression of <i>MIR824</i> and <i>AGL16</i> in rosette leaves of 28 day old silencing mutants . . . . .	52
4.9. Promoter expression studies of <i>MIR824</i> and <i>AGL16</i> by leaf infiltration . . . . .	54
4.10. Characterization of mutants with T-DNA insertions in the <i>MIR824</i> locus . . . . .	55
4.11. miR824 cleavage of target mRNA and location of <i>agl16-1</i> . . . . .	57
4.12. Expression of <i>AGL16</i> transcript in rosette leaves of silencing deficient mutants . . . . .	59
4.13. Expression of <i>AGL16</i> transcript in rosette leaves of the <i>AGL16</i> deficient mutant . . . . .	60
4.14. miR426 mediated regulation of AGL17 clade members . . . . .	62
4.15. Expression of <i>AGL16</i> in different plant organs and parts of the organ of Arabidopsis . . . . .	63
4.16. Expression of miR824 in rosette leaves of Arabidopsis plants upon several stress conditions and hormonal treatments . . . . .	64

4.17. Expression of <i>MIR824</i> and <i>AGL16</i> in rosette leaves of Arabidopsis plants upon several stress conditions and hormonal treatments . . . . .	65
5.1. Schematic presentation of the <i>AGL16m</i> transgene . . . . .	69
5.2. Expression of miR824 and <i>AGL16</i> mRNA in <i>AGL16.1/2</i> and <i>AGL16m1/2</i> rosette leaves . . . . .	70
5.3. Phenotypical differences caused by <i>AGL16</i> overexpression . . . . .	72
5.4. SEM images of mesophyll cells and trichomes of <i>AGL16m</i> transformants and control plants . . . . .	73
5.5. The positioning of stomatal complexes on the abaxial epidermis of transgenic Arabidopsis plants altered in <i>AGL16</i> mRNA expression . . . . .	74
5.6. The positioning of stomatal complexes on the adaxial epidermis of transgenic Arabidopsis plants altered in <i>AGL16</i> mRNA expression . . . . .	75
5.7. Effects of altered <i>AGL16</i> mRNA expression on stomatal density and stomatal index . . . . .	76
5.8. Promoter expression studies in stomatal complexes of rosette leaves of transgenic Arabidopsis plants . . . . .	78
5.9. Effects of altered <i>AGL16</i> expression on the proportion of primary and higher-order stomatal complexes . . . . .	79
6.1. Transcriptional profiling of rosette leaves of Col-0 and Col-0 <i>AGL16m1</i> . . . . .	83
6.2. <i>AGL16</i> binds CArG motifs . . . . .	86
A.1. Vector map of pPro <sub>2x35S</sub> : <i>MIR824ΔE1E2(+)</i> . . . . .	G
A.2. Vector map of pPro <sub>MIR824</sub> : <i>Luc</i> (Amp <sup>R</sup> ) . . . . .	H
A.3. Vector map of pPro <sub>2x35S</sub> : <i>Luc</i> (Amp <sup>R</sup> ) . . . . .	I
A.4. Vector map of pΔ: <i>Luc</i> (Amp <sup>R</sup> ) . . . . .	J
A.5. Vector map of pProΔ: <i>GUS</i> . . . . .	K
A.6. Vector map of pPro <sub>MIR824</sub> : <i>GUS</i> . . . . .	L
A.7. Vector map of pPro <sub>MIR824-LTRE</sub> : <i>GUS</i> . . . . .	M
A.8. Vector map of pPro <sub>2x35S</sub> : <i>GUS</i> . . . . .	N
A.9. Vector map of pPro <sub>MIR824</sub> : <i>GFP</i> . . . . .	O
A.10. Vector map of pPro <sub>2x35S</sub> : <i>AGL16</i> . . . . .	P
A.11. Vector map of pPro <sub>2x35S</sub> : <i>AGL16m</i> . . . . .	Q
A.12. Vector map of pPro <sub>AGL16</sub> : <i>GUS</i> . . . . .	R
A.13. Vector map of pPro <sub>AGL16</sub> : <i>GUS</i> . . . . .	S

---

## List of Tables

1.1. Genes involved in Arabidopsis stomatal development in rosette leaves . . . .	28
2.1. Concentrations of antibiotics used for standard plasmids . . . . .	32
4.1. smRNA sequences of miR824 precursor . . . . .	46
4.2. miR824 target prediction . . . . .	57
4.3. smRNA mediated cleavage of AGL17 clade members . . . . .	61
6.1. Biological and molecular function of gene candidates up- and downregulated in <i>AGL16m1</i> . . . . .	82
6.2. Expression levels and relevant motifs of genes upregulated in <i>AGL16m1</i> . . .	84
6.3. Comparison of microarray expression values and quantitative RT-PCR expres- sion values of candidate genes . . . . .	85
A.1. Arabidopsis microRNA families and their target genes . . . . .	C
A.2. Applied primers . . . . .	E
A.3. Characterization of mutant lines . . . . .	T

---

# Acronyms

<b>2,4-D</b>	2,4-dichlorophenoxy acetic acid
<b>aa</b>	amino acid
<b>ABC</b>	ATP-binding-cassette
<b>AG</b>	agamous
<b>AGI</b>	Arabidopsis gene identifier
<b>AGL</b>	agamous-like
<b>AGO</b>	argonaute
<b>AP</b>	apetala
<b>APS</b>	ATP sulfurylases
<b>ARF</b>	auxin response factor
<b>as</b>	anti-sense
<b>bHLH</b>	basic helix-loop-helix
<b>bp</b>	base-pair
<b>C</b>	carbon
<b>C-</b>	carboxy
<b>CaMV</b>	cauliflower mosaic virus
<b>cDNA</b>	copy DNA
<b>CMC</b>	chromatin-modifying complex
<b>Col-0</b>	<i>Arabidopsis thaliana</i> ecotype Columbia
<b>CSD</b>	Cu-Zn superoxide dismutase
<b>DCL</b>	dicer-like
<b>DEF</b>	deficiens
<b>DEPC</b>	diethylpyrocarbonate
<b>dCTP</b>	deoxy-cytidine-5'-triphosphate
<b>DNA</b>	desoxyribonucleic acid
<b>dNTP</b>	deoxy-nucleoside-5'-triphosphate

---

<b>DRP</b>	double strand RNA binding protein
<b>ds</b>	double strand
<b>DUF</b>	domain of unknown function
<b>EDTA</b>	ethylenediamine tetraacetic acid
<b>e. g.</b>	<i>exempli gratia</i> (Latin = for example)
<b>EST</b>	expressed sequence tag
<b>ER</b>	endoplasmic reticulum
<b><i>et al.</i></b>	<i>et alii</i> (Latin = and others)
<b>EtBr</b>	ethidium bromide
<b><i>etc.</i></b>	<i>et cetera</i> (Latin = and so on)
<b>GABI-Kat</b>	<i>Genomanalyse im biologischen System Pflanze - Kölner Arabidopsis T-DNA lines</i>
<b>GFP</b>	green fluorescent protein
<b>GUS</b>	$\beta$ -glucuronidase
<b>h</b>	hours
<b>H</b>	hydrogen
<b>H<sup>+</sup></b>	proton
<b>HDACs</b>	histone deacetylases
<b>HEN</b>	hua enhancer
<b>HST</b>	hasty
<b>HYL</b>	hyponastic leaves
<b>IAA</b>	indolyl-3-acetic acid
<b>i. e.</b>	<i>id est</i> (Latin = that is to say)
<b>IRT</b>	iron regulated transporter
<b>kb</b>	kilo base-pairs
<b>kDa</b>	kilodalton
<b>LD</b>	long day
<b>Loq</b>	loquacious
<b>MAP</b>	mitogen-activated protein
<b>MCM</b>	minichromosome-maintenance

<b>mi</b>	micro
<b>min</b>	minutes
<b>MPSS</b>	massively parallel signature sequencing
<b>N-</b>	amino
<b>NASC</b>	Nottingham Arabidopsis Stock Center
<b>nat</b>	natural
<b>NOS</b>	nopaline synthase
<b>NPTII</b>	nopaline phosphotransferase gene
<b>nt</b>	nucleotides
<b>OD</b>	optical density
<b>ORF</b>	open reading frame
<b>PCR</b>	polymerase chain reaction
<b>PHB</b>	phabulosa
<b>PHV</b>	phavulota
<b>PI</b>	pistillata
<b>PLE</b>	plena
<b>pre</b>	precursor
<b>pri</b>	primary
<b>Pol</b>	polymerase
<b>PTGS</b>	post-transcriptional gene silencing
<b>RACE</b>	rapid amplification of cDNA ends
<b>RdDM</b>	RNA-directed DNA methylation
<b>RDRP</b>	RNA-directed DNA methylation
<b>REV</b>	revoluta
<b>RISC</b>	RNA-induced silencing complex
<b>RNA</b>	ribonucleic acid
<b>RNAi</b>	RNA interference
<b>RT</b>	room temperature
<b>SCL</b>	scarecrow-like

---

<b>SD</b>	short day
<b>se</b>	serrate
<b>SDS</b>	sodium dodecyl sulfate
<b>si</b>	small interfering
<b>sm</b>	small
<b>sn</b>	small nucleolar
<b>SPL</b>	squamosa promoter binding protein like
<b>SQUA</b>	squamosa
<b>SRF</b>	serum response factor
<b>ss</b>	single-stranded
<b>st</b>	small temporal
<b>ta</b>	trans acting
<b>TGS</b>	transcriptional gene silencing
<b>TIGR</b>	The Institute for Genomic Research
<b>TRBP</b>	TAR RNA-binding protein
<b>Tris</b>	tris(hydroxymethyl)-amino-methane
<b>TrisHCl</b>	tris(hydroxymethyl)-amino-methane hydrochloric acid
<b>Tween20</b>	polyoxyethylene-sorbitan monolaurate
<b>U</b>	units
<b>UV</b>	ultraviolet
<b>UTP</b>	uridine-5'-triphosphate
<b>vol</b>	volume
<b>WRN</b>	Werner syndrome protein
<b>Ws</b>	<i>Arabidopsis thaliana</i> ecotype Wassilewskija
<b>WT</b>	wild-type
<b>X-Gluc</b>	5-bromo-4-chloro-3-indolyl- $\beta$ -D-glucuronide
<b>XRN</b>	exoribonuclease

## Part I

# Introduction



# 1. Introduction

Development of multi-cellular organisms is characterized by the specification and differentiation of diverse cell types and organs. Specification is controlled by proteins and other regulatory elements present in specific locations and at specific times in adequate concentrations. In Eukaryotes, several layers of gene regulation, including: transcription and chromatin modifications; RNA capping, RNA polyadenylation, RNA splicing; and mechanisms of protein modification, localization, compartmentation, and degradation; have important roles in differentiation processes (Alberts *et al.*, 2002). Transcription factors are key components in the spatio-temporal regulation of genes involved in cell differentiation. They can bind to regulatory elements in genes and increase or decrease their expression. More recent findings have shown that the steady-state level of mRNAs, including those encoding transcription factors, can be regulated by smRNAs (Chen and Rajewsky, 2007). This form of regulation by smRNAs is major topic of this dissertation.

## 1. Small RNA pathways

### 1.1. Classes of smRNAs

Many levels of gene regulation in both plants and animals can be influenced by different classes of non-coding smRNAs 19-30 nucleotides in length (Bartel, 2004; Zamore and Haley, 2005) that are distinguished by their biogenesis and genomic origin. smRNA-mediated regulation is often referred to as RNA silencing, gene silencing, or RNA interference (RNAi) because of their repressing function on gene expression. smRNAs are known to play essential roles in Eukaryotes, with the surprising exception of *Saccharomyces cerevisiae* (brewer's yeast) (Cerutti and Casas-Mollano, 2006). In plants small RNAs are involved in a variety of phenomena that are essential for genome stability, development, and adaptive responses to biotic and abiotic stresses.

### 1.1.1. small interfering RNA (siRNA)

siRNAs are produced either by exogenously triggered RNA silencing (double-stranded RNA (dsRNA), viruses, and transgenes) resulting in transcript cleavage or by endogenous RNA silencing pathways. Endogenously derived siRNAs are subdivided into: repeat-associated siRNAs (ra-siRNAs) (Hamilton *et al.*, 2002; Xie *et al.*, 2004), trans-acting siRNAs (ta-siRNAs) (Peragine *et al.*, 2004; Vazquez *et al.*, 2004), and natural antisense siRNAs (nat-siRNAs) (Borsani *et al.*, 2005). ra-siRNAs arise from loci with repeat sequences and are involved in DNA methylation and establishment or maintenance of transcriptionally silent chromatin (Lippmann *et al.*, 2004). ta-siRNAs are generated from non-coding RNA precursors that are initially targeted for cleavage by a microRNA (miRNA) and play an important developmental role in the juvenile-to-adult transition (Hunter *et al.*, 2003; Fahlgren *et al.*, 2006). Partial overlapping genes on opposite strands of DNA from the same locus (cis-antisense genes) can anneal, form dsRNAs, and give rise to nat-siRNAs. Nat-siRNAs are capable of regulating target mRNA expression of one of the two parent transcripts at the post-transcriptional levels by guiding mRNA cleavage, mainly in response to stress (Borsani *et al.*, 2005).

### 1.1.2. micro RNA (miRNA)

The first miRNA, *lin-4*, was identified in a forward genetic screen in *C. elegans* to identify genes that cause defects in timing in larval development. However, in this case *lin-4* did not encode a protein but a smRNA called at this time a small temporal RNA (stRNA) (Lee *et al.*, 1993). *lin-4* inhibits translation of the heterochronic gene *lin-14*, with which it shares short elements of partial sequence complementarity in its 3'UTR (Lee *et al.*, 1993; Wightman *et al.*, 1993). miRNAs were later identified by cloning in many other organisms including *Drosophila* (Aravin *et al.*, 2003), mouse, human (Lagos-Quintana *et al.*, 2003; Lagos-Quintana *et al.*, 2002), various plant species (Billoud *et al.*, 2005; Jones-Rhoades and Bartel, 2004; Lu *et al.*, 2005; Reinhart *et al.*, 2002; Wang *et al.*, 2004a; Zhang *et al.*, 2005; Zhang *et al.*, 2007) and the green algae *Chlamydomonas reinhardtii* (Molnar *et al.*, 2007; Zhao *et al.*, 2007).

### 1.1.3. piwi-interacting RNA (piRNA)

piwi-interacting RNAs (piRNAs) are smRNAs that associate with members of the Piwi sub-family of Argonaute (AGO) proteins found in the germline of *Drosophila* (Brennecke *et al.*, 2007; Gunawardane *et al.*, 2007; Saito *et al.*, 2006; Vagin *et al.*, 2006), zebrafish (Houwing *et al.*, 2007), and rodents (Aravin *et al.*, 2006; Carmell *et al.*, 2007; Girard *et al.*, 2006; Grivna *et al.*, 2006; Lau *et al.*, 2006; Watanabe *et al.*, 2006). They are 24 to 29 nt with methylated

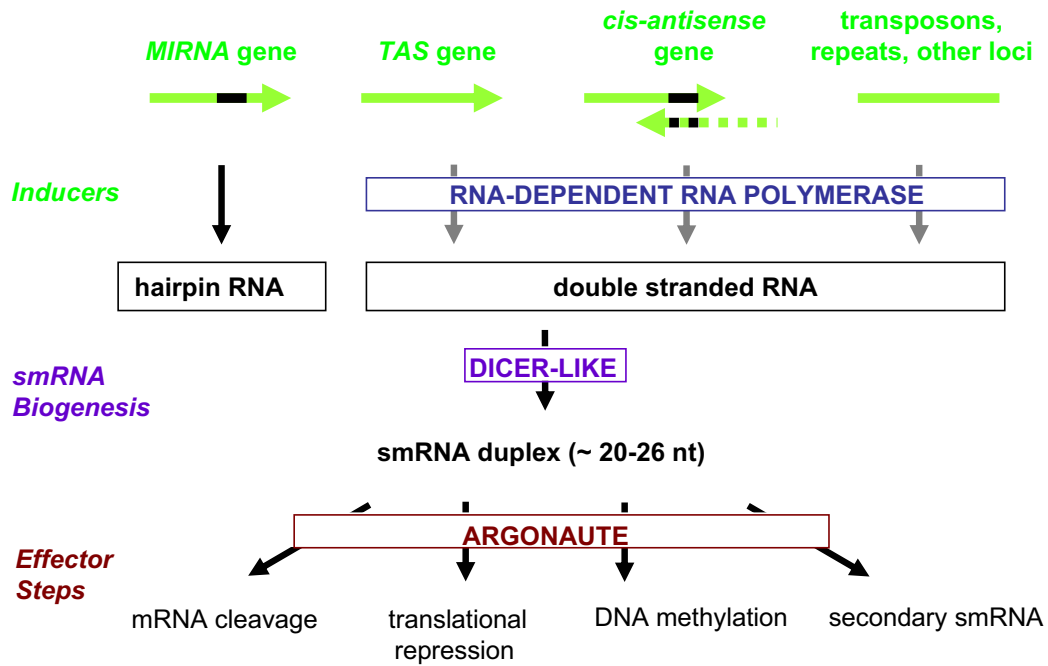


**Figure 1.1: Generalized core RNA silencing pathways.**

RNA silencing is triggered by several inducers that adapt a double-stranded (ds) RNA structure, achieved either by a hairpin structure or reverse transcription by an RNA-dependent RNA polymerase (RDR). The dsRNA is processed by a member of the Dicer family of proteins into small (sm) RNA duplex intermediates. smRNA duplexes are unwound and one (passenger) strand (smRNA\*) is degraded while the guiding strand (smRNA) is incorporated into RISC (RNA-induced silencing complex), an Argonaute protein containing complex. RISC programmed with a smRNA lead to specific degradation of a target sequence.

3' ends, map to euchromatic transposon loci, and their biogenesis occurs through a mechanism distinct from that of siRNAs and miRNAs. piRNAs are evolutionary conserved with a potential role in maintenance of transposon silencing in the germline (O'Donnell and Boeke, 2007).

## 1.2. smRNA biogenesis and mechanistic basis of smRNA-mediated gene regulation

RNA silencing pathways (Figure 1.1) have in common the processing of a dsRNA intermediate by a member of the Dicer family to produce smRNAs that are incorporated into an Argonaute protein-containing complex. The smRNA guides the Argonaute complex to a target in a sequence-specific manner. Figure 1.2 highlights the miRNA pathway in Arabidopsis.

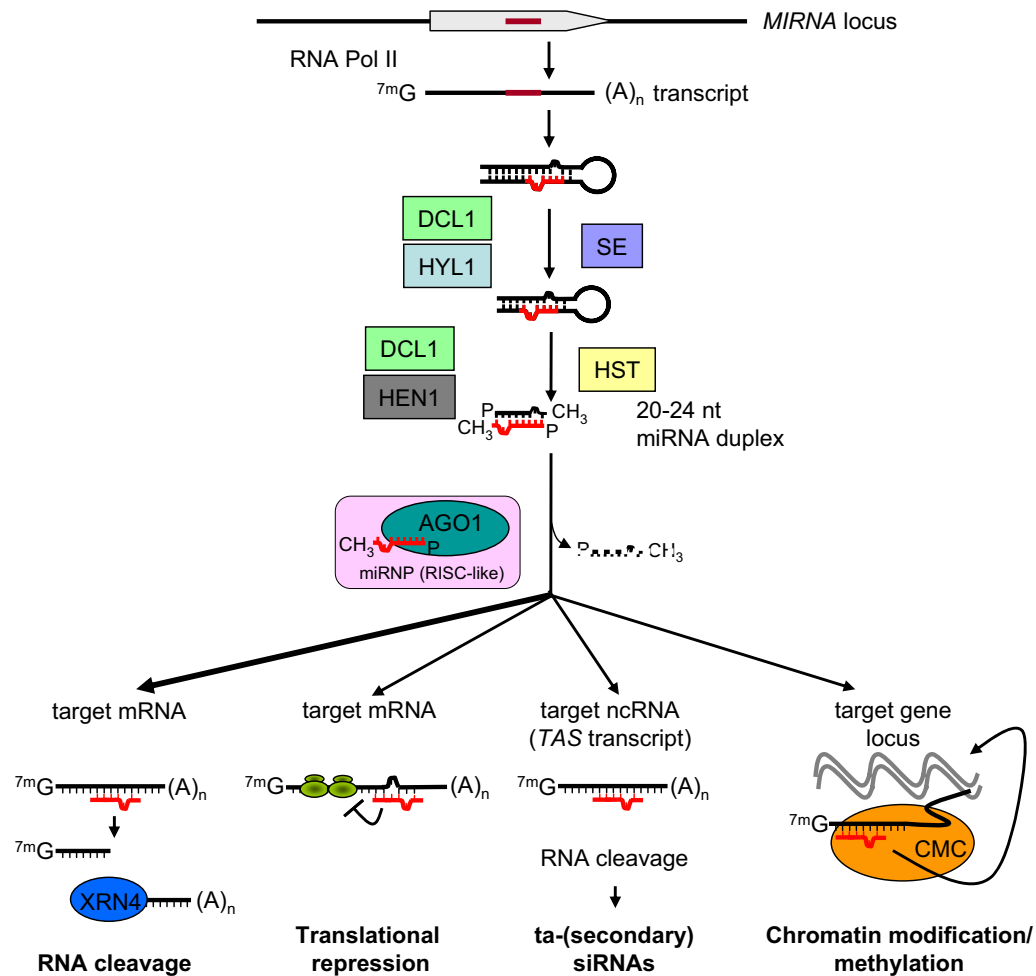


**Figure 1.2: The microRNA pathway in Arabidopsis.**

miRNAs are encoded on a genetic locus. Most miRNA genes are transcribed by an RNA Polymerase II (RNA Pol II) and have core promoter elements like TATA boxes. The transcripts contain both 5' guanosine caps, 3' poly-adenosine tails, and may be spliced, like conventional protein-coding transcripts. *MIRNA* transcripts fold back forming a stem loop region that contains the future mature miRNA sequence. Processing of the precursor transcript is mediated by an RNase III type enzyme DICER-LIKE 1 (DCL1), a double strand binding protein HYPERNASTIC LEAVES 1 (HYL1), and the zinc-finger protein SERRATE (SE) to form a miRNA duplex. Each 3' end of the duplex is protected from polyuridylation and probably degradation by a methyl group mediated by the methyltransferase HUA ENHANCER 1 (HEN1). The miRNA duplex is shuttled to the cytoplasm by HASTY (HST). The guiding strand (miRNA) of the miRNA duplex will be incorporated into the RNA-induced silencing complex (RISC) with ARGONAUTE 1 (AGO1) as its main component. The miRNA will guide RISC to the target mRNA leading either to mRNA degradation by cleavage or translational repression. The miRNA can also act on the target gene locus of a cleaved mRNA by recruiting a chromatin-modifying complex (CMC). Additionally, miRNAs can direct trans-acting (ta)-siRNA phasing. In this case the miRNA cleavage products of a non-protein coding transcript are reversed transcript by an RNA-dependent RNA polymerase (RDR6), that can be processed by Dicer-like proteins into pairs of 21 nt siRNAs. Because of the positioning of the miRNA-directed cleavage, one ta-siRNA will be in correct register to direct cleavage of an mRNA.

## 1.2.1. smRNA processing enzymes - Type III Ribonucleases (RNase III) (Dicer family)

The Dicer family of proteins are large type III ribonucleases that process smRNA precursors. Cleavage by type III RNases produces a characteristic terminal dsRNA structure consisting of a 5' phosphate group and a 2 nt overhang at the 3' end (Robertson *et al.*, 1968). They have been divided into three classes. The bacterial class 1 RNase III contains a single RNase III domain and a dsRNA-binding domain (dsRBD). Class 2 (Drosha) and class 3 (Dicer) proteins have two RNase III (a and b) domains and one dsRBD. Class 3 enzymes have in addition functional domains, a DExD and DExC ATPase/helicase domain at their amino (N)- terminal end, a domain of unknown function (DUF283), and a PAZ domain, which is thought to specifically bind the single stranded tails of smRNA duplexes (Bernstein *et al.*, 2003; Tomari and Zamore 2005).

Drosha as well as Dicer RNases have been shown to mediate processing of siRNA or miRNA precursors. They require a double-stranded RNA-binding protein (DRB) partner to mediate RNA cleavage at the required positions (Liu *et al.*, 2003). In *Drosophila* Drosha and its binding partner Pasha are required for primary (pri-) miRNA maturation in the nucleus (Denli *et al.*, 2004). Dicer-1 (Dcr-1) and Loquacious (Loq) then act in the cytoplasm for further processing of the precursor (pre-) miRNA into mature miRNAs (Forstemann *et al.*, 2005; Lee *et al.*, 2004; Saito *et al.*, 2005). R2D2, the binding partner of siRNA-producing Dicer-2 in *Drosophila*, was shown to selectively bind to the siRNA/siRNA\* double stranded end with the higher thermodynamical stability. This orients the Dicer-2/R2D2 complex and stabilizes the functional guide strand (Tomari *et al.*, 2004), while the other strand, the passenger strand, is degraded. *C. elegans* and mammals contain only a single Dicer enzyme, generating both siRNAs and miRNAs, whereas other species have split these functions between different proteins. The miRNA biogenesis pathway in mammals and *Drosophila* are similar. the Pasha homolog DGCR8 is required for pri-miRNA recognition and pre-miRNA formation by Drosha in the nucleus (Han *et al.*, 2004) and pre-miRNAs are subsequently processed in the cytoplasm by Dicer associated with the Loq homologues HIV-1 TAR RNA-binding protein (TRBP) (Chendrimada *et al.*, 2005; Haase *et al.*, 2005) and PACT (Kok *et al.*, 2007; Lee *et al.*, 2006).

Four different DICER-LIKE (DCL) proteins have been described in Arabidopsis with different, partially overlapping functions in smRNA biogenesis (Gascioli *et al.*, 2005). DCL1 is the main enzyme generating miRNAs (Golden *et al.*, 2002; Park *et al.*, 2002; Reinhart *et al.*, 2002). HYPONASTIC LEAVES 1 (HYL1), one of the five DRBs in Arabidopsis, has been shown to interact with DCL1 (Hiraguri *et al.*, 2005; Vazquez *et al.*, 2004a). DCL1 and HYL1 co-localize in the nucleus where HYL1 interacts directly with miRNA precursors (Hiraguri *et*

*al.*, 2005; Kurihara *et al.*, 2006; Song *et al.*, 2007). DCL2 processes viral and nat-siRNAs (Borsani *et al.*, 2005; Xie *et al.*, 2004). DCL3 is involved in the formation of viral and endogenous siRNAs related to chromatin silencing (Qi *et al.*, 2005; Xie *et al.*, 2004), while DCL4 has been implicated in the formation of secondary ta-siRNAs (Dunoyer *et al.*, 2005; Gascioli *et al.*, 2005; Xie *et al.*, 2005) but also of some miRNAs (Rajagopalan *et al.*, 2007). DRB4 interacts with DCL4 *in vitro* (Hiraguri *et al.*, 2005) to ensure production of ta-siRNAs (Adenot *et al.*, 2005). Examining the *C. reinhardtii*, poplar, and rice genomes revealed that they contain three, five, and six DCL genes, respectively.

### 1.2.2. Additional smRNA processing enzymes in Arabidopsis

Proper miRNA processing in Arabidopsis depends on the interaction between HYL1 and SERRATE (SE) which encodes a zinc-finger protein (Lobbes *et al.*, 2006; Yang *et al.*, 2006). It also depends on HUA ENHANCER 1 (HEN1) which adds methyl groups to the 3' terminal riboses of both strands in the miRNA/miRNA\* duplex (Yu *et al.*, 2005) and stabilizes the miRNA by preventing addition of one or several uridyl residues (Li *et al.*, 2005). Similar observations have been made for siRNA in plants and piRNAs in animals (Carmell *et al.*, 2007; Houwing *et al.*, 2007; Horwich *et al.*, 2007; Saito *et al.*, 2007). HASTY, the plant Exportin-5 ortholog has been implicated in shuttling miRNAs into the cytoplasm, where they can exert their function (Bollman *et al.*, 2003, Hunter *et al.*, 2003).

RNA-DEPENDENT RNA POLYMERASES (RDRs) converts RNA transcripts into dsRNA structures that serve as template for DCL processing and the RNA silencing response. The Arabidopsis genome encodes six RDRs. Biological functions have been assigned only for RDR1, RDR2, and RDR6. RDR6 was first shown to be involved in antiviral defense by mutant screens that also implicated AGO1, HEN1, an RNA helicase (SDE3), and a coiled-coiled protein (SGS3) (Dalmay *et al.*, 2000, 2001; Mourrain *et al.*, 2000). In this screen RDR6 was required for resistance against Cucumber Mosaic Virus (CMV) infection; whereas, RDR1 was required for resistance against infection by tobamoviruses and tobaviruses (Yu *et al.*, 2003). In addition to its function in siRNAs biogenesis and viral defense, and transgene silencing (Himber *et al.*, 2003), RDR6 is required to produce endogenous, ta-siRNAs. Using miRNA cleavage products of the *TAS* locus as templates, RDR6 produces dsRNAs that are then cleaved in phase to give 21 nt ta-siRNAs (Peragine *et al.*, 2004; Vazquez *et al.*, 2004). A similar role for RDR6 in the processing of nat-siRNAs after DCL2 cleavage has been proposed (Borsani *et al.*, 2006). RDR2 is required for the formation of heterochromatin-associated 24 nt siRNAs (Lu *et al.*, 2006; Xie *et al.*, 2004). Pontes *et al.* (2006) showed that DCL3 colocalizes in nucleolar processing bodies with RDR2 and acts downstream of

RDR2 and Pol IVa, a plant-specific RNA polymerase (Herr *et al.*, 2005; Pontier *et al.*, 2005; Onodera *et al.*, 2005).

### 1.2.3. Assembly of smRNA containing ribonucleoprotein complexes and slicing activity - the Argonaute (Ago) family

smRNAs serve as specificity components of the protein RNA induced silencing complex (RISC). RISC is required for miRNA-mediated RNA cleavage (Baumberger and Baulcombe, 2005; Qi *et al.*, 2005). RISC has also been shown to recruit RDRs and the DNA methylation machinery (Bartel, 2004). AGO proteins are the central players of RISC-like complexes and specifically bind small RNAs with their PAZ domain (Lingel *et al.*, 2003; Song *et al.*, 2003; Song *et al.*, 2004; Yan *et al.*, 2003). A second functional region of Ago proteins, the PIWI domain, possesses endonucleolytic activity required for cleaving transcripts in the middle of the region of complementarity to smRNAs ("slicer" activity) (Kasschau *et al.*, 2003; Llave *et al.*, 2002b). This slicer activity was shown for *Drosophila* Ago2 (Liu *et al.*, 2004), human Ago2 (Meister *et al.*, 2004), and Arabidopsis AGO1 (Baumberger and Baulcombe, 2005). Studies of RISC assembly show that Dicer, associates with AGO proteins in the RISC complex. Dicer cleavage products are therefore directly exposed to the AGO PAZ domain, where passenger strands are selectively degraded. Similar to Dicer proteins, AGO proteins are not unique in many genomes, suggesting that they have acquired specialized functions. The Arabidopsis genome encodes 10 AGO family members, whose functions are only partially understood. AGO1 functions in both miRNA and siRNA target regulation (Vaucheret *et al.*, 2004). Unlike animal AGO proteins, which are normally found as part of a larger protein complex, AGO1 directs miRNA and siRNA target cleavage without requiring any protein partners (Baumberger and Baulcombe 2005). AGO4 is involved in siRNA-dependent silencing of transposons and repeats (Zilberman *et al.*, 2004). Although the mechanism of AGO4-mediated chromatin modifications in combination with Pol IV-RDR2-DCL3 complex is still unclear, AGO4 slicer activity is dispensable for maintenance of heterochromatin at some loci (Qi *et al.*, 2006). AGO7 (ZIPPY) has been implicated in mediating slicing of ta-siRNAs gene targets (Axtell *et al.*, 2007; Fahlgren *et al.*, 2006). Once the target mRNA is "sliced" by Ago proteins, the 5' and 3' cleavage fragments are degraded respectively, by the exosome complex and the 5'-3' exonuclease XRN4 (Souret *et al.*, 2004).

### 1.3. Evolution of miRNA genes in plants

Currently, there are 1220 plant miRNAs catalogued in the miRNA sequence database release 10.0 (miRBase, <http://microrna.sanger.ac.uk>, Griffith-Jones, 2004), with the majority identified in *Arabidopsis* (184 miRNAs grouped into 108 families) (Appendix Table A.1), rice (243 miRNAs grouped into 63 families), and poplar (215 miRNAs grouped into 33 families). The majority of miRNAs are conserved across plant species and even between flowering plants and non-flowering plants such as ferns and mosses (Axtell and Bartel, 2005; Zhang *et al.*, 2006), indicating also the conservation of an ancient mechanism for miRNA processing enzymes. Some miRNAs are unique for *Arabidopsis* and believed to be non-conserved (e.g. miR778, miR780, miR824, and miR856) beyond this plant species, leading to a model for the evolution of miRNA genes in plants that distinguishes between “old” and “young” miRNAs (Allen *et al.*, 2004; Fahlgren *et al.*, 2007; Rajagopalan *et al.*, 2006). This suggests that the *MIRNA* locus evolved recently in the *Arabidopsis* genome and possibly occurred by aberrant transposition, inverted gene duplication or recombination of the expressed target gene sequence. Duplication of protein-coding sequences creates new gene regulatory networks and occurred frequently in plant genomes (Teichmann and Babu, 2004). The current model (inverted duplication hypothesis) is supported by the discovery of loci representing intermediate stages in this process (Figure 1.3) and proposes that the newly formed *MIRNA* gene has been co-expressed with the target gene sequence (called founder gene), adopt a foldback structure to produce a miRNA, and is finally kept in the genome to negatively regulate the founder gene (Allen *et al.*, 2004). The *MIRNA* locus initially shows extensive complementarity to its target and over time accumulates mutations and therefore becomes highly divergent from the founder gene sequence except in small regions corresponding to the miRNA and miRNA\* sequences.

### 1.4. miRNA function in *Arabidopsis* - a developmental view

The number of putative transcripts regulated posttranscriptionally by miRNAs or other small RNAs is potentially large in plants and animals (Jones-Rhoades *et al.*, 2006; Rajewsky, 2006). In humans, for example, computational and indirect experimental evidence indicates that miRNAs regulate expression of up to one third of all genes (Bentwich *et al.*, 2005; Farh *et al.*, 2005; John *et al.*, 2006). The crucial roles of miRNAs in *Arabidopsis* development were exemplified by studying plants overexpressing miRNAs and a miRNA-resistant form of the target gene (Jones-Rhoades *et al.*, 2006) (Figure 1.4).



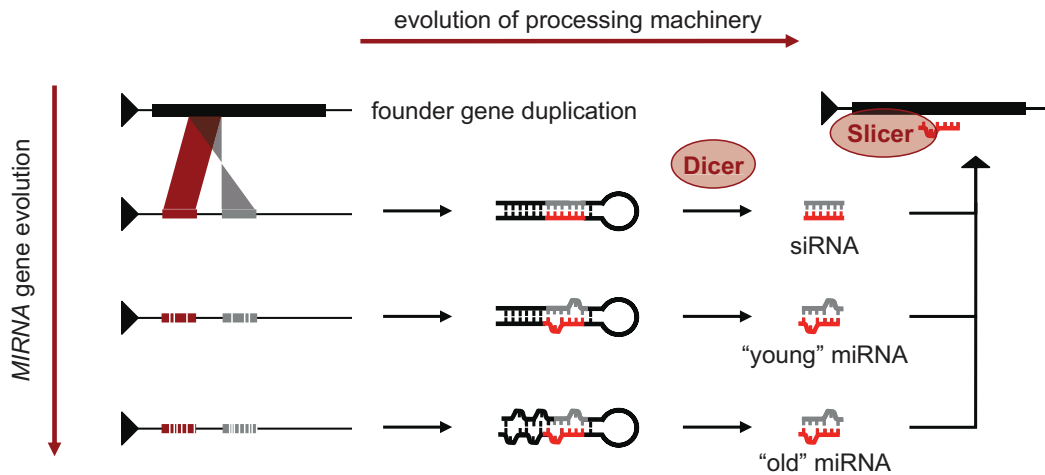


**Figure 1.3: Inverted gene duplication model for evolution of *MIRNA* genes.**

*MIRNA* genes evolve *de novo* by inverted duplication of their future target genes (y axis). The inverted duplication initially forms the arms of an almost perfect double stranded foldback transcript that progressively, through adaptive selection, acquires bulged structures. During evolution “young” miRNA precursors will show extensive complementarity to their targets, and then acquire nt divergence to the point that only the mature miRNA sequence resembles the founder gene sequence as seen in “old” miRNAs. However, the formation of miRNAs requires also the evolution of miRNA processing enzymes (x axis).

#### 1.4.1. miRNAs targeting mRNAs encoding SCL transcription factors

Studies of miR170 and miR171 provided the first experimental evidence for miRNA guided cleavage of plant mRNAs (Llave *et al.*, 2002). Based on sequence analysis, three members of the GRAS family of transcription factors *SCARECROW-LIKE 6 (SCL6)*, *SCL22*, and *SCL27* are potential targets for miR170/171 (Rhoades *et al.*, 2002). While the developmental roles of miR170/171 and its SCL target genes have not been reported yet, studies of this miRNA-mRNA interaction made crucial contributions in the understanding of miRNA functions. Parizotto *et al.* (2004) showed that the foldback structure of pre-miR171 is sufficient for miRNA processing by DCL1. This study also highlighted that the upstream region of *MIR171* contains highly specific promoter elements ensuring tissue-specific expression of miR171.

#### 1.4.2. miR156/157 targeting mRNAs encoding SPL transcription factors

miR156 is a 20 nt long miRNA that differs from the 21 nt long miR157 by one nucleotide and two additional mismatches. Ten out of the 16 *SQUAMOSA PROMOTER BINDING PROTEIN LIKE (SPL)* gene family have target sites for miR156/157. All of the genes are downregulated

miRNA Overexpression		miRNA-resistant target	
Promoter used	Phenotype	Promoter used	Phenotype
Pro35S:miR172	Early flowering Transformation of sepals to carpels <small>Aukerman et al., 2003; Chen, 2004.</small>	miR172 target Pro35S:AP2m	Late flowering Excess of petals and stamens <small>Chen, 2004.</small>
Pro35S:miR159	Male sterility Delayed flowering <small>Achard et al., 2004.</small>	miR159 target Pro35S:MYB33m ProMYB33:MYB33m	Upward curling of leaves <small>Palatnik et al., 2003; Millar et al., 2005.</small>
Pro35S:miR164	Organ fusion Reduced lateral rooting <small>Laufs et al., 2004; Mallory et al., 2004; Guo et al., 2005.</small>	miR164 targets Pro35S:CUC2m ProalcA:CUC2m ProCUC1:CUC1m Pro35S:NAC1m	Aberrant leaf shape Extra petals Increased sepal separation Missing sepals Increased number of lateral roots <small>Guo et al., 2005; Laufs et al., 2005; Mallory et al., 2004.</small>
Pro35S:miR166	Fasciated apical meristems Female sterility <small>Kim et al., 2005; Williams et al., 2005.</small>	miR166 targets Pro35S:PHBm ProREV:REVm	Adaxialized leaves Radialized vasculature <small>Emery et al., 2003; Mallory et al., 2004.</small>
Pro35S:miR319	Uneven leaf shape and curvature Delayed flowering <small>Palatnik et al., 2003.</small>	miR319 targets Pro35S:TCP2m/4m ProTCP2/4:TCP2m/4m	Upward curling of leaves <small>Palatnik et al., 2003.</small>
Pro35S:miR160	Agravitropic roots Abnormal root caps Increased lateral rooting <small>Wang et al., 2005.</small>	miR160 target Pro35S:ARF16m/17m ProARF16/17:ARF16m/17m	Few and abnormal lateral roots <small>Wang et al., 2005; Mallory et al., 2004.</small>
Pro35S:miR156	Increased leaf initiation Decreased apical dominance Delayed flowering <small>Schwab et al., 2005.</small>	miR399 target Pro35S:UBC <sub>ΔUTR</sub>	Reduced response to low phosphate <small>Fujii et al., 2006.</small>
		miR398 targets Pro35S:CSD1m Pro35S:CSD2m	High tolerance to high light, heavy metals, and other oxidative stresses. <small>Sunkar et al., 2006.</small>
		miR168 target ProAGO1:AGO1m	Curled leaves Disorganized phyllotaxy <small>Vaucheret et al., 2004.</small>

**Figure 1.4: Phenotypical consequences of Arabidopsis plants impaired in miRNA and target gene expression**

miRNA overexpression (left panel; controlled by the 35S promoter) and miRNA-resistant target gene expression (right panel; controlled by either the 35S or the endogenous target gene promoter) result in obvious phenotypes of Arabidopsis as described and shown by a picture.

in plants constitutively overexpressing miR156b (Schwab *et al.*, 2005) but only five of these transcripts have been shown to be cleaved by these miRNAs (Chen *et al.*, 2004; Kasschau *et al.*, 2003; Vazquez *et al.*, 2004; Wu and Poethig, 2006). miR156/157 is responsible for the change in *SPL3* expression in vegetative phase change and floral induction (Wu and Poethig, 2006). Interestingly, Gandikota *et al.* (2007) report that miR156/157 prevents early flowering in seedlings by translational inhibition of *SPL3*. The phenotype is similar to that of mutants deficient in *ZIP* and *RDR6* that are required for the ta-siRNA pathway. Indeed, both either directly or indirectly repress the expression of *SPL3* during vegetative development (Wu and Poethig, 2006). The heterochronic maize mutant *corngrass 1 (cg1)* is formed by overexpressing a tandem arranged miR156 locus that is probably caused by retrotransposon insertion (Chuck *et al.*, 2007) and the phenotype is so severe that it causes reversion to a more ancestral grass-like state (Singleton, 1951). This leads to the conclusion that altering miR156/157 level can either prolong or shorten juvenile development in maize thus providing a mechanism for how species-level heterochronic changes can occur in nature.

#### 1.4.3. miRNAs targeting mRNA encoding TCP transcription factors

The sequence of miR159 and miR319/JAW differ by only three nucleotides (Palatnik *et al.*, 2003; Reinhart *et al.*, 2002). The effects of overexpression, as well as the position of target cleavage, indicated that miR159 and miR319 have largely nonoverlapping effects *in vivo*. miR159 targets several MYB transcription factor genes involved in flowering and male fertility, while miR319 primarily affects five TCP transcription factor genes controlling leaf shape (Achard *et al.*, 2004; Millar and Gubler, 2005; Palatnik *et al.*, 2003; Schwab *et al.*, 2005). Cross regulation by cleavage has been shown by using a mutational approach of miR159 and miR319 targets (Palatnik *et al.*, 2007). Surprisingly, Hikosaka *et al.* (2007) reported that miR159 was found in the *Xenopus tropicalis* miRNA cDNA library and is assembled with transposons raising the possibility that *MIR159* genes were horizontally transferred from plants to animals.

#### 1.4.4. miR172 targeting of AP2 transcription factors

miR172, which targets AP2 and AP2-like genes, was identified in screens for early flowering and floral defects. For example, the early flowering eat-D mutant and late-flowering *toe1-D* mutants turned out to have increased expression of *MIR172b* and the *miR172* target gene *TOE1*, respectively (Aukerman and Sakai, 2003). Interestingly, miR172 regulates AP2 via repression of translation rather than cleavage (Aukerman and Sakai, 2003; Chen, 2004).

miRNA resistant alleles of *AP2* result in phenotypes similar to *agamous* (*ag*) mutants that have stamens and carpels replaced by additional whorls of petals and sepals (Chen, 2004). This phenotype is consistent with models of floral organ identity establishment in which *AP2* and *AG* activities are antagonistic (Bowman *et al.*, 1991). Activation of miR172 in flower meristem could be a mechanism for cell fate specification by clearing *AP2* transcripts rapidly (Bartel and Bartel, 2002).

#### 1.4.5. miR164 targeting of NAC transcription factors

miR164 targets mRNAs encoding *CUC-like* NAC transcription factors. *cuc1* and *cuc2* mutants exhibit fused lateral organs, fusions of cotyledons, and failure in apical meristem formation (Aida *et al.*, 1997). Constitutive expression of miR164 phenocopies a *cuc1cuc2* double mutant (Laufs *et al.*, 2004; Mallory *et al.*, 2004). So far, *eep1/mir164c* is the only recessive loss-of-function miRNA mutant that has been identified in plants by a forward genetic screen (Baker *et al.*, 2005). Constitutive expression of a wild-type *CUC1* gene results in a dramatic phenotype in which ectopic meristems developed from the adaxial sites of both cotyledons and rosette leaves and root branching is reduced (Guo *et al.*, 2005; Mallory *et al.*, 2004; Takada *et al.*, 2001). This suggests that local miR164 expression helps to clear transcripts from cells rapidly following cell divisions and thus, limits the expansion of the meristem boundary domain.

#### 1.4.6. miR165/166 targeting of class III HD-ZIP transcription factors

Two miRNAs (miR165/166) target the five class III HD-ZIP gene family members, *PHABULOSA* (*PHB*), *PHAVULOTA* (*PHV*), *REVOLUTA* (*REV*), *ATHB8*, and *CNA/ATHB15* (Reinhart *et al.*, 2002; Rhoades *et al.*, 2002). *PHB*, *PHV*, and *REV* are involved in establishment of adaxial leaf identity, development of the apical meristem, and the vascular bundles (Emery *et al.*, 2003; McConnell and Barton, 1998; McConnell *et al.*, 2001; Zhong and Ye, 2004). Cleavage products were detected for all the miR165/166 targeted class III HD-ZIP gene family members (Emery *et al.*, 2003; Mallory *et al.*, 2004; Zhong and Ye, 2004). miR166 overexpressor *jba1-D* and *men* mutants exhibited fasciated stems that primarily resulted from the downregulation of *PHB*, *PHV* and *CNA/ATHB15* mRNAs, but not from *REV* and *ATHB8*, pointing to the importance of the tissue-specific regulation of miRNA expression during development (Kim *et al.*, 2005; Williams *et al.*, 2005). Transgenic plants carrying a miRNA-resistant *PHB* and *REV* gene exhibited a phenotype similar to a gain-of-function mutant having a point mutation in the miR165/166 binding site. However, constitutive ex-

pression of the wild-type versions of *PHB* and *REV* did not result in aberrant phenotypes. By investigating DNA methylation patterns Bao *et al.* (2004) came to the conclusion that miR165/166 direct more stable epigenetic changes by influencing chromatin remodeling at the *PHB* loci rather than a rapid developmentally induced clearing of transcripts. Additionally, it has been shown that histone deacetylases (HDACs) control levels and/or pattern of miR165/166 (Ueno *et al.*, 2007). The study of Nogueira *et al.* (2007) highlighted that ta-siRNAs targeting the *AUXIN RESPONSE FACTOR (ARF)* genes accumulate on the adaxial side where they restrict the expression of miR166.

#### 1.4.7. miRNAs implicated in hormonal regulation

Several links between hormonal signal transduction pathways in plants and miRNA regulation have been identified. For example, miR159 levels are regulated by gibberellic acid during flower development (Achard *et al.*, 2004; Millar and Gubler, 2005) and by abscisic acid during seed germination (Reyes and Chua, 2007). Auxins directly stimulate or inhibit the expression of specific genes by targeting for degradation members of the Aux/IAA family of transcriptional repressor proteins. The auxin receptor TIR1 is an F-box protein of the SCF ubiquitin ligase complex (Dharmasiri *et al.*, 2005; Kepinski and Leyser, 2005), which mediates ubiquitination of the AUX/IAA protein and subsequent proteolysis through the 26S proteasome pathway (Gray *et al.*, 2001; Rogg and Bartel, 2001; Kepinski and Leyser, 2002). miR393 targets *TIR1* mRNA and the three most closely related F-box proteins (Jones-Rhoades and Bartel, 2004; Sunkar and Zhu, 2004). miR164 targets the mRNA encoding NAC1 (Rhoades *et al.*, 2002; Mallory *et al.*, 2004), a putative transcription factor that acts downstream of *TIR1* to promote lateral root development (Xie *et al.*, 2002). AUX/IAA proteins heterodimerize with AUXIN RESPONSE FACTORS (ARFs), which bind auxin-response elements and activate or repress gene expression (Ulmasov *et al.*, 1997a,b; Ulmasov *et al.*, 1999a,b). Several clades within the ARF family are negatively regulated by small RNAs. *ARF6* and *ARF8* mRNAs are targeted by miR167 while *ARF10*, *ARF16*, and *ARF17* mRNAs are targeted by miR160 (Rhoades *et al.*, 2002; Kasschau *et al.*, 2003; Jones-Rhoades and Bartel, 2004; Vazquez *et al.*, 2004). *ARF6* and *ARF8* regulate ovule and anther development (Ru *et al.*, 2006; Wu *et al.*, 2006). miR160-resistant mutants have been used to study phenotypic changes (Chen, 2004; Guo *et al.*, 2005; Laufs *et al.*, 2004; Mallory *et al.*, 2004; Millar and Gubler, 2005) revealing that downregulation of *ARF10* is needed for seed germination (Liu *et al.*, 2007), *ARF16* and *ARF17* are essential in root, leaf, and flower organ development (Mallory *et al.*, 2005; Wang *et al.*, 2005). Additionally, miR390 guides in-phase processing of the *TAS3* locus that generate ta-siRNAs, which in turn target *ARF2*, *ARF3* (ETTIN), and *ARF4* (Allen *et*

*et al.*, 2005; Williams *et al.*, 2005).

#### 1.4.8. miRNAs implicated in responses to abiotic stress and nutrient deficiency

Plant miRNAs play important roles in plant resistance to abiotic and biotic stresses. miR398 targets COX5b-1, a subunit of the mitochondrial cytochrome c oxidase, and both the cytosolic Cu-Zn superoxide dismutase (CSD1) and plastidic CSD2 that are involved in antioxidant response (Jones-Rhoades and Bartel, 2004; Sunkar and Zhu, 2004). Under copper limiting conditions miR398 degrades both CSD2 and COX5b-1 (Yamasaki *et al.*, 2007). In response to oxidative stress miR398 is transcriptionally downregulated to release its suppression of *CSD1* and *CSD2* genes (Sunkar *et al.*, 2006). miR398 can determine normal growth and development on one hand or stress tolerance on the other hand. miR395 and miR399 have been shown to function in nutrient homeostasis; miR395 are induced by low-sulfate treatment (Jones-Rhoades and Bartel, 2004) and miR399 is induced by low-phosphate treatment (Fujii *et al.*, 2005; Chiou *et al.*, 2006). miR395 targets ATP sulfurylases (*APS1*, *APS3*, and *APS4*) that play a crucial role in sulfur assimilation pathways (Jones-Rhoades and Bartel, 2004; Sunkar and Zhu, 2004), while miR399 was predicted to target a phosphate transporter (Jones-Rhoades and Bartel, 2004) and a putative ubiquitin conjugating enzyme-E2 (*UBC24*, *PHO2*) (Sunkar and Zhu, 2004). Downregulation of *PHO2* mRNA levels under low phosphate conditions is important for primary root elongation (Fujii *et al.*, 2005). In addition to its role in auxin signaling, miR393 was found to be induced in response to biotic stress such as treatment with flagellin (Navarro *et al.*, 2006) or *Pseudomonas syringae* (Fahlgren *et al.*, 2007).

#### 1.4.9. Feedback regulation of miRNA pathways

DCL1 and AGO1, proteins involved in miRNA biogenesis and/or function, are themselves negatively regulated by miRNAs. This negative feedback regulation provides probably cell type specificity in the production or activity of miRNA by restricting them to certain cell or tissue types (Rajagopalan *et al.*, 2006; Vaucheret *et al.*, 2004; Xie *et al.*, 2003). miR162 targets *DCL1* mRNA spanning exon 12 and 13 (Reinhart *et al.*, 2002; Rhoades *et al.*, 2002). Interestingly, miR838, targeting a gene encoding Armadillo/ $\beta$ -catenin protein, derives from a hairpin within intron 14 of the *DCL1* mRNA (Rajagopalan *et al.*, 2006). Alternative splicing of *DCL1* leads to several transcript isoforms, which all accumulate in embryonic lethal *dcl1* mutants (Hirsch *et al.*, 2006; Xie *et al.*, 2003). The intronic miR838 might help to enable a self-regulatory mechanism to maintain *DCL1* homeostasis. These findings suggest that

splicing of this miR838 primary transcript and miR162 processing are competitive nuclear events. miR168 targets *AGO1* mRNA and helps to maintain AGO1 homeostasis. Disturbing levels of miR168 has a global consequence on miRNA-programmed silencing complex leading to accumulation of mRNA levels of other miRNA targets (Vaucheret *et al.*, 2006).

To summarize, a diverse set of genes is regulated by miRNAs. miRNAs therefore ensure rapid clearing of transcripts during cell fate decisions in addition to the control of developmental and physiological processes. miRNAs can act as key components or modulators in signaling and metabolic pathways to ensure robustness or set a threshold for activation switches. They adjust their own formation by targeting genes of their own biosynthesis and take therefore also part in the regulation of endogenous and exogenous siRNA including RNAi-dependent epigenetic mechanisms. The examples described and localization studies (Valoczi *et al.*, 2006) show that both miRNAs and their targets are spatial-temporal regulated to ensure correct gene function.

## 2. The MADS-box gene family

The miRNA, miR824, described in this thesis targets for degradation AGAMOUS-LIKE 16 (AGL16) belonging to the MADS-box gene family. MADS-box genes encode a eukaryotic family of transcriptional regulators involved in diverse biological functions. These proteins contain a conserved MADS-box domain named after the founding members of this family: the *MINICHROMOSOME MAINTENANCE 1 (MCM1)* genes in yeast (Passmore *et al.*, 1989), *AGAMOUS (AG)* in Arabidopsis (Yanofsky *et al.*, 1990), *DEFICIENS (DEF)* in *Antirrhinum* (Sommer *et al.*, 1990), and *SERUM RESPONSE FACTOR (SRF)* in humans (Norman *et al.*, 1988).

Before the divergence of plants from fungi and animals, a duplication occurred in the MADS-box lineage, resulting in type I (SRF-like) and type II (MYOCYTE ENHANCER FACTOR 2 [MEF2]-like) MADS-box genes (Alvarez-Buylla, *et al.*, 2000 Pelaz; *et al.*, 2000; Svensson *et al.*, 2000). The type II MADS-box proteins are composed of an N-terminal MADS-box domain involved in DNA binding and dimerization domain, followed by an intervening (I) region and a keratin-like (K) box that are involved in protein-protein interactions (Theissen *et al.*, 2000), and the carboxyl-terminus (C) that is necessary for activity and ternary complex formation (Egea-Cortines *et al.*, 1999; Honma and Goto, 2001; Lamb and Irish 2003). Some type II MADS-box proteins possess an additional N-terminal extension (Theissen *et al.*, 1996). In contrast, type I MADS-box proteins lack the K-box (Alvarez-Buylla *et al.*, 2000; Boffelli *et al.*, 2003).

## 2.1. The modular structure of plant MADS-box proteins

Mutational and functional analysis demonstrated that MADS-box proteins consist of a DNA-binding region which serves as an interface for dimerization and interactions with other proteins. There is a considerable overlap between these functional domains and the M, I, K, and C structural domains, although none of the functions can exclusively be assigned to just one single domain.

### 2.1.1. Protein interaction networks of MADS-box proteins

MADS domain proteins act as homo- or heterodimer to recognize AT-rich consensus sequences with a highly conserved 10 bp core. This common DNA motif, designated CArG-box (CC(A/T)<sub>6</sub>GG) (Riechmann and Meyerowitz, 1997; Treisman, 1990), was used to generate crystal structures of SRF-core homodimers. The crystal structure revealed that the N-terminus of the MADS domain is imbedded in the major groove of the DNA helix and causes conformation changes of DNA (bending) upon binding (Pellegrini *et al.*, 1995). Studies to identify the minimal DNA binding domain of the *Antirrhinum* MADS-box proteins SQUAMOSA (SQUA) and PLENA (PLE) demonstrated that the MADS- and I-domains are sufficient to permit sequence-specific DNA binding by the proteins (West *et al.*, 1998). Similar results were obtained for the *Arabidopsis* MADS-box proteins APETALA1 (AP1), APETALA3 (AP3), PISTILLATA (PI), and AGAMOUS (AG). In the case of AP3 and PI the regions involved to form a protein-DNA complex are the MADS box, the entire I region and the first putative amphipathic helix of the K box, while for AP1 and AG only the MADS-box and part of the I region is needed (Riechmann *et al.*, 1996a, b). For DNA binding the MADS-box proteins have to homo- and/or heterodimerize. The differences in organization and partner specificity of the AP1, AG, and AP3 and PI proteins support the idea that selective interactions achieve their functional specificity. Since the DNA-binding activities of the dimers (AP1-AP1, AP3-PI and AG-AG) are very similar, it is suggested that their biological specificity is achieved through selective interactions with additional transcription factors. This mechanism appears to be a common theme for MADS-box proteins of animals and fungi. DNA binding is often accompanied by transcription factor-induced DNA bending, which is important in determining local promoter architecture and is thought to be a key determinant of their function, but the mechanism is still unclear (West and Sharrocks, 1999).

In principle, the formation of dimers and multimers of MADS-box transcription factors provides a mechanism to increase the diversity of DNA-binding functions that could enhance target gene specificity. The MADS domain proteins preferentially form heterodimers (Kauf-



mann *et al.*, 2005). A comprehensive yeast two-hybrid screen revealed that at least 269 MADS domain dimers can be formed in *Arabidopsis* (de Folter *et al.*, 2005). The first *in vitro* experiments showed that three *Antirrhinum* MADS proteins (SQUA, DEF, and GLOBOSA (GLO)) form ternary complexes via their C-termini. Gel-shift assays have established that the ternary complex shows enhanced DNA binding to consensus binding sites (CArG motifs) relative to DEF/GLO heterodimers or SQUA/SQUA homodimers (Egea-Cortines *et al.*, 1999). Additional genetic and yeast-two/three-hybrid screens confirmed higher-order complex formation for many MADS domain proteins (Goto *et al.*, 2001; Honma and Goto, 2001; Krizek and Meyerowitz 1996ab; Mizukami *et al.*, 1996; Pelaz *et al.*, 2001; Sridhar *et al.*, 2006). Other studies showed the involvement of other interacting cofactors to facilitate DNA binding (Gamboa *et al.*, 2001; Pelaz *et al.*, 2001; Remenyi *et al.*, 2004).

### 2.1.2. Transcriptional regulation of MADS-box proteins

MADS-box proteins form cross- or auto-regulatory circuits to control their own or their partner activity. MADS-box proteins DEF and GLO in *Antirrhinum* bind to their own promoter sequences (Schwarz-Sommer *et al.*, 1992; Trobner *et al.*, 1992; Zachgo *et al.*, 1995), similar to AP3 and PI in *Arabidopsis* (Chen *et al.*, 2000; Goto and Meyerowitz, 1994; Honma and Goto, 2000; Jack *et al.*, 1992). Autoregulation of AG (Espinosa-Soto, 2004; Gomez-Mena *et al.*, 2005) and AGL15 (Zhu and Perry, 2005) has also been described. Transcriptional regulatory networks involving MADS-box proteins have been proposed for flower formation (Espinosa-Soto, 2004). The floral MADS-box gene AG requires sequences located in a 3 kb intron for proper expression (Busch *et al.*, 1999; Deyholos and Sieburth, 2000; Sieburth and Meyerowitz, 1997). Expression of MADS-box genes FLOWERING LOCUS C (FLC) and PLENA (PLE) are also regulated by intragenic regions (Bradley *et al.*, 1993; Sheldon *et al.*, 2002). Three transcription factors LEAFY (LFY), WUSCHEL (WUS), and BELLRINGER (BLR) bind to sequences within this intron (Boa *et al.*, 2004; Busch *et al.*, 1999; Lohmann *et al.*, 2001) that control AG enhancer activity. Interestingly, CArG-boxes are located in the second intron of AG. Other MADS-box transcription factors bind to these intronic CArG motif and control AG regulation on the transcriptional level (Hong *et al.*, 2003).

### 2.2. Functions of MADS-box genes in *Arabidopsis*

In contrast to animals, homeotic genes (Hox genes) in plants do not code for homeodomain-containing proteins, but in almost all cases for MADS domain proteins (Meyerowitz, 2002). The gene family encoding MADS domain transcription factors in plants encompasses a rel-

atively large family with 107 members in the Arabidopsis genome (Parenicova *et al.*, 2003). They are further subdivided into two groups: the class II MADS box proteins, comprising the MIKC<sup>c</sup> (Henschel *et al.*, 2002; Kaufmann *et al.*, 2005) and M $\delta$ / MIKC\* types (M $\delta$  in Parenicova *et al.*, 2003; MIKC\* in Becker and Theissen, 2003), and the class I proteins that are further subdivided into the M $\alpha$ , M $\beta$ , and M $\gamma$  types (Alvarez-Buylla *et al.*, 2000; Parenicova *et al.*, 2003). The majority of MIKC-type MADS-box genes are involved in the determination of flowering time, floral meristem, and floral organ identity (overview given in Figure 1.5).

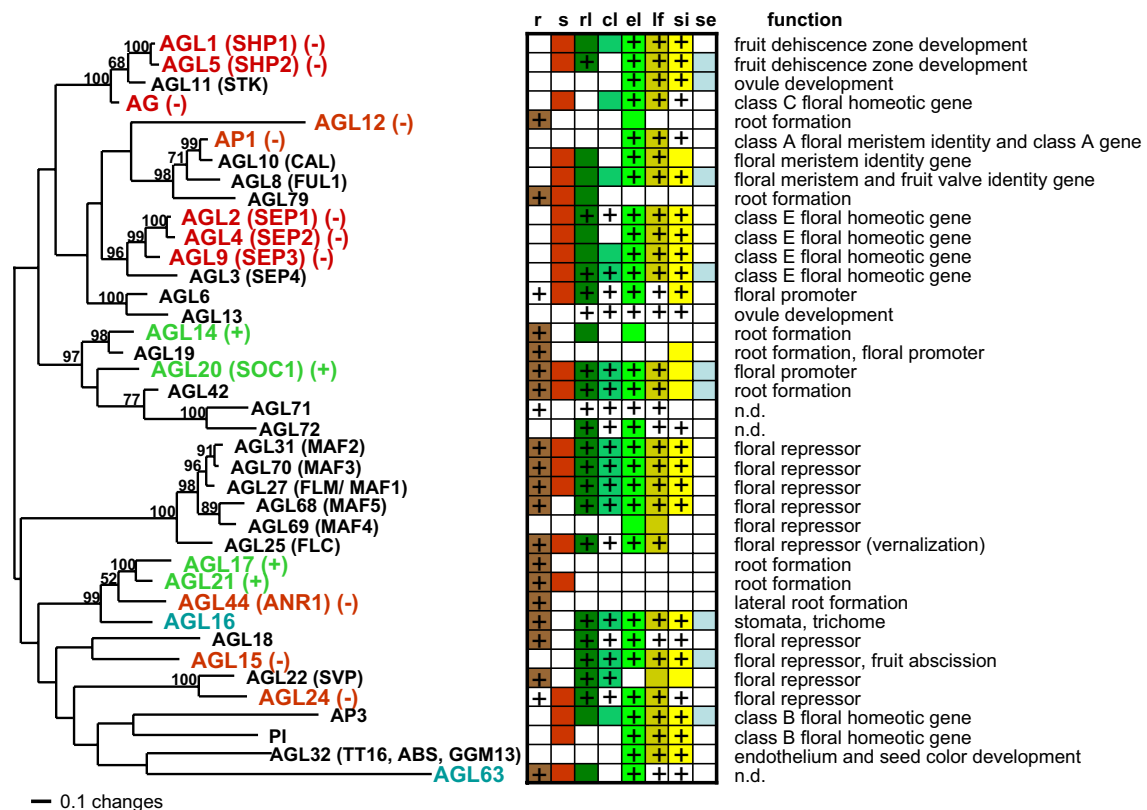


**Figure 1.5: The Arabidopsis MIKC-type of MADS box protein interaction map.**

MADS box protein are arranged according to their phylogenetic relationship as has been reported by Parenicova *et al.* (2003) and de Folter *et al.* (2005). The phylogenetic tree is shown on the left. For example: AGL16 forms a homodimer. Protein-protein interactions with AGL16 are represented in red (inhibition) or in green (activation) blocks, and interactions that could not be tested in gray. Gene expression pattern were determined by RT-PCR. A positive signal is indicated by a plus in each box in the study of Parenicova *et al.* (2003) and by colored boxes in the study of Hillemann *et al.* (2006). Validated function of each MADS-box transcription factor is presented on the right. r, roots; s, seedlings; rl, rosette leaves; cl, cauline leaves; el, early flowers; lf, late flowers; si, siliques; se, seeds. Note: rl and cl analyzed as “leaves”, el and lf analyzed as “inflorescence” in Parenicova *et al.* (2003)

### 2.2.1. Control of flowering time by MADS-box genes

The function of MADS-box genes in the reproductive development of plants has been studied in detail. Flowering time is influenced by environmental conditions, such as day length, temperature, light quality, nutrient deprivation, as well as by developmental parameters associated with the age of the plant (Koornneef *et al.*, 1998). The MADS-box genes *FLC* and *SHORT VEGETATIVE PHASE (SVP)* belong to the autonomous pathway and regulate negatively the transition from vegetative to reproductive development under both long-day and short-day conditions (Michaels and Amasino, 1999; Hartmann *et al.*, 2000). *CONSTANS (CO)*, a zinc-finger protein is involved in the photoperiodic pathway (also called the long-day pathway) which promotes flowering only under long-day conditions but has no effect under short days (Putterill *et al.*, 1995). The day-length independent pathway (also called the gibberellin pathway) stimulates flowering by the plant hormone gibberellin. It has been shown that the MADS-box gene *SUPPRESSOR OF OVEREXPRESSION OF CO 1 (SOC1)* can integrate signals from all three pathways (Moon *et al.*, 2003; Onouchi *et al.*, 2000; Samach *et al.*, 2000) and that it is a direct target of *CO* (Onouchi *et al.*, 2000; Samach *et al.*, 2000). Compared to late-flowering genes, less is known about early-flowering genes. *TERMINAL FLOWER (TFL)* controls both flowering time and the identity of the shoot meristem (Shannon and Meekss-Wagner, 1991). Therefore, *TFL* provides a link between the control of flowering time and flower initiation. How MADS-box genes like *AP1*, *CAULIFLOWER (CAL)*, *FRUITFULL (FUL)* and *SVP*, which also control flowering time, are integrated into the current framework is still unclear (Mandel *et al.*, 1992; Kempin *et al.*, 1995; Mandel and Yanofsky 1995; Ferrandiz *et al.*, 2000; Hartmann *et al.*, 2000).

### 2.2.2. Control of floral meristem identity

The switch from vegetative to reproductive development involves the production of flowers instead of leaves or shoots and requires the activity of floral meristem identity genes whose expression is upregulated in developing floral primordia during the transition (Cary *et al.*, 2002; Bowman *et al.*, 2002). Mutants affecting these genes develop shoots or shoot-like structures in place of flowers. These genes include *AP1*, *CAL*, and *FUL*, as well as the non-MADS-box gene *LFY*. The *AP1* and *CAL* genes have overlapping functions in promoting flower meristem identity and *ap1 cal* double mutants have a massive proliferation of a shoot-like meristem in positions normally occupied by a single flower (Bowman *et al.*, 1991). This phenotype is further enhanced by mutations in *FUL*, such that *ful;ap1;cal* triple mutants never flower under standard growth conditions, and continuously elaborate leafy shoots in

place of flowers (Ferrandiz *et al.*, 2000). This observation indicates that these three genes act together to control meristem identity. The failure to flower in the triple mutant is due to loss of *LFY* upregulation, because introducing a transgene that constitutively expresses *LFY* into the *ful;ap1;cal* background restores flowering (Ferrandiz *et al.*, 2000).

### 2.2.3. Control of floral organ identity - the “ABCDE” and “quartet” models

The “ABC” model, based on homeotic mutants affecting floral organs, was proposed to account for the function of specific classes of transcription factors in flower development (Coen and Meyerowitz, 1991; Weigel and Meyerowitz, 1994). According to this model, A class genes *APETALA1* (*AP1*) and the non-MADS-box gene *APETALA2* (*AP2*) specify sepals in the first whorl. A class genes in combination with the B class genes *APETALA3* (*AP3*) and *PISTILLATA* (*PI*) specify petals in the second whorl. B class genes and C class genes *AGAMOUS* (*AG*) specify stamens (male reproductive organs) in the third whorl; and, C class genes specify carpels (female reproductive organs) in the fourth whorl of a typical *Arabidopsis* flower (Coen and Meyerowitz, 1991; Weigel and Meyerowitz, 1994). In addition to ABC class genes, D class genes *SEEDSTICK* (*STK*), important for ovule development, and E class genes *SEPALLATA1* (*SEP1*), *SEPALLATA2* (*SEP2*), *SEPALLATA3* (*SEP3*), and *SEPALLATA4* (*SEP4*), which encode additional transcription factors playing a role in determining the identity of all four whorls, have been described. This led to an extension of the ABC model to the current “ABCDE” model (Theissen, 2001; Ditta *et al.*, 2004). Moreover, evidence is growing on the formation of multimers, possibly tetramers according to the “quartet” model (Figure 1.6), consisting of proteins encoded by these different MADS-box gene classes and regulating different aspects of floral organ development (Honma and Goto, 2001; Theissen and Saedler, 2001; de Folter *et al.*, 2005; Kaufmann *et al.*, 2005b).

### 2.2.4. Additional functions of MIKC-type MADS-box genes

MIKC-type MADS-box genes also play roles in the vegetative development of *Arabidopsis* (Figure 1.5). The *ARABIDOPSIS NITRATE REGULATED 1* (*ANR1*) gene controls root growth in response to nitrate (Zhang and Forde, 1998; Gan *et al.*, 2005). Other MADS-box genes are involved in the specification of cell fates in the fruit. *FRUITFULL* (*FUL*), *AGL13*, *SHATTERPROOF 1* (*SHP1*), and *SHATTERPROOF 2* (*SHP2*) determine cell fate in the development of the fruit (Rounsley *et al.*, 1995). *SHP1* and *2* are closely related, functionally redundant, and involved in the differentiation of the dehiscence zone (Liljegren *et al.*, 2000). Differentiation of the valves (peripheral wall of the silique) separating seed compartments

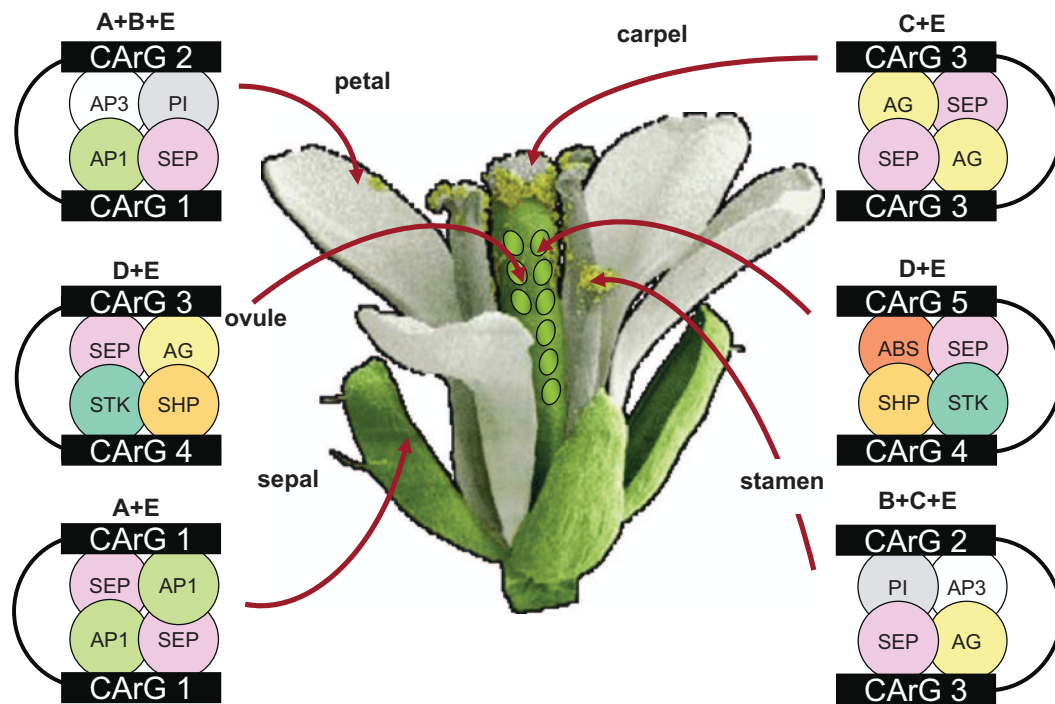


**Figure 1.6: The “ABCDE” and “quartet model” in Arabidopsis.**

ABCDE model maintains that class A+E genes are required to specify sepals, A+B+E petals, B+C+E stamens, C+E carpels, and D+E ovules. The combinatorial protein complexes represent transcription factors that exert their function by binding to promoters of target genes leading to their activation or repression. Endothelium, the inner layer in the integument of ovules. ABS, Arabidopsis *B<sub>sister</sub>*; for all other names see text

in Arabidopsis requires the activity of *FUL*, which negatively regulates *SHP1* and *SHP2* expression (Ferrandiz *et al.*, 2000). Other MADS-box genes regulate different aspects of root (*AGL12*, *AGL14*, and *AGL17*) (Rounsley *et al.*, 1995) and embryo (*AGL15* and *AGL18*) (Heck *et al.*, 1995; Lehti-Shiu *et al.*, 2005) development. *AGL16* is expressed in guard cells and trichomes (Alvarez-Buylla *et al.*, 2000) but its biological function is unknown.

### 2.3. Evolutionary complexity of MADS-box gene family members

Natural variation and selection of MADS-box genes implicated in flowering are believed to have played a key role in the structural evolution of flowers (Becker and Theissen 2003). Phylogenetic studies of MADS-box genes showed that the MIKC-type diversified extensively in land plants. MIKC-type MADS box genes have independently duplicated in different plant lineages, with 39 paralogous genes present in the Arabidopsis genome (Kofuji *et al.*, 2003; Parenicova *et al.*, 2003) and ca. 47 copies in the rice genome (Nam *et al.*, 2004). A gene duplication event is the simplest form to produce two functional redundant, paralogous genes.

It has been demonstrated that after the duplication of an ancestral gene, one copy accumulates mutations, especially in the C-terminal domain, while the MIK domain is retained. Insertions or deletions causing a frameshift in the coding sequence may have yielded to novel functional motifs and were integrated in regulatory networks (Litt and Irish, 2003; Vandenbusche *et al.*, 2003). However, the extent that these networks are conserved and act to specify similar developmental outcomes across angiosperms is unclear. For example, in Arabidopsis, the CONSTANS transcription factor activates *FT*, which encodes a key integrator of flowering signals (Samach *et al.*, 2000). In contrast, the rice homolog of CONSTANS functions to repress the *FT* homolog, suggesting that a switch in the mode of transcriptional regulation of *FT* is responsible for long day versus short day flowering (Causier *et al.*, 2005; Davies *et al.*, 1999; Hayama *et al.*, 2003; Kramer *et al.*, 2004; Zachgo *et al.*, 1997). Conversely there are examples of paralogous MADS-box genes that appear to have taken on equivalent developmental functions (Martienssen and Irish, 1999; Irish, 2003; Causier *et al.*, 2005). In many cases, (partial) functional redundancy between paralogous MADS-box genes (e.g., AP1-CAL, SHP1-SHP2, and SEP1-SEP2-SEP3-SEP4) has been described (Ditta *et al.*, 2004; Ferrandiz *et al.*, 2000; Malcomber and Kellogg, 2005; Pinyopich *et al.*, 2003). In summary, DNA-binding and multimerization properties of MADS-box proteins evolved to ensure proper interaction between the family members (e.g. “quartet” model) required for the specification of sophisticated organ development such as flowers (Theissen and Saedler, 2001).

### 3. Stomatal development and patterning

The MADS-box gene *AGL16* targeted by miR824 was shown to be expressed in guard cells of stomata in Arabidopsis (Alvarez-Buylla *et al.*, 2000). Stomata are epidermal structures that are responsible for modulating the exchange of gases between the plant and the environment. The epidermis provides the major boundary between the plant and the external world.

#### 3.1. Evolution and function of epidermal structures

When higher plants started to colonize land, only their subterranean organs found an environment with relatively high water potential whereas the aerial organs did not. Plants adapted to the new environment by developing specialized cell types within the epidermis: at first rhizoids and later on root hairs for the acquisition of water and mineral nutrients as well as stomata within the aerial epidermis for the control of water loss and regulation of gas exchange. The fossil evidence shows that stomata first arose in moss 400 million years ago.

Functional considerations suggest that stomata evolution is linked to the development of the surrounding epidermal cells. Thus, stomatal complex refers to the stoma (i.e. the pore), the surrounding pair of guard cells with chloroplasts, plus its associated two to four contact cells (subsidiary cells) that lack chloroplasts (Carpenter, 2005). Other specialized cell types of the aerial epidermis are the trichomes or hairs which developed first in fern. The function of trichomes is less obvious. Mostly, their role is thought to be reflectance of light (Benz and Martin, 2006) and protection against herbivores (Gassmann and Hare, 2005). Some epiphytes (*Tillandsia*) have foliar trichomes that can absorb water from moist air (Benz and Martin, 2006). Hydropotes and ethereal oil cells are another type of specialized epidermal cells that are often considered to be a type of trichomes (Esau, 1965). Studies of angiosperm origins and early evolution have directed several phylogenetic analyses of multiple genes that arose from earliest lineage-splitting events within the extant angiosperm clade. An intriguing role of MYB-bHLH-WD40-type of transcription factors in the evolution of epidermal patterning has been addressed (Larkin *et al.*, 2003; Ramsay and Glover, 2005).

### 3.2. Anatomy of stomata

Stomatal architecture - the number, form, and arrangement of specialized epidermal cells associated with stomatal guard cells - are valuable taxonomic and systematic features of present-day and fossil plants (Metcalf and Chalk, 1950; Pant, 1965) that have been important in the development of hypotheses for early angiosperm evolution (Upchurch, 1984). Angiosperm stomatal complexes exhibit two fundamental mode of architecture. In monocots stomata appear in ordered arrays adjacent to cell files near vascular bundles whereas in eudicots stomata arise from multiple locations (Croxdale, 2000). Studies in maize suggest that an inhibitory signal derives from the veins of the leaf to control the ordered patterning of stomata in rows (Hernandez *et al.*, 1999). In eudicots a set number of epidermal cells surround the stoma leading to the morphological classification into 14 types (Metcalf and Chalk, 1950). In *Arabidopsis* and other members of Brassicaceae the stoma is surrounded by three epidermal cells, one of them is smaller than the other two. This arrangement is called anisocytic and accounts as a taxonomic feature of Brassicaceae (Pant and Kidway, 1967).

The epidermis of most leaves shows dorsoventral anatomy: the upper (adaxial) and lower (abaxial) surfaces have somewhat different construction and may serve different functions. The number of stomata (stomatal density) varies from about 10 to over 1000 per mm<sup>2</sup> of leaf surface. Stomata are more numerous over the abaxial epidermis of the leaf than the adaxial epidermis probably because heating of leaves is less on the abaxial surface and therefore

loss of water through transpiration can be reduced (Geisler and Sack, 1998).

### 3.2.1. Stomatal development

The stomatal lineage in *Arabidopsis* is initiated by a subset of protodermal cells called meristemoid mother cells (MMC). The MMC undergoes an asymmetric "entry" division that produces a small triangular cell called a meristemoid, and a larger sister cell called a stomatal-lineage ground cell (SLGC), which often becomes a cuticularized epidermal pavement cell. The meristemoid will undergo two more asymmetric divisions and differentiate into a round guard mother cell (GMC) that will subsequently divide symmetrically to produce a pair of guard cells, which work in concert to control the size of the pore. Meristemoids are self-renewing and can give rise to another meristemoid, called satellite meristemoid (SM), which will undergo the same division process. The asymmetric division ensures that the satellite meristemoid is always oriented away from the existing GMC or stoma and separated by one intervening cell. The mature guard cells are terminally differentiated and do not divide further (Pillitteri and Torii, 2007) (Figure 1.7 A).

The placement of stomata on the epidermal surface is regulated and appears to depend on the elaboration and perception of local as well as long-distance signals. The present understanding of the underlying mechanisms has come primarily from studies of *Arabidopsis* mutants impaired in the stomatal development or patterning (Figure 1.7 B, Table 1.1). A current model for stomatal development is shown in Figure 1.7 A. According to this model an extracellular, inhibitory signal helps regulate spacing of stomata. STOMATAL DENSITY AND DISTRIBUTION 1 (SDD1), a subtilisin-like serine protease, acts to process a yet unidentified ligand to generate this signal (Berger and Altmann, 2000). Another possible signal is the small protein EPIDERMAL PATTERNING FACTOR 1 (EPF1), which does not depend on SDD1 (Hara *et al.*, 2007). The signals are perceived by TOO MANY MOUTHS (TMM) which is a leucine-rich repeat receptor-like protein (LRR-RLP). TMM is localized in the plasma membrane (Yang and Sack, 1995) and is thought to interact with three LRR receptor-like kinases (RLK), ERECTA (ER) and ERECTA-LIKE (ERL) proteins (ER, ERL1, and ERL2) (Nadeau and Sack, 2002; Shpak *et al.*, 2005; Torii *et al.*, 1996). Only *er;erl1;erl2* triple mutants exhibited an excess of guard cells and spacing abnormalities, indicating that the ER-family members are functionally redundant (Shpak *et al.*, 2005). The identification of several mutants has implicated a mitogen activated protein kinase cascade in transduction of the receptor signal to the ultimate gene targets. Mutations in the MAP kinase kinase kinase (MAPKKK) gene, YODA (YDA), cause the formation of large stomatal clusters (Bergmann *et al.*, 2004). Two MAP kinase kinase genes and two MAP kinase genes, MKK4/MKK5 and



MPK3/MPK6, respectively, were shown to act downstream of YDA in this signaling pathway (Wang *et al.*, 2007). The proteins described above are all required for proper orientation of divisions, density of stomata, and control of entry and amplifying divisions but not for differentiating cell types within the stomatal lineage. Stomatal differentiation requires the successive action of three closely related bHLH proteins, SPEECHLESS (SPCH), MUTE, and FAMA. A mutation in any one of these gene results in aerial organs that lack stomata. They have a distinct role in key transitional states of the stomatal lineage: first, the transition from MMC to meristemoid is maintained by SPCH because the epidermis of *spch* mutants exhibited only jigsaw-puzzle-shaped pavement cells (MacAlister *et al.*, 2007; Pillitteri *et al.*, 2007). MUTE activity drives the second transition from meristemoid to GMC. Meristemoids in *mute* mutants undergo an excessive number of amplifying divisions but fail to form GMCs (Pillitteri *et al.*, 2007). FAMA acts at the third transition from GMC to guard cell. *fama-1* mutant produces abnormal “caterpillar-like” rows of GMCs (Bergmann *et al.*, 2004; Ohashi-Ito and Bergmann, 2006). The strong *fama-1* phenotype is similar to that described for a double mutant knockout of *FOUR LIPS (FLP)* (Yang and Sack, 1995) and MYB88 (R2R3 MYB-type transcription factors) (Lai *et al.*, 2005). MYB-like proteins can form complexes with bHLH to control cell-fate specification as seen in root epidermal patterning (Lee and Schiefelbein, 1999; Zimmermann *et al.*, 2004). However, no interaction was observed between FAMA and MYB88/ FLP (Ohashi-Ito and Bergmann, 2006).

### 3.3. Environmental factors affecting stomatal development

Stomatal density and function needed to adapt to global climatic changes environmental changes (Hetherington and Woodward, 2003). Stomatal densities are sensitive to atmospheric CO<sub>2</sub> concentrations. In eudicot leaves, stomatal density decreases as atmospheric CO<sub>2</sub> levels increase, but in conifers, the number of rows of cells that are determined to form stomata is decreased rather than stomatal density (Kouwenberg *et al.*, 2004). The *high in carbon dioxide (hic)* mutant of *Arabidopsis* increases stomatal density in response to elevated CO<sub>2</sub> (Gray *et al.*, 2000). *HIC* encodes a 3-keto acyl CoA synthetase that is involved in synthesizing the long chain fatty acids of epicuticular waxes. It has been suggested that HIC affects the permeability of the guard cell walls to a mobile signal, influencing stomatal density, or that the signal itself might be a product or a by-product of wax biosynthesis (Holroyd *et al.*, 2002). The mobile signal that affects stomatal density could be a plant hormone. Decreased stomatal conductance caused in response to increases in atmospheric CO<sub>2</sub> levels or to decreased light, might affect transpirational water flow significantly. Changes in the rate of transpiration might in turn affect the flux of hormones (abscisic acid [ABA] and cytokinins

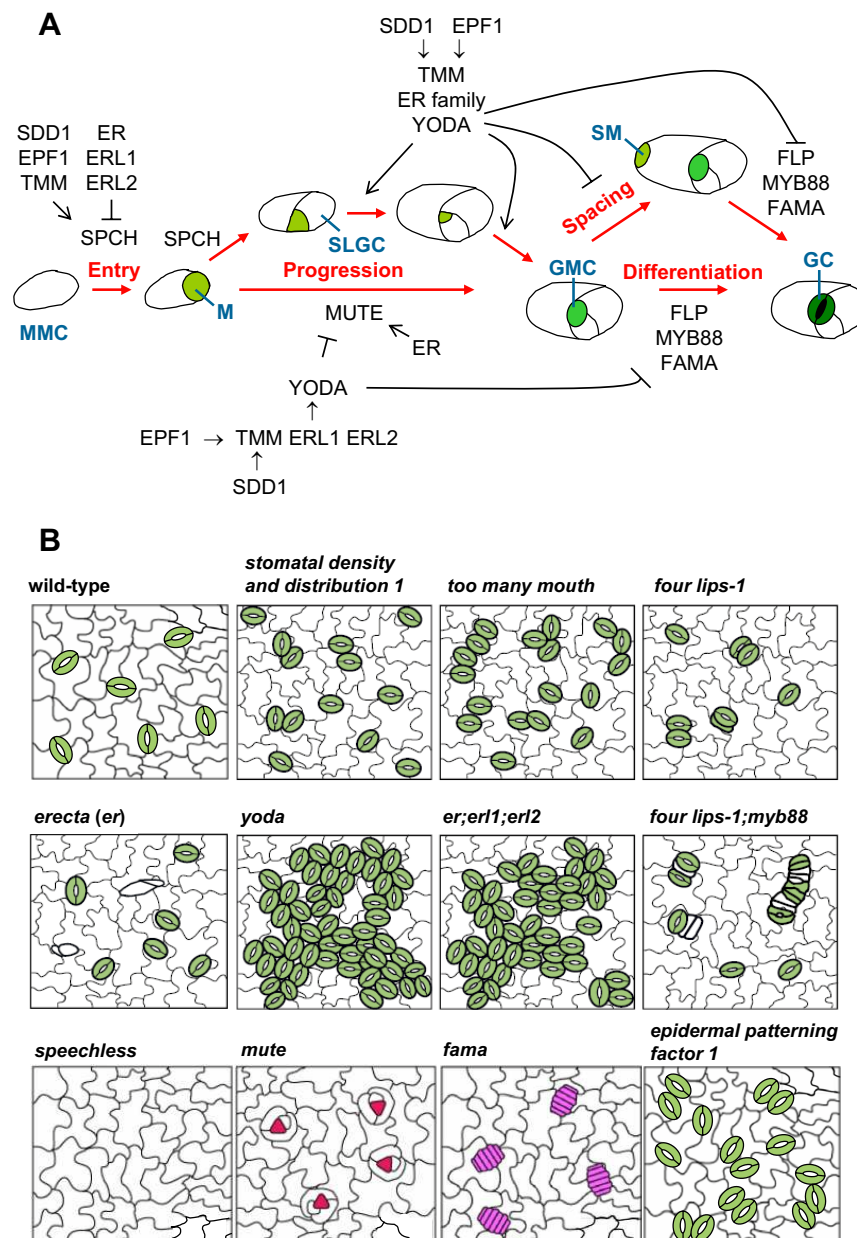


**Figure 1.7: Lineage-based mechanism for the patterning and determination of stomata in Arabidopsis.**

A. Stages of divisions (red) during stomatal development and their genetic control (black). A protodermal cell (not shown) is converted into a meristemoid mother cell (MMC) through an unknown process. The MMC undergoes an asymmetric entry division to create a meristemoid (M). Meristemoids go through additional rounds of asymmetric divisions before differentiation into a guard mother cell (GMC). GMCs divide symmetrically to produce two guard cells (GCs), which form mature stomata. The stomatal lineage ground cell (SLGCs) or subsidiary cells, produced from amplifying divisions, can initiate an entry division to form a satellite meristem (SM) that is placed away from an existing precursor cell or stoma. Negative regulation is indicated by T-shaped lines, positive regulation by an arrow. Abbreviation of proteins altered in mutants indicated under Figure 1.7 B.

B. Drawing of terminal leaf phenotypes in stomatal mutants indicating the typical number and arrangement of stomata (green) or terminal cell type (red for M, pink for GMC). White cells in *erecta* and *flp;myb88* panels represent cells of indeterminate identity.

**Table 1.1.: Genes involved in Arabidopsis stomatal development in rosette leaves.**

Gene name	Symbol	Molecular homology	Mutant Phenotype	Overexpression/Constitutively Active Phenotype
<b>Patterning genes</b>				
<i>STOMATAL DENSITY AND DISTRIBUTION 1</i>	<i>SDD1</i>	Subtilisin-like protease	Increased SI, small clusters	Represses stomatal divisions Arrested meristemoids and GMCs
<i>EPIDERMAL PATTERNING FACTOR 1</i>	<i>EPF1</i>	secretory signal peptide	Increased SD, small clusters	Represses stomatal divisions
<i>TOO MANY MOUTHS</i>	<i>TMM</i>	Leucine-rich repeat receptor-like protein	Increased SD, clusters	ND
<i>ERECTA-</i> and <i>ERECTA-LIKE</i> family	<i>ER.ERL1, ERL2</i>	Leucine-rich repeat receptor-like kinase	Greatly increased SD, large clusters	<i>erecta</i> - no phenotype <i>erl1</i> and <i>erl2</i> -ND
<i>YODA</i>	<i>YDA</i>	Mitogen-activated protein kinase kinase kinase	Greatly increased SD, large clusters	No stomata, pavement cell only
<i>MAPKK4/MAPKK5</i>	<i>MKK4/MKK5</i>	Mitogen-activated protein kinase kinase	Entire epidermis converted to stomata	No stomata, pavement cell only
<i>MAPK3/MAPK6</i>	<i>MPK3/MPK6</i>	Mitogen-activated protein kinase	Entire epidermis converted to stomata	No stomata, pavement cell only
<b>Differentiation genes</b>				
<i>SPEECHLESS</i>	<i>SPCH</i>	bHLH protein	No initiation of asymmetric cell division in the epidermis - no stomata	Excessive epidermal divisions, no extra stomata
<i>MUTE</i>	<i>MUTE</i>	bHLH protein	Initiation and reiteration of asymmetric cell division in the epidermis - no stomata	Entire epidermis converted to stomata
<i>FAMA</i>	<i>FAMA</i>	bHLH protein	Reiterative divisions of the GMC - no stomata	Entire epidermis converted to single guard cells
<i>FOUR LIPS</i>	<i>FLP</i>	R2R3 MYB protein	Reiterative divisions of the GMC, small clusters	ND
<i>MYB88</i>	<i>MYB88</i>	R2R3 MYB protein	None, enhances flp phenotype	ND

[CK]) to the leaves from the roots. Application of either ABA or CK can increase stomatal densities in a variety of plant species (Bradford *et al.*, 1983; Franks and Farquhar, 2001). Serna and Fenoll (1997) showed that growing Arabidopsis plants in enclosed environments (i.e. at high humidity) could significantly affect the lineage-based patterning mechanism and give rise to clustered stomata that phenocopies the *tmm* and *flp* mutant phenotypes. Stomatal densities or stomatal index (the proportion of epidermal cells that are stomata) are influenced by several other environmental conditions, including light intensity (Lake *et al.*, 2002), light quality (Liu-Gitz *et al.*, 2000), UV-B radiation (Dai *et al.*, 1995), drought (Franks and Farquhar, 2001), and ozone (Pääkkönen *et al.*, 1997).

## 4. Aim of the dissertation

The initial motivation for my thesis project was the cloning of numerous naturally occurring smRNAs by our laboratory. Our group, like many other groups, was interested in how these smRNAs are generated and function. *In silico* analyses had shown that Arabidopsis genome encodes 184 miRNAs targeting for degradation genes with various functions. So far only eleven Arabidopsis miRNAs were characterized regulating mostly transcription factors with an established function in cell patterning and specification. My objective was to fully elucidate a plant miRNA pathway from its biogenesis to repression of target-gene expression and biological function. I focused on one miRNA identified in our screen, now called miR824, that is encoded at a single locus and appeared to target a single gene, *AGAMOUS-LIKE 16* (*AGL16*) belonging to the MADS-box family of transcription factors. Using informative mutants and a transgenic-plant approach I established the molecular requirements for miR824 biogenesis and confirmed *AGL16* mRNA as the single target for miR824-guided degradation. Combined with bioinformatic studies I showed that miR824 is a member of the class of non-conserved miRNAs that is conserved in *Brassica* species and Arabidopsis, but not in more distantly related monocots and eudicots. The reported expression of *AGL16* in mature guard cells focused my attention on the possible function of *AGL16* in stomatal development. This study shows that miR824 negatively regulates *AGL16* in stomatal complexes to control the pattern and number of stomata on the leaf surface. The stomatal developmental pathway has not been shown to be regulated neither by miRNAs nor by MADS-box proteins. This mechanism of regulation is conserved in *Brassica* species and, therefore, provides some of the first evidence for important roles of non-conserved miRNAs in determining species-specific taxonomic features.

## Part II

# Materials and Methods

## 2. Materials and Methods

### 1. Materials

#### 1.1. Chemicals and enzymes

Unless otherwise indicated, all molecular biology grade chemicals and organic solvents were purchased from Merck (Darmstadt, Germany), Fluka (Buchs, Switzerland), Sigma (St. Louis MO, USA) or BioRAD (Richmond CA, USA). Restriction endonucleases and DNA modifying enzymes were purchased from New England Biolabs NEB (Beverly MA, USA), Fermentas (St. Leon-Rot, Germany), Invitrogen (Carlsbad CA, USA), Promega (Madison WI, USA), and Roche (Basel, Switzerland). RNA modifying enzymes were purchased from Ambion (Austin, TX, USA), Epicentre (Madison WI, USA) and Roche. Taq DNA Polymerases were purchased from Eppendorf (Schönenbuch, Switzerland), and Invitrogen. The proofreading DNA Polymerases used in this study were included in the kit “Expand High Fidelity” and “Expand Long template” PCR systems (Roche). Other proofreading enzymes were the Pfu and Pfu Turbo<sup>®</sup> purchased respectively from Promega, and from Stratagene (La Jolla, CA, USA) respectively. Kits for DNA and RNA extraction were purchased from Qiagen (Basel, Switzerland), GE Healthcare Biosciences (Piscataway NJ, USA) and Promega (Madison WI, USA). DNA and RNA Oligonucleotides were synthesized by Microsynth (Balgach, Switzerland).

#### 1.2. Plasmids

The TOPO-TA cloning kit (Invitrogen), which allows direct ligation of amplified fragments with single 3'-A overhangs, was used for cloning PCR products. pBluescript SK(+) (Stratagene) or pLitmus 28 (NEB) were used for subcloning of DNA fragments. The binary vectors pBI121 (Clontech) and pCambia 1300 (CAMBIA, Canberra, Australia) were used to make constructs designed to overexpress genes in plants. The concentrations of antibiotics used for each plasmid are given in Table 2.1.

**Table 2.1.: Concentrations of antibiotics used for standard plasmids.**

Plasmid	Origin	Antibiotic concentration( $\mu\text{g/ml}$ )
pBluescript SK(+)	Stratagene	Ampicillin <sup>100</sup>
pLitmus 28	NEB	Ampicillin <sup>100</sup>
pBI121	Clontech	Kanamycin <sup>50</sup>
pCAMBIA 1300	CAMBA, Australia	Kanamycin <sup>50</sup>

### 1.3. Bacterial strains

*Escherichia coli* strain DH5 $\alpha$ MCR (Stratagene) was used for the propagation of all plasmids. Bacteria were grown overnight at 37°C with shaking at 225 rpm in Luria-Bertani (LB) medium or grown on solid LB medium plates containing 1% (w/v) agar (Difco-Bacto) at 37°C. Depending on the plasmid, 50 g/ml kanamycin or 50 g/ml ampicillin were added to the LB medium. *Agrobacterium* strain GV3101 pPM6000 (Bonnard *et al.*, 1989) used for plant transformation was provided by Barbara Hohn's laboratory.

### 1.4. Plant materials and condition of culture

*Arabidopsis thaliana* plants were grown from seeds on standard soil (GS90) under 20°C day/16°C night; 50% relative humidity day/night; 16 h photoperiod at 250  $\mu\text{mol/m}^2/\text{s}$ . *Brassica* and rice seeds were obtained from Syngenta. *Brassica rapa* ssp. *pekinensis*, *Brassica napus* ssp. *oleifera*, and *Brassica oleracea* var. *alboglabra* plants grown axenically in liquid  $\frac{1}{2}$  MS medium were raised at 21°C (16h 100  $\mu\text{E/m}^2 \text{ s}^{-1}$  light/ 8h dark). *Oryza sativa* var. *japonica* and *Nicotiana benthamiana* and *Nicotiana tabacum* plants grown in GS90 soil were raised at 26°C (16h 300  $\mu\text{E/m}^2/\text{s}$  light/ 8h dark). Seeds of the T-DNA insertion mutants were obtained from the SAIL or the SALK collections.

## 2. Methods

### 2.1. Cloning and construction of the plasmids

Standard PCR protocols were used to amplify genes of interest using proofreading DNA polymerases. Oligonucleotide primers used are described in Appendix Table A.2. Unless otherwise indicated, the primers used for PCR amplification do not contain restriction sites and the amplified PCR products were directly cloned in TOPOII vector using TOPO-TA cloning kit (Invitrogen) according to the manufacturer's protocol. The genes were sequenced

and used for subcloning in the appropriate expression vector described in Appendix C. The ligation of insert and vectors was the same for all plasmids and was performed using the Rapid DNA ligation kit (Roche). For blunt-end ligations the recipient vector was previously dephosphorylated using the Antarctic phosphatase from NEB. Bacteria were transformed with 2  $\mu$ l of the ligation and incubated on Luria Broth (LB) plates containing the appropriate antibiotic. The positive bacterial colonies identified by PCR were put in liquid LB culture and plasmid miniprep was performed using the alkaline method as described in Sambrook and Russell (2001). The right orientation of inserts and open reading frames were checked by sequencing. T-DNA binary plasmids further used for plant transformation were introduced in *Agrobacterium tumefaciens* GV3101 by electroporation using Gene Pulser II (BioRAD). After incubation on 2xYT plates containing 100  $\mu$ g/ml Rifampicin and 50  $\mu$ g/ml Kanamycin, the positive *Agrobacterium* colonies were identified by PCR.

## 2.2. Transformation and agroinfiltration

*A. tumefaciens* strain GV3101 containing T-DNA binary vectors were cultivated in 2xYT medium containing Rifampicin (100  $\mu$ g/ml) and Kanamycin (50  $\mu$ g/ml) overnight or until an  $OD_{600} = 1.0$ . *Agrobacterium* were collected by centrifugation and resuspended in transformation solution which consists of  $\frac{1}{2}$  MS medium supplemented with 5% sucrose and 0.005% Silwet L-77 (Helena Chemical, Fresno, USA). Plant transformation was carried out using the floral dip method of Clough *et al.* (1998). Transformed *Arabidopsis* seeds were surface sterilized for 3 min with 70% (v/v) ethanol, 10 min with bleach solution (3% (w/v) NaOCl, 0.05% (w/v) Tween 20, and washed four times with sterile deionized water. A total of 100 sterilized seeds from the second generation after *Agrobacterium* transformation were sown on  $\frac{1}{2}$  MS medium containing  $\frac{1}{2}$  MS salts (Duchefa), 0.5% (w/v) sucrose, 0.7% (w/v) agar, pH 5.7, containing 25  $\mu$ g/ml Hygromycin and 50  $\mu$ g/ml Claforan/Timentin. After two weeks the number of non-germinating seeds, rapidly growing Hygromycin-resistant seedlings, and arrested Hygromycin-sensitive seedlings were scored.

For agroinfiltration, *A. tumefaciens* was resuspended to an  $OD_{600} = 1.0$  in infiltration medium which contains 5% (w/v) saccharose, 0.22% MS salt (Duchefa), 0.005% 2-(N-morpholino) ethanesulfonic (MES) acid buffer (Duchefa), 500  $\mu$ l Silwet L-77, and the pH adjusted to 5.75 with KOH. The *Agrobacterium* suspension was infiltrated into leaves of four week-old plants using a 2 ml syringe.



### 2.3. Characterization of T-DNA insertion

The T3 generations obtained from these lines were genotyped by using LBb1 or LB1 left border primers respectively for SALK and SAIL T-DNA lines and a primer specific for the gene of interest. Oligonucleotide primers used are described in Appendix Table A.2. The T-DNA insertion was mapped by using thermal asymmetric interlaced PCR (TAIL-PCR) as described by Liu *et al.* (1995).

### 2.4. Isolation of plant nucleic acids

#### 2.4.1. Isolation of DNA

Plant material was pulverized to fine powder in liquid nitrogen and 1g was used to isolate genomic DNA using Nucleon plant DNA extraction kit (GE Healthcare) following manufacturer's protocol.

#### 2.4.2. Isolation of RNA

All RNA isolations were carried out in an RNase-free environment and using DEPC treated water (0.1% DEPC). One gram of plant material frozen in liquid nitrogen, ground to fine powder was resuspended in 10 ml Trizol<sup>®</sup> (Invitrogen) and total RNA was extracted following the manufacturer's protocol. Isolated total RNA was separated into high- and low-molecular weight fractions using the RNeasy Midi Kit protocol (Qiagen) as modified by DiSerio *et al.* (2001). The high molecular weight were recovered by elution from the column and the small RNAs were precipitated with one volume of isopropanol and washed with DEPC treated 75% ethanol.

### 2.5. Southern analysis

DNA was digested overnight with appropriate restriction endonucleases (5U/ $\mu$ g DNA). Genomic DNA was separated on a 0.7% agarose gel and prepared for the DNA transfer as described in Sambrook and Russell (2001). Subsequently, the DNA was transferred to a Hybond<sup>™</sup>-N+ nylon transfer membrane (GE Healthcare). Membranes were incubated in a self made hybridization buffer (0.25M Na-phosphate buffer  $\text{Na}_2\text{HPO}_4/\text{NaH}_2\text{PO}_4$ , 1mM EDTA, 6.6% (w/v) SDS, 10 g/l BSA). DNA probes were radiolabeled with [ $\alpha$ -<sup>32</sup>P]-dCTPs using Random Labeling kit (Invitrogen). Denatured probes were applied to the hybridization buffer and incubated at 60°C overnight. Washes were carried out at 60°C using a 2x SSC, 0.1% (w/v) SDS solution after initial brief rinsing in 0.5x SSC, 0.1% (w/v) SDS.

## 2.6. RNA blot hybridization

For analysis of high molecular weight RNA, total RNA was mixed with 2x RNA loading buffer (17% formaldehyde, 50% formamide, 1x MOPS, 5% glycerol, 0.05% bromophenol blue, 0.05% xylene cyanol, and 10  $\mu\text{g/ml}$  ethidium bromide) and denatured on a 1.2% agarose/formaldehyde gel. The RNA was transferred to a Hybond<sup>TM</sup>-N+ nylon transfer membrane (GE Healthcare). Probes were radiolabeled with [ $\alpha^{32}\text{P}$ ]-dCTPs using the Random Labeling kit (Invitrogen). Hybridization using PerfectHyb<sup>TM</sup>Plus buffer (Sigma) and washes were carried out according to the manufacturer's protocol. Exposure to Phospho-Imager screens and Biomax MS/MR radiofilms (Kodak) were carried out for different times. The same hybridization buffer and protocol was used for mRNA blot using poly(A+)-RNA.

smRNAs were dried using a SpeedVac and resuspended in 15  $\mu\text{l}$  5x loading buffer (95% formamide, 20 mM EDTA, 0.05% (w/v) bromophenol blue and 0.05% (w/v) xylene cyanol) and separated on a 15% polyacrylamide gel (19:1) (8M urea, 0.1% APS, and 0.1% TEMED in 1xTBE). Blotting was performed on a Hybond<sup>TM</sup>-N+ nylon membrane (GE Healthcare). Hybridization and labeling of oligo probes were carried out according to Akbergenov *et al.* (2006) except that PerfectHyb<sup>TM</sup>Plus buffer was used.

## 2.7. RNA ligation mediated rapid amplification of cDNA ends (RLM-RACE)

Total RNA was directly ligated to the provided RNA adapter in the RLM-RACE kit (Ambion) without applying the mRNA decapping protocol. SuperScript<sup>TM</sup>III RT (Invitrogen) was used for reverse transcription using primers specific for the 3' gene UTRs. A first PCR was carried out using the 5' RLM-RACE outer primer on the RNA adapter and a gene specific primer designated upstream of the 3'UTR. A nested PCR was then performed using the 5' RLM-RACE inner primer on the RNA adapter and a second inner gene specific primer. PCR products were gel-purified, cloned into the TOPO-II vector, and at least 10 independent clones sequenced.

## 2.8. RT-PCR and quantitative RT-PCR (RT-qPCR)

Total RNA (5  $\mu\text{g}$ ) was treated with DNase I (Promega) for 15 minutes. Poly-A RNA was reverse transcribed using oligo-dT or gene-specific primers and SuperScript<sup>TM</sup>III RT (Invitrogen). Second strand synthesis for RT-qPCR was carried out in the presence of the SYBR green fluorescent dye for quantitative analysis. Oligonucleotides for RT-qPCR were designed to amplify 80 to 200 nucleotides in the cDNA of interest, if possible spanning an exon-intron boundary. qPCR reactions were performed in an optical 96-well plate with an ABI PRISM

7000 Sequence Detection System (Applied Biosystems). Triplet reactions for each sample contained 12.5  $\mu$ l SYBR Green Master Mix reagent (Applied Biosystems), 10  $\mu$ l of cDNA (0.25  $\mu$ g/ $\mu$ l), and 2.5  $\mu$ l of each gene-specific primer (2.5  $\mu$ M) in a final volume of 25  $\mu$ l. The standard thermal profile used for all PCR reactions was 50°C for 2 min, 95°C for 10 min, 50 cycles of 95°C for 15 s, and 60°C for 40 s. Data were analyzed using the SDS 1.1 software (Applied Biosystems). Levels of amplified mRNAs were normalized to the *TIP41*-like gene (Czechowski *et al.*, 2005) using the comparative  $C_T$  method (Ramakers *et al.*, 2003). For semi-quantitative RT-PCR, regular PCR protocols were used. *TIP41*, *ACTIN*, *eIF4 $\alpha$* , or *TUBULIN* was amplified as references to detect differences in loading.

### 2.9. Microarray analysis

RNA purification, cRNA preparation, and hybridization to microarrays were performed by the FMI Microarray Service. The Affymetrix ATH1 chip used contains probe sets representing approximately 24,000 genes ([www.affymetrix.com](http://www.affymetrix.com)). Expression data was analyzed using Expressionist software 4.5 (GeneData, Basel).

### 2.10. In situ hybridization (ISH)

For *in situ* hybridization of *AGL16* mRNA, whole mounts leaves were hybridized with DIG-labeled probes as described by Friml *et al.* (2003). The probes used were sense and antisense RNAs complementary to the *AGL16* transcript (At3g57230). For miR824 and miR824\*, the hybridization procedure with DIG-labeled miRCURY<sup>®</sup> LNA probes (Exiqon Vedbaek, Denmark) was used (Bhattacharyya *et al.*, 2006). Hybridization signals were detected by using nitroblue tetrazolium/5-bromo-4-chloro-3-indolyl phosphate (NBT/BCIP) staining procedure (Roche).

### 2.11. Physiological experiments

Surface-sterilized *Arabidopsis* seeds were grown axenically. One month after germination liquid MS medium was supplemented with NaCl, abscisic acid (Sigma) or 24-epibrassinolide (Sigma) at the concentration indicated. The stock solutions used were 5M, 1M, and 0.1M respectively.

### 2.12. Staining for $\beta$ -glucuronidase (GUS) activity

Plant transformed or infiltrated with GUS expression vectors (Appendix Figure A.5-A.8, A.12, A.13) were assayed by GUS staining according to Jefferson *et al.* (1987). Samples were

stored at 4°C in 90% (v/v) ethanol for imaging.

### 2.13. Analysis of luciferase (LUC) activity

LUC expression vectors (Appendix Figure A.2-A.4, Kutter *et al.*, 2007) were delivered biolistically into leaves of three-week old Col-0 plants as described by Klahre *et al.* (2004). Images were collected using a N<sub>2</sub>-cooled CCD camera (Gloor Instruments) and *in vivo* LUC activity was measured 48 hours post-bombardment as described by Fritsch *et al.* (2004).

### 2.14. Electro mobility shift assays (EMSA)

Standard Electro mobility shift assays (EMSA) was performed according to Sambrook and Russell, 2001. Radiolabeled double-stranded deoxyoligonucleotides were labeled with [ $\gamma$ <sup>32</sup>P]-ATP using polynucleotide kinase (Roche). Oligonucleotides primers used are described in Appendix Table A.2.

### 2.15. Imaging experiments

GFP expression in plants transformed with pPro<sub>MIR824</sub>:GFP (Appendix Figure A.9) was imaged by confocal laser scanning microscopy (Leica TCS SP2, Leica Microsystem, Wetzlar, Germany) with excitation at 488 nm. Green fluorescence was detected between 490 nm and 510 nm. Digital images were recorded using the Leica confocal operating system software. For Scanning Electron Microscopy (SEM) samples were prepared using a Balzers SCU 020 cryopreparation unit. Images were collected with a JEOL JSM 6300 scanning electron microscope at 15 kV. Comparable regions of epidermis were recorded for each type of plant in the same experiment.

### 2.16. Dental resin imprinting technique

Stomatal development was monitored using the dental resin impression method described by Berger *et al.* (2000) and Geisler *et al.* (2000). For the time course of stomatal development Coltène® President Light body dental resin (Coltene/Whaledent AG Altstätten, Switzerland) was gently applied daily to the abaxial side of the first emerging leaf of a 6-10 day old seedling grown axenically on  $\frac{1}{2}$  MS agar. After hardening of the resin transparent nail polish was applied to the imprints. Images of nail-polish copies were collected using a Kappa CF 8/5 camera and Zeiss Axioplan 2 microscope. The time course of stomatal development was determined from tracings made of images of the same stomatal complexes. Stomatal

density, stomatal index and the proportion of primary and higher-order stomatal complexes were quantified from images of nail polish copies of dental resin imprints of the surfaces of the fifth rosette leaf. Comparable regions of epidermis were scored for each type of plant in the same experiment.

Part III

Results

### 3. Establishing a Collection of RNA Silencing Mutants

Contributions to this chapter:

I carried out all experiments and their analysis described in this chapter, if not mentioned otherwise.

## 1. Elucidation of RNA silencing pathways using deficiency mutants

The majority of proteins involved in RNA silencing pathways, e.g. DCL1, HYL1, and HEN1, were identified in genetic screens aimed to identify mutants impaired in certain aspects of plant growth, development, and reproduction. Their discovery in those screens indicated the importance of RNA silencing in a broad range of regulatory functions (Figure 3.1). Biochemical studies are rarely done in plants and RNA silencing pathways have been elucidated primarily by accessing the effect of deficiency mutants on the expression of smRNA and their putative targets. None of the known silencing mutants were available in the laboratory in the beginning of my thesis. Therefore, my first objective was to establish a collection of deficiency mutants as a tool for detailed studies.

## 2. Partial Characterization of T-DNA Insertion mutants

In a reverse genetic approach several lines with single T-DNA insertions in genes known to affect RNA silencing were obtained from the Nottingham Arabidopsis Biological Stock Centre (NASC) or from the SAIL collection (Syngenta). Segregating T3-generation T-DNA lines with a *NPTII* kanamycin resistance gene (SALK) or BASTA resistance cassette (SAIL) were characterized (Appendix Table D). Characterization of the T-DNA insertion involved determination of the genotype (homozygosity), the copy number in the genome, and mapping of the insertion site. Additionally, transcript expression of the gene altered by the T-DNA insertion site was measured.

Some of the mutants analyzed exhibited different molecular phenotypes indicating that the alleles differ in expression. When published mutants became available, they were included in the study as controls. For example the *dcl1-x* mutant (allele undetermined, Appendix Table D) with a T-DNA insertion in the 3' UTR exhibited normal growth and miRNA formation and was not impaired in smRNA production (data not shown). *dcl1* mutants with point mutations in the RNA helicase domain (*dcl1-7* and *dcl1-8*) or truncation of the second dsRNA binding domain (*dcl1-9*) have developmental defects including sterility, late flowering, and show reduced miRNA accumulation (Park *et al.*, 2002; Reinhart *et al.*, 2002; Schauer *et al.*, 2002). Initially only heterozygous mutants could be identified for *dcl4-2* and *rdr6-15* although alterations in smRNA accumulation were found. TAIL-PCR (Liu *et al.*, 1995) revealed that the T-DNA insertion was located differently than indicated before. After several generation of self-fertilization a drug resistance phenotype

Characterized RNA silencing deficient mutants were used routinely for the study of miRNA biogenesis and function during my thesis and by members of the Meins laboratory. Some of



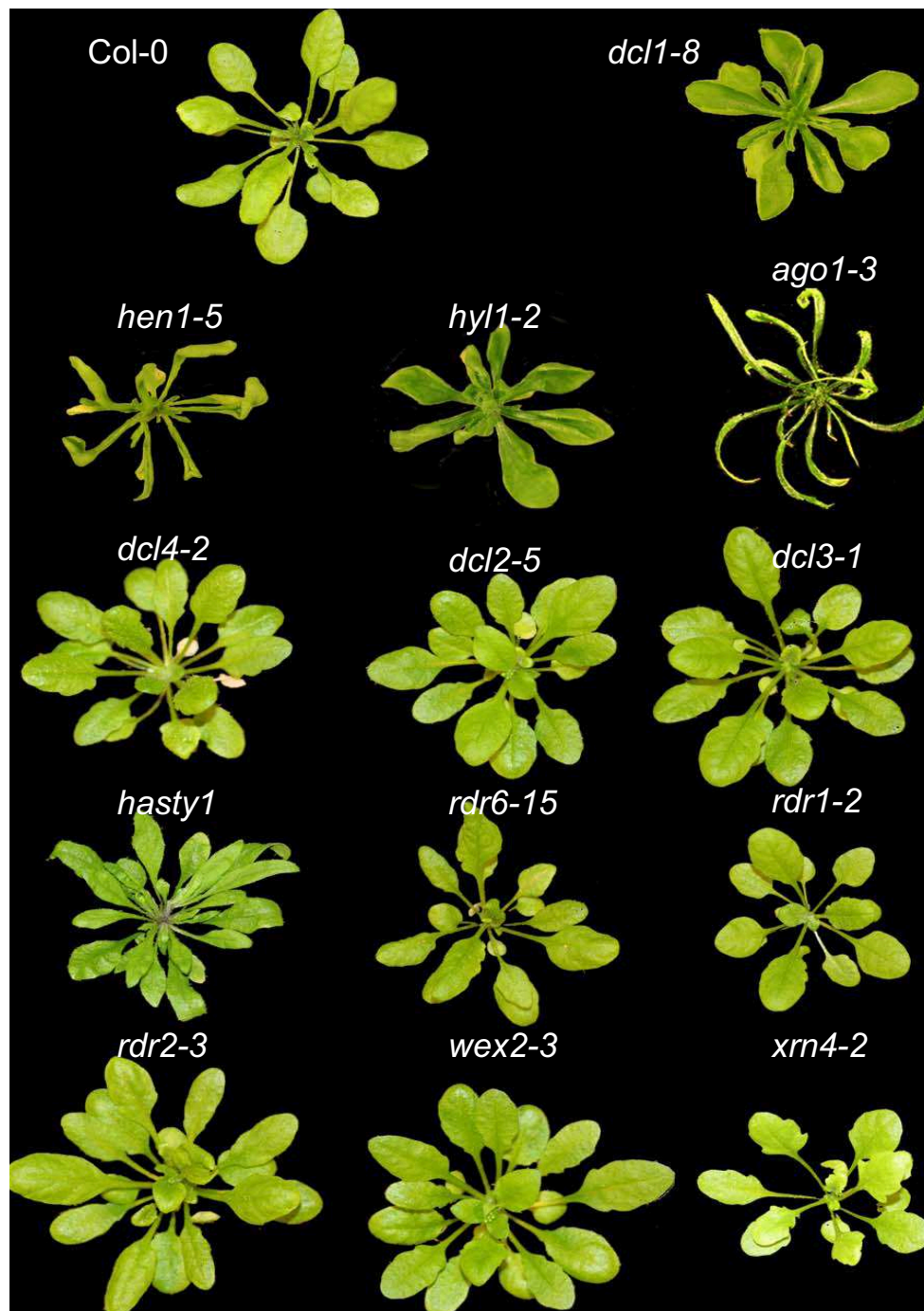


**Figure 3.1: Phenotypes of Arabidopsis mutants impaired in smRNA biogenesis.**

The wild-type is shown on the left. RNA silencing mutants are shown below. *ago1* (*argonate 1*), *hen1* (*hua enhancer 1*), *hyl1* (*hyponastic leaves 1*), and *hst* (*hasty*) mutants all have pleiotropic developmental defects that overlap with those of hypomorphic *dcl1* (*dicer-like 1*) plants. Although many or all of these developmental defects may result from impaired miRNA activity, they may also reflect disruption of other pathways in which these genes act, such as in the generation and function of siRNAs. However, mutations in genes required for the accumulation of various siRNAs, such as *RDR6* (*RNA-DEPENDENT RNA POLYMERASE 6*), *DCL2*, *DCL3*, and *DCL4*, result in few, if any, developmental abnormalities. *wex*, *werner syndrome-like exonuclease*; *xrn4*, *exoribonuclease 4*

these mutants were also used to gain insights in the regulation of other smRNA pathways in collaboration with other research groups (Akbergenov *et al.*, 2006; Blevins *et al.*, 2006).

## 4. Identification and characterization of the *miR824/AGL16* regulatory pathway

Contributions to this chapter:

I carried out all experiments and their analysis described in this chapter often under the supervision of Azeddine Si-Ammour. Hanspeter Schöb cloned smRNAs. Azeddine Si-Ammour constructed plasmids for plant transformation and made the cleavage assay for *AGL16*.

## 1. Characterization of the miR824 locus

### 1.1. Identification of miR824 and its precursor

miR824 was originally cloned in the Meins laboratory by Hanspeter Schöb in 2001 using a smRNA cloning protocol designed to obtain 18 nt to 30 nt RNAs with 5'-phosphate and 3'-hydroxyl groups (Elbashir *et al.*, 2001). An *in silico* analysis performed in the beginning of my thesis identified miR824 as a potential miRNA. In addition to miR824, sixteen miRNAs and two known ta-siRNAs were identified from a total of ca. 350 unique small RNA clones obtained from pooled tissues of Arabidopsis plants at different developmental stages. Blast searches against the Arabidopsis database ([www.arabidopsis.org](http://www.arabidopsis.org)) revealed a unique genomic location of miR824 on chromosome IV (NC\_003075.3, position 12625136 to 12625157). RNA blot hybridization confirmed that miR824 is a 21 nt long RNA and ubiquitously expressed in stems, leaves, cauline leaves, inflorescences, and roots (Kutter *et al.*, 2007). It was recently shown that miR824 accumulation in Arabidopsis depends on HYPONASTIC LEAVES 1 (HYL1), HUA ENHANCER 1 (HEN1), DICER-LIKE 1 (DCL1), (DCL1) (Rajagopalan *et al.*, 2006, Kutter *et al.*, 2007), and ARGONAUTE 1 (AGO1) but not on DCL2, DCL3, DCL4, AGO3, AGO5, AGO7, AGO10, RNA DEPENDENT RNA POLYMERASE 1 (RDR1), RDR2, RDR6, SILENCING DEFECTIVE (SDE3), WERNER SYNDROME-LIKE EXONUCLEASE (WEX-2), or EXORIBONUCLEASE 4 (XRN4) (Figure 4.1 A-C). As shown for other miRNAs, a passenger miR824\* sequence bearing 2 nt 3' overhang to the complementary miR824 was identified computationally and by deep pyrophosphate sequencing (Fahlgren *et al.*, 2007; Rajagopalan *et al.*, 2007). miR824\* was detectable at low abundance with a ratio of 4 to 5 molecules of miR824 to 1 molecule of miR824\* as quantified by RNA blot hybridization. miR824\* accumulation depends on *hyl1-2*, *hen1-5*, *dcl1-8*, and *ago1-3* but not on *dcl2-5*, *dcl3-1*, *dcl4-2*, or *rdr6-15* (Figure 4.1 A). Identification of miR824\* indicates exact processing of the miRNA from the hairpin precursor by DCL1-like activity as described by a previous study (Talmor-Neiman *et al.*, 2006a). Other potential smRNA molecules obtained by deep sequencing most likely do not act as miR824\* sequences because of low complementarity towards miR824 and their orientation (Table 4.1, Figure 4.2). The minimum free energy structure for the miR824 locus was analyzed algorithm with a folding temperature set to 20°C (Zucker, 2003). This algorithm evaluates paired regions of an RNA secondary structure and predicts stem loop hairpin structure, a characteristic feature of precursor (pre)-miRNAs. miR824 is present in the 5' arm of the stable predicted 689 nt stem-loop hairpin structure and miR824\* is located on the opposite 3' arm of the foldback structure (Figure 4.3). The precise ends of the 5' and 3' arm could not be mapped by using a method based on

**Table 4.1.: smRNA sequences of miR824 precursor.**

name	sequence	length in nt	orientation	reference
AGO4_01585	UAGACCAUUUGUGAGAAGGGAG	22	plus/plus	Qi <i>et al.</i> , 2006
Ath_wt_11860	UAGACCAUUUGUGAGAAGGGA	21	plus/plus	Qi <i>et al.</i> , 2006
AGO1_1555	UAGACCAUUUGUGAGAAGGGA	21	plus/plus	Qi <i>et al.</i> , 2006
AGO4_13392	UAGACCAUUUGUGAGAAGGGA	21	plus/plus	Qi <i>et al.</i> , 2006
Ath_wt_04764	AGACCAUUUGUGAGAAGGGA	20	plus/plus	Qi <i>et al.</i> , 2006
AGO1_0931	GACCAUUUGUGAGAAGGGA	19	plus/plus	Qi <i>et al.</i> , 2006
BarFl4288	UAGACCAUUUGUGAGAAGAGA	21	plus/plus	Axtell <i>et al.</i> , 2006
BarRL6665	CAAGGAUUUUUAAAAAGGGUUAGC	24	plus/minus	Axtell <i>et al.</i> , 2006
AGO4_03753	CGAAACAAUAAACUAACGAAUCUC	24	plus/minus	Qi <i>et al.</i> , 2006
BarFL4394	UGAAGAGAUUAUUCUCUUGUGGU	24	plus/plus	Axtell <i>et al.</i> , 2006
AGO4_07237	AUAUUAUCUCUUGUGGUUGAUGUA	24	plus/plus	Qi <i>et al.</i> , 2006
BarSee277	AGAAGGGUUUUUAAAAGUUUAGUA	24	plus/minus	Axtell <i>et al.</i> , 2006
BarSil3147	CAAAAUCAUAUAAAACACUUAGAA	24	plus/plus	Axtell <i>et al.</i> , 2006
BarSil1431	UCUAAGUGUUUUUAUGAUUUUG	24	plus/minus	Axtell <i>et al.</i> , 2006
AGO4_00058	UCAAAAUCAUAUCAUCACCAAC	24	plus/plus	Qi <i>et al.</i> , 2006
Ath_wt_17349	CCUUCUCAUCGAUGGUCUAGA	21	plus/plus	Qi <i>et al.</i> , 2006
AGO1_4080	CCUUCUCAUCGAUGGUCUAGA	21	plus/plus	Qi <i>et al.</i> , 2006

circularization of RNA molecules through self-ligation as used in other studies (e.g., miR163 [Kurihara and Watanabe, 2004] or human let-7 [Basyuk *et al.*, 2003]). Sequence analysis of the 60 to 70 bp cloned molecules aligned either to the intronic region upstream of the predicted miR824 precursor or aligned to the region between miR824 and miR824\*. These fragments represent most likely degradation products obtained from precursor processing.

Taken together these data confirm that miR824 is a bona fide miRNA produced exclusively by the known miRNA pathway and that pre-miR824 is a long precursor, a common feature of recently evolved Arabidopsis miRNAs.

## 1.2. Characterization of the *MIR824* locus

The stem loop hairpin containing miR824 is encoded by a transcribed gene, designated *MIR824*, corresponding to the gene At4g24415.1. The capped, polyadenylated 2897 nt transcript, named primary miR824 (pri-miR824), is non-coding, capped, polyadenylated mRNA. RT-PCR using primers annealing at the ends of pri-miR824 confirmed expression of two splice variants: the 1640 nt variant pri-miR824.1 represented and the 1497 nt variant pri-miR824.2 (Figure 4.4, Kutter *et al.*, 2007). The stem loop is present in the third exon of the pri-miR824. Transgenic plants expressing only the third and fourth exon driven by the strong, double-enhancer Cauliflower mosaic virus 35S RNA promoter (*Pro*<sub>2x35S</sub>), named *pPro*<sub>2x35S</sub>:*MIR824*Δ*E1E2*(+), showed increased miR824 expression (Figure 4.5) indicating that the last two exons are sufficient for the formation of the stem loop structure and miR824 processing. Similar results were obtained by Parizotto *et al.* (2004) for another miRNA

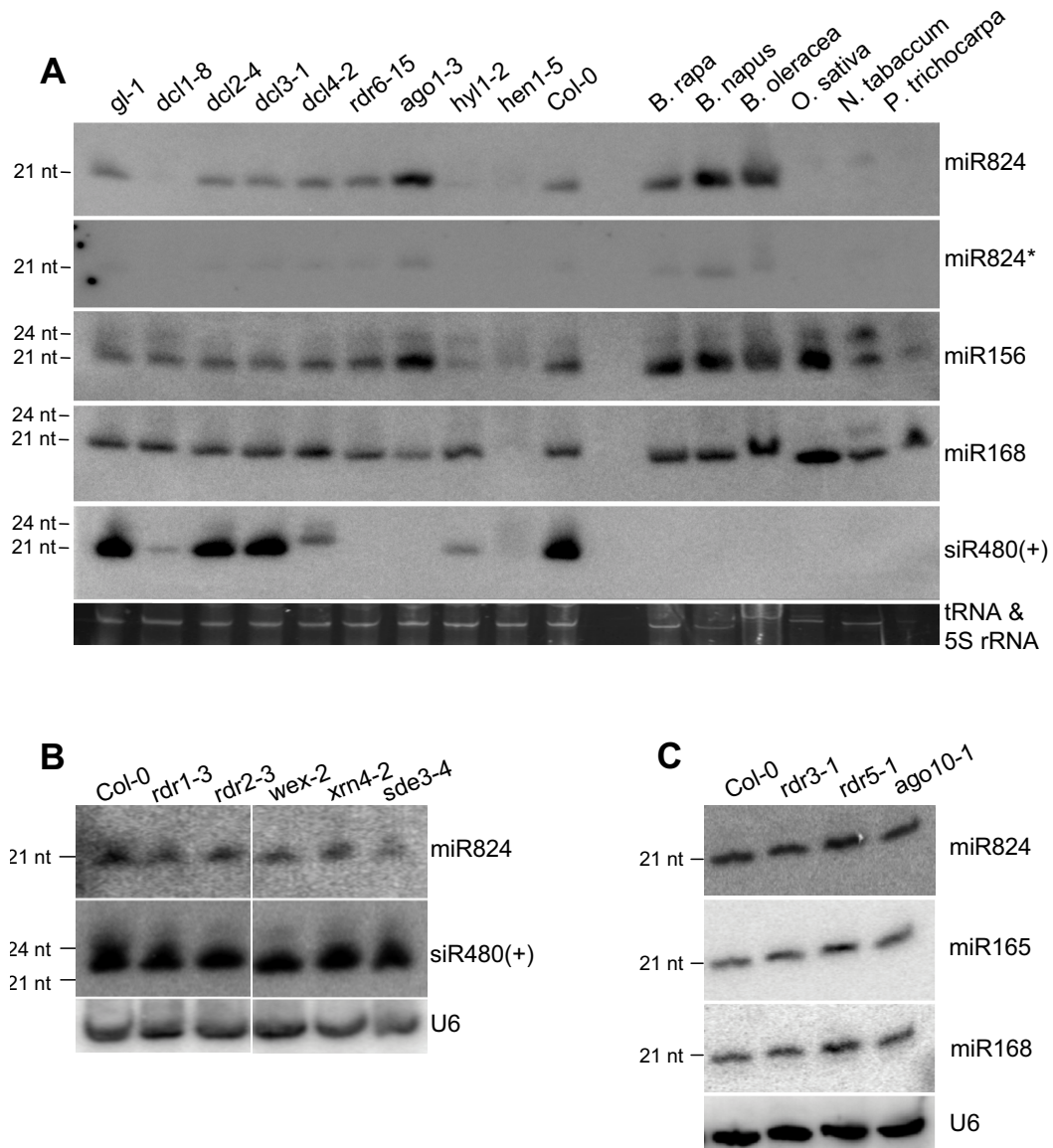


**Figure 4.1: Expression of miR824 in leaves of Arabidopsis miRNA mutants and other plant species.**

(A-C) RNA blot hybridization of Arabidopsis smRNAs using probes for miR824, miR824\*, miR156, miR165, miR168, TAS1, and siRNA480(+) or with U6 as loading standard. 5S rRNA and tRNA loading standards are stained with ethidium bromide. The sizes of smRNAs are indicated on the left. (A) Expression of miR824, miR824\*, miR156, miR168, and TAS1 in deficiency mutants *dcl1-8*, *dcl2-4*, *dcl3-1*, *dcl4-2*, *rdr6-15*, *ago1-3*, *hyl1-2*, *hen1-5* and *Brassica rapa*, *B. napus*, *B. oleracea*, *Oryza sativa*, *Nicotiana tabaccum*, and *Populus trichocarpa*. (B) Expression of miR824 and siRNA480(+) in deficiency mutants *rdr1-3*, *rdr2-3*, *wex-2*, *xrn4-2*, and *sde3-4*. (C) Expression of miR824, miR165, and miR168 in deficiency mutants *rdr3-1*, *rdr5-1*, and *ago10-1*.

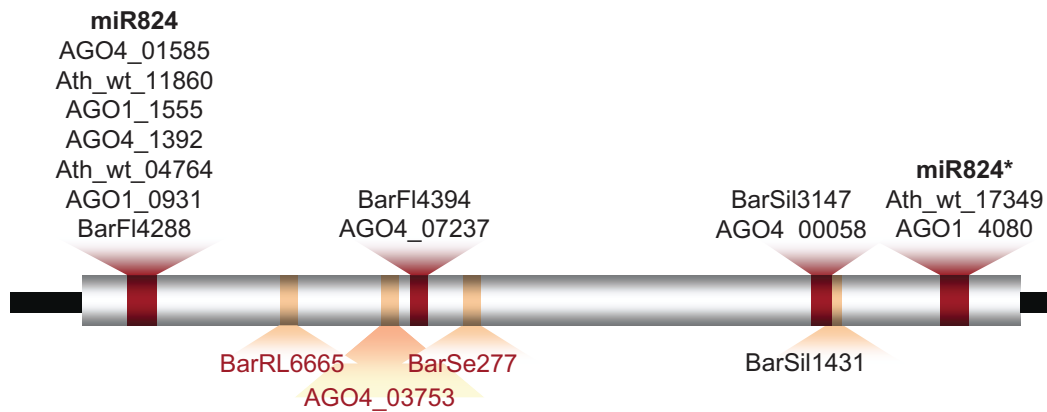


**Figure 4.2: Genomic locations of smRNA sequences of the miR824 precursor.** (also see Table 4.1)

smRNA sequences highlighted in red align in plus (5' to 3') and in orange in minus (3' to 5') orientation towards miR824 precursor sequences. Sequences were obtained from the NCBI Gene Expression Omnibus web site: <http://www.ncbi.nlm.nih.gov/geo/> (Barrett *et al.*, 2007). BLAST search against the miR824 precursor identified smRNAs. smRNA with identification number (ID) >AGO1\_XXXX (GSM149080) and AGO4\_XXXX (GSM149081) were isolated by immunoprecipitation (IP) of smRNAs associated with AGO1 and AGO4 complex, respectively. The set used as control without IP (whole extract) was designated >Ath\_wtXXXX (GSM149079) (Qi *et al.*, 2006). smRNA sequences with the ID number ">Bar" derive from high-throughput sequencing of *Arabidopsis thaliana* endogenous small RNAs by 454 pyrosequencing dataset submitted by Axtell *et al.* (2006). The following ID were used according to the library used:

- >BarRLXXX: GSM118373: smRNAs from rosette leaves
- >BarFLXXX: GSM118372: smRNAs from whole flowers
- >BarSeeXXXX: GSM118374: smRNAs from whole seedlings
- >BarSilXXXX: GSM118375: smRNAs from whole siliques

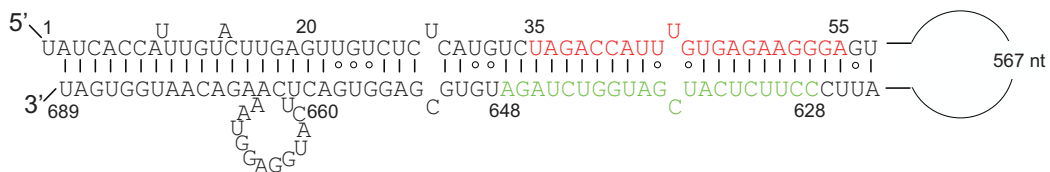


**Figure 4.3: Fold back structure of miR824 precursor.**

5' to 3' stem loop hairpin structures of the pre-miR824 predicted for *Arabidopsis*. The mature miR824 sequence is indicated in red and the miR824\* in green. G:U wobble pairing is shown by a circle.

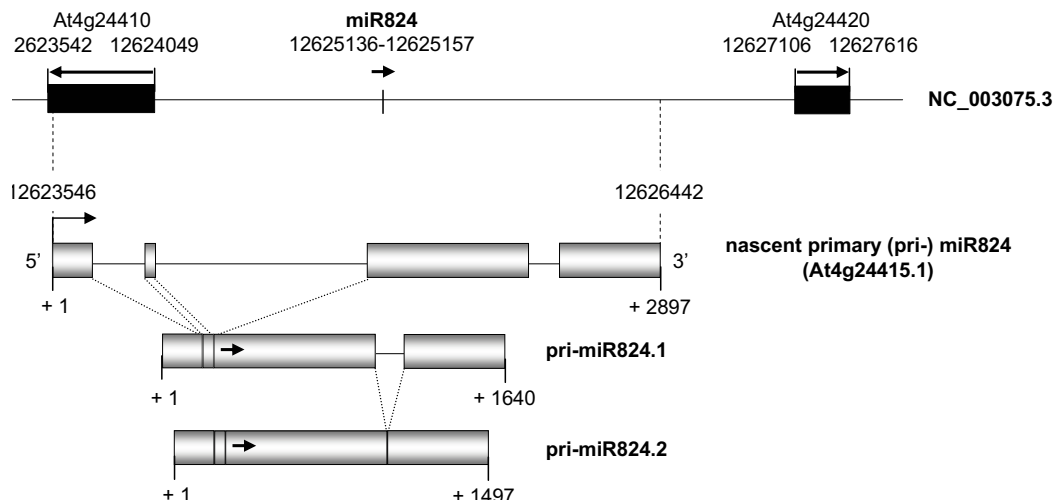


**Figure 4.4: Genomic organization of the *MIR824* locus.**

Schematic presentation of the *MIR824* locus on chromosome IV based on the alignment of ESTs with genomic sequences. The direction of transcription and 5'-3' orientation of *miR824* are indicated by arrows. Exons (grey boxes for *MIR824* and black boxes for gene accessions), introns (horizontal lines), start of transcription (+1), transcript length, and the position and orientation of *miR824* (short arrows) are indicated. The figure is not drawn to scale.

showing that only the fold-back pre-miRNA is sufficient for *miR171* processing. The first two exons of *MIR824* may function as a proximal promoter enabling transcription of *MIR824*. A CT-rich motif leading to enhancement of gene expression (Pauli *et al.*, 2004) was found in those regions suggesting that *miR824* is encoded at the *MIR824* locus as a polyadenylated pri-miRNA that undergoes splicing and further processing.

BLAST searches of the entire Arabidopsis genome established that the first two exons of the *MIR824* (*At4g24415.1*) gene are in antisense orientation to the predicted gene *At4g24410*. Recent reports demonstrate that endogenous siRNAs derive from the overlapping region of a pair of natural antisense transcripts (NATs) (Borsani *et al.*, 2005; Katiyar-Agarwal *et al.*, 2006). No smRNAs deriving from the locus could be detected by RNA blot hybridization even under stringent hybridization conditions. Furthermore, no smRNAs corresponding to this region were found in the MPSS database (<http://mpss.udel.edu>; Lu *et al.*, 2005) and no methylation signals were detected (Lu *et al.*, 2006; Zhang *et al.*, 2006). Reverse transcription with gene-specific primers followed by PCR analysis of the *At4g24415.1* locus (Figure 4.6 A) confirmed that the *in silico* predicted gene *At4g24410* is a misannotated gene entry in the TAIR database. Furthermore, no EST derived from this gene locus could be identified. This result shows that



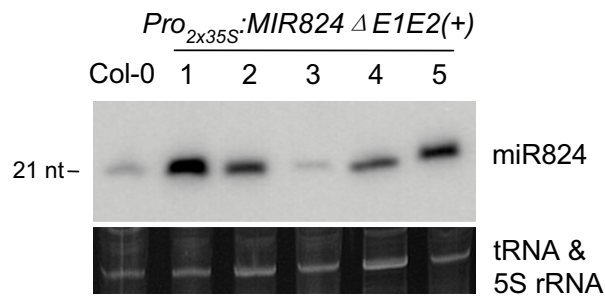


**Figure 4.5: Expression of miR824 in leaves of Col-0 and independent transgenic lines expressing *Pro*<sub>2x35S</sub>:*MIR824* $\Delta$ *E1E2*(+).**

RNA blot hybridization probed with miR824. tRNA and 5S rRNA was stained with ethidium bromide. The size of the smRNA is indicated on the left.

no natural antisense transcript is produced that could give rise to nat-siRNAs acting in *cis* to facilitate cleavage of the *MIR824* transcript.

The impairment of the miRNA pathway in *dcl1-8* and *hyl1-1* mutants resulted in increased steady-state levels of pri-miR824 compared with their corresponding wild-types Col-0 (*gl-1*) and No-0 (Figure 4.7). Furthermore, miR824 processing was partially impaired in *hyl1-1* but not in *dcl1-8* mutants. In *hyl1-1* mutants a shift in a band with lower molecular weight was observed. Misplaced cleavage of pri-miR163 was previously reported in *dcl1-8* and *hyl1-2* mutants (Kurihara and Watanabe, 2004; Kurihara *et al.*, 2006). Cloning analysis showed that the band shift of pri-miR824 in the *hyl1-1* mutant (Figure 4.7) was caused by the absence of the second exon. This data lead to the conclusion that beside the involvement of HYL1 in positioning of the cleavage sites in miRNA processing, another function in splicing of pri-miR824 and probably other pri-miRNAs can be proposed.

Northern blot analysis and quantitative real time PCR (RT-qPCR) confirmed that DCL1 and HYL1 but not HEN1, DCL2, DCL4, RDR1, RDR2, RDR6, SDE3, WEX, or XRN4 are involved in pri-miR824 processing. In the *dcl1-8*, *hyl1-2*, *ago1-3*, and *dcl3-1* mutant an increase of pri-miR824 expression of 3.2-, 3.1-, 3.8-, and 2.0- fold was obtained (Figure 4.8). No function for AGO1 or other DCLs, except DCL1, in miRNA precursor processing is known. Redundancy of DCLs in Arabidopsis as described previously (Blevins *et al.*, 2006; Deleris *et al.*, 2006; Henderson *et al.*, 2006; Moissiard and Voinnet, 2006) might explain a DCL3-dependent role in miR824 formation.

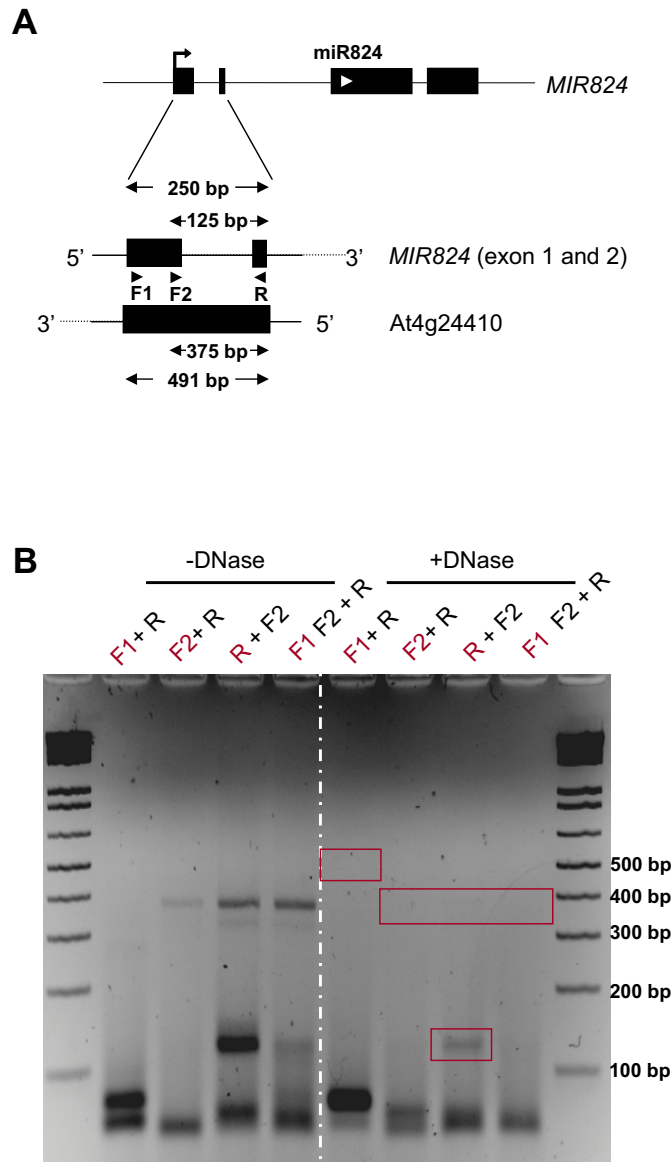


**Figure 4.6: Genomic organization of the *MIR824* locus and the annotated gene *At4g24410*.**

(A) Schematic presentation of the *MIR824* locus with emphasis on the first two exons and *At4g24410* on chromosome IV. The direction of transcription in 5'-3' orientation is indicated. White arrow represents location and orientation of *miR824*. Exons (black boxes) and introns (horizontal lines) are shown. F1, F2, and R represent forward (F) and reverse (R) primer and small black arrows their 5'-3' orientation. Expected length (in bp) of RT-PCR products is represented by double-headed arrow. The figure is not drawn to scale.

(B) Image of 2% agarose gel electrophoreses showing RT-PCR products with (+) and without (-) DNase treatment and primer (F and R) combinations stained with ethidium bromide. The primer in red is used for reverse transcriptase, followed by PCR amplification using primer(s) in black. Red box demonstrates postulated location of RT-PCR products. The size of the DNA size marker is indicated on the right. Note: absence of PCR fragments (red box) indicative for *At4g24410*.

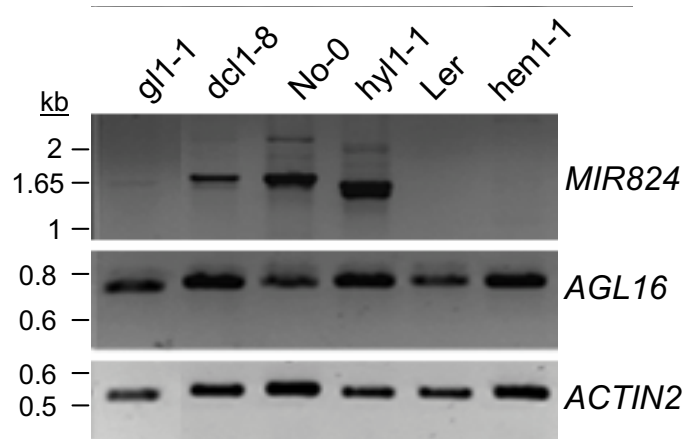


**Figure 4.7: Expression of *MIR824*, *AGL16*, and *ACTIN2* in leaves of miRNA mutants and corresponding wild-type backgrounds.**

Image of native 1% agarose gel electrophoreses showing semiquantitative RT-PCR products of *MIR824*, *AGL16*, and *ACTIN2* stained with ethidium bromide in *dcl1-8*, *hyl1-1*, and *hen1-1* and corresponding wild-type backgrounds *gl1-1* (Col-0), *No-0*, and *Ler*. Primers used amplify whole gene products. Note: sequence differences in *Ler* cause that *MIR824* is not amplified by primer pair designed for Col-0. The length of the DNA is determined by the DNA size marker indicated on the left.

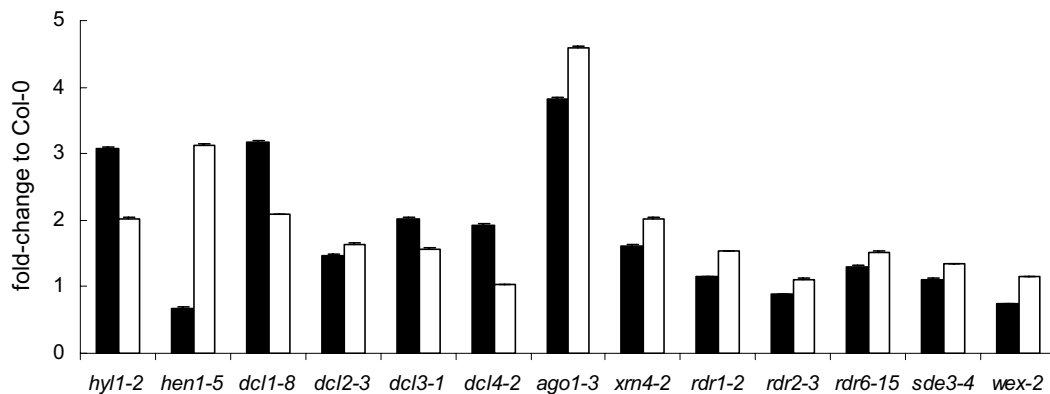


**Figure 4.8: Expression of *MIR824* and *AGL16* in rosette leaves of 28 day old silencing mutants.**

Quantitative RT-PCR determining fold-change of expression of *MIR824* (black column) and uncleaved target *AGL16* (white column) in deficiency mutants *hyl1-2*, *hen1-5*, *dcl1-8*, *dcl2-4*, *dcl3-1*, *dcl4-2*, *ago1-3*, *xrn4-2*, *rdr1-3*, *rdr2-3*, *rdr6-15*, *sde3-4*, and *wex-2*. Quantifications were normalized to *TIP41*. The values in wild-type plants were arbitrarily fixed to 1.

### 1.3. Promoter analysis of *MIR824*

Functional promoters of other Arabidopsis *MIRNA* genes contain cis-elements for polymerase II-type transcription (Xie *et al.*, 2005). The region upstream of the transcription start of pri-miR824 contains a TATA box with the conserved TATAAA-motif at position -30 (Kutter *et al.*, 2007) as well as the recently reported CT-repeat microsatellite motifs found in putative *MIRNA* promoters (Zhou *et al.*, 2007). Several distal *cis*-acting elements implicated in transcriptional regulation including a CArG motif with site for AGAMOUS-LIKE 15 (AGL15) (Tang and Perry, 2003) at position -100, and a low temperature responsive element (LTRE) specific to the *COLD REGULATED 15a* promoter (Baker *et al.*, 1994) at position -450 (Figure 4.9 A). *MIR824* promoter activity was visualized by expression of the *uidA*, encoding the reporter protein  $\beta$ -glucuronidase (GUS) (*pPro<sub>MIR824</sub>:GUS*) (Figure 4.9 C, C') infiltrated into rosette leaves of *Brassica rapa*. GUS expression controlled by the double 35S promoter (*Pro<sub>2x35S</sub>*) was used as positive control (Figure 4.9 B, B'). No GUS expression was visible in expression studies using a promoterless construct or truncated versions of the *MIR824* promoter. *MIR824* promoter activity was also observed in Arabidopsis plants transformed with *Pro<sub>MIR824</sub>:GFP*. However, the green fluorescence intensity of the reporter gene was weak and detectable only in tissues (e.g. roots and petiole) where less chlorophyll interfered with the GFP excitation. These results show that the region 2954 upstream of pri-miR824 is a functional promoter probably regulated by abiotic stresses and other environmental factors.

### 1.4. Characterization of *MIR824* T-DNA insertion alleles

Several homozygous and monogenetic T-DNA insertion alleles of *MIR824*, designated *m1* to *m4*, were identified from the SALK Collection of sequence-indexed T-DNA insertion mutants (<http://signal.salk.edu>) (Alonso *et al.*, 2003) (Figure 4.10 A) and characterized (Figure 4.10 B). The T-DNA insertion of the mutants *m1* (SALK\_007098) and *m2* (SALK\_000582) are located downstream of the miR824 precursor and map to the last exon of the precursor and to the 3' UTR sequence, respectively. The T-DNA insertions in *m3* (SALK\_042802) and *m4* (SALK\_099968) are positioned upstream of the transcription start to *MIR824* (Figure 4.10 A). The mutant lines *m1* and *m2* showed reduced *MIR824* expression and miR824 formation while the *m3* and *m4* lines enhance *MIR824* expression and miR824 formation (Figure 4.10 C, D). This suggests that T-DNA insertions in those mutants affect miR824 biogenesis. Enhanced expression probably results from read-through transcription because the T-DNA promoter is in the same orientation as pri-miR824 transcription (Kutter *et al.*, 2007), as reported by others using the same T-DNA vector (Ren *et al.*, 2004).

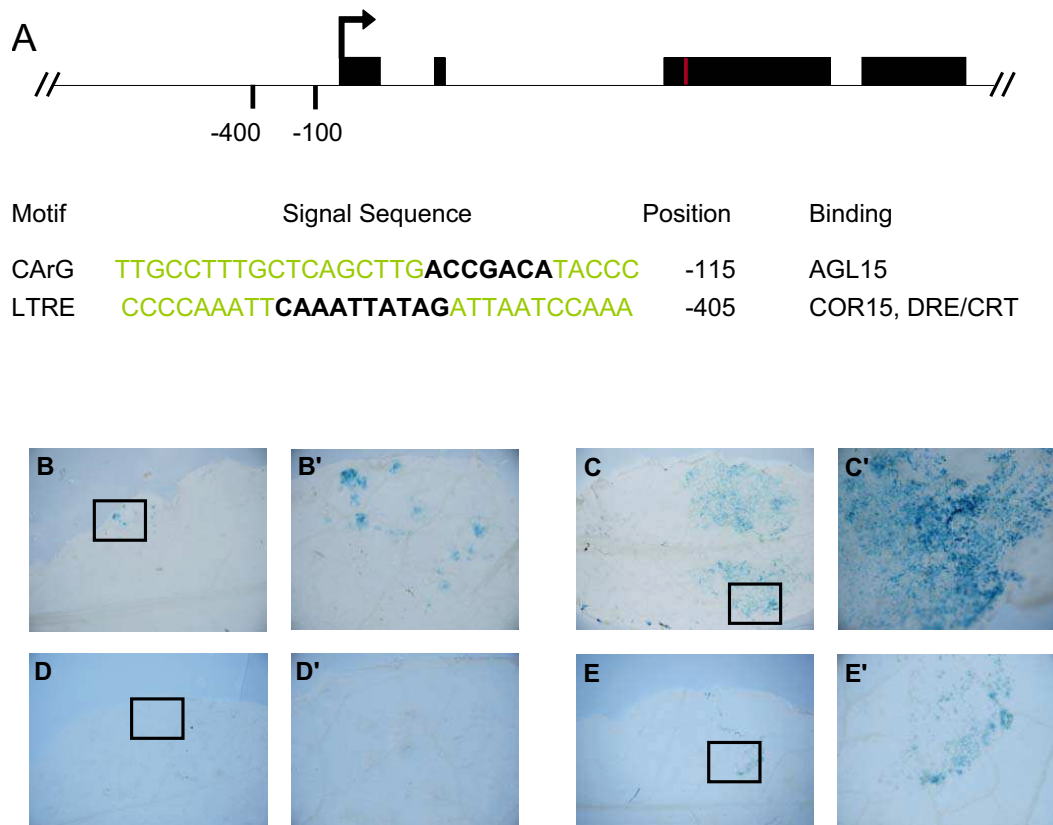


**Figure 4.9: Promoter expression studies of *MIR824* and *AGL16* by leaf infiltration.**

(A) Schematic presentation and indication of the localization of predicted promoter motifs upstream of *MIR824*. (B-E) Staining of the abaxial epidermis of leaves of *Arabidopsis* four week after germination is shown. B' to E' represent magnified images of regions (highlighted by black square) of B to E, respectively. Region with positive promoter activity appear blue due to GUS reporter gene expression. Infiltrated plants with (B-B') pPro<sub>2x35S</sub>:GUS as positive control carrying the GUS reporter gene regulated by the Pro<sub>2x35S</sub> promoter, (C-C') pPro<sub>MIR824</sub>:GUS carrying 2954 bp of genomic region upstream of the pri-miR824 start of transcription fused to the reporter gene. (D-D') pPro<sub>AGL16-11</sub>:GUS carrying the full-length genomic region upstream of the *AGL16* start of transcription plus the genomic region up to and including intron 1 of *AGL16* fused to the reporter gene, (E-E') pPro<sub>AGL16-12</sub>:GUS carrying the full-length genomic region upstream of the *AGL16* start of transcription plus the genomic region up to and including intron 2 of *AGL16* fused to the reporter gene.

## 2. miR824 target gene prediction and validation

Plant miRNA target genes show high complementarity in pairing (0-4 mismatches) to the respective miRNAs. This feature of plant miRNAs facilitated the computational identification of almost all plant miRNA target genes (Jones-Rhoades and Bartel 2004; Park *et al.*, 2002; 2002; Rhoades *et al.*, 2002). A confirmation or validation of the cleavage site by 5' RACE

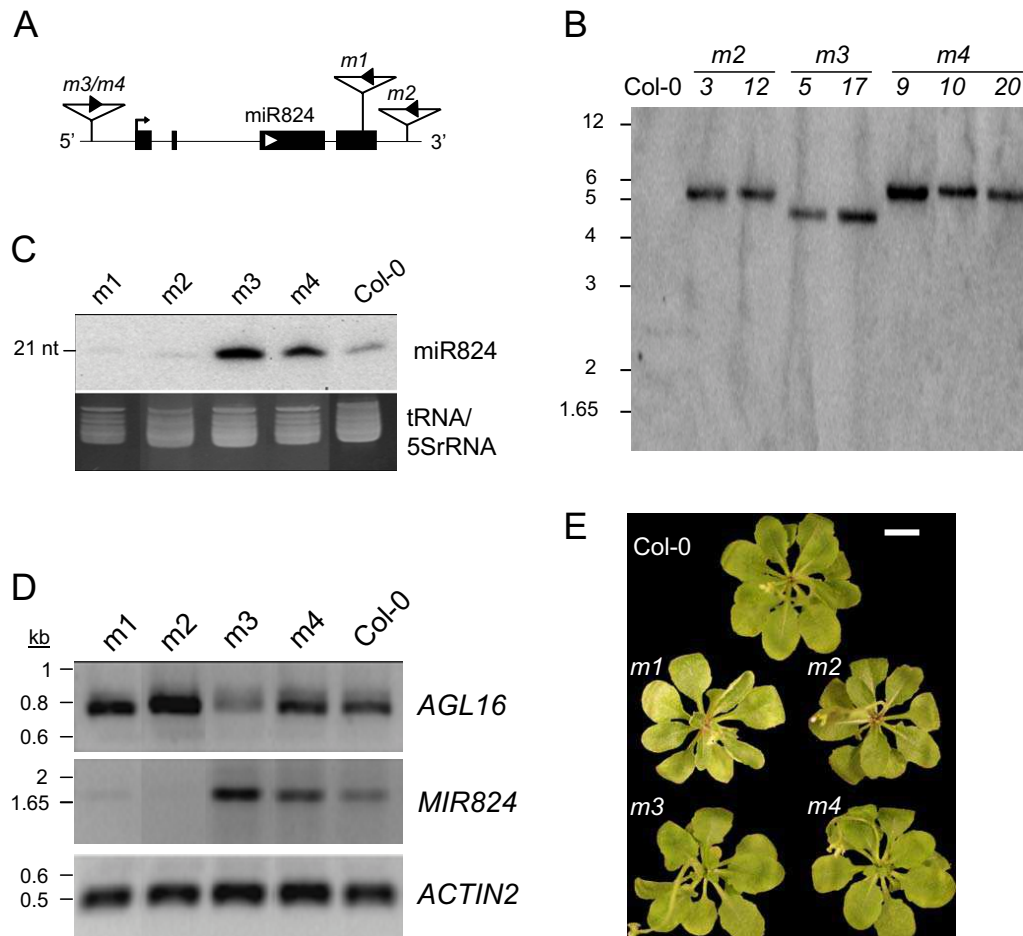


**Figure 4.10: Characterization of mutants with T-DNA insertions in the *MIR824* locus.**

(A) Schematic presentation of the localization of T-DNA insertions of mutant *m1* to *m4* in the *MIR824* locus. Black arrows indicate orientation of 35S promoter within the T-DNA insertion. White arrow represents location and orientation of miR824. Exons (black boxes) and introns (horizontal lines) are shown. (B) Determination of T-DNA copy number in *m2* to *m4* mutants: genomic DNA was prepared from rosette leaves of *m2* to *m4* mutants, digested with *Bam*HI and separated by agarose gel electrophoresis. Detection of the *NPTII* gene by using a  $^{32}$ P-labeled PCR fragment of *NPTII* as probe for hybridization. The probe does not span an intron and none of the used enzymes cuts within the probe sequence. The size of the DNA in kb is indicated by molecular size marker on the left. (C) Detection of miR824 in rosette leaves of Col-0 and *m1* to *m4* by RNA blot hybridization. tRNA and 5S rRNA were stained with ethidium bromide. Size of smRNA is shown on the left. (D) Image of native 1% agarose gel electrophoreses showing semiquantitative RT-PCR products of *MIR824*, *AGL16*, and *ACTIN2* stained with ethidium bromide in *m1* to *m4* mutants. The length of the DNA is determined by the DNA size marker indicated on the left. (E) Representative Col-0 and *m1* to *m4* mutant plants grown under the same conditions and photographed 28 days after germination. Mutants appear normal in growth habit and development. Bar: 1 cm.

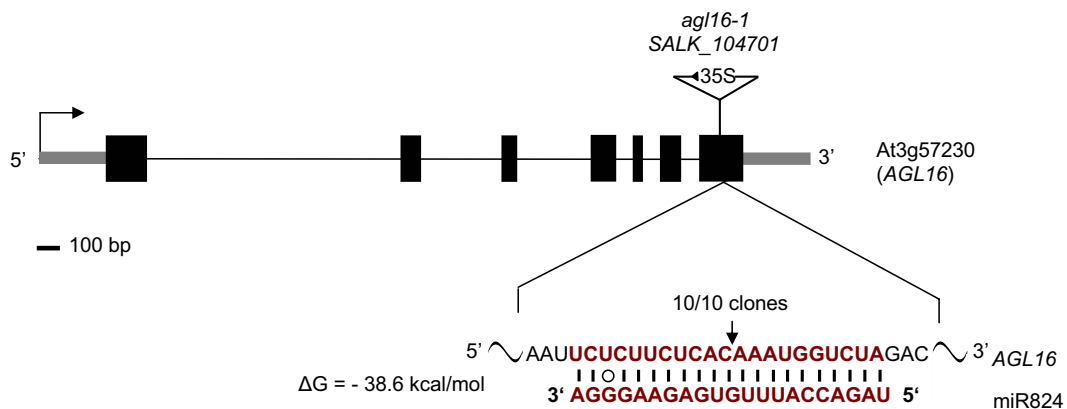
(also called RNA ligase mediated cDNA ends, RLM-RACE) is indicative of miRNA-mediated processing and has been described for many of those target genes (Allen *et al.*, 2004; Aukerman and Sakai, 2003; Kasschau *et al.*, 2003; Llave *et al.*, 2002b; Mallory *et al.*, 2005; Mallory *et al.*, 2004a; Palatnik *et al.*, 2003; Park *et al.*, 2002).

### 2.1. Identification of *AGL16* (*AGAMOUS-LIKE 16*) as the unique miR824 target gene

Target genes of miR824 were predicted by BLAST searches against the *Arabidopsis* coding sequences including introns and untranslated regions. Up to four mismatches, deletions, or substitutions were allowed and exclude therefore non-biological miRNA targets showing less than 85% sequence identity with the reverse complement sequence of miR824 (Allen *et al.*, 2005). Several complementarities to miR824 were identified in exonic sequence of the genes At3g57230 (*AGL16*), At1g05930 (hypothetical protein), At1g65370 (neprin and TRAF homology domain-containing protein), and At1g65150 (neprin and TRAF homology domain-containing protein) and in intronic sequence of the gene At1g65050 (neprin and TRAF homology domain-containing protein) (Table 4.2). Previous studies showed that mismatches at the 5' and central regions of the miRNA (Allen *et al.*, 2005; Schwab *et al.*, 2005) are more disruptive than those at the 3' region (Mallory *et al.*, 2004). These criteria were fulfilled only by *AGL16* and At1g05930. The base pairing at the site of *AGL16* is almost perfect except for one G:U wobble pairing at the 3' end of miR824 and has the predicted free energy of pairing -38.6 kcal/mol (Reeder *et al.*, 2006) (Figure 4.11). miR824 sequence pairs to At1g05930 with three G:U wobble pairings at position 1, 10, and 15 and with a mismatch at position 21. The predicted free energy of pairing is therefore increased to -29.5 kcal/mol. At1g65370, At1g65150, and At1g65050 pair to the miR824 sequence with four mismatches at position 1, 5, 6, and 15 and have a predicted free energy of pairing -26.7, -26.7, and -26.4 kcal/mol, respectively. Potential miR824 target genes were validated by RLM-RACE in which the precise cleavage site was mapped. Fragments with the correct size were only obtained for *AGL16*, At1g05930, and At1g65150 after the third round of nested PCR using gene-specific primers for each of the target genes. All 10 clones sequenced, showed that cleavage of the *AGL16* transcript occurs between nucleotides 10 and 11 of the miR824 pairing (Figure 4.11) like targets of many other miRNAs. None of the 30 clones sequenced mapped to the predicted target genes At1g05930, At1g65370, At1g65150, or At1g65050. These results indicate that *AGL16* is the only cleaved target gene of miR824.

Table 4.2.: miR824 target prediction.

AGI	protein domain	% pairing identity	sequence alignment in plus/minus orientation (miR824 [5'-3'] in bold to target mRNA [3'-5'])	targeting sequence	cleavage validation by RLM-RACE	$\Delta G$ [kcal/mol]
At3g57230	AGL16 (Agamous-like AGL16, MADS-box containing transcription factor protein)	95	<b>uagacc</b> auuuugugaga <b>aggga</b>       uagacc <u>auuuugugaga</u> agaga	exon 7	yes	-38.6
At1g05930	hypothetical protein	89	<b>uagacc</b> auuuugugaga <b>aggga</b>                gagacc <u>auuuugugau</u> aagggu	exon 1	no	-29.5
At1g65370	neprin and TRAF homology domain-containing protein	85	<b>uagacc</b> auuuugugaga <b>aggga</b>                 aagaga <u>auuuugugaa</u> aggga	exon 2	no	-26.7
At1g65150	neprin and TRAF homology domain-containing protein	85	<b>uagacc</b> auuuugugaga <b>aggga</b>                 aagaga <u>auuuugugaa</u> aggga	exon 3	no	-26.7
At1g65050	neprin and TRAF homology domain-containing protein	85	<b>uagacc</b> auuuugugaga <b>aggga</b>                 aagaga <u>auuuugugaa</u> aggga	intron 3	no	-26.4

Figure 4.11: miR824 cleavage of target mRNA and location of *agl16-1*.

Black boxes symbolize exon, grey boxes UTR, and horizontal lines intron sequences. The arrow represents transcription start. miR824 binding site is emphasized with the nucleotide positions relative to the transcription start of *AGL16* indicated (dashed line perfect match, circle represents G:U wobble pairing). The frequency of 5'-RACE clones corresponding to the cleavage site (vertical arrows) is shown. The free energy of binding ( $\Delta G$ ) is indicated. Localization of T-DNA insertion *agl16-1* is shown. Black triangle indicates orientation of 35S promoter within the T-DNA insertion.



## 2.2. *AGL16* expression in RNA silencing and *MIR824* locus mutants

RNA blot hybridization showed that relative to wild-type, *AGL16* mRNA consistently accumulated at higher concentrations in the miRNA defective mutants *dcl1-8*, *hyl1-1*, *hen1-1*, compared to their corresponding wild-types Col-0 (*gl-1*), No-0, and Ler (Figure 4.12 A) and *ago1-3* (Figure 4.12 B). Slight increases in *AGL16* transcripts were also observed in the XRN4- and RDR1-deficient mutant (Figure 4.12 B). The 5' to 3' exoribonuclease activity of AtXRN4 causes often an accumulation of short 3' end cleavage fragments in *xrn4* mutants (Souret *et al.*, 2004). However, the *AGL16* 3' cleavage product of 386 nt could not be detected. No alterations in *AGL16* transcript levels occurred in *dcl2-5*, *dcl3-1*, *dcl4-2*, *rdr2-3*, *rdr6-15*, *sde3-4*, or *wex-2* (Figure 4.12 B). Quantitative RT-PCR with primer pairs detecting *AGL16* transcripts either 5' upstream or 3' downstream of the *miR824* cleavage site confirmed the DCL1-, HYL1-, HEN1-, AGO1-, and XRN4-mediated regulation of *AGL16* expression. The 5' transcript levels of *AGL16* were increased in the *dcl1-8*, *hyl1-2*, *hen1-5*, *ago1-3*, and *xrn4-2* mutant by 2.1-, 2.0-, 3.1-, 4.6-, and 2.0-fold, respectively (Figure 4.8). *AGL16* transcript levels were slightly increased in the precursor mutants *m1* and *m2* that show reduced *miR824* accumulation and slightly decreased in *m3* and *m4* that show enhanced *miR824* accumulation (Figure 4.10).

A homozygous, monogenic mutant *agl16-1* (Figure 4.13 A) carrying a T-DNA insertion in the last exon of *AGL16* was identified (Figure 4.11). The T-DNA insertion in the last exon impaired *AGL16* accumulation. This mutant showed a ca. 14-fold reduction in *AGL16* mRNA relative to wild-type (Figure 4.13 B). *miR824* accumulation remained unchanged since the insertion is independent of the *MIR824* locus (Figure 4.13 C). Taken together, these results indicate that *AGL16* is negatively regulated by miRNA-mediated cleavage as shown for other miRNA targets (Vazquez *et al.*, 2004).

## 2.3. miRNA-mediated regulation of other Arabidopsis MADS-box genes

*AGL16* is one of the four *AGL17*-like subfamily members of the MIKC-type MADS-box genes encoding eukaryotic transcription factors (Alvarez-Buylla *et al.*, 2000; Bitter *et al.*, 2003). BLAST analysis of all the known MADS-box genes to the computationally predicted or experimentally validated Arabidopsis miRNAs was performed. The analysis showed that the predicted *miR426* (Wang *et al.*, 2004) might target other MADS-box genes in addition to *miR824*. *miR426* shows complementarity to the other members of the *AGL17*-like subfamily *ANR1* (At2g14210), *AGL17* (At2g22630), and *AGL21* (At4g37940) but not *AGL16* or any other MADS-box gene (Table 4.3). RNA blot hybridizations were performed since *miR426*

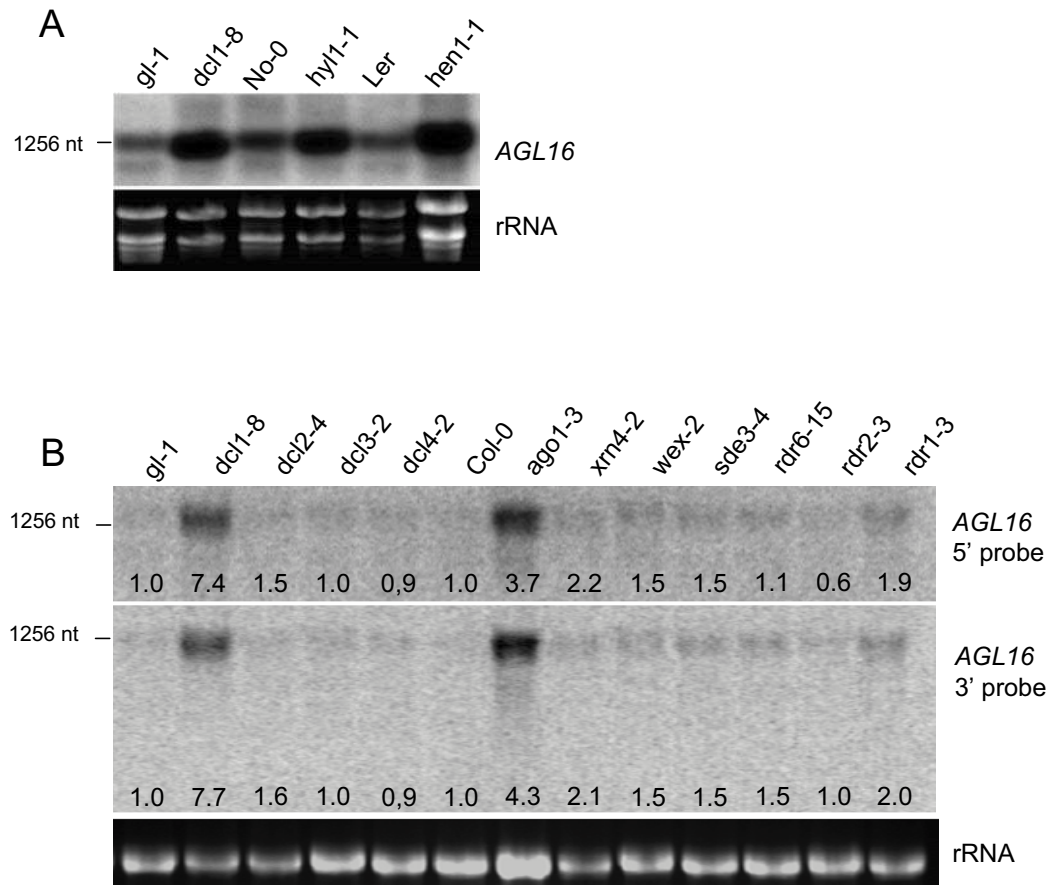


**Figure 4.12: Expression of *AGL16* transcript in rosette leaves of silencing deficient mutants.**

RNA blot hybridization of total RNAs using probes to detect *AGL16* (full-length *AGL16* coding region, 5' and 3' products of *AGL16* coding region after cleavage). rRNA loading standards are stained with ethidium bromide. The size of the transcript is indicated on the left. (A) Expression of *AGL16* (full-length probe) in deficiency mutants *dcl1-8*, *hyl1-1*, and *hen1-1* and their corresponding backgrounds Col-0 (*gl-1*), No-0, and Ler. (B) Expression of *AGL16* (5' and 3' probe) in deficiency mutants *dcl1-8*, *dcl2-4*, *dcl3-1*, *dcl4-2*, *ago1-3*, *xrn4-2*, *wex-2*, *sde3-4*, *rdr6-15*, *rdr2-3*, and *rdr1-3*. Fold-changes to their backgrounds are indicated below.

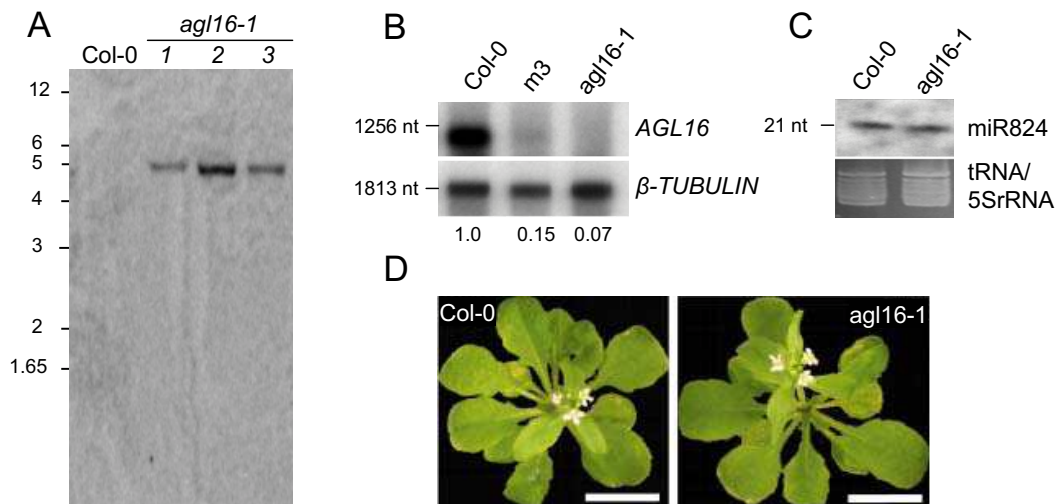


**Figure 4.13: Expression of *AGL16* transcript in rosette leaves of the *AGL16* deficient mutant.**

(A) Determination of T-DNA copy number in *agl16-1* mutants: genomic DNA was prepared from rosette leaves of *agl16-1*, digested with *Bam*HI and separated by agarose gel electrophoresis. Detection of the *NPTII* gene by using a  $^{32}$ P-labeled PCR fragment of *NPTII* as probe for hybridization. The probe does not span an intron and none of the used enzymes cuts within the probe sequence. The size of the DNA in kb is indicated by molecular size marker on the left. (B) RNA-blot hybridization of 2  $\mu$ g poly (A+) RNA prepared from Col-0, *m3*, and *agl16-1* plants. The blot was hybridized with probes for  $\beta$ -*TUBULIN* mRNA or the full-length *AGL16* coding region. The sizes of transcripts are indicated on the left and the fold expression of *AGL16* mRNA in *m3* and *agl16-1* relative to Col-0 after normalization for the  $\beta$ -*TUBULIN* loading standard is shown below. (C) RNA blot hybridization of miR824 in 20  $\mu$ g of low molecular weight RNA of Col-0 and *agl16-1*. tRNA and 5S rRNA were stained with ethidium bromide. The size of the miRNA is indicated on the left. (D) Representative Col-0 and *agl16-1* plants grown under the same conditions and photographed 28 days after germination. The *agl16-1* mutant appears normal in growth habit and development. Bar: 1 cm

**Table 4.3.: smRNA mediated cleavage of AGL17 clade members.**

AGI	protein domain	sequence alignment in plus/minus orientation (miR824 [5'-3'] in bold to target mRNA [3'-5'])	targeting sequence	cleavage validation by RLM-RACE	$\Delta G$ [kcal/mol]
At3g57230	AGL16 (Agamous-like AGL16, MADS-box containing transcription factor protein)	miR824 <b>uagacc</b> auuugugagaagga       uagacc <u>auuugugaga</u> agaga	exon 7	yes	-38.6
At2g14210	ANR1 (Arabidopsis nitrate response, MADS-box containing transcription factor protein)	miR426 <b>uuuuggaa-uuu</b> gucc-uuacg             uuuuggaugauuuguccuuacg	exon 5 and exon 6 junction	no	-20.4
At2g22630	AGL17 (Agamous-like AGL17, MADS-box containing transcription factor protein)	miR426 <b>uu-uugg---</b> aaauuugu-ccuuacg                 :  uuc <u>auu</u> gucaaaa <u>uu</u> gu <u>ccuuuu</u>	exon 4 and exon 5 junction	no	-12.9
At4g37940	AGL21 (Agamous-like AGL21, MADS-box containing transcription factor protein)	miR426 <b>uu-uug-g--aa-</b> uuuugu-ccuuacg              :         : : uuc <u>u</u> gaguc <u>u</u> c <u>u</u> g <u>u</u> g <u>u</u> cc <u>u</u> u <u>u</u> cu	exon 4 and exon 5 junction	no	-16.1

expression was not validated. miR826 could be detected after prolonged exposure in samples of 80  $\mu$ g of smRNAs, but not in 20  $\mu$ g samples (Figure 4.14 A, B). These results and the finding that miR426 could not be detected in the *hyl1-2* mutants suggest that miR426 is generated by a smRNA pathway, but is far less abundant in rosette leaves than other known miRNAs. miR426 has 18, 11, and 12 base-pair matches with the putative targets *ANR1*, *AGL17*, and *AGL21* respectively. miR426 pairs at the splicing junctions between exon 5 and exon 6 of *ANR1*, and between exon 4 and exon 5 for *AGL17* and *AGL21* (Table 4.3). No gene-specific cleavage fragments with the correct size were obtained by RLM-RACE for any of the putative targets tested. This shows that *ANR1*, *AGL17*, and *AGL21* are not degraded by miRNA-mediated RNA cleavage. Furthermore, no MPSS smRNA signatures were found in of *ANR1*, *AGL17*, and *AGL21* transcribed regions. These findings strongly support my working hypothesis that *AGL16* is the sole member of MADS-box gene family regulated by miRNA-directed cleavage.

#### 2.4. Analysis of *AGL16* expression

Several reports showed that *AGL16* is expressed in all aerial parts of the plant and roots (Alvarez-Buyalla *et al.*, 2000; Gan *et al.*, 2005; Gong *et al.*, 2004; Kofuji *et al.*, 2003; Nawy *et*

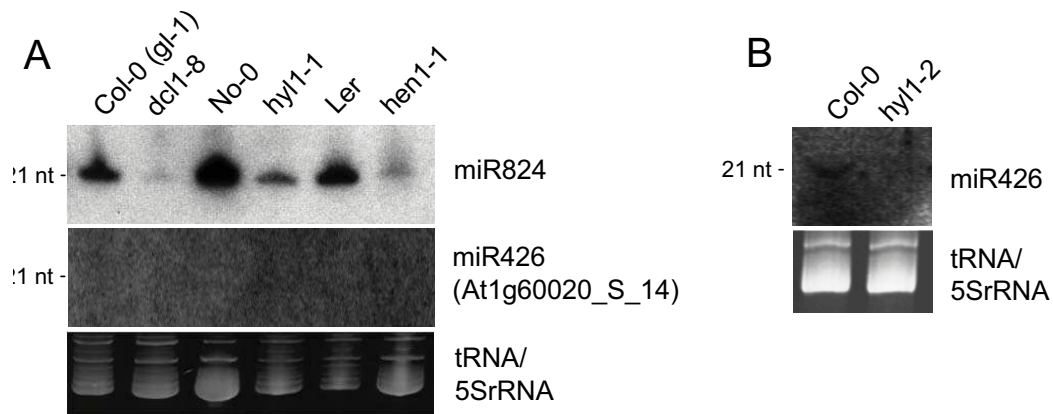


**Figure 4.14: miR426 mediated regulation of AGL17 clade members.**

(A and B) RNA blot hybridization probed with miR824 and miR426. tRNA and 5S rRNA was stained with ethidium bromide. The size of the miRNAs is indicated on the left. (A) RNA blot hybridization of 20  $\mu$ g low molecular weight RNA of rosette leaves of *dcl1-8*, *hyl1-1*, and *hen1-1* mutants and their corresponding backgrounds Col-0 (*gl-1*), No-0, and Ler. (B) RNA blot hybridization of 80  $\mu$ g low molecular weight RNA of rosette leaves of *hyl1-2* and Col-0.

*al.*, 2005). In two independent biological experiments *AGL16* transcript levels of six-week-old Arabidopsis plants were tested by quantitative RT-PCR at this developmental stage *AGL16* transcript was highly expressed in stems as well as in rosette and cauline leaves but lower in roots or inflorescences. Dissection of the rosette leaf showed that *AGL16* is similarly expressed in major vein, leaf blade, and leaf margin (Figure 4.15).

## 2.5. Promoter regulation of *AGL16*

To identify the *AGL16* gene promoter region, a genomic region 611 bp upstream of the *AGL16* transcription start was fused to a  $\beta$ -glucuronidase (GUS) (*pPro<sub>AGL16</sub>:GUS*) reporter gene. While GUS activity was detected after infiltrating leaves of *Brassica rapa* with the positive control *Pro<sub>2x35S</sub>:GUS*. No activity was detected with (*pPro<sub>AGL16</sub>:GUS*). Because regions important for transcription are located within the second intronic region of the related *AGAMOUS* gene (Sieburth and Meyerowitz, 1997), the experiment were repeated with *pPro<sub>AGL16</sub>:GUS* vectors that included the first (*pPro<sub>AGL16-11</sub>:GUS*) or second intron (*pPro<sub>AGL16-12</sub>:GUS*). Only vector *pPro<sub>AGL16-12</sub>:GUS* (Figure 4.9 E, E') but not *pPro<sub>AGL16-11</sub>:GUS* (Figure 4.9 D, D') gave expression of GUS in *B. rapa* leaves suggesting that regions in the second intron are required for high-level transcription of *AGL16*. Interestingly, CArG motifs were found in these intronic regions, which are known to be important for regulation by

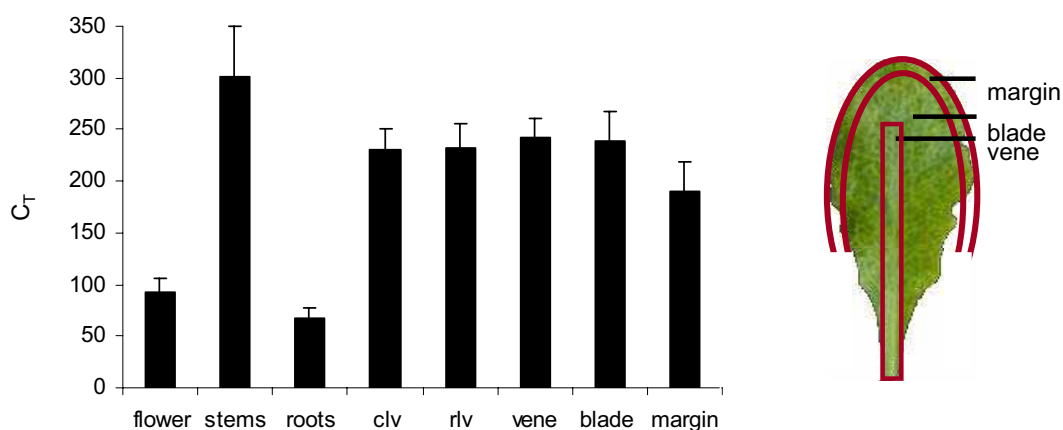


**Figure 4.15: Expression of *AGL16* in different plant organs and parts of the organ of Arabidopsis.**

Quantitative RT-PCR determined absolute ( $C_T$ ) values of *AGL16* gene expression in different organs of the plant. The bar represents the standard error. clv, cauline leaves; rlv, rosette leaves. Different parts of the leaf used for RT-PCR are illustrated on the right.

5'-upstream sequences in AGL genes.

### 3. Role of miR824 and *AGL16* upon abiotic stress and hormonal treatment

The response of plants to abiotic and biotic stress is associated with specific, global patterns of changes in gene expression (www.geneinvestigator.ehz.ch; Zimmermann *et al.*, 2004). Novel miRNAs have also been associated with abiotic stress (Jones-Rhoades and Bartel, 2004; Sunkar and Zhu, 2004). These reports and the predicted low temperature responsive element (LTRE) of *COLD REGULATED 15a* in the promoter region of *MIR824* suggested that miR824 expression might be affected by stress. miR824 expression was tested in response to cold, heat, and salt stress as well as in response to hormone treatment. RNA-blot hybridization showed that, relative to controls, RNA blot analysis was performed on 5-week-old wild-type plants grown on  $\frac{1}{2}$  MS-agar plates subjected to cold (6.5°C for 24h), increased temperature (37°C for 3h), and treated with 0.25 M NaCl (for 3h), 0.1 M abscisic acid (ABA) (for 3h), or 2  $\mu$ M 24-epibrassinolide. Control plants were left at 21°C or treated with water and kept under same light conditions as plants subjected to stress. An increased accumulation of miR824 was observed after exposure to all stress conditions tested (Figure 4.16). Treatments with hormones ABA and 24-epibrassinolide caused the greatest change of 1.3-

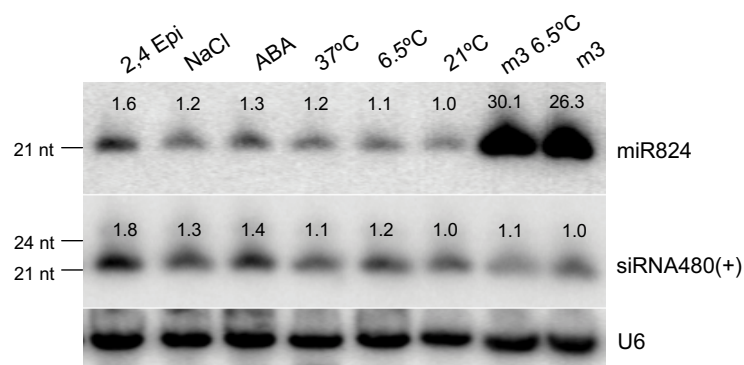


**Figure 4.16: Expression of miR824 in rosette leaves of Arabidopsis plants upon several stress conditions and hormonal treatments.**

RNA blot hybridization of smRNAs using probes for miR824 and siRNA480(+). Labelling with a U6 probe was used as standard control. The sizes of smRNAs are indicated on the left and the fold expression of miR824 and siRNA480(+) relative to the untreated Col-0 control after normalization for the U6 loading standard is shown below. Conditions tested: cold stress (6.5°C for 24h), increased temperature (37°C for 3h), 0.25 M NaCl (for 3h), 0.1 M abscisic acid (ABA) (for 3h), or 2  $\mu$ M 24-epibrassinolide (Epi).

and 1.6-fold, respectively. miR824 overexpressing *m3* plants responded to cold-treatment like wild-type plants. Both showed a similar fold increase in miR824 relative to controls. The same pattern of increase with all treatments was observed using siRNA480(+) as control. These findings suggest that altered miR824 accumulation may be a general effect of abiotic and hormonal stress on smRNA formation.

Transcript levels of the same plant samples were analyzed by quantitative RT-PCR. Cold induced the expression of pri-miR824 by 12.2-fold. Salt stress, abscisic acid, and 24-epibrassinosteroids caused moderate elevated transcript levels (2.9-, 2.5-, and 2.2-fold, respectively). No changes were observed by 37°C treatment. *AGL16* transcripts were altered upon temperature changes. Like pri-miR824, a 2.7-fold increase of *AGL16* transcript was determined upon cold stress. However, heat stress causes a decrease in *AGL16* transcript (2.5-fold) (Figure 4.17). Induction of precursor accumulation leading to increased miRNA formation was not correlated with decreased accumulation of the target transcript under the conditions tested. Thus, it seems likely that cold stress affects stabilization of mRNA transcripts by interfering with the processing machinery as shown for RNA splicing (Lee *et al.*, 2006).

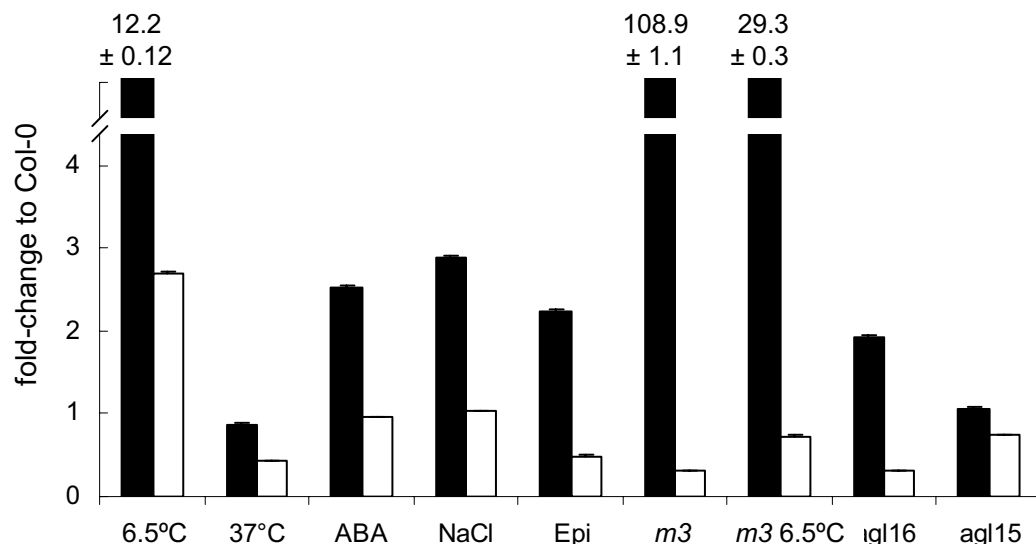


**Figure 4.17: Expression of *MIR824* and *AGL16* in rosette leaves of *Arabidopsis* plants upon several stress conditions and hormonal treatments.**

Quantitative RT-PCR determining fold-change of expression of *MIR824* (black column) and uncleaved target *AGL16* (white column). Quantifications were normalized to *TIP41*. The values in wild-type plants were arbitrarily fixed to 1. Conditions tested: cold stress (6.5°C for 24h), increased temperature (37°C for 3h), 0.25 M NaCl (for 3h), 0.1 M abscisic acid (ABA) (for 3h), or 2 µM 24-epibrassinolide (Epi).



#### 4. Evolutionary conservation of miR824 and *AGL16*

Most miRNAs are conserved among flowering and non-flowering plants (Axtell and Bartel, 2005). Similarly, homologs of many *Arabidopsis* miRNA targets have conserved miRNA complementary site in monocots and eudicots implying that these miRNA-target interactions have functions since the divergence of monocots and eudicots (Rhoades *et al.*, 2002; Jones-Rhoades and Bartel, 2004; Sunkar and Zhu, 2004). A BLAST search of all available plant genome databases detected miR824 sequence only in other Brassicaceae, specifically, *B. rapa*, *B. napus*, and *B. oleracea*. In each case, this sequence was present on the 5' arm of the predicted hairpin structure, which was identical in the subspecies *B. napus* and *B. rapa* (Kutter *et al.*, 2007). RNA-blot hybridization showed that miR824 and miR824\* are expressed in these *Brassica* species (Kutter *et al.*, 2007). As control, the 21 and 24 nt band of miR158 and the 21 nt band of miR168 was detectable in all *Brassica* species, rice, tobacco, and poplar (Figure 4.1 A). As known for other plant species (Axtell and Bartel, 2005), the transacting siRNA480(+) was also not detectable in any of the *Brassica* species tested, indicating that *TAS1* is *Arabidopsis* specific. The miRNA miR173 or its target transcript *TAS1* itself might be not present in other plant species beyond *Arabidopsis*. It is also possible that the sequence arrangement of the *TAS* locus varies in other plant species and therefore gives rise to differently phased ta-siRNA to which the probe used for detection in *Arabidopsis* does not hybridize. Taken together, these results suggests that miR824 is a member of the class of recently evolved *Arabidopsis* miRNA genes (Allen *et al.*, 2004) that have been conserved in the same eudicot family, but not in more distantly related eudicots and monocots. In addition, the highly conserved miR824 pairing region was also identified in *B. rapa* (AC189325.1), *B. napus* (CX281097), and *B. oleracea* (EH417933) ESTs encoding *AGL16* orthologs (Kutter *et al.*, 2007) but not in any other plant genome sequenced so far suggesting that miR824-mediated regulation of *AGL16* has been conserved in the evolution of the Brassicaceae .

## 5. The biological function of the miR824/*AGL16* pathway

Contributions to this chapter:

I did most of the experiments described in this chapter often under the supervision of Azeddine Si-Ammour. Azeddine Si-Ammour constructed plasmids for plant transformation. Daniel Mathys at the Basel University Microscopy Center helped with SEM imaging.

## 1. Molecular characterization of transgenic lines altered in *AGL16* mRNA expression

To determine the biological function of miR824-mediated regulation of *AGL16* mRNA, transgenics showing decreased *AGL16* mRNA expression (*agl16-1* and *m3*), increased ectopic expression of *AGL16* mRNA (*AGL16.1/2*), and a miRNA-resistant version of *AGL16* (*AGL16m1/2*) were studied in detail (Kutter *et al.*, 2007). *AGL16m* transformants carry a miR824-resistant form of *AGL16* generated by seven silent mutations to block cleavage at the miR824 pairing site (Figure 5.1). Several T2 lines were obtained. Two independent lines overexpressing wild-type *AGL16* (named *AGL16.1/2*) in the Col-0 background and the miRNA-resistant form *AGL16m* in the Col-0 (named Col-0 *AGL16m1/2*) and *m3* background (named *m3 AGL16m1/2*) were studied in detail. Quantitative RT-PCR of *AGL16* mRNA confirmed that, relative to wild-type Col-0, *AGL16* transcripts were increased by 5- to 7-fold in *AGL16.1/2* plants, by 16- to 19-fold in Col-0 *AGL16m1/2*, and by 14- to 16-fold in *m3 AGL16m1/2* whereas the relative accumulation of the unrelated *SCL6-III* mRNA that is targeted by miR171 was not affected in the *AGL16m1/2* and *AGL16.1/2* lines (Figure 5.2 A). miR824 and miR171 levels were not altered in the *AGL16.1/2* or *AGL16m1/2* lines compared to their backgrounds (Figure 5.2 B), indicating that overexpression of *AGL16* and *AGL16m* does not have a general effect on miRNA biogenesis and targeting. Overexpression of miR824, as shown in *m3*, leads to degradation of wild-type *AGL16* transcripts (Figure 4.13 B). However, elevated miR824 accumulation is insufficient to cause increased degradation of the miR824-resistant *AGL16* transcript in *m3 AGL16m1/2*. Because the probe used for RNA blot hybridization does not distinguish between *AGL16* and *AGL16m* transcripts, *AGL16m* RNA expression in the *AGL16m* transformants were confirmed by treating RT-PCR products with *HincII* restriction endonuclease that only cuts the miRNA resistant form (Figure 5.2 C). Interestingly, the 163 bp fragment obtained by RT-PCR, representing the endogenous *AGL16* transcript, was reduced in *AGL16m* lines relative to controls. This might reflect negative regulation of *AGL16* RNA by *AGL16m* RNA as reported for other miRNA resistant targets (Schwab *et al.*, 2005; Sunkar *et al.*, 2006). These results show that miR824-mediated regulation of *AGL16* mRNA requires complementarity with miR824 and demonstrates that very small sequence alterations in the miR824 binding site of *AGL16* impair miR824 cleavage activity.

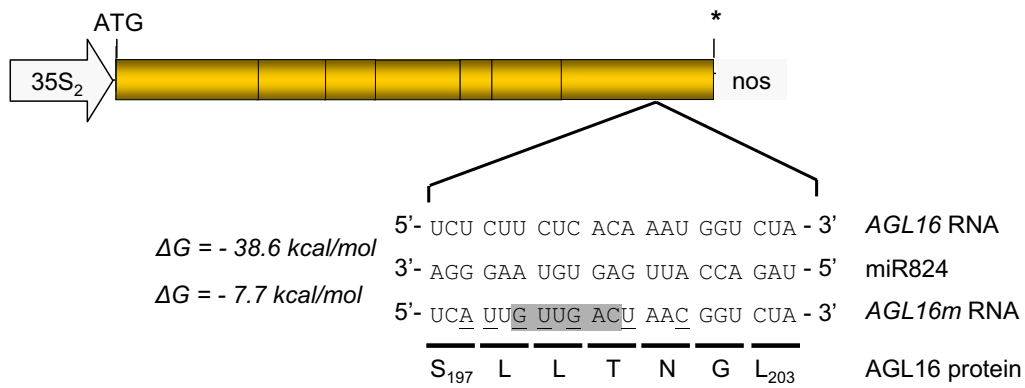


**Figure 5.1: Schematic presentation of the *AGL16m* transgene.**

The nucleotide sequence of a resistant version of *AGL16* (*AGL16m*) with silent mutations in the miR824 recognition site is shown. miR824 pairs to *AGL16* RNA at the nucleotide segment corresponding to the amino acids S<sub>197</sub> and L<sub>203</sub>. The seven mutations introduced to create *AGL16m* are shown by underlined nucleotides with predicted free energies of pairing to miR824 indicated on the left. Vertical lines indicate perfect base pairing; circles indicate G:U wobble pairing; gray shading indicates the *HincII* restriction site (GTT/GAC) introduced into *AGL16m*.

## 2. Phenotypical characterization of transgenic lines altered in *AGL16* mRNA expression

### 2.1. Leaf abnormalities

Comparison of flowering plants revealed no differences in the general macroscopic defects in growth or development in the *agl16-1* mutant (Figure 4.13 D). Similar findings were obtained for the miR824-overexpressing mutant *m3* and *m4*, which showed reduced *AGL16* mRNA accumulation (Figure 4.10 E). Furthermore, the sizes (leaf area) and the forms (length and width of the leaf blade) of rosette leaves were evaluated and no differences were observed. This results show that *AGL16*-deficiency lead to inconspicuous changes in morphology.

A slight upward curling of leaves was observed in the mutant *m1* and *m2* (Figure 4.10 E), which showed reduction in miR824-expression but increased *AGL16* mRNA accumulation. These macroscopically visible abnormalities were much more dramatic in the *AGL16m* transgenic lines in both the Col-0 (Figure 5.3 E, F) and *m3* backgrounds (Figure 5.3 H, I). The plants exhibited a bushy growth habit and increased numbers of leaves that were reduced in size. Distortions in leaf morphology included elongation, increased green pigmentation, twisting along the apical-basal axis, and upward curling of the margin and lamella (Figure 5.3 E', F' and H', I'). To examine the structure of the internal leaf tissue, semi thin sections

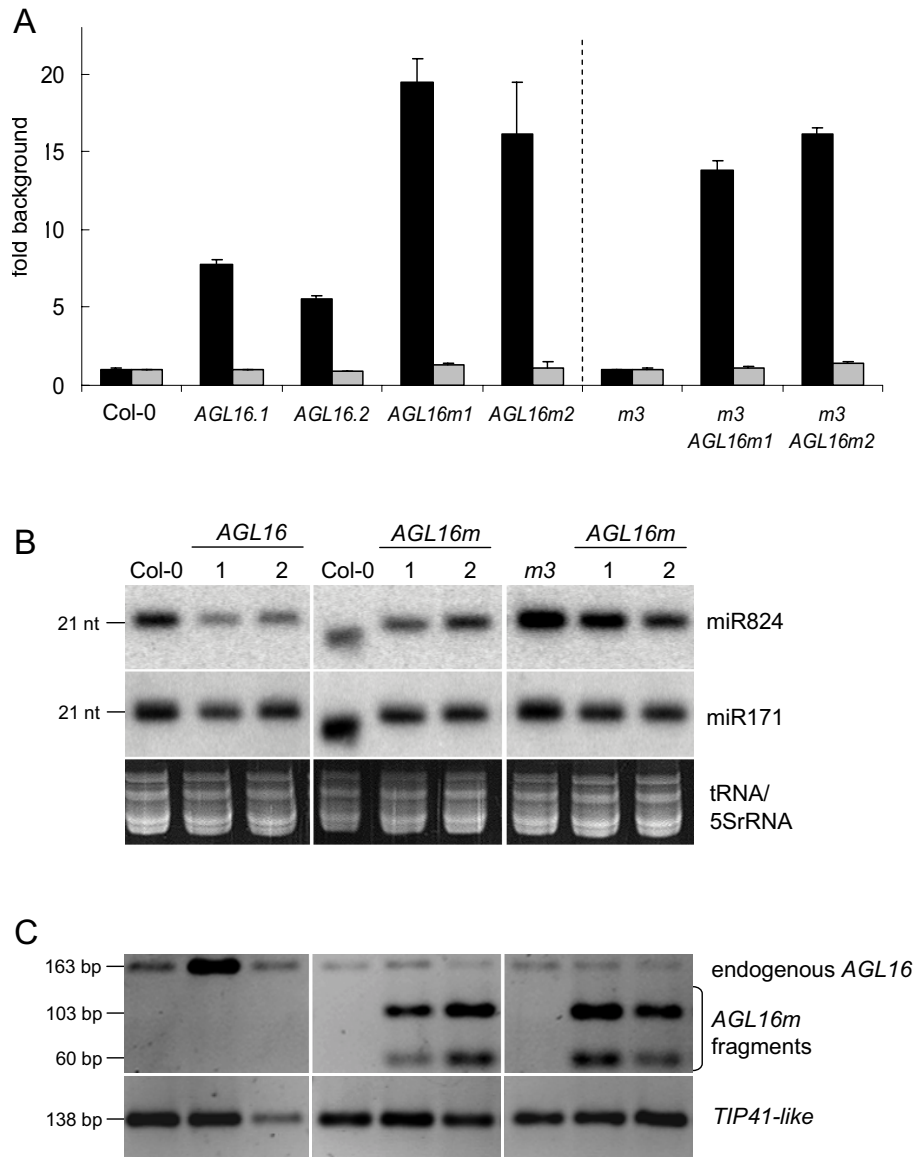


**Figure 5.2: Expression of miR824 and *AGL16* mRNA in *AGL16.1/2* and *AGL16m1/2* rosette leaves.**

(A) Steady-state levels of uncleaved target *AGL16* mRNA (black bar) and *SCL6-III* mRNA (grey bar) in leaves of Col-0, Col-0 *AGL16.1/2*, Col-0 *AGL16m1/2*, *m3*, and *m3 AGL16m1/2* determined by RT-qPCR using primers spanning the miR824 and the miR171 complementary site. Quantifications were normalized to *TIP41-like* gene (At4g34270). The values in wild-type Col-0 and *m3* were arbitrarily fixed to 1. Bars indicate standard error. (B) RNA blot hybridization of low molecular weight RNAs. Low molecular weight RNAs were detected by using probes for miR824 and the unrelated miR171. Equal loading was verified by ethidium bromide staining of tRNA/5S rRNA. Equal loading was verified by ethidium bromide staining of rRNA. The size of RNAs is indicated on the left. (C) *AGL16* and *AGL16m* transcripts were distinguished by *HincII* digestion, which only digests *AGL16m* cDNA, after RT-PCR amplification of endogenous and *AGL16m* transcripts.

of mature rosette leaves were analyzed by light microscopy. No differences in tissue organization, cell numbers, or cell sizes could be observed between wild-type and mutants. The parenchyma is composed of a single layer of adaxial palisade parenchyma and four to five layers of spongy parenchyma. A rosette leaf thus consists of seven to eight cell layers including the abaxial and the adaxial epidermis. As shown by SEM, no apparent abnormalities were detected in either the shape or dorso-ventral symmetry of parenchyma cells of Col-0 (Figure 5.4 A), *AGL16m* transformants (Figure 5.4 B, D), *m3* (Figure 5.4 C), or *agl16-1* (Figure 5.4 E) that could account for the observed alterations in leaf shape. However, the cellular structure of epidermal derivatives on the leaf surface, like trichomes, was altered. Trichomes in the *AGL16m1/2* lines formed sometimes two branches or, more frequently four branches, rather than three branches as expected for wild-type Col-0 (Figure 5.4 F-H).

## 2.2. Alteration in stomatal density

The report that *AGL16* mRNA accumulates in guard cells of leaves (Alvarez-Buylla *et al.*, 2000), suggested that miR824-mediated regulation of *AGL16* might have a role in stomatal development. Mutants altered in stomatal development often exhibit changes in stomatal density, i.e., the number of stomata per mm<sup>2</sup> of epidermis (Bergmann and Sack, 2007) or in stomatal index (SI) defined as the ratio of the number of stomata to the number of epidermal cells plus stomata (Berger and Altmann, 2000). Scanning electron microscopy (SEM) of the abaxial, i.e., lower surface (Figure 5.5) and the adaxial, i.e., upper surface (Figure 5.6) of the fifth rosette leaf of Col-0, Col-0 *AGL16.1/2*, Col-0 *AGL16m1/2*, *m3*, *m3 AGL16m1/2*, and *agl16-1* were performed. Both leaf surfaces were investigated in the beginning since it has been shown that stomatal density can vary in different organs (Bergmann, 2006). Figure 5.7 A show that the average stomatal densities of the abaxial and adaxial surface of Col-0 *AGL16.1/2* plants did not differ significantly from Col-0. Stomatal density of both surfaces was significantly reduced in *agl16-1* (abaxial: 1.2-fold, adaxial: 1.3-fold) and in the *m3* mutant (abaxial: 1.2-fold, adaxial: 1.7-fold), but was drastically increased in the two independent lines of Col-0 *AGL16m1/2* (abaxial: 2.2- to 2.9-fold, adaxial: 2.4- to 3.2-fold) and of *m3 AGL16m1* (abaxial: 2.6-fold, adaxial: 1.4- to 2.7-fold). Taken together, these results show that stomatal density is decreased in mutants with reduced or no *AGL16* expression and increased in *AGL16m* mutants with increased *AGL16* expression on both the abaxial and adaxial leaf surface. None of the lines altered in *AGL16* expression showed dramatic changes of stomatal index on both the abaxial and adaxial leaf surface (Figure 5.7 B).

In addition, stomatal density of the abaxial and adaxial leaf surface of the fifth rosette leaf was measured for representative RNA silencing mutants (Figure 5.7 C). Stomatal den-

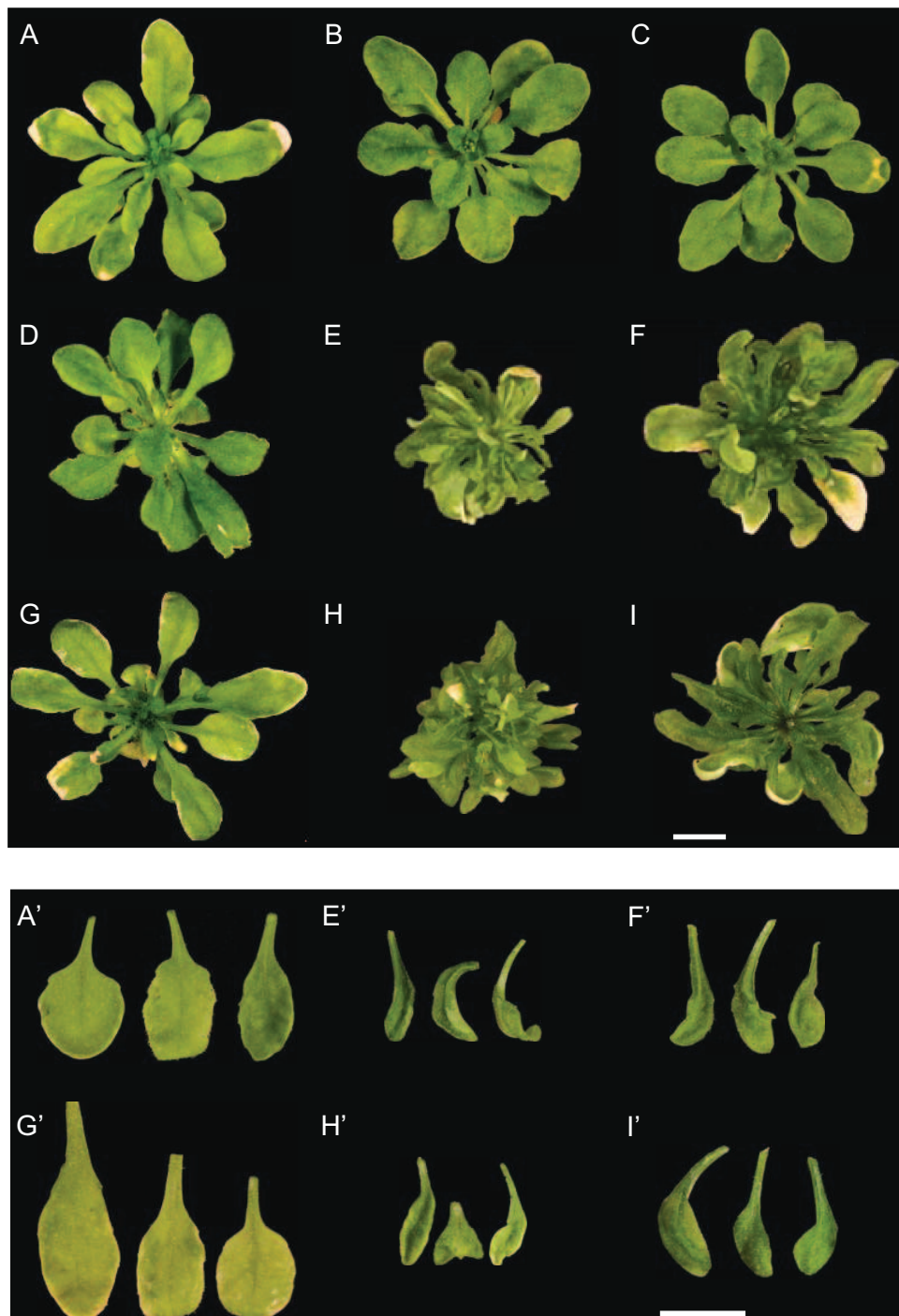


**Figure 5.3: Phenotypical differences caused by *AGL16* overexpression.**

Representative images of (A) Col-0, (B and C) Col-0 *AGL16.1/2*, (D) *agl16-1*, (E and F) Col-0 *AGL16m1/2*, (G) *m3*, and (H and I) *m3 AGL16m1/2* grown under the same conditions and photographed with roots and inflorescences removed of 28 day old plants. Individual rosette leaves magnified 1.8 times are shown below. The number corresponds to the plants above. The representative images show that independent transformants expressing *AGL16m* RNA in both the Col-0 and *m3* backgrounds consistently exhibit, a bushy growth habit and curled, abnormal-appearing rosette leaves. Bar: 1 cm.

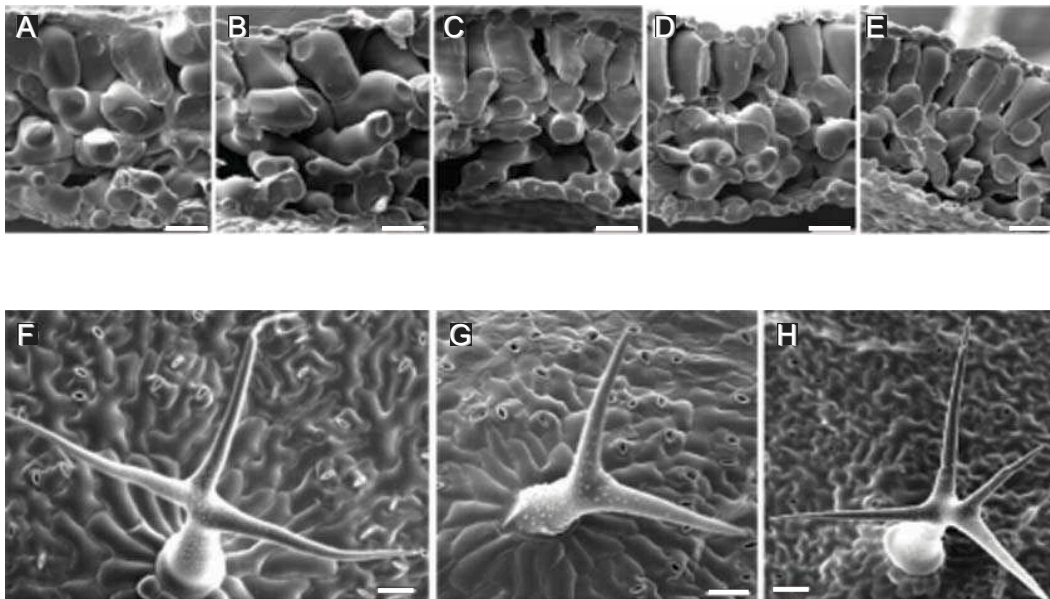


**Figure 5.4: SEM images of mesophyll cells and trichomes of *AGL16m* transformants and control plants.**

(A-E) Transverse sections of rosette leaves showing adaxial epidermal cells (top), vertically elongated palisade mesophyll cells directly beneath the adaxial epidermis, and the loosely packed spongy mesophyll cells with intercellular air spaces directly above the abaxial epidermis (bottom). No conspicuous differences were detected in the arrangement of the mesophyll in (A) Col-0, (B) Col-0 *AGL16m1*, (C) *m3*, (D) *m3 AGL16m1*, or (E) *agl16-1* leaves. (F-H) Morphology of trichomes on the adaxial surface of rosette leaves. (F) Col-0, *m3*, and *agl16-1* plants (not shown) form unicellular trichomes, almost always with three branches. In contrast Col-0 *AGL16m2* plants develop aberrant trichomes with two branches (G), or more frequently, four branches (H). Bar: 50  $\mu$ m.

sity of both surfaces was highly increased in *hen1-5* (abaxial/adaxial: 3.3-fold) and *dcl1-8* (abaxial/adaxial: 1.6-fold) and moderately in *hyl1-2* and *dcl4-2* (abaxial/adaxial: 1.1-fold, in both cases). In these mutants increased *AGL16* transcript levels were also detectable, like in the miR824 resistant *AGL16* mutant. However, it is inconclusive whether the increase in stomatal density is only caused by altered *AGL16* mRNA since other miRNA targets are regulated by HYL1, HEN1, DCL1, and DCL4 as well. The miRNA targets might be involved in developmentally controlled pathways, making interpretations of the stomatal phenotype of *hyl1-2*, *hen1-5*, *dcl1-8*, and *dcl4-2* difficult.



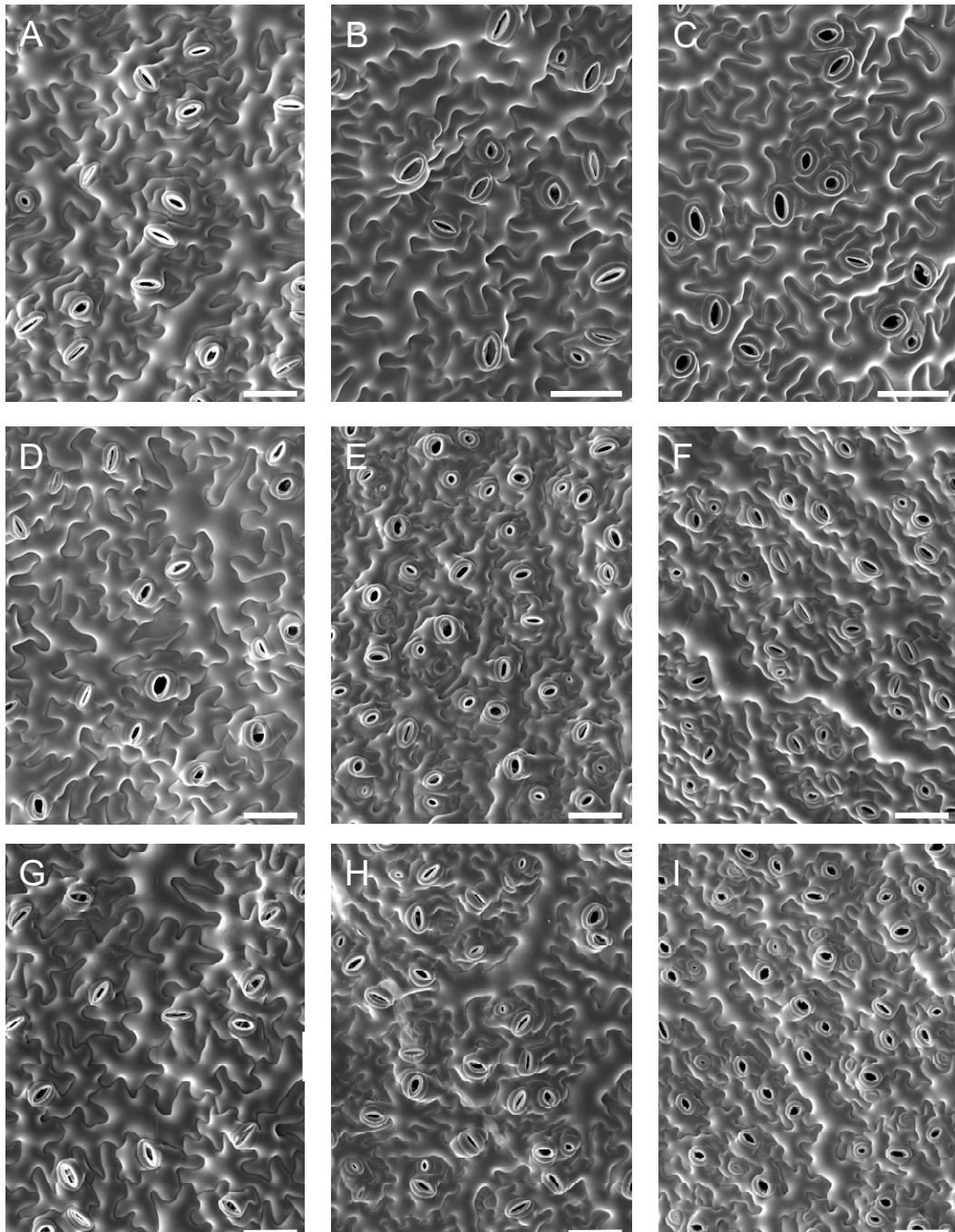


**Figure 5.5: The positioning of stomatal complexes on the abaxial epidermis of transgenic *Arabidopsis* plants altered in *AGL16* mRNA expression.**

(A-I) Representative low-magnification SEM images of the abaxial surface of rosette leaves 4-6 numbered from the bottom of the plant. (A) Col-0, (B and C) Col-0 *AGL16.1/2*, (D) *agl16-1*, (E and F) Col-0 *AGL16m1/2*, (G) *m3*, and (H and I) *m3 AGL16m1/2*. Bar: 50  $\mu$ m.

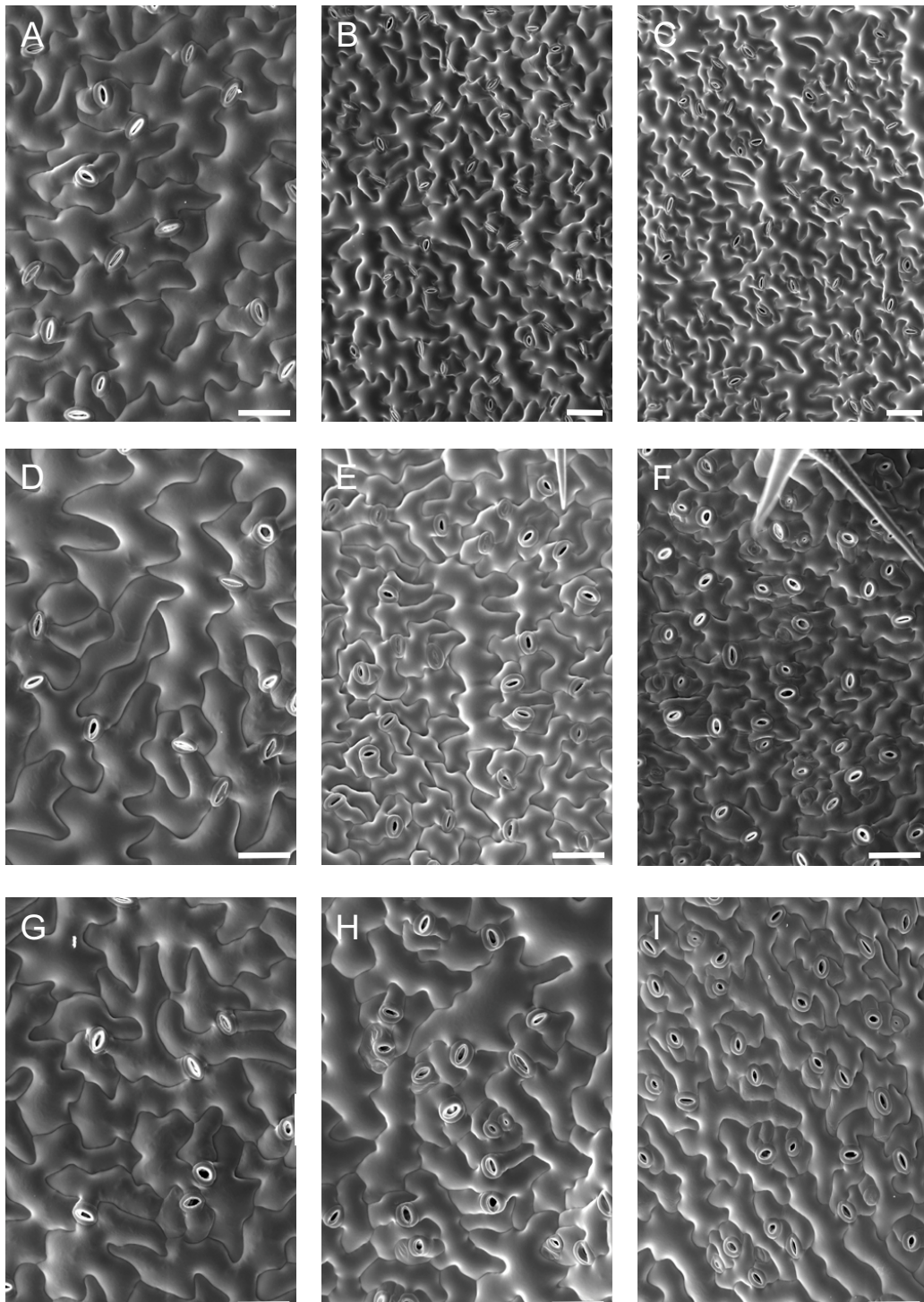


**Figure 5.6: The positioning of stomatal complexes on the adaxial epidermis of transgenic *Arabidopsis* plants altered in *AGL16* mRNA expression.**

(A-I) Representative low-magnification SEM images of the adaxial surface of rosette leaves 4-6 numbered from the bottom of the plant. (A) Col-0, (B and C) Col-0 *AGL16.1/2*, (D) *agl16-1*, (E and F) Col-0 *AGL16m1/2*, (G) *m3*, and (H and I) *m3 AGL16m1/2*. Bar: 50  $\mu$ m.

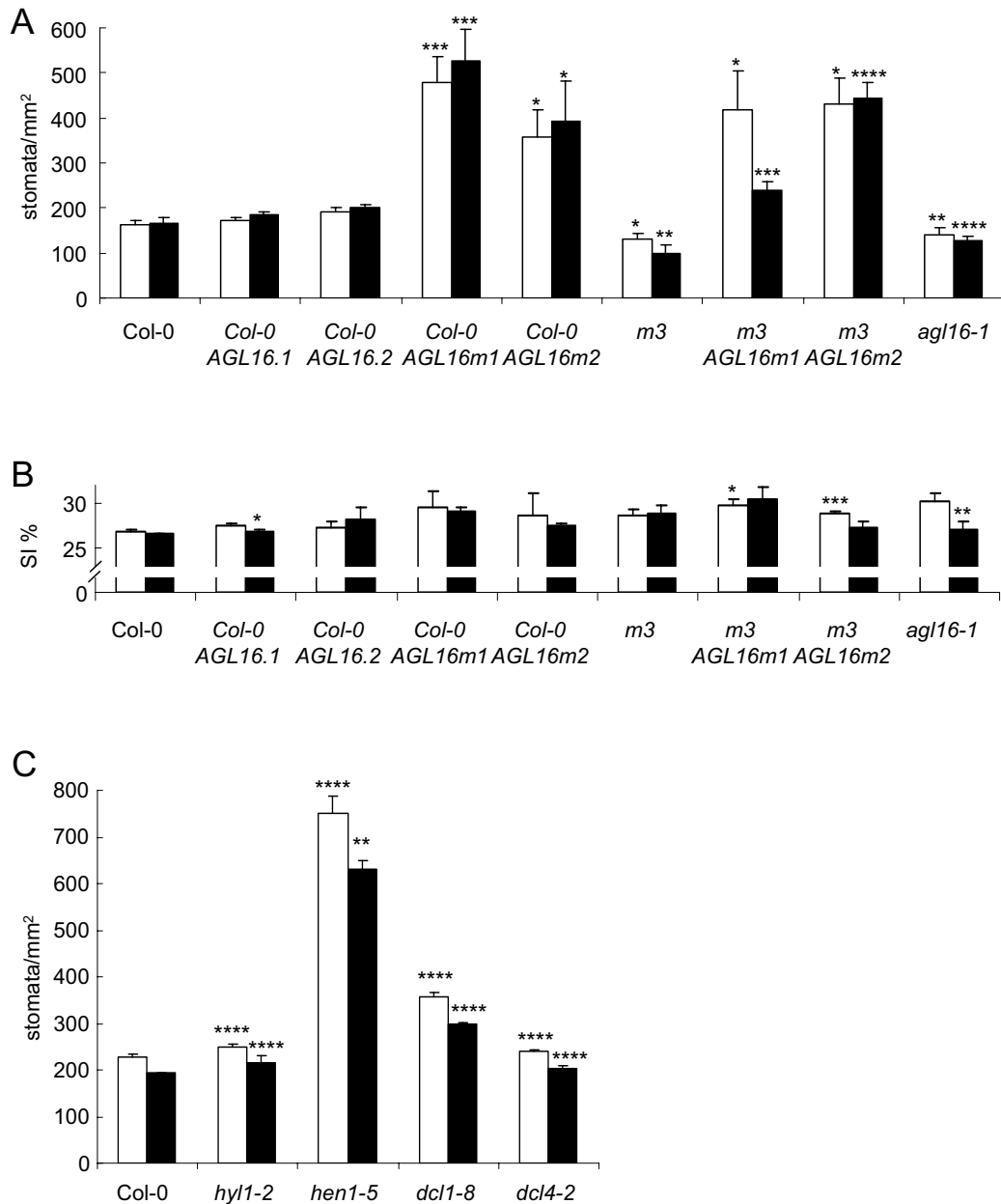


**Figure 5.7: Effects of altered AGL16 mRNA expression on stomatal density and stomatal index.**

(A) Average stomatal density and (B) average stomatal index (SI%)  $\pm$  s.e.m for 3-4 replicates of the abaxial and adaxial surface of the fifth rosette leaves of Col-0, Col-0 AGL16.1/2, Col-0 AGL16m1/2, m3, and m3 AGL16m1/2 was determined. (C) Average stomatal density for 3-4 replicates of the abaxial and adaxial surface of the fifth rosette leaves of Col-0, hyl1-2, hen1-5, dcl1-8, dcl4-2. Significance levels (t-test of means) relative to the Col-0 controls: \*p<0.05, \*\*p<0.025, \*\*\*p<0.01, and \*\*\*\*p<0.005.

### 2.3. Alterations in the density of higher-order stomatal complexes

Three sequential unequal divisions of the initial cell result in the formation of three neighboring cells that surround the central guard cell mother cell, leading to the Brassicaceae-specific anisocytic stomatal phenotype. All lines studied have this anisocytic structure. The guard cell morphology was also normal in *AGL16m* mutants. Fused stomata (Figure 5.8 A), typical for stomatal mutants impaired in the symmetric division of guard mother cells, like *tmm* (Yang and Sack, 1995) or *flp* (Geisler *et al.*, 1998), were observed in ca. 2% of Col-0 *AGL16m* (6 in 285 stomatal complexes) and wild-type (2 in 112 stomatal complexes) plants indicating that this rare abnormality is not a specific result of the mutation. However, alterations in the density of higher-order stomatal complexes were observed. Representative SEM images of individual primary- (Figure 5.9 A) and quaternary-stomatal complexes (Figure 5.9 B) are demonstrated. Figure 5.9 C shows the percentage of primary, secondary, and higher order stomatal complexes estimated for comparable abaxial regions of the fifth fully expanded leaves for Col-0, Col-0 *AGL16.1/2*, Col-0 *AGL16m1/2*, *m3*, and *agl16-1* plants. Similar results were obtained in three independent experiments. The proportion of stomatal-complex types of Col-0 *AGL16.1/2* did not differ significantly from that of Col-0 ( $\chi^2$ , df=2,  $P>0.94$ ). These three lines developed predominantly primary stomatal complexes (69-71%), with considerably lower incidences of higher-order secondary (26-28%), tertiary (3-4%) stomatal complexes, and no quaternary stomatal complexes. The distributions obtained with *agl16-1* and *m3* plants deficient in *AGL16* mRNA accumulation also differed significantly from that of Col-0 ( $\chi^2$ , df=1,  $P<2.7 \times 10^{-5}$ ), but unlike *AGL16m1/2* showed a higher percentage of primary complexes relative to Col-0, 91% and 93% respectively, and lacked tertiary complexes. In contrast, the distributions of Col-0 *AGL16m1/2* plants and *m3 AGL16m1/2* plants differed significantly from that of Col-0 ( $\chi^2$ , df=2,  $P<3.0 \times 10^{-9}$ ) and *m3* ( $\chi^2$ , df=2,  $P<3.0 \times 10^{-9}$ ) and consistently showed a dramatic shift to higher-order stomatal complexes in which secondary and tertiary forms predominate. Moreover, 2-5% of the complexes in Col-0 *AGL16m1/2* and *m3 AGL16m1/2* plants were quaternary forms, which were never detected in Col-0 or Col-0 *AGL16.1/2* plants. By performing a time course of stomatal development on the abaxial surface of the first emerging leaf we showed that reduced *AGL16* expression (*m3* and *agl16-1*) abolishes the formation of satellite meristemoids but did not alter the kinetics of primary stomatal complex development. Expression of miR824-resistant *AGL16m* mRNA, on the other hand, increased the incidence of early meristemoid formation, prolonged the period of SM initiation, and therefore significantly increased the proportion of higher-order stomatal complexes (Kutter *et al.*, 2007).



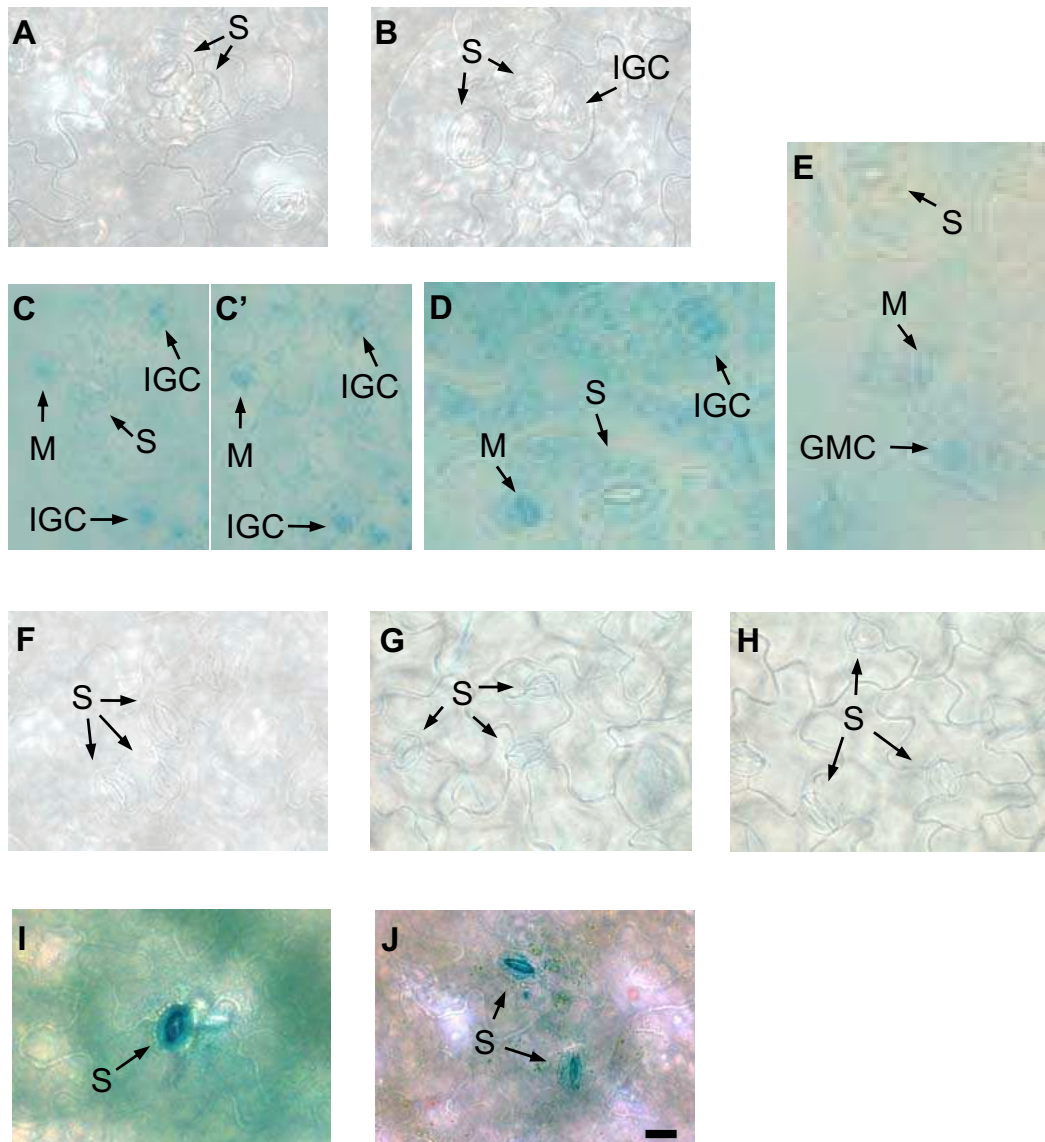


**Figure 5.8: Promoter expression studies in stomatal complexes of rosette leaves of transgenic *Arabidopsis* plants.**

(A-J) Staining of the abaxial epidermis of the first true leaves of *Arabidopsis thaliana* two week after germination is shown. Region with positive promoter activity appear blue due to GUS reporter gene expression. (A-B) untransformed wild-type plants, transformed plants with (C-E) *Pro<sub>MIR824</sub>:GUS*, (F) *Pro<sub>AGL16</sub>:GUS*, (G-H) *Pro<sub>AGL16-1</sub>:GUS*, (I-J) *Pro<sub>AGL16-12</sub>:GUS*. Regions hybridizing with the probe appear dark gray. Mature stomata (S), meristemoids and satellite meristemoids (M), and immature guard cell (IGC) are indicated. Bar: 10  $\mu$ m.

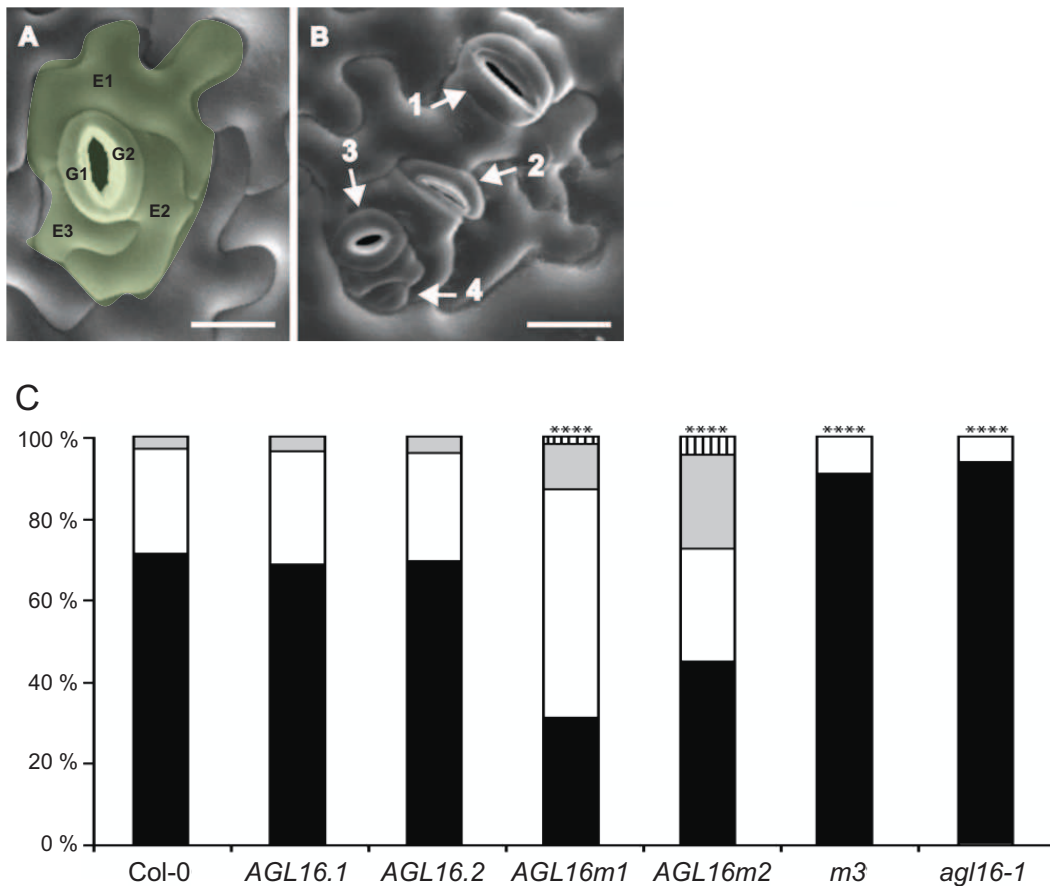


**Figure 5.9: Effects of altered *AGL16* expression on the proportion of primary and higher-order stomatal complexes.**

(A and B) Representative SEM images of stomatal complexes on the abaxial surface of the fifth rosette leaf. (A) A primary Col-0 stomatal complex consisting of a central pair of guard cells (G1 and G2) and stoma surrounded by neighboring cells (E1, E2, and E3). (B) A quaternary stomatal complex of *AGL16m1* with primary, secondary, tertiary, and quaternary complexes is shown. The numbered arrows indicate the apparent order in which stomata form. Note that the fourth order stomata is at the early, SM stage of development. Bar: 10  $\mu\text{m}$ . (C) The relative proportion of primary (black bars), secondary (white bars), tertiary (gray bars) and quaternary (vertical-hatched bars) stomatal complexes on the abaxial surface of the fifth rosette leaf of Col-0, *AGL16.1/2*, *AGL16m1/2*, *m3* and *agl16-1* plants. At least 110 stomatal complexes were scored for each line. Asterisks above the bars indicate distributions significantly different ( $P < 5 \times 10^{-5}$ ) from that of the Col-0 distribution by the  $\chi^2$  test.

#### 2.4. Localization studies of miR824 and AGL16 mRNA in different cell types of the stomatal complex

In situ hybridization (ISH) of whole mounts of *B. rapa* developing leaves showed that miR824 is expressed in SMs and GMCs, but not in mature guard cells. In contrast, AGL16 mRNA was only detected in mature guard cells and not in cells of stomatal complexes where miR824 is localized (Kutter *et al.*, 2007). Whole mount ISH could not be done in Arabidopsis plants because of technical problems. To better understand the cell-type specific expression pattern, transgenic Arabidopsis plants were generated by introducing a  $\beta$ -glucuronidase (*GUS*) reporter gene fused either to the full-length *MIR824* promoter (*Pro<sub>MIR824</sub>:GUS*), to the full-length *AGL16* promoter (*Pro<sub>AGL16</sub>:GUS*), to the full-length *AGL16* promoter with the first intron sequence (*Pro<sub>AGL16-I</sub>:GUS*) or with the first and second intron sequence (*Pro<sub>AGL16-I2</sub>:GUS*). Reporter expression was analyzed in developing T1 plants. As expected, no *GUS* staining was detectable in untransformed wild-type plants (Figure 5.8 A and B). The reporter signal in *Pro<sub>MIR824</sub>:GUS* plants was detectable in young leaves at the time when the stomatal lineage is initiated and was restricted to meristemoids, GMCs, and young guard cells (Figure 5.8 C-E). Like in infiltration assays in *B. rapa*, no *GUS* staining was detected in transformed plants with *Pro<sub>AGL16</sub>:GUS* (Figure 5.8 F) or *Pro<sub>AGL16-I</sub>:GUS* (Figure 5.8 G-H). *GUS* activity was detected in mature stomata of *Pro<sub>AGL16-I2</sub>:GUS* plants (Figure 5.8 I-J). ISH studies with *B. rapa* and the *GUS* reporter gene studies with Arabidopsis lead to the conclusion that although both miR824 and its target are localized in stomatal complexes, they are never detected in the same cell type.

## 6. The molecular basis for *AGL16* function

Contributions to this chapter:

I did most of the experiments described in this chapter. Herbert Angelika processed Affymetrix microarrays. Edward J. Oakeley helped with the experimental design, statistics, and analysis of the Affymetrix data.



## 1. Specific effects of ectopic expression of *AGL16* on the plant transcriptome

### 1.1. Ectopic expression of *AGL16* regulates genes with diverse functions

Expression profiling experiments surveying 22,810 Arabidopsis genes were performed to identify genes regulated downstream of AGL16. *AGL16m1* plants ectopically expressing the miR824-resistant *AGL16m* transcript and wild-type Col-0 were grown axenically on  $\frac{1}{2}$  x MS medium. Leaves from each type of plant were harvested after 25 days. This time point was selected to minimize non-specific changes due to the faster growth and development of Col-0 plants. The scatterplot (Figure 6.1 A) shows that 14990 genes are expressed in *AGL16m1* and Col-0. About 91% of the expressed genes were identical in both groups, only 126 genes showed a significant (t-test,  $P < 0.05$ ), 2.0-fold difference in expression in the two genotypes. Of these, 97 genes were upregulated and 29 genes downregulated in *AGL16m1* relative to wild-type (Figure 6.1 B).

These genes were classified by putative functions based on Arabidopsis Gene Ontology (GO) annotations in the TIGR and TAIR (version 7.0) database, Affymetrix GO platform. The functional clusters enriched in *AGL16m1* upregulated genes include gene products known to be induced in response to abiotic or biotic stress. Many genes encoding proteins that regulate developmental processes, such as transcription factors, signaling proteins, senescence-related proteins, and hormone metabolism were also enriched in *AGL16m1*. Other candidate genes encode hydrolases, transferases, and kinases that are involved in protein, carbohydrate, lipid, and secondary metabolism (Figure 6.1 C, Table 6.1).

**Table 6.1.: Biological and molecular function of gene candidates up- and downregulated in *AGL16m1*.**

GO biological and molecular function	number best candidates	number of genes upregulated in <i>AGL16m1</i>	number of genes downregulated in <i>AGL16m1</i>
secondary metabolism & cell wall	10 (8%)	7 (70%)	3
fatty acid & lipid metabolism, transport	12 (10%)	7 (58%)	5
carbohydrate metabolism	7 (6%)	7 (100%)	-
protein catabolism/metabolism	13 (11%)	9 (69%)	4
abiotic & biotic stress, signaling	28 (23%)	23 (92%)	5
transcription factor	13 (11%)	11 (85%)	2
senescence	4 (3%)	4 (100%)	-
unknown functions	39 (31%)	30 (77%)	9

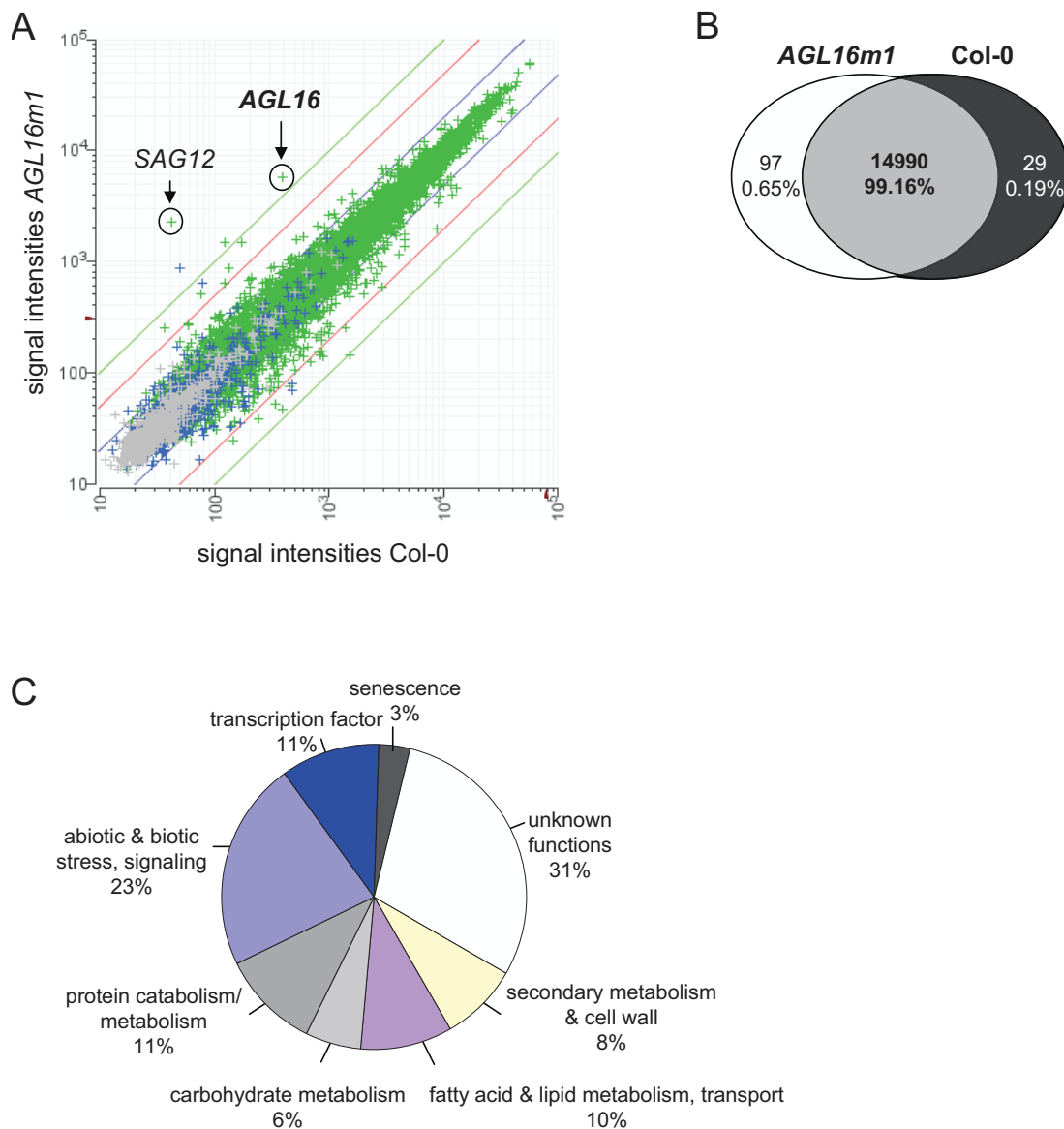


**Figure 6.1: Transcriptional profiling of rosette leaves of Col-0 and Col-0 *AGL16m1*.**

(A) For each chip experiment, overall intensity normalization for the entire probe set was performed as described by Zhu *et al.* (2001). Scatterplot comparing signal intensities of genes in Col-0 (x-axis) and Col-0 *AGL16m1* (y-axis). Invalid counts (723) in grey, valid counts (852) in either Col-0 or Col-0 *AGL16m1* in green, and valid counts (13415) in both Col-0 and Col-0 *AGL16m1* in blue. Fold-changes greater than 1.3, 1.7, and 2.0 are marked by respectively a blue, red, and green line. Expression of *AGL16* and *SAG12* are indicated by an arrow. (B) Expression of transcripts in Col-0 and Col-0 *AGL16m1* after grouping of replicates, performing TTEST  $p < 0.05$ , and expression differences of 2-fold. 14 990 genes are expressed in both Col-0 and Col-0 *AGL16m1* (grey), 29 genes are altered in Col-0 (black), and 97 genes in *AGL16m1*. (C) Functional categorization of differential expressed genes.

**Table 6.2.: Expression levels and relevant motifs of genes upregulated in *AGL16m1*.**

Description	AGI	Expression <sup>a)</sup>		Fold <sup>b)</sup>		Motif <sup>c)</sup>		Reference <sup>d)</sup>	expression gene atlas <sup>e)</sup>
		Col-0	<i>AGL16m1</i>	Ratio <i>AGL16m1</i>	Regulation score	CArG- motif	TAATG- motif		
MADS-box protein ( <i>AGL16</i> )	At3g57230	386.9	5054.1	13.1	13.1	+	+	1, 8, 9	lv, ro
senescence-specific SAG12 protein/ putative cysteine proteinase	At5g45890	21.6	233.3	10.8	10.8	+	+	2, 3, 5, 6, 7	sen lv, fl
putative pathogenesis-related protein	At2g19970	26.0	145.3	5.6	5.6	+	+		lv, ro, em
expressed protein	At1g55265	27.6	124.5	4.5	4.5	+	+		sen lv, fl
expressed protein	At3g21520	27.0	98.6	3.7	3.7	+	+		sen lv, em
glutathione S-transferase, putative	At5g62480	23.9	71.1	3.0	3.0		+	10	em, dry se
putative AP2 domain-containing transcription factor	At4g34410	698.7	230.5	0.3	3.0	+	+	9	ro, y lv, sdl
expressed protein	At1g30135	146.6	46.6	0.3	3.1	+	+		em, y lv
MATE efflux family protein	At1g61890	6420.5	2040.4	0.3	3.1	+	+		em, lv, fl
organic cation transporter family protein	At3g20660	206.9	49.6	0.2	4.2	+			em, se
expressed protein	At1g73120	375.4	74.7	0.2	5.0	+	+		dry se
pectinesterase family protein	At4g02330	1427.2	299.5	0.2	4.8	+	+	4	lv
putative cytochrome P <sub>450</sub>	At2g27690	706.0	122.9	0.2	5.7	+	+		lv, em
expressed protein	At5g13220	568.2	86.8	0.2	6.5	+	+		fl, em

<sup>a)</sup> Expression value represents mean, normalized expression level for 3 independent plants measured by quantitative PCR.

<sup>b)</sup> Fold expression relative to Col-0

<sup>c)</sup> Presence (+) or absence(-) in the promote region of the MADS box transcription factor CArG motif and the guard-cell specific TAATG motif.

<sup>d)</sup> References:

<sup>1)</sup> Alvarez Buylla et al., 2000; <sup>2)</sup> Gan & Amasino, 1986; <sup>3)</sup> Grbic & Bieecker, 1995; <sup>4)</sup> Micheli et al., 1998; <sup>5)</sup> Noh & Amasino, 1999; <sup>6)</sup> Lohman et al., 1994; <sup>7)</sup> Otegui et al., 2005; <sup>8)</sup> Parenicova et al., 2003; <sup>9)</sup> Riechmann et al., 2000; <sup>10)</sup> Wagner et al., 2002

dry se, dry seeds; em, embryo; fl, flowers; lv, leaves; ro, roots; sdl, seedlings; se, seeds; sen lv, senescence leaves; y lv, young leaves

<sup>e)</sup> [www.genevestigator.ehz.ch](http://www.genevestigator.ehz.ch) (Zimmermann et al., 2004)

As expected, *AGL16* showed the highest induction (13.1-fold) in *AGL16m1* (Table 6.2). The gene showing the second highest induction (10.8-fold) was *SAG12* (*SENESCENCE ASSOCIATED GENE 12*) encoding a cysteine-protease (At5g45890) that is specifically involved in senescence. Interestingly, *SAG12* was shown to be expressed in stress vacuoles of guard cells (Otegui *et al.*, 2005).

Quantitative PCR was used to measure the expression of the 14 genes showing >3-fold upregulation in *AGL16m1* in the array experiment. For ten of these genes, expression levels obtained from the array experiment and by quantitative PCR were correlated (Table 6.3) In general; however, the quantitative PCR values were lower than those from the array experiment. Interestingly, expression of 9 of the genes upregulated in *AGL16m1* were unchanged in *AGL16.1*. Only *AGL16* itself was upregulated in both *AGL16m1* (9.3-fold) and *AGL16.1* (5.6-fold). Together these results suggest that increased expression of the 9 candidate genes is a specific effect of increased, ectopic expression of the miR824-resistant form of *AGL16*.

## 1.2. Identification and analysis of promoter motifs of the candidate genes

MADS domain proteins generally bind to a consensus DNA sequence called a CArG motif with the canonical sequence CC(A/T)<sub>6</sub>GG (Riechmann *et al.*, 1996) To investigate whether

**Table 6.3.: Comparison of microarray expression values and quantitative RT-PCR expression values of candidate genes.**

Description	AGI	Ratio			match to RT-qPCR
		profiling <i>AGL16m1</i>	RT-qPCR <i>AGL16m1</i>	RT-qPCR <i>AGL16.1</i>	
MADS-box protein (AGL16)	At3g57230	13.1	9.3	5.6	+++
senescence-specific SAG12 protein	At5g45890	10.8	6.4	1.5	+++
putative pathogenesis-related protein	At2g19970	5.6	3.7	2.0	+
expressed protein	At1g55265	4.5	2.4	1.0	++
expressed protein	At3g21520	3.7	3.7	0.8	+++
putative glutathione S-transferase	At5g62480	3.0	2.9	1.9	+
putative AP2 domain-containing transcription factor	At4g34410	0.3	0.7	1.4	-
expressed protein	At1g30135	0.3	0.8	0.9	-
MATE efflux family protein	At1g61890	0.3	0.5	0.7	+
organic cation transporter family protein	At3g20660	0.2	0.9	1.8	-
expressed protein	At1g73120	0.2	0.4	0.9	++
pectinesterase family protein	At4g02330	0.2	0.4	0.7	+
putative cytochrome P <sub>450</sub>	At2g27690	0.2	0.3	1.8	+++
expressed protein	At5g13220	0.2	1.0	0.9	-
MIR824	At4g24415	n.d.	1.3	1.1	n.d.

a) Fold expression relative to Col-0 (mean, normalized expression level for 3 independent plants measured by profiling or quantitative (q) PCR)

b) Consensus of profiling and qPCR data are indicated (-, no; +, low; ++, middle; +++ high)

AGL16 has DNA binding properties and binds to CARG motifs, total protein extracts of Col-0 and *AGL16m1* were tested with an AG- and AGL15-specific CARG sequences and their mutated versions of binding sites by EMSA (electro mobility shift assay). CARG 1 is an AG-selected CC-6-GG type motif, CARG 2 is a C-8-G type of motif to which AGL15 preferentially binds and CARG 3 is a modified form of CARG2 C-8m-G type. A representative EMSA is shown in Figure 6.2. Protein extracts of Col-0 plants show binding to a AG-specific sequence but not to AGL15-specific or AGL15-modified sequences. Much higher affinity was obtained with protein extracts of cleavage-resistant *AGL16m1* plant suggesting that these plants might accumulate more AGL16 proteins than Col-0. These results indicate that AGL16 has CARG motif binding capacity and prefers CARG motifs with longer AT stretches. This raises the possibility that AGL16 is a transcription factor that enables expression of genes containing AG-like or even AG-specific CARG cis-acting elements in their promoter regions.

The 14 candidate genes (Table 6.2) were screened for transcriptional regulatory sequences in the PLACE database (Higo *et al.*, 1999). The region screen was upstream of the ATG initiation codon of the candidate to the stop codon of the next upstream genes predicted by

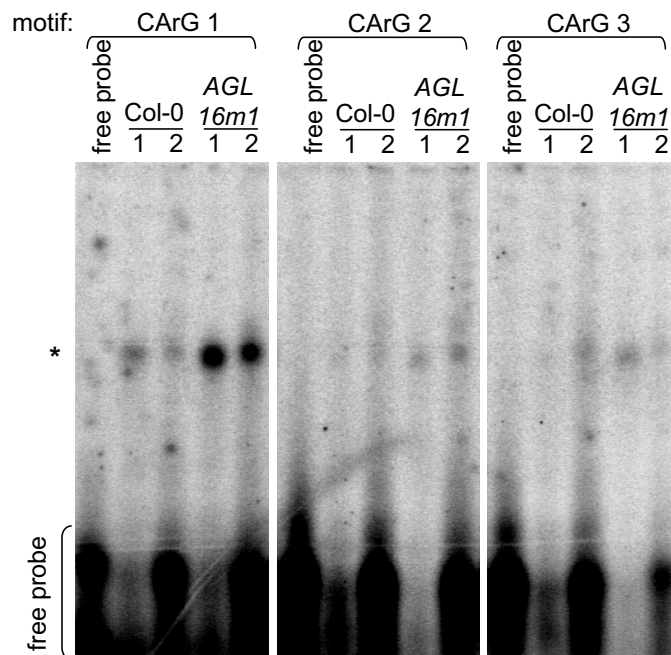


**Figure 6.2: AGL16 binds CARG motifs.**

Relative binding affinity of 5  $\mu\text{g}$  (1) and 10  $\mu\text{g}$  (2) total protein extracts of Col-0 and *AGL16m1* plants to different CARG motifs are shown by EMSA (electro mobility shift assay). *CARG1*, AG-selected CC-6-GG type canonical CARG; *CARG2*, AGL15-selected C-8-G type CARG; *CARG3*, AGL15-mutated C-8m-G type. Cleavage-resistant *AGL16* mutants, with presumably higher AGL16 protein accumulation, showed preferentially binding to a CARG motif with a shorter A/T-rich core. Shifted probes, corresponding to protein-DNA complexes, are indicated with an asterisk. All of the shifted bands were exposed to  $1.5 \times 10^6$ ,  $1.7 \times 10^6$ , or  $2.1 \times 10^6$  cpm of labeled *CARG1*, *CARG2*, or *CARG3* probes, respectively.

the TAIR (version 7) annotation (Haas *et al.*, 2005). The region 5' of the transcription start of all the candidates contained typical promoter regulators such as the TATA box. All candidates except the gene encoding a putative glutathione S-transferase (At5g62480) had a CARG-box known to be binding sites for MADS domain transcription factors (de Folter and Angenent, 2006; Kaufmann *et al.*, 2005); and, all candidates except the gene encoding an organic cation transporter family protein (At3g20660) had the TAATG motif sufficient for regulating guard cell-specific gene transcription (Plesch *et al.*, 2001). The upregulation of the candidate genes specifically in AGL16m plants, which show increased AGL16 expression and these findings suggest that AGL16 could bind the CARG-box motifs directly or in combination with other MADS-box domain transcription factors to activate expression of these candidates. The presence of the guard-cell specific motif in all but one of the candidates is consistent with the localization and putative function of AGL16 in guard cells.

Part IV

Discussion

## 7. General Discussion

The first smRNA sequencing efforts in plants (Llave *et al.*, 2002b; Park *et al.*, 2002; Reinhart *et al.*, 2002) identified only the most abundant miRNAs. These initially discovered miRNAs were highly conserved in other plant species, leading to the hypothesis that miRNAs are ancient posttranscriptional regulators of plant developmental processes. Recent high-throughput smRNA sequencing attempts identified miRNAs that are weakly expressed (Fahlgren *et al.*, 2007; Henderson *et al.*, 2006; Kasschau *et al.*, 2007; Lu *et al.*, 2005, 2006; Rajagopalan *et al.*, 2006; Zhang *et al.*, 2007). Most of these miRNAs lack identifiable homologs in other species. The finding presented here and in Kutter *et al.* (2007) show for the first time that one member of the class of non-conserved miRNAs, miR824, is important for posttranscriptional control of a taxonomically important developmental trait, namely, stomatal complexes.

### 1. Evolutionary relevance of miR824 in its biological function

My studies and those of Rajagopalan *et al.* (2006) lead to the conclusion that miR824 is a non-conserved miRNA since no miR824 orthologs could be identified in other plant species even by lowering stringency in BLAST analysis. However, miR824 is conserved in at least three *Brassica* species, *B. rapa*, *B. napus*, and *B. oleracea* for which genomic sequences are available. The target gene *AGL16*, a member of the MADS-box protein family, is also highly conserved in the *Brassica* species tested, and is likely to be present in other Brassicaceae as well. Phylogenetic analysis of the miRNA target genes provides insight into the possible evolutionary significance of miRNA-mediated regulation. For example, the highly conserved miR169 family members regulates a *HAP2* transcription factor that is important for root nodulation in alfalfa, which is a function specific to the legume clade (Comber *et al.*, 2006) but is also important for secondary growth in the distantly related species *Populus trichocarpa* (Ko *et al.*, 2006). This shows that while conserved miRNAs can regulate the same target gene in different species, these targets have acquired different functions in the course of evolution. The OsMADS57 gene in rice and PPM1, Pp MADS1, and Phypa1\_1 109598 genes in moss encoding MADS-box proteins have been shown to be targeted by miR444

(Sunkar *et al.*, 2005) and miR538 (Arazi *et al.*, 2005; Axtell *et al.*, 2007), respectively; but, no *MIR824* syntenic region in rice and moss or similarity to the *MIR444* and *MIR538* loci were detectable suggesting that miRNA sequences may be different in several plant species but still regulate a gene with a potential similar function. Interestingly, among the miR538 targets PPM1 has been demonstrated to play a role in moss development. Antisense knockdown of PPM1 results in delayed gametangia development and aberrant leaf development (Singer *et al.*, 2007). These findings indicate that miRNA-mediated regulation of MADS-box genes is distinct for at least three plant lineages.

## 2. *AGL16* is a novel player in stomatal development

Members of the MADS-box proteins family have many established functions in plant growth and development (Kaufmann *et al.*, 2005). This work shows that a MADS-box protein also functions in stomatal development and is subjected to miRNA regulation. The MADS-box gene *AGL16* is cleaved at the miR824 recognition site. Decreased accumulation of *AGL16* mRNA, both in the *agl16-1* deficiency mutant and in the miR824-overexpressing *m3* mutant, resulted in a decrease in the density of higher-order stomata. Overexpression of *AGL16m* mRNA resistant to miR824-mediated cleavage had the opposite effect: the density of higher-order stomata was increased. The fact that this increase was not observed with the *AGL16.1/2* lines indicates that this effect depends on miR824 resistance rather than on ectopic expression of *AGL16* mRNA. These results suggest that normal development of stomatal complexes depends on proper downregulation of *AGL16* by miR824.

The incidence of higher-order stomatal complexes depends on the number of entry divisions and subsequent asymmetric divisions that give rise to SMs (von Groll *et al.*, 2001, Bergmann and Sack, 2007). Reduced *AGL16* expression in deficient mutants markedly decreased the incidence of higher-order stomata, but did not affect the incidence of primary stomata, which arise directly from the MMC lineage (Kutter *et al.*, 2007). Therefore, *AGL16* is a positive regulator that functions downstream of the entry division in the SM lineage. *AGL16* acts, presumably as a transcription factor, to promote expression of genes required for continued asymmetric divisions, SM identity, or both processes. Cells with low levels of *AGL16* enter the specification and differentiation pathway leading to GCs. The plane of SM division is controlled by *SDD1* (Berger and Altmann, 2000), *EPF1* (Hara *et al.*, 2007), and *TMM* (Yang and Sack, 1995). *AGL16* seems not to be involved in this process since the one cell spacing pattern is not disturbed by altered *AGL16* transcripts levels. The fact that *AGL16* is expressed in mature stomata and that SM formation occurs on the opposite site



of the neighbor cell favors the hypothesis of an AGL16-dependent signal of unknown nature travelling from the mature stoma to activate cellular programs leading to SM formation. This type of regulation ensures that new SMs are formed only if the preexisting stoma is mature. Non destructive methods for example Pro<sub>MIR824</sub> and Pro<sub>AGL16-12</sub> fused to a fluorescent reporter gene would allow the study of miR824 on its target gene *AGL16* within the stomatal complex *in planta* and in time.

Bergmann *et al.* (2004) identified a set of genes by transcriptome profiling of *yda* mutants whose pattern of differential expression correlated with known genes that were later shown to affect stomatal development. Transcriptome profiling study of *AGL16m1* did not show significant changes in any of the stomatal mutants identified so far. This suggests that AGL16 acts more likely on an unknown stomatal pathway. The subtilisin-like serine protease SDD1 probably processes a peptide signal perceived by TMM/YDA that activates the MAPK signaling cascade (Bergmann and Sack, 2007). Interestingly, the most upregulated gene in *AGL16m1* is SAG12, a cysteine protease belonging to the same protease family as SDD1. It is tempting to speculate that AGL16 is involved in a signaling pathway with SAG12 acting as a protease for the production of an intercellular peptide signal whereas SDD1 is a protease processing an extracellular signal peptide. This hypothesis could be tested by phenotypical studies of *sag12* mutants. Additionally, *agl16;sag12* double mutants might reveal the epistatic relationship of AGL16 and SAG12.

It was shown that environmental factors influence stomatal density and distribution. For example, stomatal density and distribution is increased upon lower temperature (Aronne and De Micco, 2001). However, it is still unclear how environmental factors can modulate stomatal developmental pathways. It is possible that the biogenesis and/or formation of miR824 is affected upon environmental changes and would therefore affect the steady-state level of *AGL16* and thus, stomatal development. It would be interesting to test this hypothesis by comparing stomatal developmental of *AGL16m1* and Col-0 subjected to low temperature since it was shown that miR824 expression is considerably increased upon cold stress.

### 3. Pleiotropic effects of AGL16 in gene transcription

Deficiencies in *AGL16* mRNA did not have detectable developmental effects other than on the SM lineage. This suggests there is functional compensation for extra-stomatal deficiencies as has been reported for other members of the highly redundant MADS-box protein family (Ferrandiz *et al.*, 2000; Liljegren *et al.*, 2000; Pinyopich *et al.*, 2003; Ditta *et al.*, 2004; Gregis *et al.*, 2006). However, increased AGL16 expression in *AGL16m* lines cause abnor-

malities in growth habit, leaf shape, and branching of trichomes, which have been reported to accumulate *AGL16* mRNA (Alvarez-Buylla *et al.*, 2000). RNA profiling experiment showed that most genes having altered mRNA expression in the miR824-resistant line *AGL16m1* contain a CArG motif to which AGL16 might bind and therefore facilitates the regulation of gene expression directly. It is also possible that AGL16 regulates gene expression in a complex network by heterodimerization to other MADS-box proteins. Both possibilities might lead to the observed pleiotropic developmental abnormalities. Identification of interaction partners of AGL16 by yeast-two hybrid system or pull-down experiment will provide information of the AGL16 interaction network.

#### 4. Evolution of species specific miRNA regulation

Many *MIRNA* loci in plants appear to arise continuously through inverted gene duplication of a founder gene that can constitute a starting point in the evolution of fold-back structures found at *MIRNA* loci (Allen *et al.*, 2004). However, this might be only one possibility of *MIRNA* loci evolution. The insertion of transposable elements into new genomic sites also seems to be one of the driving forces that creates new miRNAs during mammalian, and perhaps, plant gene evolution (Smalheiser and Torvik, 2005). Some *MIRNA* genes might also be occasionally acquired by direct horizontal transfer through genomic integration of foreign nucleic acids, e.g. several mammalian DNA viruses encode and produce miRNAs during infection (Sullivan *et al.*, 2005). It is possible that plant viruses or other pathogens that use nucleic acids to infect plants might use miRNAs as virulence factors and their genes could integrate into host genomes.

*MIR824*, like *MIR161*, *MIR163* (Allen *et al.*, 2004; Rajagopalan *et al.*, 2006), *MIR778*, *MIR780*, and *MIR856* (Fahlgren *et al.*, 2007), seem to be a rather recently evolved gene generated by duplication of its unique *AGL16* target that probably evolved 12 to 20 million years ago before the divergence of *Brassica* and *Arabidopsis* lineages (Town *et al.*, 2006). It is likely that *MIR824* originated by duplication of *AGL16* rather than by insertion of transposable elements into new genomic sites because no repetitive sequences, diagnostic for transposition were identified in the genomic region of *MIR824*. Gene duplication events, diversification, and/or fixation contributed to the establishment of different MADS-box gene clades (Alvarez-Buylla *et al.*, 2000; Theissen *et al.*, 1996). Previous studies showed that after the duplication of an ancestral gene, one copy of the MADS-box gene accumulates mutations especially in the C-terminal domain (Litt and Irish, 2003; Vandenbusche *et al.*, 2003). Sequence alignments demonstrated that *AGL16* differs the most in the C-terminal

domain from other members of *AGL17*-like MADS-box clade (Becker and Theissen, 2003; Kofiju *et al.*, 2003). Interestingly, the *miR824* binding site is located in this domain of *AGL16*. A molecular analysis in *Brassica oleracea* var. *botrytis* has shown that the cauliflower phenotype is due to a C-terminal non-sense mutation in *BoCAL* (Kempin *et al.*, 1995; Smith and King, 2000). This indicates that the C-terminal domain is required for protein function despite its highest rate of evolutionary change. Other studies lead to the conclusion that sequence changes, including loss of a C-terminal domain, may indeed be associated with morphological variation (Galant and Carroll, 2002; Omland, 1997; Ronshaugen *et al.*, 2002). If these mutations in the coding sequence of the C-terminal domain occurred after the divergence of Brassicaceae, then they may result in Brassicaceae-specific functions. My studies raise the possibility that the *miR824-AGL16* interaction accounts for some *Brassica*-specific taxonomic features of stomatal organization. This hypothesis could be tested by functionally characterizing ortholog and stomatal development in the Capparaceae and Resadaceae, which are closely related to the Brassicaceae. This experimental approach might identify additional links between molecular and morphological diversity explain why no *AGL16* ortholog is present in either rice or poplar.

## 5. *AGL16* might be regulated by both *miR824* and *miR824\**

The *miR824* arm aligned best to exon 7 of the *AGL16*. Interestingly, the *miR824\** arm also aligned to the *AGL16* gene, but in this case with highest scores corresponding a duplicated region located within intron 3 of the *AGL16* gene At3g57230.1 or to intron 2 of splice variant At3g57230.2. This suggests that during evolution selection might act on both *MIR824* arms (Rajagopalan *et al.*, 2006). It has been reported that some miRNA and miRNA\* sequences are indistinguishable (Rajagopalan *et al.*, 2006). It seems more likely that *miR824* is more efficiently incorporated into the RISC machinery rather than *miR824\** because the 5' end of *miR824* ( $\Delta G = -15.9$  kcal/mol) starts with a U and is less stable than the 5' end *miR824\** ( $\Delta G = -16.4$  kcal/mol) with a C at the first position. Nevertheless, in principle *miR824\** could also guide RISC-mediated cleavage since *miR824\** is stable and its expression was detectable by RNA blot hybridization. This hypothesis could be tested by an RLM-RACE detecting cleavage activity of *miR824\** on the *AGL16* intronic sequence. *AGL16* promoter activity, like that of several other MADS-box domain genes (Busch *et al.*, 1999; Deyholos and Sieburth, 2000; Sieburth and Meyerowitz, 1997) depends on cis-regulatory enhancer elements in introns. *miR824\** might disrupt any enhancer or repressor elements by targeting the intronic region of *AGL16*. It would be important to confirm this by testing *AGL16* promoter activity in a trans-

genic line where a miR824\*-cleavage resistant full-length *AGL16* gene is fused to a reporter gene. If confirmed, this would suggest that the *AGL16* gene is controlled by miRNAs in two ways: by transcript degradation and by novel regulation of its own promoter activity.

## 6. Role of AGO1 in miR824 processing

Biogenesis of miR824 and miR824\* depends on DCL1, HYL1, and HEN1 but surprisingly not on AGO1. In Arabidopsis it is not clear if AGO1 associates with DCL1 to process miRNAs from the precursor as shown in animal systems (Matranga *et al.*, 2005). If this is the case, the accumulation of miR824 should be reduced in *ago1* mutants. Intriguingly, miR824 and miR824\*, as well as miR156, accumulate in the strong *ago1-3* null-mutant. This can be explained by an inefficient loading of miR824 and/or miR824\* into RISC containing AGO1. Vaucheret *et al.* (2004) argued that certain miRNAs, such as miR156/157 and miR167, whose expression is not strongly AGO1-dependent result from inefficient turn-over of miRNA/miRNA\*. However, AGO1 is involved in the RISC-mediated target degradation (Baumberger and Baulcombe, 2005) since *AGL16* transcript accumulated in the *ago1-3* mutant. Therefore, the endonucleolytic activity of AGO1 is crucial for RNA cleavage mediated by miRNAs but it seems unlikely that AGO1 is the only AGO protein that associates with DCL1 to process miRNAs from the precursor. miR824 but not miR824\* co-immunoprecipitated with AGO4 (Qi *et al.*, 2006) suggesting a complex mechanism involving both miRNA processing and RISC loading. Accumulation of miR824 in mutants being impaired in AGO function (AGO2 to AGO10) might indicate which AGO protein is associated for miR824 biogenesis. Redundant function of AGO proteins, as described for DCLs (Blevins *et al.*, 2006; Henderson *et al.*, 2006; Moissiard and Voinnet, 2006), in miR824 processing can be tested by combinatorial crosses of *ago* mutants. Alternatively, functional studies of AGO proteins *in vitro* may help to understand the regulatory requirements for RISC assembly and maturation in plants. miR824 seems to be a good candidate for those studies because of its structural features and genetic advantages.

Part V

# Bibliography

# Bibliography

- Achard, P., Herr, A., Baulcombe, D. C., and Harberd, N. P.** (2004) Modulation of floral development by a gibberellin-regulated microRNA. *Development* **131**, 3357-3365.
- Adenot, X., Elmayan, T., Lauressergues, D., Boutet, S., Bouche, N., Gascioli, V., and Vaucheret, H.** (2006) DRB4-dependent TAS3 trans-acting siRNAs control leaf morphology through *AGO7*. *Curr Biol* **16**, 927-932.
- Aida, M., Ishida, T., Fukaki, H., Fujisawa, H., and Tasaka, M.** (1997) Genes involved in organ separation in *Arabidopsis*: an analysis of the cup-shaped cotyledon mutant. *Plant Cell* **9**, 841-857.
- Akbergenov, R., Si-Ammour, A., Blevins, T., Amin, I., Kutter, C., Vanderschuren, H., Zhang, P., Gruissem, W., Meins, F., Jr., Hohn, T., and Pooggin, M. M.** (2006) Molecular characterization of gemini-virus-derived small RNAs in different plant species. *Nucleic Acids Res.* **34**, 462-471.
- Allen, E., Xie, Z., Gustafson, A. M., and Carrington, J. C.** (2005) microRNA-directed phasing during trans-acting siRNA Biogenesis in Plants. *Cell* **121**, 207-221.
- Allen, E., Xie, Z., Gustafson, A. M., Sung, G. H., Spatafora, J. W., and Carrington, J. C.** (2004) Evolution of microRNA genes by inverted duplication of target gene sequences in *Arabidopsis thaliana*. *Nat. Genet.* **36**, 1282-1290.
- Alonso, J. M., Stepanova, A. N., Lisse, T. J., Kim, C. J., Chen, H., Shinn, P., Stevenson, D. K., Zimmerman, J., Barajas, P., Cheuk, R., Gadrinab, C., Heller, C., Jeske, A., Koesema, E., Meyers, C. C., Parker, H., Prednis, L., Ansari, Y., Choy, N., Deen, H., Geralt, M., Hazari, N., Hom, E., Karnes, M., Mulholland, C., Ndubaku, R., Schmidt, I., Guzman, P., Aguilar-Henonin, L., Schmid, M., Weigel, D., Carter, D. E., Marchand, T., Risseuw, E., Brogden, D., Zeko, A., Crosby, W. L., Berry, C. C., and Ecker, J. R.** (2003) Genome-wide insertional mutagenesis of *Arabidopsis thaliana*. *Science* **301**, 653-657.
- Alvarez-Buylla, E. R., Pelaz, S., Liljegren, S. J., Gold, S. E., Burgeff, C., Ditta, G. S., Ribas de Pouplana, L., Martinez-Castilla, L., and Yanofsky, M. F.** (2000) An ancestral MADS-box gene duplication occurred before the divergence of plants and animals. *Proc Natl Acad Sci USA* **97**, 5328-5333.
- Aravin, A. A., Sachidanandam, R., Girard, A., Fejes-Toth, K., and Hannon, G. J.** (2007) Developmentally regulated piRNA clusters implicate MILI in transposon control. *Science* **316**, 744-747.
- Arazi, T., Talmor-Neiman, M., Stav, R., Riese, M., Huijser, P., and Baulcombe, D. C.** (2005) Cloning and characterization of microRNAs > »from moss. *Plant J* **43**, 837-848.
- Aronne, G. and De Micco, V.** (2001) Seasonal dimorphism in the mediterranean *Cistus in-*

- canus* L. *subsp. incanus*. *Ann Bot* **87**, 789-794.
- Aukerman, M. J. and Sakai, H.** (2003) Regulation of flowering time and floral organ identity by a microRNA and its *APETALA2-LIKE* target genes. *Plant Cell* **15**, 2730-2741.
- Axtell, M. J. and Bartel, D. P.** (2005) Antiquity of microRNAs and their targets in land plants. *Plant Cell* **17**, 1658-1673.
- Axtell, M. J., Jan, C., Rajagopalan, R., and Bartel, D. P.** (2006) A two-hit trigger for siRNA biogenesis in plants. *Cell* **127**, 565-577.
- Baker, C. C., Sieber, P., Wellmer, F., and Meyerowitz, E. M.** (2005) The early extra petals1 mutant uncovers a role for microRNA miR164c in regulating petal number in *Arabidopsis*. *Curr Biol* **15**, 303-315. **Baker, S. S., Wilhelm, K. S., and Thomashow, M. F.** (1994) The 5'-region of *Arabidopsis thaliana* *COR15a* has cis-acting elements that confer cold-, drought- and ABA-regulated gene expression. *Plant Mol Biol* **24**, 701-713.
- Bao, N., Lye, K. W., and Barton, M. K.** (2004) MicroRNA binding sites in *Arabidopsis* class III *HD-ZIP* mRNAs are required for methylation of the template chromosome. *Dev Cell* **7**, 653-662.
- Bao, X., Franks, R. G., Levin, J. Z., and Liu, Z.** (2004) Repression of *AGAMOUS* by *BELL-RINGER* in floral and inflorescence meristems. *Plant Cell* **16**, 1478-1489.
- Barrett, T., Troup, D. B., Wilhite, S. E., Ledoux, P., Rudnev, D., Evangelista, C., Kim, I. F., Soboleva, A., Tomashevsky, M., and Edgar, R.** (2007) NCBI GEO: mining tens of millions of expression profiles-database and tools update. *Nucleic Acids Res* **35**, 760-765.
- Bartel, B. and Bartel, D. P.** (2003) MicroRNAs: at the root of plant development? *Plant Physiol* **132**, 709-717.
- Bartel, D. P.** (2004) MicroRNAs: Genomics, biogenesis, mechanism, and function. *Cell* **116**, 281-297.
- Basyuk, E., Suavet, F., Doglio, A., Bordonne, R., and Bertrand, E.** (2003) Human let-7 stem-loop precursors harbor features of RNase III cleavage products. *Nucleic Acids Res* **31**, 6593-6597.
- Baumberger, N. and Baulcombe, D. C.** (2005) *Arabidopsis* ARGONAUTE1 is an RNA Slicer that selectively recruits microRNAs and short interfering RNAs. *Proc Natl Acad Sci USA* **102**, 11928-11933.
- Becker, A. and Theissen, G.** (2003) The major clades of MADS-box genes and their role in the development and evolution of flowering plants. *Mol. Phylogenet. Evol.* **29**, 464-489.
- Bentwich, I.** (2005) A postulated role for microRNA in cellular differentiation. *FASEB J* **19**, 875-879.
- Benz, B. W. and Martin, C. E.** (2006) Foliar trichomes, boundary layers, and gas exchange in 12 species of epiphytic *Tillandsia* (Bromeliaceae). *J Plant Physiol* **163**, 648-656.
- Berger, D. and Altmann, T.** (2000) A subtilisin-like serine protease involved in the regulation of stomatal density and distribution in *Arabidopsis thaliana*. *Genes Dev.* **14**, 1119-1131.

- Bergmann, D.** (2006) Stomatal development: from neighborly to global communication. *Curr Opin Plant Biol* **9**, 478-483.
- Bergmann, D. C., Lukowitz, W., and Somerville, C. R.** (2004) Stomatal development and pattern controlled by a MAPKK Kinase. *Science* **304**, 1494-1497.
- Bergmann, D. C. and Sack, F. D.** (2007) Stomatal Development. *Annu. Rev. Plant Biol.* **58**, 163-181.
- Bernstein, E., Kim, S. Y., Carmell, M. A., Murchison, E. P., Alcorn, H., Li, M. Z., Mills, A. A., Elledge, S. J., Anderson, K. V., and Hannon, G. J.** (2003) Dicer is essential for mouse development. *Nat Genet* **35**, 215-217.
- Bhattacharyya, S. N., Habermacher, R., Martine, U., Closs, E. I., and Filipowicz, W.** (2006) Relief of microRNA-mediated translational repression in human cells subjected to stress. *Cell* **125**, 1111-1124.
- Billoud, B., De Paepe, R., Baulcombe, D., and Boccara, M.** (2005) Identification of new small non-coding RNAs from tobacco and Arabidopsis. *Biochimie* **87**, 905-910.
- Blevins, T., Rajeswaran, R., Shivaprasad, P. V., Beknazariants, D., Si-Ammour, A., Park, H. S., Vazquez, F., Robertson, D., Meins, F., Hohn, T., and Pooggin, M. M.** (2006) Four plant Dicers mediate viral small RNA biogenesis and DNA virus induced silencing. *Nucleic Acids Res* **34**, 6233-6246.
- Boffelli, D., McAuliffe, J., Ovcharenko, D., Lewis, K. D., Ovcharenko, I., Pachter, L., and Rubin, E. M.** (2003) Phylogenetic shadowing of primate sequences to find functional regions of the human genome. *Science* **299**, 1391-1394.
- Bollman, K. M., Aukerman, M. J., Park, M. Y., Hunter, C., Berardini, T. Z., and Poethig, R. S.** (2003) *HASTY*, the Arabidopsis ortholog of exportin 5/MSN5, regulates phase change and morphogenesis. *Development* **130**, 1493-1504.
- Bonnard, G., Vincent, F., and Otten, L.** (1989) Sequence and distribution of IS866, a novel T region-associated insertion sequence from *Agrobacterium tumefaciens*. *Plasmid* **22**, 70-81.
- Borsani, O., Zhu, J., Verslues, P. E., Sunkar, R., and Zhu, J. K.** (2005a) Endogenous siRNAs derived from a pair of natural cis-antisense transcripts regulate salt tolerance in Arabidopsis. *Cell* **123**, 1279-1291.
- Bowman, J. L., Drews, G. N., and Meyerowitz, E. M.** (1991a) Expression of the Arabidopsis floral homeotic gene *AGAMOUS* is restricted to specific cell types late in flower development. *Plant Cell* **3**, 749-758.
- Bowman, J. L., Smyth, D. R., and Meyerowitz, E. M.** (1991b) Genetic interactions among floral homeotic genes of Arabidopsis. *Development* **112**, 1-20.
- Bowman, J. L., Eshed, Y., and Baum, S. F.** (2002) Establishment of polarity in angiosperm lateral organs. *Trends Genet* **18**, 134-141.
- Bradford, K. J., Sharkey, T. D., and Farquhar, G. D.** (1983) Gas exchange, stomatal behavior, and delta C values of the flacca tomato mutant in relation to abscisic acid. *Plant Physiol* **72**, 245-250.



- Bradley, D., Carpenter, R., Sommer, H., Hartley, N., and Coen, E.** (1993) Complementary floral homeotic phenotypes result from opposite orientations of a transposon at the *plena* locus of *Antirrhinum*. *Cell* **72**, 85-95.
- Brennecke, J., Aravin, A. A., Stark, A., Dus, M., Kellis, M., Sachidanandam, R., and Hannon, G. J.** (2007) Discrete small RNA-generating loci as master regulators of transposon activity in *Drosophila*. *Cell* **128**, 1089-1103.
- Busch, M. A., Bomblies, K., and Weigel, D.** (1999) Activation of a floral homeotic gene in *Arabidopsis*. *Science* **285**, 585-587.
- Carmell, M. A., Girard, A., van de Kant, H. J. G., Bourchis, D., Bestor, T. H., de Rooij, D. G., and Hannon, G. J.** (2007) MIWI2 is essential for spermatogenesis and repression of transposons in the mouse male germline. *Dev Cell* **12**, 503-514.
- Carpenter, K. J.** (2005) Stomatal architecture and evolution in basal angiosperms. *Amer. J. Bot.* **92**, 1595-1615.
- Cary, A. J., Che, P., and HOWELL, S. H.** (2002) Developmental events and shoot apical meristem gene expression patterns during shoot development in *Arabidopsis thaliana*. *Plant J* **32**, 867-877.
- Causier, B., Castillo, R., Zhou, J., Ingram, R., Xue, Y., Schwarz-Sommer, Z., and Davies, B.** (2005) Evolution in action: following function in duplicated floral homeotic genes. *Curr Biol* **15**, 1508-1512.
- Cerutti, H. and Casas-Mollano, J. A.** (2006) On the origin and functions of RNA-mediated silencing: from protists to man. *Curr Genet* **50**, 81-99.
- Chen, J., Li, W. X., Xie, D., Peng, J. R., and Ding, S. W.** (2004) Viral virulence protein suppresses RNA silencing-mediated defense but upregulates the role of microRNA in host gene expression. *Plant Cell* **16**, 1302-1313.
- Chen, K. and Rajewsky, N.** (2007) The evolution of gene regulation by transcription factors and microRNAs. *Nat Rev Genet* **8**, 93-9103.
- Chen, X.** (2003) A microRNA as a translational repressor of *APETALA2* in *Arabidopsis* flower development. *Science* **303**, 2022-2025.
- Chendrimada, T. P., Gregory, R. I., Kumaraswamy, E., Norman, J., Cooch, N., Nishikura, K., and Shiekhattar, R.** (2005) TRBP recruits the Dicer complex to Ago2 for microRNA processing and gene silencing. *Nature* **436**, 740-744.
- Chiou, T. J.** (2007) The role of microRNAs in sensing nutrient stress. *Plant Cell Environ* **30**, 323-332.
- Chuck, G., Cigan, A. M., Saeteurn, K., and Hake, S.** (2007) The heterochronic maize mutant *Corngrass1* results from overexpression of a tandem microRNA. *Nat Genet* **39**, 544-549.
- Coen, E. S. and Meyerowitz, E. M.** (1991) The war of the whorls: genetic interactions controlling flower development. *Nature* **353**, 31-37.
- Comber, J. P., Frugier, F., de Billy, F., Boualem, A., El Yahyaoui, F., Moreau, S., Vernie, T.,**

- Ott, T., Gamas, P., Crespi, M., and Niebel, A.** (2006) MtHAP2-1 is a key transcriptional regulator of symbiotic nodule development regulated by microRNA169 in *Medicago truncatula*. *Genes Dev* **20**, 3084-3088.
- Croxdale, J. L.** (2000) Stomatal patterning in angiosperms. *Amer. J. Bot.* **87**, 1069-1080.
- Czechowski, T., Stitt, M., Altmann, T., Udvardi, M. K., and Scheible, W. R.** (2005) Genome-wide identification and testing of superior reference genes for transcript normalization in *Arabidopsis*. *Plant Physiol.* **139**, 5-17.
- Dai, Q., Peng, S., Chavez, A. Q., and Vergara, B. S.** (1995) Effects of UV-B radiation on stomatal density and opening in rice (*Oryza sativa* L.). *Ann Bot* **76**, 65-70.
- Dalmay, T., Hamilton, A., Rudd, S., Angell, S., and Baulcombe, D. C.** (2000) An RNA-dependent RNA polymerase gene in *Arabidopsis* is required for posttranscriptional gene silencing mediated by a transgene but not by a virus. *Cell* **101**, 543-553.
- Dalmay, T., Horsefield, R., Braunstein, T. H., and Baulcombe, D. C.** (2001) SDE3 encodes an RNA helicase required for post-transcriptional gene silencing in *Arabidopsis*. *EMBO J* **20**, 2069-2078.
- Davies, B., Motte, P., Keck, E., Saedler, H., Sommer, H., and Schwarz-Sommer, Z.** (1999) *PLENA* and *FARINELLI*: redundancy and regulatory interactions between two Antirrhinum MADS-box factors controlling flower development. *EMBO J* **18**, 4023-4034.
- de Folter, S., Immink, R. G. H., Kieffer, M., Parenicová, L., Henz, S. R., Weigel, D., Busscher, M., Kooiker, M., Colombo, L., Kater, M. M., Davies, B., and Angenent, G. C.** (2005) Comprehensive interaction map of the *Arabidopsis* MADS-box transcription factors. *Plant Cell* **17**, 1424-1433.
- de Folter, S. and Angenent, G. C.** (2006) Trans meets cis in MADS science. *Trends Plant Sci* **11**, 224-231.
- Deleris, A., Gallego-Bartolome, J., Bao, J., Kasschau, K. D., Carrington, J. C., and Voinet, O.** (2006) Hierarchical action and inhibition of plant Dicer-Like proteins in antiviral defense. *Science* **313**, 68-71.
- Denli, A. M., Tops, B. B. J., Plasterk, R. H. A., Ketting, R. F., and Hannon, G. J.** (2004) Processing of primary microRNAs by the microprocessor complex. *Nature* **432**, 231-235.
- Deyholos, M. K. and Sieburth, L. E.** (2000) Separable whorl-specific expression and negative regulation by enhancer elements within the *AGAMOUS* second intron. *Plant Cell* **12**, 1799-1810.
- Dharmasiri, N., Dharmasiri, S., and Estelle, M.** (2005) The F-box protein TIR1 is an auxin receptor. *Nature* **435**, 441-445.
- Di Serio, F., Schöb, H., Iglesias, A., Tarina, C., Bouldoires, E., and Meins, F. Jr.** (2001) Sense- and antisense-mediated gene silencing in tobacco is inhibited by the same viral suppressors and is associated with accumulation of small RNAs. *Proc. Natl. Acad. Sci. USA* **98**, 6506-6510.
- Ditta, G., Pinyopich, A., Robles, P., Pelaz, S., and Yanofsky, M. F.** (2004) The *SEP4* gene

- of *Arabidopsis thaliana* functions in floral organ and meristem identity. *Curr. Biol.* **14**, 1935-1940.
- Dunoyer, P., Himber, C., and Voinnet, O.** (2005) *DICER-LIKE 4* is required for RNA interference and produces the 21-nucleotide small interfering RNA component of the plant cell-to-cell silencing signal. *Nat Genet* **37**, 1356-1360.
- Egea-Cortines, M., Saedler, H., and Sommer, H.** (1999) Ternary complex formation between the MADS-box proteins SQUAMOSA, DEFICIENS and GLOBOSA is involved in the control of floral architecture in *Antirrhinum majus*. *EMBO J* **18**, 5370-5379.
- Elbashir, S. M., Lendeckel, W., and Tuschl, T.** (2001) RNA interference is mediated by 21 and 22 nt RNAs. *Genes Dev.* **15**, 188-200.
- Emery, J. F., Floyd, S. K., Alvarez, J., Eshed, Y., Hawker, N. P., Izhaki, A., Baum, S. F., and Bowman, J. L.** (2003) Radial patterning of Arabidopsis shoots by class III *HD-ZIP* and *KANADI* genes. *Curr. Biol.* **13**, 1768-1774.
- Esau, K.** (1965) Fixation images of sieve elements plastids in Beta. *Proc Natl Acad Sci USA* **54**, 429-437.
- Espinosa-Soto, C., Padilla-Longoria, P., and Alvarez-Buylla, E. R.** (2004) A gene regulatory network model for cell-fate determination during *Arabidopsis thaliana* flower development that is robust and recovers experimental gene expression profiles. *Plant Cell* **16**, 2923-2939.
- Fahlgren, N., Howell, M. D., Kasschau, K. D., Chapman, E. J., Sullivan, C. M., Cumbie, J. S., Givan, S. A., Law, T. F., Grant, S. R., Dangl, J. L., and Carrington, J. C.** (2007) High-throughput sequencing of Arabidopsis microRNAs: evidence for frequent birth and death of *MIRNA* genes. *PLoS ONE* **2**, e219.
- Fahlgren, N., Montgomery, T. A., Howell, M. D., Allen, E., Dvorak, S. K., Alexander, A. L., and Carrington, J. C.** (2006) Regulation of *AUXIN RESPONSE FACTOR3* by TAS3 ta-siRNA affects developmental timing and patterning in Arabidopsis. *Curr Biol* **16**, 939-944.
- Farh, K. K. H., Grimson, A., Jan, C., Lewis, B. P., Johnston, W. K., Lim, L. P., Burge, C. B., and Bartel, D. P.** (2005) The widespread impact of mammalian microRNAs on mRNA repression and evolution. *Science* **310**, 1817-1821.
- Forstemann, K., Tomari, Y., Du, T., Vagin, V. V., Denli, A. M., Bratu, D. P., Klattenhoff, C., Theurkauf, W. E., and Zamore, P. D.** (2005) Normal microRNA maturation and germ-line stem cell maintenance requires Loquacious, a double-stranded RNA-binding domain protein. *PLoS Biol* **3**.
- Franks, P. J. and Farquhar, G. D.** (2001) The effect of exogenous abscisic acid on stomatal development, stomatal mechanics, and leaf gas exchange in *Tradescantia virginiana*. *Plant Physiol* **125**, 935-942.
- Friml, J., Benkova, E., Mayer, U., Palme, K., and Muster, G.** (2003) Automated whole mount localisation techniques for plant seedlings. *Plant J.* **34**, 115-124.
- Fritsch, O., Benvenuto, G., Bowler, C., Molinier, J., and Hohn, B.** (2004) The INO80 protein

- controls homologous recombination in *Arabidopsis thaliana*. *Mol. Cell* **16**, 479-485.
- Fujii, H., Chiou, T. J., Lin, S. I., Aung, K., and Zhu, J. K.** (2005) A miRNA involved in phosphate-starvation response in *Arabidopsis*. *Curr Biol* **15**, 2038-2043.
- Galant, R. and Carroll, S. B.** (2002) Evolution of a transcriptional repression domain in an insect Hox protein. *Nature* **415**, 910-913.
- Gamboa, A., Paz-Valencia, J., Acevedo, G. F., Vázquez-Moreno, L., and Alvarez-Buylla, R. E.** (2001) Floral transcription factor AGAMOUS interacts *in vitro* with a leucine-rich repeat and an acid phosphatase protein complex. *Biochem Biophys Res Commun* **288**, 1018-1026.
- Gan, Y., Filleur, S., Rahman, A., Gotensparre, S., and Forde, B. G.** (2005) Nutritional regulation of *ANR1* and other root-expressed MADS-box genes in *Arabidopsis thaliana*. *Planta* **222**, 730-742.
- Gandikota, M., Birkenbihl, R. P., Hohmann, S., Cardon, G. H., Saedler, H., and Huijser, P.** (2007) The miRNA156/157 recognition element in the 3' UTR of the *Arabidopsis* SBP box gene *SPL3* prevents early flowering by translational inhibition in seedlings. *Plant J* **49**, 683-693.
- Gascioli, V., Mallory, A. C., Bartel, D. P., and Vaucheret, H.** (2005) Partially redundant functions of *Arabidopsis* DICER-like enzymes and a role for DCL4 in producing trans-acting siRNAs. *Curr Biol* **15**, 1494-1500.
- Gassmann, A. J. and Hare, J. D.** (2005) Indirect cost of a defensive trait: variation in trichome type affects the natural enemies of herbivorous insects on *Datura wrightii*. *Oecologia* **144**, 62-71.
- Geisler, M., Nadeau, J., and Sack, F. D.** (2000) Oriented asymmetric divisions that generate the stomatal spacing pattern in *Arabidopsis* are disrupted by the *too many mouths* mutation. *Plant Cell* **12**, 2075-2086.
- Geisler, M., Yang, M., and Sack, F. D.** (1998) Divergent regulation of stomatal initiation and patterning in organ and suborgan regions of the *Arabidopsis* mutants *too many mouths* and *four lips*. *Planta* **205**, 522-530.
- Girard, A., Sachidanandam, R., Hannon, G. J., and Carmell, M. A.** (2006) A germline-specific class of small RNAs binds mammalian Piwi proteins. *Nature* **442**, 199-202.
- Golden, T. A., Schauer, S. E., Lang, J. D., Pien, S., Mushegian, A. R., Grossniklaus, U., Meinke, D. W., and Ray, A.** (2002) *SHORT INTEGUMENTS1/SUSPENSOR1/CARPEL FACTORY*, a Dicer homolog, is a maternal effect gene required for embryo development in *Arabidopsis*. *PLANT PHYSIOL* **130**, 808-822.
- Gomez-Mena, C., de Folter, S., Costa, M. M., Angenent, G. C., and Sablowski, R.** (2005) Transcriptional program controlled by the floral homeotic gene *AGAMOUS* during early organogenesis. *Development* **132**, 429-438.
- Gong W., Shen Y. P., Ma L. G., Pan Y., Du Y. L., Wang D. H., Yang J. Y., Hu L. D., Liu X. F., Dong C. X., Ma L., Chen Y. H., Yang X. Y., Gao Y., Zhu D., Tan X., Mu J. Y., Zhang D. B., Liu Y. L., Dinesh-Kumar S. P., Li Y., Wang X. P., Gu H. Y., Qu L. J., Bai S. N., Lu Y. T., Li**

- J. Y., Zhao J. D., Zuo J., Huang H., Deng X. W., Zhu Y. X.** (2004) Genome-wide ORFeome cloning and analysis of Arabidopsis transcription factor genes. *Plant Physiol.* **135**, 773-782.
- Goto, K., Kyojuka, J., and Bowman, J. L.** (2001) Turning floral organs into leaves, leaves into floral organs. *Curr Opin Genet Dev* **11**, 449-456.
- Goto, K. and Meyerowitz, E. M.** (1994) Function and regulation of the Arabidopsis floral homeotic gene *PISTILLATA*. *Genes Dev.* **8**, 1548-1560.
- Gray, J. E., Holroyd, G. H., van der Lee, F. M., Bahrami, A. R., Sijmons, P. C., Woodward, F. I., Schuch, W., and Hetherington, A. M.** (2000) The HIC signalling pathway links CO<sub>2</sub> perception to stomatal development. *Nature* **408**, 713-716.
- Gray, W. M., Kepinski, S., Rouse, D., Leyser, O., and Estelle, M.** (2001) Auxin regulates SCF(TIR1)-dependent degradation of AUX/IAA proteins. *Nature* **414**, 271-276.
- Gregis, V., Sessa, A., Colombo, L., and Kater, M. M.** (2006) *AGL24*, *SHORT VEGETATIVE PHASE*, and *APETALA1* redundantly control *AGAMOUS* during early stages of flower development in Arabidopsis. *Plant Cell* **18**, 1373-1382.
- Griffith-Jones, S. A. M., Grocock, R. J., van Dongen, S., Bateman, A., and Enright, A. J.** (2006) miRBase: microRNA sequences, targets and gene nomenclature. *Nucleic Acids Res.* **34**, D140-D144.
- Grivna, S. T., Beyret, E., Wang, Z., and Lin, H.** (2006) A novel class of small RNAs in mouse spermatogenic cells. *Genes Dev* **20**, 1709-1714.
- Gunawardane, L. S., Saito, K., Nishida, K. M., Miyoshi, K., Kawamura, Y., Nagami, T., Siomi, H., and Siomi, M. C.** (2007) A slicer-mediated mechanism for repeat-associated siRNA 5' end formation in *Drosophila*. *Science* **315**, 1587-1590.
- Guo, H. S., Xie, Q., Fei, J. F., and Chua, N. H.** (2005) MicroRNA directs mRNA cleavage of the transcription factor *NAC1* to downregulate auxin signals for Arabidopsis lateral root development. *Plant Cell* **17**, 1376-1386.
- Gutierrez, R. A., Ewing, R. M., Cherry, J. M., and Green, P. J.** (2002) Identification of unstable transcripts in Arabidopsis by cDNA microarray analysis: Rapid decay is associated with a group of touch- and specific clock-controlled genes. *Proc. Natl. Acad. Sci. USA* **99**, 11513-11518.
- Haas, B. J., Wortman, J. R., Ronning, C. M., Hannick, L. I., Smith, R. K., Maiti, R., Chan, A. P., Yu, C., Farzad, M., Wu, D., White, O., and Town, C. D.** (2005) Complete reannotation of the Arabidopsis genome: methods, tools, protocols and the final release. *BMC Biol* **3**, 7.
- Haase, A. D., Jaskiewicz, L., Zhang, H., Laine, S., Sack, R., Gatignol, A., and Filipowicz, W.** (2005) TRBP, a regulator of cellular PKR and HIV-1 virus expression, interacts with Dicer and functions in RNA silencing. *EMBO Rep* **6**, 961-967.
- Hamilton, A., Voinnet, O., Chappell, L., and Baulcombe, D.** (2002) Two classes of short interfering RNA in RNA silencing. *EMBO J.* **21**, 4671-4679.
- Han, J., Lee, Y., Yeom, K. H., Kim, Y. K., Jin, H., and Kim, V. N.** (2004) The Drosha-DGCR8 complex in primary microRNA processing. *Genes Dev* **18**, 3016-3027.

- Hara, K., Kajita, R., Torii, K. U., Bergmann, D. C., and Kakimoto, T.** (2007) The secretory peptide gene EPF1 enforces the stomatal one-cell-spacing rule. *Genes Dev* **21**, 1720-1725.
- Hartmann, U., Hohmann, S., Nettekheim, K., Wisman, E., Saedler, H., and Huijser, P.** (2000) Molecular cloning of *SVP*: a negative regulator of the floral transition in *Arabidopsis*. *Plant J* **21**, 351-360.
- Hayama, R., Yokoi, S., Tamaki, S., Yano, M., and Shimamoto, K.** (2003) Adaptation of photoperiodic control pathways produces short-day flowering in rice. *Nature* **422**, 719-722.
- Heck, G. R., Perry, S. E., Nichols, K. W., and Fernandez, D. E.** (1995) *AGL15*, a MADS domain protein expressed in developing embryos. *Plant Cell* **7**, 1271-1282.
- Henderson, I. R., Zhang, X., Lu, C., Johnson, L., Meyers, B. C., Green, P. J., and Jacobsen, S. E.** (2006) Dissecting *Arabidopsis thaliana* DICER function in small RNA processing, gene silencing and DNA methylation patterning. *Nat Genet* **38**, 721-725.
- Henschel, K., Kofuji, R., Hasebe, M., Saedler, H., Munster, T., and Theissen, G.** (2002) Two ancient classes of MIKC-type MADS-box genes are present in the moss *Physcomitrella patens*. *Mol Biol Evol* **19**, 801-814.
- Hernandez, M. L., Passas, H. J., and Smith, L. G.** (1999) Clonal analysis of epidermal patterning during maize leaf development. *Dev Biol* **216**, 646-658.
- Herr, A. J., Jensen, M. B., Dalmay, T., and Baulcombe, D. C.** (2005) RNA polymerase IV directs silencing of endogenous DNA. *Science* **308**, 118-120.
- Hetherington, A. M. and Woodward, F. I.** (2003) The role of stomata in sensing and driving environmental change. *Nature* **424**, 901-908.
- Higo, K., Ugawa, Y., Iwamoto, M., and Korenaga, T.** (1999) Plant cis-acting regulatory DNA elements (PLACE) database: 1999. *Nucleic Acids Res* **27**, 297-300.
- Hikosaka, A., Takaya, K., Jinno, M., and Kawahara, A.** (2007) Identification and expression-profiling of *Xenopus tropicalis* miRNAs including plant miRNA-like RNAs at metamorphosis. *FEBS Lett* **581**, 3013-3018.
- Himber, C., Dunoyer, P., Moissiard, G., Ritzenthaler, C., and Voinnet, O.** (2003) Transitivity-dependent and -independent cell-to-cell movement of RNA silencing. *EMBO J* **22**, 4523-4533.
- Hiraguri, A., Itoh, R., Kondo, N., Nomura, Y., Aizawa, D., Murai, Y., Koiwa, H., Seki, M., Shinozaki, K., and Fukuhara, T.** (2005) Specific interactions between Dicer-like proteins and HYL1/DRB-family dsRNA-binding proteins in *Arabidopsis thaliana*. *Plant Mol Biol* **57**, 173-188.
- Hirsch, J., Lefort, V., Vankersschaver, M., Boualem, A., Lucas, A., Thermes, C., d'Aubenton-Carafa, Y., and Crespi, M.** (2006) Characterization of 43 non-protein-coding mRNA genes in *Arabidopsis*, including the *MIR162a*-derived transcripts. *Plant Physiol* **140**, 1192-1204.
- Holroyd, G. H., Hetherington, A. M., and Gray, J. E.** (2002) A role for the cuticular waxes in the environmental control of stomatal development. *New Phytologist* **153**, 433-439.

- Hong, R. L., Hamaguchi, L., Busch, M. A., and Weigel, D.** (2003) Regulatory elements of the floral homeotic gene *AGAMOUS* identified by phylogenetic footprinting and shadowing. *Plant Cell* **15**, 1296-1309.
- Honma, T. and Goto, K.** (2000) The Arabidopsis floral homeotic gene *PISTILLATA* is regulated by discrete cis-elements responsive to induction and maintenance signals. *Development* **127**, 2021-2030.
- Honma, T. and Goto, K.** (2001) Complexes of MADS-box proteins are sufficient to convert leaves into floral organs. *Nature* **409**, 525-529.
- Horwich, M. D., Li, C., Matranga, C., Vagin, V., Farley, G., Wang, P., and Zamore, P. D.** (2007) The Drosophila RNA methyltransferase, DmHen1, modifies germline piRNAs and single-stranded siRNAs in RISC. *Curr Biol* **17**, 1265-1272.
- Houwing, S., Kamminga, L. M., Berezikov, E., Cronembold, D., Girard, A., van den Elst, H., Filippov, D. V., Blaser, H., Raz, E., Moens, C. B., Plasterk, R. H. A., Hannon, G. J., Draper, B. W., and Ketting, R. F.** (2007) A role for Piwi and piRNAs in germ cell maintenance and transposon silencing in Zebrafish. *Cell* **129**, 69-82.
- Huang, T., Bohlenius, H., Eriksson, S., Parcy, F., and Nilsson, O.** (2005) The mRNA of the Arabidopsis gene *FT* moves > »from leaf to shoot apex and induces flowering. *Science* **309**, 1694-1696.
- Hunter, C., Sun, H., and Poethig, R. S.** (2003a) The Arabidopsis heterochronic gene *ZIPPY* is an *ARGONAUTE* family member. *Curr. Biol.* **13**, 1734-1739.
- Hunter, C. A., Aukerman, M. J., Sun, H., Fokina, M., and Poethig, R. S.** (2003b) *PAUSED* encodes the Arabidopsis exportin-t ortholog. *Plant Physiol* **132**, 2135-2143.
- Irish, V. F.** (2003) The evolution of floral homeotic gene function. *BioEssays* **25**, 637-646.
- Jack, T., Brockman, L. L., and Meyerowitz, E. M.** (1992) The homeotic gene *APETALA3* of *Arabidopsis thaliana* encodes a MADS-box and is expressed in petals and stamens. *Cell* **68**, 683-697.
- John, B., Sander, C., and Marks, D. S.** (2006) Prediction of human microRNA targets. *Methods Mol Biol* **342**, 101-113.
- Jones-Rhoades, M. W. and Bartel, D. P.** (2004) Computational identification of plant microRNAs and their targets, including a stress-induced miRNA. *Mol. Cell* **14**, 787-799.
- Jones-Rhoades, M. W., Bartel, D. P., and Bartel, B.** (2006) MicroRNAs and their regulatory roles in plants. *Ann. Rev. Plant Biol.* **57**, 19-53.
- Kasschau, K. D., Xie, Z., Allen, E., Llave, C., Chapman, E. J., Krizan, K. A., and Carrington, J. C.** (2003) P1/HC-Pro, a viral suppressor of RNA silencing, interferes with Arabidopsis development and miRNA function. *Developmental Cell* **4**, 205-217.
- Katiyar-Agarwal, S., Morgan, R., Dahlbeck, D., Borsani, O., Villegas, A., Zhu, J. K., Staskawicz, B. J., and Jin, H.** (2006) A pathogen-inducible endogenous siRNA in plant immunity. *Proc Natl Acad Sci USA* **103**, 18002-18007.

- Kaufmann, K., Anfang, N., Saedler, H., and Theissen, G.** (2005a) Mutant analysis, protein-protein interactions and subcellular localization of the Arabidopsis B sister (ABS) protein. *Mol Genet Genomics* **274**, 103-118.
- Kaufmann, K., Melzer, R., and Theissen, G.** (2005b) MIKC-type MADS-domain proteins: structural modularity, protein interactions and network evolution in land plants. *Gene* **347**, 183-198.
- Kempin, S. A., Savidge, B., and Yanofsky, M. F.** (1995) Molecular basis of the cauliflower phenotype in Arabidopsis. *Science* **267**, 522-525.
- Kepinski, S. and Leyser, O.** (2002) Ubiquitination and auxin signaling: a degrading story. *Plant Cell* **14**, 81-95.
- Kepinski, S. and Leyser, O.** (2005) The Arabidopsis F-box protein TIR1 is an auxin receptor. *Nature* **435**, 446-451.
- Kim, J., Jung, J. H., Reyes, J. L., Kim, Y. S., Kim, S. Y., Chung, K. S., Kim, J. A., Lee, M., Lee, Y., Narry Kim, V., Chua, N. H., and Park, C. M.** (2005) microRNA-directed cleavage of *ATHB15* mRNA regulates vascular development in Arabidopsis inflorescence stems. *Plant J* **42**, 84-94.
- Klahre, U. and Meins, F. Jr.** (2004) RNA silencing in plants- biolistic delivery of RNAi reagents. In gene silencing by RNA interference: Technology and application, M. Sohail, ed (Boca Raton, FL: CRC Press), pp. 343-355.
- Ko, J. H., Prassinos, C., and Han, K. H.** (2006) Developmental and seasonal expression of *PtaHB1*, a *Populus* gene encoding a class III HD-Zip protein, is closely associated with secondary growth and inversely correlated with the level of microRNA (miR166). *New Phytol* **169**, 469-478.
- Kofuji, R., Sumikawa, N., Yamasaki, M., Kondo, K., Ueda, K., Ito, M., and Hasebe, M.** (2003) Evolution and divergence of the MADS-box gene family based on genome-wide expression analyses. *Mol Biol Evol* **20**, 1963-1977.
- Kok, K. H., Ng, M. H. J., Ching, Y. P., and Jin, D. Y.** (2007) Human TRBP and PACT directly interact with each other and associate with dicer to facilitate the production of small interfering RNA. *J Biol Chem* **282**, 17649-17657.
- Koornneef, M., Alonso-Blanco, C., Peeters, A. J. M., and Soppe, W.** (1998) Genetic control of flowering time in Arabidopsis. *Annu Rev Plant Physiol Plant Mol Biol* **49**, 345-370.
- Kouwenberg, L. L. R., Kurschner, W. M., and Visscher, H.** (2004) Changes in stomatal frequency and size during elongation of *Tsuga heterophylla* needles. *Ann Bot (Lond)* **94**, 561-569.
- Kramer, E. M., Jaramillo, M. A., and Di Stilio, V. S.** (2004) Patterns of gene duplication and functional evolution during the diversification of the *AGAMOUS* subfamily of MADS-box genes in angiosperms. *Genetics* **166**, 1011-1023.
- Krizek, B. A. and Meyerowitz, E. M.** (1996a) Mapping the protein regions responsible for the functional specificities of the Arabidopsis MADS domain organ-identity proteins. *Proc Natl*



- Acad Sci USA **93**, 4063-4070.
- Krizek, B. A. and Meyerowitz, E. M.** (1996b) The Arabidopsis homeotic genes *APETALA3* and *PISTILLATA* are sufficient to provide the B class organ identity function. *Development* **122**, 11-22.
- Kurihara, Y. and Watanabe, Y.** (2004) Arabidopsis microRNA biogenesis through Dicer-like 1 protein functions. *Proc Natl Acad Sci USA* **101**, 12753-12758.
- Kurihara, Y., Takashi, Y., and Watanabe, Y.** (2006) The interaction between DCL1 and HYL1 is important for efficient and precise processing of pri-miRNA in plant microRNA biogenesis. *RNA* **12**, 206-212.
- Kutter, C., Schob, H., Stadler, M., Meins, F., and Si-Ammour, A.** (2007) MicroRNA-mediated regulation of stomatal development in Arabidopsis. *Plant Cell* PMID: 17704216.
- Lagos-Quintana, M., Rauhut, R., Yalcin, A., Meyer, J., Lendeckel, W., and Tuschl, T.** (2002) Identification of tissue-specific microRNAs from mouse. *Curr Biol* **12**, 735-739.
- Lagos-Quintana, M., Rauhut, R., Meyer, J., Borkhardt, A., and Tuschl, T.** (2003) New microRNAs from mouse and human. *RNA* **9**, 175-179.
- Lai, L. B., Nadeau, J. A., Lucas, J., Lee, E. K., Nakagawa, T., Zhao, L., Geisler, M., and Sack, F. D.** (2005) The Arabidopsis R2R3 MYB proteins *FOUR LIPS* and *MYB88* restrict divisions late in the stomatal cell lineage. *Plant Cell* **17**, 2754-2767.
- Lake, J. A., Woodward, F. I., and Quick, W. P.** (2002) Long-distance CO(2) signalling in plants. *J Exp Bot* **53**, 183-193.
- Lamb, R. S. and Irish, V. F.** (2003) Functional divergence within the *APETALA3/PISTILLATA* floral homeotic gene lineages. *Proc Natl Acad Sci USA* **100**, 6558-6563.
- Larkin, J. C., Brown, M. L., and Schiefelbein, J.** (2003) How do cells know what they want to be when they grow up? Lessons from epidermal patterning in Arabidopsis. *Ann. Rev. Plant Biol.* **54**, 403-430.
- Lau, N. C., Seto, A. G., Kim, J., Kuramochi-Miyagawa, S., Nakano, T., Bartel, D. P., and Kingston, R. E.** (2006) Characterization of the piRNA complex from rat testes. *Science* **313**, 363-367.
- Laufs, P., Peaucelle, A., Morin, H., and Traas, J.** (2004) MicroRNA regulation of the *CUC* genes is required for boundary size control in Arabidopsis meristems. *Development* **131**, 4311-4322.
- Lee, B. h., Kapoor, A., Zhu, J., and Zhu, J. K.** (2006a) STABILIZED1, a stress-upregulated nuclear protein, is required for pre-mRNA splicing, mRNA turnover, and stress tolerance in Arabidopsis. *Plant Cell* **18**, 1736-1749.
- Lee, M. M. and Schiefelbein, J.** (2002) Cell pattern in the Arabidopsis root epidermis determined by lateral inhibition with feedback. *Plant Cell* **14**, 611-618.
- Lee, R. C., Feinbaum, R. L., and Ambros, V.** (1993) The *C. elegans* heterochromic gene *lin-4* encodes small RNAs with antisense complementarity to *lin-14*. *Cell* **75**, 843-854.

- Lee, Y., Hur, I., Park, S. Y., Kim, Y. K., Suh, M. R., and Kim, V. N.** (2006b) The role of PACT in the RNA silencing pathway. *EMBO J* **25**, 522-532.
- Lehti-Shiu, M. D., Adamczyk, B. J., and Fernandez, D. E.** (2005) Expression of MADS-box genes during the embryonic phase in Arabidopsis. *Plant Mol Biol* **58**, 89-8107.
- Li, J., Yang, Z., Yu, B., Liu, J., and Chen, X.** (2005) Methylation protects miRNAs and siRNAs from a 3'-end uridylation activity in Arabidopsis. *Curr Biol* **15**, 1501-1507.
- Liljegen, S. J., Ditta, G. S., Eshed, Y., Savidge, B., Bowman, J. L., and Yanofsky, M. F.** (2000) *SHATTERPROOF* MADS-box genes control seed dispersal in Arabidopsis. *Nature* **404**, 766-770.
- Lingel, A., Simon, B., Izaurralde, E., and Sattler, M.** (2003) Structure and nucleic-acid binding of the Drosophila Argonaute 2 PAZ domain. *Nature* **426**, 465-469.
- Lippman, Z., Gendrel, A. V., Black, M., Vaughn, M. W., Dedhia, N., Richard McCombie, W., Lavine, K., Mittal, V., May, B., Kasschau, K. D., Carrington, J. C., Doerge, R. W., Colot, V., and Martienssen, R.** (2004) Role of transposable elements in heterochromatin and epigenetic control. *Nature* **430**, 471-476.
- Litt, A. and Irish, V. F.** (2003) Duplication and diversification in the *APETALA1/FRUITFULL* floral homeotic gene lineage: implications for the evolution of floral development. *Genetics* **165**, 821-833.
- Liu, J., Carmell, M. A., Rivas, F. V., Marsden, C. G., Thomson, J. M., Song, J. J., Hammond, S. M., Joshua-Tor, L., and Hannon, G. J.** (2004) Argonaute2 is the catalytic engine of mammalian RNAi. *Science* **305**, 1437-1441.
- Liu, P. P., Montgomery, T. A., Fahlgren, N., Kasschau, K. D., Nonogaki, H., and Carrington, J. C.** (2007) Repression of *AUXIN RESPONSE FACTOR10* by microRNA160 is critical for seed germination and post-germination stages. *Plant J.*
- Liu, Q., Rand, T. A., Kalidas, S., Du, F., Kim, H. E., Smith, D. P., and Wang, X.** (2003) R2D2, a bridge between the initiation and effector steps of the Drosophila RNAi pathway. *Science* **301**, 1921-1925.
- Liu-Gitz, L., Britz, S. J., and Wergin, W. P.** (2000) Blue light inhibits stomatal development in soybean isolines containing kaempferol-3-O-2G-glycosyl-gentiobioside (K9), a unique flavonoid glycoside. *Plant, Cell & Environment* **23**, 883-891.
- Llave, C., Xie, Z., Kasschau, K. D., and Carrington, J. C.** (2002) Cleavage of Scarecrow-like mRNA targets directed by a class of Arabidopsis miRNA. *Science* **297**, 2053-2056.
- Lobbes, D., Rallapalli, G., Schmidt, D. D., Martin, C., and Clarke, J.** (2006) SERRATE: a new player on the plant microRNA scene. *EMBO Rep* **7**, 1052-1058.
- Lohmann, J. U., Hong, R. L., Hobe, M., Busch, M. A., Parcy, F., Simon, R., and Weigel, D.** (2001) A molecular link between stem cell regulation and floral patterning in Arabidopsis. *Cell* **105**, 793-803.
- Lu, C., Kulkarni, K., Souret, F. F., MuthuValliappan, R., Tej, S. S., Poethig, R. S., Henderson, I. R., Jacobsen, S. E., Wang, W., Green, P. J., and Meyers, B. C.** (2006) MicroRNAs

- and other small RNAs enriched in the Arabidopsis RNA-dependent RNA polymerase-2 mutant. *Genome Res* **16**, 1276-1288.
- Lu, C., Tej, S. S., Luo, S., Haudenschild, C. D., Meyers, B. C., and Green, P. J.** (2005) Elucidation of the small RNA component of the transcriptome. *Science* **309**, 1567-1569.
- MacAlister, C. A., Ohashi-Ito, K., and Bergmann, D. C.** (2007) Transcription factor control of asymmetric cell divisions that establish the stomatal lineage. *Nature* **445**, 537-540.
- Malcomber, S. T. and Kellogg, E. A.** (2005) *SEPALLATA* gene diversification: brave new whorls. *Trends Plant Sci* **10**, 427-435.
- Mallory, A. C., Dugas, D. V., Bartel, D. P., and Bartel, B.** (2004) MicroRNA regulation of NAC-domain targets is required for proper formation and separation of adjacent embryonic, vegetative, and floral organs. *Curr. Biol.* **14**, 1035-1106.
- Mallory, A. C., Bartel, D. P., and Bartel, B.** (2005) MicroRNA-directed regulation of Arabidopsis *AUXIN RESPONSE FACTOR17* is essential for proper development and modulates expression of early auxin response genes. *Plant Cell* **17**, 1360-1375.
- Mandel, M. A., Gustafson-Brown, C., Savidge, B., and Yanofsky, M. F.** (1992) Molecular characterization of the Arabidopsis floral homeotic gene *APETALA1*. *Nature* **360**, 273-277.
- Mandel, M. A. and Yanofsky, M. F.** (1995) A gene triggering flower formation in Arabidopsis. *Nature* **377**, 522-524.
- Martienssen, R. and Irish, V.** (1999) Copying out our ABCs: the role of gene redundancy in interpreting genetic hierarchies. *Trends Genet* **15**, 435-437.
- Martinez-Zapater, J. M. and Somerville, C. R.** (1990) Effect of Light quality and vernalization on late-flowering mutants of *Arabidopsis thaliana*. *Plant Physiol* **92**, 770-776.
- Matranga, C., Tomari, Y., Shin, C., Bartel, D. P., and Zamore, P. D.** (2005) Passenger-strand cleavage facilitates assembly of siRNA into Ago2-containing RNAi enzyme complexes. *Cell* **123**, 607-620.
- McConnell, J. R. and Barton, M. K.** (1998) Leaf polarity and meristem formation in Arabidopsis. *Development* **125**, 2935-2942.
- McConnell, J. R., Emery, J., Eshed, Y., Bao, N., Bowman, J., and Barton, M. K.** (2001) Role of *PHABULOSA* and *PHAVOLUTA* in determining radial patterning in shoots. *Nature* **411**, 709-713.
- Meister, G., Landthaler, M., Patkaniowska, A., Dorsett, Y., Teng, G., and Tuschl, T.** (2004) Human Argonaute2 mediates RNA cleavage targeted by miRNAs and siRNAs. *Mol Cell* **15**, 185-197.
- Metcalfe CR, Chalk L. Anatomy of the dicotyledons.** (1950). Oxford: Clarendon Press. Ref Type: Generic
- Meyerowitz, E. M.** (2002) Plants compared to animals: the broadest comparative study of development. *Science* **295**, 1482-1485.

- Michaels, S. D. and Amasino, R. M.** (1999) *FLOWERING LOCUS C* encodes a novel MADS domain protein that acts as a repressor of flowering. *Plant Cell* **11**, 949-956.
- Millar, A. A. and Gubler, F.** (2005) The Arabidopsis *GAMYB-LIKE* genes, *MYB33* and *MYB65*, are microRNA-regulated genes that redundantly facilitate anther development. *Plant Cell* **17**, 705-721.
- Mizukami, Y., Huang, H., Tudor, M., Hu, Y., and Ma, H.** (1996) Functional domains of the floral regulator AGAMOUS: characterization of the DNA binding domain and analysis of dominant negative mutations. *Plant Cell* **8**, 831-845.
- Moissiard, G., Parizotto, E. A., Himber, C., and Voinnet, O.** (2007) Transitivity in Arabidopsis can be primed, requires the redundant action of the antiviral Dicer-like 4 and Dicer-like 2, and is compromised by viral-encoded suppressor proteins. *RNA* **13**, 1268-1278.
- Molnar, A., Schwach, F., Studholme, D. J., Thuenemann, E. C., and Baulcombe, D. C.** (2007) miRNAs control gene expression in the single-cell alga *Chlamydomonas reinhardtii*. *Nature* **447**, 1126-1129.
- Moon, J., Suh, S. S., Lee, H., Choi, K. R., Hong, C. B., Paek, N. C., Kim, S. G., and Lee, I.** (2003) The *SOC1* MADS-box gene integrates vernalization and gibberellin signals for flowering in Arabidopsis. *Plant J* **35**, 613-623.
- Mourrain, P., Béclin, C., Elmayan, T., Feuerbach, F., Godon, C., Morel, J. -B., Jouette, D., Lacombe, A. -M., Nikic, S., Picault, N., Réjoué, K., Sanial, M., Vo, T. -A., and Vaucheret, H.** (2000) Arabidopsis *SGS2* and *SGS3* genes are required for posttranscriptional gene silencing and natural virus resistance. *Cell* **101**, 533-542.
- Nadeau, J. A. and Sack, F. D.** (2002) Control of stomatal distribution on the Arabidopsis leaf surface. *Science* **296**, 1697-1700.
- Nam, J., Kim, J., Lee, S., An, G., Ma, H., and Nei, M.** (2004) Type I MADS-box genes have experienced faster birth-and-death evolution than type II MADS-box genes in angiosperms. *Proc Natl Acad Sci USA* **101**, 1910-1915.
- Navarro, L., Dunoyer, P., Jay, F., Arnold, B., Dharmasiri, N., Estelle, M., Voinnet, O., and Jones, J. D. G.** (2006) A plant miRNA contributes to antibacterial resistance by repressing auxin signaling. *Science* **312**, 436-439.
- Nawy, T., Lee, J. Y., Colinas, J., Wang, J. Y., Thongrod, S. C., Malamy, J. E., Birnbaum, K., and Benfey, P. N.** (2005) Transcriptional profile of the Arabidopsis root quiescent center. *Plant Cell* **17**, 1908-1925.
- Nogueira, F. T. S., Sarkar, A. K., Chitwood, D. H., and Timmermans, M. C. P.** (2006) Organ polarity in plants is specified through the opposing activity of two distinct small regulatory RNAs. *Cold Spring Harb Symp Quant Biol* **71**, 157-164.
- Norman, C., Runswick, M., Pollock, R., and Treisman, R.** (1988) Isolation and properties of cDNA clones encoding SRF, a transcription factor that binds to the c-fos serum response element. *Cell* **55**, 989-981003.
- O'Donnell, K. A. and Boeke, J. D.** (2007) Mighty Piwis defend the germline against genome

- intruders. *Cell* **129**, 37-44.
- Ohashi-Ito, K. and Bergmann, D. C.** (2006) Arabidopsis *FAMA* controls the final proliferation/differentiation switch during stomatal development. *Plant Cell* **18**, 2493-2505.
- Omland, K. E.** (1997) Correlated rates of molecular and morphological evolution. *Evolution* **51**, 1381-1393.
- Onodera, Y., Haag, J. R., Ream, T., Nunes, P. C., Pontes, O., and Pikaard, C. S.** (2005) Plant nuclear RNA polymerase IV mediates siRNA and DNA methylation-dependent heterochromatin formation. *Cell* **120**, 613-622.
- Onouchi, H., Igeno, M. I., Perilleux, C., Graves, K., and Coupland, G.** (2000) Mutagenesis of plants overexpressing *CONSTANS* demonstrates novel interactions among Arabidopsis flowering-time genes. *Plant Cell* **12**, 885-900.
- Otegui, M. S., Noh, Y. S., Martinez, D. E., Vila Petroff, M. G., Staehelin, L. A., Amasino, R. M., and Guimmet, J. J.** (2005) Senescence-associated vacuoles with intense proteolytic activity develop in leaves of Arabidopsis and soybean. *Plant J* **41**, 831-844.
- Paakkonen, E. and Holopainen, T.** (1995) Influence of nitrogen supply on the response of clones of birch (*Betula pendula* Roth. ) to ozone. *New Phytologist* **129**, 595-603.
- Palatnik, J. F., Allen, E., Wu, X., Schommer, C., Schwab, R., Carrington, J. C., and Weigel, D.** (2003) Control of leaf morphogenesis by microRNAs. *Nature* **425**, 257-263.
- Palatnik, J. F., Wollmann, H., Schommer, C., Schwab, R., Boisbouvier, J., Rodriguez, R., Warthmann, N., Allen, E., Dezulian, T., Huson, D., Carrington, J. C., and Weigel, D.** (2007) Sequence and expression differences underlie functional specialization of Arabidopsis microRNAs miR159 and miR319. *Dev Cell* **13**, 115-125.
- Pant, D. D.** (1965) On the ontogeny of stomata and other homologous structures. *Pl. Set. Allahabad* **1**, 1-24.
- Pant, D. D. and Kidwai, P. F.** (1967) Development of stomata in some Cruciferae. *Ann. Bot.* **31**, 513-521.
- Parenicova, L., de Folter, S., Kieffer, M., Horner, D. S., Favalli, C., Busscher, J., Cook, H. E., Ingram, R. M., Kater, M. M., Davies, B., Angenent, G. C., and Colombo, L.** (2003) Molecular and phylogenetic analyses of the complete MADS-box transcription factor family in Arabidopsis: new openings to the MADS world. *Plant Cell* **15**, 1538-1551.
- Parizotto, E. A., Dunoyer, P., Rahm, N., Humber, C., and Voinnet, O.** (2004) *In vivo* investigation of the transcription, processing, endonucleolytic activity, and functional relevance of the spatial distribution of a plant miRNA. *Genes Dev* **18**, 2237-2242.
- Park, W., Li, J., Song, R., Messing, J., and Chen, X.** (2002) *CARPEL FACTORY*, a Dicer homolog, and *HEN1*, a novel protein, act in microRNA metabolism in Arabidopsis thaliana. *Curr Biol* **12**, 1484-1495.
- Passmore, S., Elble, R., and Tye, B. K.** (1989) A protein involved in minichromosome maintenance in yeast binds a transcriptional enhancer conserved in eukaryotes. *Genes Dev* **3**, 921-935.

- Pauli, S., Rothnie, H. M., Chen, G., He, X., and Hohn, T.** (2004) The cauliflower mosaic virus 35S promoter extends into the transcribed region. *J Virol* **78**, 12120-12128.
- Pelaz, S., Gustafson-Brown, C., Kohalmi, S. E., Crosby, W. L., and Yanofsky, M. F.** (2001) *APETALA1* and *SEPALLATA3* interact to promote flower development. *Plant J* **26**, 385-394.
- Pellegrini, L., Tan, S., and Richmond, T. J.** (1995) Structure of serum response factor core bound to DNA. *Nature* **376**, 490-498.
- Peragine, A., Yoshikawa, M., Wu, G., Albrecht, H. L., and Poethig, R. S.** (2004) *SGS3* and *SGS2/SDE1/RDR6* are required for juvenile development and the production of trans-acting siRNAs in *Arabidopsis*. *Genes Dev.* **18**, 2368-2379.
- Pillitteri, L. J., Sloan, D. B., Bogenschutz, N. L., and Torii, K. U.** (2007a) Termination of asymmetric cell division and differentiation of stomata. *Nature* **445**, 501-505.
- Pillitteri, L. J. and Torii, K. U.** (2007b) Breaking the silence: three bHLH proteins direct cell-fate decisions during stomatal development. *BioEssays* **29**, 861-870.
- Pinyopich, A., Ditta, G. S., Savidge, B., Liljegren, S. J., Baumann, E., Wisman, E., and Yanofsky, M. F.** (2003) Assessing the redundancy of MADS-box genes during carpel and ovule development. *Nature* **424**, 85-88.
- Plesch, G., Ehrhardt, T., and Mueller-Roeber, B.** (2001) Involvement of TAAAG elements suggests a role for *DOF* transcription factors in guard cell-specific gene expression. *Plant J* **28**, 455-464.
- Pontes, O., Li, C. F., Nunes, P. C., Haag, J., Ream, T., Vitins, A., Jacobsen, S. E., and Pikaard, C. S.** (2006) The *Arabidopsis* chromatin-modifying nuclear siRNA pathway involves a nucleolar RNA processing center. *Cell* **126**, 79-92.
- Pontier, D., Yahubyan, G., Vega, D., Bulski, A., Saez-Vasquez, J., Hakimi, M. A., Lerbs-Mache, S., Colot, V., and Lagrange, T.** (2005) Reinforcement of silencing at transposons and highly repeated sequences requires the concerted action of two distinct RNA polymerases IV in *Arabidopsis*. *Genes Dev* **19**, 2030-2040.
- Putterill, J., Robson, F., Lee, K., Simon, R., and Coupland, G.** (1995) The *CONSTANS* gene of *Arabidopsis* promotes flowering and encodes a protein showing similarities to zinc finger transcription factors. *Cell* **80**, 847-857.
- Qi, Y., Denli, A. M., and Hannon, G. J.** (2005) Biochemical specialization within *Arabidopsis* RNA silencing pathways. *Mol Cell* **19**, 421-428.
- Qi, Y., He, X., Wang, X. J., Kohany, O., Jurka, J., and Hannon, G. J.** (2006) Distinct catalytic and non-catalytic roles of ARGONAUTE4 in RNA-directed DNA methylation. *Nature* **443**, 1008-1012.
- Rajagopalan, R., Vaucheret, H., Trejo, J., and Bartel, D. P.** (2006) A diverse and evolutionarily fluid set of microRNAs in *Arabidopsis thaliana*. *Genes Dev.* **20**, 3407-3425.
- Rajewsky, N.** (2006) Lousy miRNA targets? *Nat Struct Mol Biol* **13**, 754-755.
- Ramakers, C., Ruijter, J. M., Deprez, R. H. L., and Moorman, A. F. M.** (2003) Assumption-

- free analysis of quantitative real-time polymerase chain reaction (PCR) data. *Neurosci. Lett.* **339**, 62-66.
- Ramsay, N. A. and Glover, B. J.** (2005) MYB-bHLH-WD40 protein complex and the evolution of cellular diversity. *Trends Plant Sci* **10**, 63-70.
- Reeder, J., Hochsmann, M., Rehmsmeier, M., Voss, B., and Giegerich, R.** (2006) Beyond mfold: recent advances in RNA bioinformatics. *J. Biotechnol.* **124**, 41-55.
- Reinhart, B. J., Weinstein, E. G., Rhoades, M. W., Bartel, B., and Bartel, D. P.** (2002) MicroRNAs in plants. *Genes Dev.* **16**, 1616-1626.
- Remenyi, A., Schoeler, H. R., and Wilmanns, M.** (2004) Combinatorial control of gene expression. *Nat Struct Mol Biol* **11**, 812-815.
- Ren, S., Johnston, J. S., Shippen, D. E., and McKnight, T. D.** (2004) *TELOMERASE ACTIVATOR1* induces telomerase activity and potentiates responses to auxin in Arabidopsis. *Plant Cell* **16**, 2910-2922.
- Reyes, J. L. and Chua, N. H.** (2007) ABA induction of miR159 controls transcript levels of two MYB factors during Arabidopsis seed germination. *Plant J* **49**, 592-606.
- Rhoades, M. W.** (2002) Prediction of plant microRNA targets. *Cell* **110**, 513-520.
- Riechmann, J. L., Krizek, B. A., and Meyerowitz, E. M.** (1996) Dimerization specificity of Arabidopsis MADS domain homeotic proteins APETALA1, APETALA3, PISTILLATA, and AGAMOUS. *Proc Natl Acad Sci USA* **93**, 4793-4798.
- Riechmann, J. L. and Meyerowitz, E. M.** (1997) Determination of floral organ identity by Arabidopsis MADS domain homeotic proteins AP1, AP3, PI, and AG is independent of their DNA-binding specificity. *Mol Biol Cell* **8**, 1243-1259.
- Riechmann, J. L. and Ratcliffe, O. J.** (2000) A genomic perspective on plant transcription factors. *Curr Opin Plant Biol* **3**, 423-434.
- Robertson, H. D., Webster, R. E., and Zinder, N. D.** (1968) Purification and properties of ribonuclease III from *Escherichia coli*. *J Biol Chem* **243**, 82-91.
- Rogg, L. E. and Bartel, B.** (2001) Auxin signaling: derepression through regulated proteolysis. *Dev Cell* **1**, 595-604.
- Ronshaugen, M., McGinnis, N., and McGinnis, W.** (2002) Hox protein mutation and macroevolution of the insect body plan. *Nature* **415**, 914-917.
- Rounsley, S. D., Ditta, G. S., and Yanofsky, M. F.** (1995) Diverse roles for MADS box genes in Arabidopsis development. *Plant Cell* **7**, 1259-1269.
- Ru, P., Xu, L., Ma, H., and Huang, H.** (2006) Plant fertility defects induced by the enhanced expression of microRNA167. *Cell Res* **16**, 457-465.
- Saito, K., Sakaguchi, Y., Suzuki, T., Suzuki, T., Siomi, H., and Siomi, M. C.** (2007) Pimet, the *Drosophila* homolog of HEN1, mediates 2'-O-methylation of Piwi-interacting RNAs at their 3' ends. *Genes Dev* **21**, 1603-1608.

- Samach, A., Onouchi, H., Gold, S. E., Ditta, G. S., Schwarz-Sommer, Z., Yanofsky, M. F., and Coupland, G.** (2000) Distinct roles of *CONSTANS* target genes in reproductive development of Arabidopsis. *Science* **288**, 1613-1616.
- Sambrook, J. and Russell, D. W.** (2000) Molecular cloning. A laboratory manual. Cold Spring Harbor, NY: Cold Spring Harbor Lab. Press.
- Schmid, M., Uhlenhaut, N. H., Godard, F., Demar, M., Bressan, R., Weigel, D., and Lohmann, J. U.** (2003) Dissection of floral induction pathways using global expression analysis. *Development* **130**, 6001-6012.
- Schwab, R., Palatnik, J. F., Riester, M., Schommer, C., Schmid, M., and Weigel, D.** (2005) Specific effects of microRNAs on the plant transcriptome. *Dev Cell* **8**, 517-527.
- Schwarz-Sommer, Z., Hue, I., Huijser, P., Flor, P. J., Hansen, R., Tetens, F., Lonig, W. E., Saedler, H., and Sommer, H.** (1992) Characterization of the *Antirrhinum* floral homeotic MADS-box gene *deficiens*: evidence for DNA binding and autoregulation of its persistent expression throughout flower development. *EMBO J* **11**, 251-263.
- Serna, L. and Fenoll, C.** (1997) Tracing the ontogeny of stomatal clusters in Arabidopsis with molecular markers. *Plant J.* **12**, 747-755.
- Shannon, S. and Meeks-Wagner, D. R.** (1991) A Mutation in the Arabidopsis *TFL1* Gene Affects Inflorescence Meristem Development. *Plant Cell* **3**, 877-892.
- Sheldon, C. C., Conn, A. B., Dennis, E. S., and Peacock, W. J.** (2002) Different regulatory regions are required for the vernalization-induced repression of *FLOWERING LOCUS C* and for the epigenetic maintenance of repression. *Plant Cell* **14**, 2527-2537.
- Shpak, E. D., McAbee, J. M., Pillitteri, L. J., and Torii, K. U.** (2005) Stomatal patterning and differentiation by synergistic interactions of receptor kinases. *Science* **309**, 290-293.
- Sieburth, L. E. and Meyerowitz, E. M.** (1997) Molecular dissection of the *AGAMOUS* control region shows that cis elements for spatial regulation are located intragenically. *Plant Cell* **9**, 355-365.
- Singer, S. D., Krogan, N. T., and Ashton, N. W.** (2007) Clues about the ancestral roles of plant MADS-box genes from a functional analysis of moss homologues. *Plant Cell Rep* **26**, 1155-1169.
- Singleton, W. R.** (1951) Inheritance of com grass, a macromutation in maize, and its possible significance as an ancestral type. *Am. Nat.* **85**, 81-96.
- Smalheiser, N. R. and Torvik, V. I.** (2005) Mammalian microRNAs derived from genomic repeats. *Trends Genet* **21**, 322-326.
- Smith, L. B. and King, G. J.** (2000) The distribution of *BoCAL-a* alleles in *Brassica oleracea* is consistent with a genetic model for curd development and domestication of the cauliflower. *Mol. Breed.* **6**, 603-613.
- Sommer, H., Beltr n, J. P., Huijser, P., Pape, H., Lonig, W. E., Saedler, H., and Schwarz-Sommer, Z.** (1990) *Deficiens*, a homeotic gene involved in the control of flower morphogenesis in *Antirrhinum majus*: the protein shows homology to transcription factors. *EMBO J* **9**,



605-613.

- Song, J. J., Liu, J., Tolia, N. H., Schneiderman, J., Smith, S. K., Martienssen, R. A., Hannon, G. J., and Joshua-Tor, L.** (2003) The crystal structure of the Argonaute2 PAZ domain reveals an RNA binding motif in RNAi effector complexes. *Nat Struct Biol* **10**, 1026-1032.
- Song, J. J., Smith, S. K., Hannon, G. J., and Joshua-Tor, L.** (2004) Crystal structure of Argonaute and its implications for RISC slicer activity. *Science* **305**, 1434-1437.
- Song, L., Han, M. H., Lesicka, J., and Fedoroff, N.** (2007) Arabidopsis primary microRNA processing proteins HYL1 and DCL1 define a nuclear body distinct from the cajal body. *Proc Natl Acad Sci USA* **104**, 5437-5442.
- Souret, F. F., Kastenmayer, J. P., and Green, P. J.** (2004) *AtXRN4* degrades mRNA in Arabidopsis and its substrates include selected miRNA targets. *Mol Cell* **15**, 173-83.
- Sridhar, V. V., Surendrarao, A., and Liu, Z.** (2006) APETALA1 and SEPALLATA3 interact with SEUSS to mediate transcription repression during flower development. *Development* **133**, 3159-3166.
- Sullivan, C. S., Grundhoff, A. T., Tevethia, S., Pipas, J. M., and Ganem, D.** (2005) SV40-encoded microRNAs regulate viral gene expression and reduce susceptibility to cytotoxic T cells. *Nature*
- Sunkar, R. and Zhu, J. K.** (2004) Novel and stress-regulated microRNAs and other small RNAs from Arabidopsis. *Plant Cell* **16**, 2001-2019. textbf435, 682-686.
- Sunkar, R., Kapoor, A., and Zhu, J. K.** (2006) Posttranscriptional induction of two Cu/Zn superoxide dismutase genes in Arabidopsis is mediated by downregulation of miR398 and important for oxidative stress tolerance. *Plant Cell* **18**, 2051-2065.
- Svensson, M. E., Johannesson, H., and Engstrom, P.** (2000) The LAMB1 gene from the clubmoss, *Lycopodium annotinum*, is a divergent MADS-box gene, expressed specifically in sporogenic structures. *Gene* **253**, 31-43
- Takada, S., Hibara, K., Ishida, T., and Tasaka, M.** (2001) The *CUP-SHAPED COTYLEDON1* gene of Arabidopsis regulates shoot apical meristem formation. *Development* **128**, 1127-1135.
- Talmor-Neiman, M., Stav, R., Frank, W., Voss, B., and Arazi, T.** (2006a) Novel micro-RNAs and intermediates of micro-RNA biogenesis > »from moss. *Plant J* **47**, 25-37.
- Talmor-Neiman, M., Stav, R., Klipcan, L., Buxdorf, K., Baulcombe, D. C., and Arazi, T.** (2006b) Identification of trans-acting siRNAs in moss and an RNA-dependent RNA polymerase required for their biogenesis. *Plant J* **48**, 511-521.
- Teichmann, S. A. and Babu, M. M.** (2004) Gene regulatory network growth by duplication. *Nat Genet* **36**, 492-496.
- Theissen, G.** (2001) Development of floral organ identity: stories from the MADS house. *Curr Opin Plant Biol* **4**, 75-85.

- Theissen, G., Becker, A., Di Rosa, A., Kanno, A., Kim, J. T., Munster, T., Winter, K. U., and Saedler, H.** (2000) A short history of MADS-box genes in plants. *Plant Mol Biol* **42**, 115-149.
- Theissen, G., Kim, J. T., and Saedler, H.** (1996) Classification and phylogeny of the MADS-box multigene family suggest defined roles of MADS-box gene subfamilies in the morphological evolution of eukaryotes. *J Mol Evol* **43**, 484-516.
- Theissen, G. and Saedler, H.** (2001) Plant biology. Floral quartets. *Nature* **409**, 469-471.
- Tomari, Y., Matranga, C., Haley, B., Martinez, N., and Zamore, P. D.** (2004) A protein sensor for siRNA asymmetry. *Science* **306**, 1377-1380.
- Tomari, Y. and Zamore, P. D.** (2005) MicroRNA biogenesis: drosha can't cut it without a partner. *Curr Biol* **15**, 61-64.
- Torii, K. U., Mitsukawa, N., Oosumi, T., Matsuura, Y., Yokoyama, R., Whittier, R. F., and Komeda, Y.** (1996) The Arabidopsis *ERECTA* gene encodes a putative receptor protein kinase with extracellular leucine-rich repeats. *Plant Cell* **8**, 735-746.
- Town, C. D., Cheung, F., Maiti, R., Crabtree, J., Haas, B. J., Wortman, J. R., Hine, E. E., Althoff, R., Arbogast, T. S., Tallon, L. J., Vigouroux, M., Trick, M., and Bancroft, I.** (2006) Comparative genomics of *Brassica oleracea* and *Arabidopsis thaliana* reveal gene loss, fragmentation, and dispersal after polyploidy. *Plant Cell* **18**, 1348-1359.
- Treisman, R.** (1990) The SRE: a growth factor responsive transcriptional regulator. *Semin Cancer Biol* **1**, 47-58.
- Troebner, W., Ramirez, L., Motte, P., Hue, I., Huijser, P., Loennig, W. E., Saedler, H., Sommer, H., and Schwarz-Sommer, Z.** (1992) *globosa* a homeotic gene which interacts with *deficiens* in the control of Antirrhinum floral organogenesis. *EMBO J.* **11**, 4693-4704.
- Ueno, Y., Ishikawa, T., Watanabe, K., Terakura, S., Iwakawa, H., Okada, K., Machida, C., and Machida, Y.** (2007) Histone deacetylases and *ASYMMETRIC LEAVES2* are involved in the establishment of polarity in leaves of Arabidopsis. *Plant Cell* **19**, 445-457.
- Ulmasov, T., Hagen, G., and Guilfoyle, T. J.** (1997a) *ARF1*, a transcription factor that binds to auxin response elements. *Science* **276**, 1865-1868.
- Ulmasov, T., Hagen, G., and Guilfoyle, T. J.** (1999a) Activation and repression of transcription by auxin-response factors. *Proc Natl Acad Sci USA* **96**, 5844-5849.
- Ulmasov, T., Hagen, G., and Guilfoyle, T. J.** (1999b) Dimerization and DNA binding of auxin response factors. *Plant J* **19**, 309-319.
- Ulmasov, T., Murfett, J., Hagen, G., and Guilfoyle, T. J.** (1997b) Aux/IAA proteins repress expression of reporter genes containing natural and highly active synthetic auxin response elements. *Plant Cell* **9**, 1963-1971.
- Upchurch, G. R.** (1984) Cuticular evolution in early cretaceous angiosperms from the potomac group of Virginia and Maryland. *Ann. Missouri Bot. Garden* **71**, 518-546.
- Vagin, V. V., Sigova, A., Li, C., Seitz, H., Gvozdev, V., and Zamore, P. D.** (2006) A distinct

- small RNA pathway silences selfish genetic elements in the germline. *Science* **313**, 320-324.
- Vandenbussche, M., Theissen, G., Van de Peer, Y., and Gerats, T.** (2003) Structural diversification and neo-functionalization during floral MADS-box gene evolution by C-terminal frameshift mutations. *Nucleic Acids Res* **31**, 4401-4409.
- Vaucheret, H., Vazquez, F., Crete, P., and Bartel, D. P.** (2004) The action of *ARGONAUTE1* in the miRNA pathway and its regulation by the miRNA pathway are crucial for plant development. *Genes Dev.* **18**, 1187-1117.
- Vaucheret, H., Mallory, A. C., and Bartel, D. P.** (2006) AGO1 homeostasis entails coexpression of *MIR168* and *AGO1* and preferential stabilization of miR168 by AGO1. *Mol Cell* **22**, 129-136.
- Vazquez, F. Vaucheret H, Rajagopalan R, Lepers C, Gasciolli V, Mallory AC, Hilbert JL, Bartel DP, Crete P.** (2004a) Endogenous trans-acting siRNAs regulate the accumulation of Arabidopsis mRNAs. *Mol. Cell* **16**, 69-79.
- Vazquez, F., Gasciolli, V., Crete, P., and Vaucheret, H.** (2004b) The nuclear dsRNA binding protein HYL1 is required for microRNA accumulation and plant development, but not posttranscriptional transgene silencing. *Curr. Biol.* **14**, 346-351.
- von Groll, U. and Altmann, T.** (2001) Stomatal cell biology. *Curr. Opin. Plant Biol.* **4**, 555-560.
- Wang, H., Ngwenyama, N., Liu, Y., Walker, J. C., and Zhang, S.** (2007) Stomatal development and patterning are regulated by environmentally responsive mitogen-activated protein kinases in Arabidopsis. *Plant Cell* **19**, 63-73.
- Wang, J. F., Zhou, H., Chen, Y. Q., Luo, Q. J., and Qu, L. H.** (2004) Identification of 20 microRNAs from *Oryza sativa*. *Nucleic Acids Res* **32**, 1688-1695.
- Wang, J. W., Wang, L. J., Mao, Y. B., Cai, W. J., Xue, H. W., and Chen, X. Y.** (2005) Control of root cap formation by microRNA-targeted auxin response factors in Arabidopsis. *Plant Cell* **17**, 2204-2216.
- Wang, X. J., Reyes, J., Chua, N. H., and Gaasterland, T.** (2004) Prediction and identification of *Arabidopsis thaliana* microRNAs and their mRNA targets. *Genome Biology* **5**, R65.
- Watanabe, T., Takeda, A., Tsukiyama, T., Mise, K., Okuno, T., Sasaki, H., Minami, N., and Imai, H.** (2006) Identification and characterization of two novel classes of small RNAs in the mouse germline: retrotransposon-derived siRNAs in oocytes and germline small RNAs in testes. *Genes Dev* **20**, 1732-1743.
- Weigel, D., Alvarez, J., Smyth, D. R., Yanofsky, M. F., and Meyerowitz, E. M.** (1992) *LEAFY* controls floral meristem identity in Arabidopsis. *Cell* **69**, 843-859.
- West, A. G., Causier, B. E., Davies, B., and Sharrocks, A. D.** (1998) DNA binding and dimerisation determinants of *Antirrhinum majus* MADS-box transcription factors. *Nucleic Acids Res* **26**, 5277-5287.
- West, A. G. and Sharrocks, A. D.** (1999) MADS-box transcription factors adopt alternative mechanisms for bending DNA. *J Mol Biol* **286**, 1311-1323.

- Wightman, B., Ha, I., and Ruvkun, G.** (1993) Posttranscriptional regulation of the heterochronic gene *lin-14* by *lin-4* mediates temporal pattern formation in *C. elegans*. *Cell* **75**, 855-862.
- Williams, L., Grigg, S. P., Xie, M., Christensen, S., and Fletcher, J. C.** (2005) Regulation of Arabidopsis shoot apical meristem and lateral organ formation by microRNA miR166g and its *AtHD-ZIP* target genes. *Development* **132**, 3657-3668.
- Wu, G. and Poethig, R. S.** (2006) Temporal regulation of shoot development in *Arabidopsis thaliana* by miR156 and its target *SPL3*. *Development* **133**, 3539-3547.
- Wu, M. F., Tian, Q., and Reed, J. W.** (2006) Arabidopsis microRNA167 controls patterns of *ARF6* and *ARF8* expression, and regulates both female and male reproduction. *Development* **133**, 4211-4218.
- Xie, Z., Kasschau, K. D., and Carrington, J. C.** (2003) Negative feedback regulation of Dicer-like1 in Arabidopsis by microRNA-guided mRNA degradation. *Curr. Biol.* **13**, 784-789.
- Xie, Z., Johansen, L. K., Gustafson, A. M., Kasschau, K. D., Lellis, A. D., Zilberman, D., Jacobsen, S. E., and Carrington, J. C.** (2004) Genetic and functional diversification of small RNA pathways in plants. *PLOS Biol.* **2**, 1-11.
- Xie, Z., Allen, E., Fahlgren, N., Calamar, A., Givan, S. A., and Carrington, J. C.** (2005) Expression of Arabidopsis *MIRNA* Genes. *Plant Physiol.* **138**, 2145-2154.
- Yamasaki, H., Abdel-Ghany, S. E., Cohu, C. M., Kobayashi, Y., Shikanai, T., and Pilon, M.** (2007) Regulation of copper homeostasis by micro-RNA in Arabidopsis. *J Biol Chem* **282**, 16369-16378.
- Yan, K. S., Yan, S., Farooq, A., Han, A., Zeng, L., and Zhou, M. M.** (2003) Structure and conserved RNA binding of the PAZ domain. *Nature* **426**, 468-474.
- Yang, L., Liu, Z., Lu, F., Dong, A., and Huang, H.** (2006) *SERRATE* is a novel nuclear regulator in primary microRNA processing in Arabidopsis. *Plant J.* **47**, 841-850.
- Yang, M. and Sack, F. D.** (1995) The *too many mouths* and *four lips* mutations affect stomatal production in Arabidopsis. *Plant Cell* **7**, 2227-2239.
- Yanofsky, M. F., Ma, H., Bowman, J. L., Drews, G. N., Feldmann, K. A., and Meyerowitz, E. M.** (1990) The protein encoded by the Arabidopsis homeotic gene *agamous* resembles transcription factors. *Nature* **346**, 35-39.
- Yu, B., Yang, Z., Li, J., Minakhina, S., Yang, M., Padgett, R. W., Steward, R., and Chen, X.** (2005) Methylation as a crucial step in plant microRNA biogenesis. *Science* **307**, 932-935.
- Yu, D., Fan, B., MacFarlane, S. A., and Chen, Z.** (2003) Analysis of the involvement of an inducible Arabidopsis RNA-dependent RNA polymerase in antiviral defense. *Mol Plant Microbe Interact* **16**, 206-216.
- Zachgo, S., Silva, E., Motte, P., Trobner, W., Saedler, H., and Schwarz-Sommer, Z.** (1995) Functional analysis of the Antirrhinum floral homeotic *DEFICIENS* gene *in vivo* and *in vitro* by using a temperature-sensitive mutant. *Development* **121**, 2861-2875.

- Zachgo, S., Saedler, H., and Schwarz-Sommer, Z.** (1997) Pollen-specific expression of *DEFH125*, a MADS-box transcription factor in *Antirrhinum* with unusual features. *Plant J* **11**, 1043-1050.
- Zamore, P. D. and Haley, B.** (2005) Ribo-gnome: the big world of small RNAs. *Science* **309**, 1519-1524.
- Zhang, B., Pan, X., Cannon, C. H., Cobb, G. P., and Anderson, T. A.** (2006a) Conservation and divergence of plant microRNA genes. *Plant J.* **46**, 243-259.
- Zhang, B., Wang, Q., Wang, K., Pan, X., Liu, F., Guo, T., Cobb, G. P., and Anderson, T. A.** (2007) Identification of cotton microRNAs and their targets. *Gene* **397**, 26-37.
- Zhang, B. H., Pan, X. P., Wang, Q. L., Cobb, G. P., and Anderson, T. A.** (2005) Identification and characterization of new plant microRNAs using EST analysis. *Cell Res* **15**, 336-360.
- Zhang, H. and Forde, B. G.** (1998) An *Arabidopsis* MADS-box gene that controls nutrient-induced changes in root architecture. *Science* **279**, 407-409.
- Zhang, X., Yazaki, J., Sundaresan, A., Cokus, S., Chan, S. W. L., Chen, H., Henderson, I. R., Shinn, P., Pellegrini, M., Jacobsen, S. E., and Ecker, J. R.** (2006b) Genome-wide high-resolution mapping and functional analysis of DNA methylation in *Arabidopsis*. *Cell* **126**, 1189-1201.
- Zhao, T., Li, G., Mi, S., Li, S., Hannon, G. J., Wang, X. J., and Qi, Y.** (2007) A complex system of small RNAs in the unicellular green alga *Chlamydomonas reinhardtii*. *Genes Dev* **21**, 1190-1203.
- Zhong, R. and Ye, Z. H.** (2004) *amphivasal vascular bundle 1*, a gain-of-function mutation of the *IFL1/REV* gene, is associated with alterations in the polarity of leaves, stems and carpels. *Plant Cell Physiol* **45**, 369-385.
- Zhou, X., Ruan, J., Wang, G., and Zhang, W.** (2007) Characterization and identification of microRNA core promoters in four model species. *PLoS Comput Biol* **3**.
- Zhu, C. and Perry, S. E.** (2005) Control of expression and autoregulation of *AGL15*, a member of the MADS-box family. *Plant J* **41**, 583-594.
- Zhu, T., Budworth, P., Han, B., Brown, D., Chang, H. S., and Wang, X.** (2001) Toward elucidating the global gene expression patterns of developing *Arabidopsis*: Parallel analysis of 8300 genes by a high-density oligonucleotide probe array. *Plant Physiol. Biochem.* **39**, 221-242.
- Zilberman, D., Cao, X., Johansen, L. K., Xie, Z., Carrington, J. C., and Jacobsen, S. E.** (2004) Role of *Arabidopsis ARGONAUTE4* in RNA-directed DNA methylation triggered by inverted repeats. *Curr Biol* **14**, 1214-1220.
- Zimmermann, P., Hirsch-Hoffmann, M., Hennig, L., and Gruissem, W.** (2004) GENEVESTIGATOR. *Arabidopsis* microarray database and analysis toolbox. *PLANT PHYSIOL* **136**, 2621-2632.
- Zuker, M.** (2003) Mfold web server for nucleic acid folding and hybridization prediction. *Nucleic Acids Res.* **31**, 3406-3415.

Part VI

Appendices

## A. Supplemental Data

A. Arabidopsis microRNA families and their target genes

**Table A.1.: Arabidopsis microRNA families and their target genes.**

miRNA family <sup>a</sup>	Number of loci	Putative or validated target gene family <sup>b</sup>	References <sup>c</sup>
miR156/157	12	<b>Squamosa-promoter binding protein-like (SPL)</b>	7, 11, 12, 13, 16
miR158	2	Pentatricopeptide repeat (PPR)	7, 11, 12, 13, 16
miR159/319	6	<b>MYB transcription factor, TCP transcription factor</b>	7, 8, 9, 11, 12, 13, 16
miR160	3	<b>Auxin response factor (ARF)</b>	7, 11, 12, 13, 16
miR161	1	<b>Pentatricopeptide repeat (PPR)</b>	7, 11, 12, 13, 16
miR162	2	<b>Dicer-like (DCL1)</b>	7, 11, 12, 13, 16
miR163	1	<b>S-adenosylmethionine-dependent methyltransferase (SAMT)</b>	7, 11, 12, 16
miR164	3	<b>NAC domain transcription factor</b>	7, 11, 12, 13, 16
miR165/166	9	<b>HD-ZIPIII transcription factor</b>	7, 11, 12, 13
miR167	4	<b>Auxin response factor (ARF)</b>	6, 11
miR168	2	<b>Argonaute (AGO1)</b>	7, 11, 12, 13, 16
miR169	14	<b>HAP2 transcription factor</b>	6, 7, 11, 16
miR170/171	4	<b>Scarecrow-like transcription factor (SCL)</b>	7, 11, 12, 13, 16
miR172	5	<b>Apetala2-like transcription factor (AP2)</b>	7, 11, 12, 13, 16
miR173	1	<b>TAS1, TAS2</b>	7, 10, 11, 16
miR390/391	3	<b>TAS3</b>	1, 5, 7, 11, 16
miR393	2	<b>Auxin receptors (TIR1, AFBs), bHLH transcription factor</b>	6, 7, 11, 14, 15
miR394	2	<b>F-box</b>	6, 7, 11, 16
miR395	6	<b>ATP-sulfurylase (APS), Sulfate transporter (AST)</b>	6, 7, 11
miR396	2	<b>Growth regulating factor (GRF)</b>	6, 7, 11, 16
miR397	2	<b>Laccase (LAC)</b>	6, 7, 11, 14, 16
miR398	3	<b>Copper superoxide dismutase (CSD) , Cytochrome-c oxidase</b>	6, 7, 11, 14
miR399	6	<b>Phosphate transporter, E2 ubiquitinating-conjugating protein (E2-UBC)</b>	6, 7, 11
miR400	1	Pentatricopeptide repeat (PPR)	7, 11, 14
miR401	1	Unknown	14
miR402	1	ROS1-like, putative DNA glycosylase	7, 11, 14
miR403	1	<b>Argonaute (AGO2)</b>	7, 11, 14, 16
miR404	1	LRR-TM protein kinase	14
miR405	3	Unknown	14
miR406	1	Spliceosomal proteins	14
miR407	1	Short-chain dehydrogenase/reductase	14
miR408	1	<b>Laccase (LAC), Plantacyanin-like (PCL)</b>	7, 11, 14
miR413	1	Splicing factor, MYB transcription factor, PPR	15
miR414	1	DEAD box RNA helicase (DRH1), F-box, nucleosome assembly protein	15
miR415	1	Cellulose synthase family, PPR	15
miR416	1	F-box	15
miR417	1	RNA-directed RNA polymerase, auxin response transcription factor	15
miR418	1	Homeobox protein	15
miR419	1	ABC transporter family protein, No apical meristem (NAM), histidine kinase	15
miR420	1	None predicted	15
miR426	1	None predicted	15
miR447	3	<b>2-phosphoglycerate kinase-related (2-PGK)</b>	2, 11, 16
miR472	1	<b>CC-NBS-LRR</b>	7, 11, 14
miR771	1	None predicted	7, 11, 14
miR773	1	<b>DNA (cytosine-5)-methyltransferase</b>	4, 7
miR774	1	<b>F-box</b>	4, 7
miR775	1	<b>Galactosyltransferase Avr9 elicitor</b>	4, 7, 11
miR776	1	Serine/threonine kinase	4, 7
miR777	1	None predicted	4, 7, 11
miR778	1	<b>SET-domain</b>	4, 7
miR779	1	None predicted	4, 7, 11
miR780	1	<b>Cation/hydrogen exchanger</b>	4, 7
miR781	1	CD2-binding, MCM	4, 7
miR782	1	Pseudogene	7
miR783	1	Extra-large G-protein-related	7
miR822	1	DC1 domain	11
miR823	1	<b>Chromomethylase, CMT3</b>	4, 11
miR824	1	<b>AGL16 MADS-box</b>	4, 11
miR825	1	Remorin, zinc finger homeobox family, frataxin-related	4, 11
miR826	1	AOP2	11



Table A.1 continued

miR827	1	<b>SPX domain/C3CH4-type RING zinc finger</b>	4, 11
miR828	1	<b>MYB transcription factor</b>	11
miR829	1	AP2 domain ethylene response factor	4, 11
miR830	1	RanBP1 domain, kinesin motor-related	4, 11
miR831	1	None predicted	11
miR832	1	Unknown	11
miR833	1	F-box	4, 11
miR834	1	COP1-interacting protein	11
miR835	1	MYB trabscription factor	11
miR836	1	None predicted	11
miR837	1	GIF transcription factor	11
miR838	1	Armadillo/ $\beta$ -catenin	11
miR839	1	None predicted	11
miR840	1	WHIRLY3	4, 11
miR841	1	Histone H2A.F/Z	11
miR842	1	<b>Jacalin lectin</b>	4, 11
miR843	1	F-box	4, 11
miR844	1	<b>Kinase</b>	4, 11
miR845	2	None predicted	4, 11
miR846	1	<b>Jacalin lectin</b>	4, 11
miR847	1	Cyclophilin-RNA interacting protein	11
miR848	1	None predicted	11
miR849	1	None predicted	11
miR850	1	None predicted	11
miR851	1	None predicted	4, 11
miR852	1	ATPase	4, 11
miR853	1	None predicted	4, 11
miR854	4	UBP1b 3'UTR	3
miR855	1	UBP1b 3'UTR	3
miR856	1	<b>Cation/hydrogen exchanger, Zinc transporter</b>	4
miR857	1	<b>Laccase</b>	4
miR858	1	<b>MYB transcription factor</b>	4
miR859	1	<b>F-box</b>	4
miR860	1	Histone deacetylase, ferrochelataze, RNA recognition motif	4
miR861	1	None predicted	4
miR862	1	None predicted	4
miR863	1	None predicted	4
miR864	1	Triacylglycerol lipase	4
miR865	1	Serine carboxypeptidase, sulfate transporter	4
miR866	1	Expressed protein, C2-domain containing protein	4
miR867	1	PHD finger-related/SET domain, kinase, phospholipase/carboxylesterase	4
miR868	1	None predicted	4
miR869	1	None predicted	4
miR870	1	None predicted	4

<sup>a</sup> Family number according to miRBase Release 10.0

<sup>b</sup> Genes for which miRNA-mediated cleavage was demonstrated experimentally are indicated in bold.

<sup>c</sup> References are indicated according to miRBase Release 10.0

<sup>1</sup> Adai *et al.*, 2005; <sup>2</sup> Allen *et al.*, 2005; <sup>3</sup> Arteaga-Vazquez *et al.*, 2006; <sup>4</sup> Fahlgren *et al.*, 2007; <sup>5</sup> Gustafson *et al.*, 2005; <sup>6</sup> Jones-Rhoades *et al.*, 2004; <sup>7</sup> Lu *et al.*, 2006; <sup>8</sup> Mette *et al.*, 2002; <sup>9</sup> Palatnik *et al.*, 2003; <sup>10</sup> Park *et al.*, 2002; <sup>11</sup> Rajagop; 2006; <sup>12</sup> Reinhart *et al.*, 2002; <sup>13</sup> Rhoades *et al.*, 2002; <sup>14</sup> Sunkar *et al.*, 2004; <sup>15</sup> Wang *et al.*, 2004; <sup>16</sup> Xie *et al.*, 2005

## B. Applied primers

Table A.2.: Applied primers.

Primer by application	Sequence 5'-3' <sup>18</sup>	Description
<b>ProMIR824 Vectors</b>		
F-275RAFL	GCTTCATCTGTGTTTGCAGTC	Cloning of <i>MIR824</i> Exon 3 and 4
R-275RAFL	TTAGAGAGAAACCTACTTGTATATCTATTCC	Cloning of <i>MIR824</i> Exon 3 and 4
F-promofull/ <i>Hind</i> III	CCCAAGCTTCTGATTTGAATACGGTCTGATGCGATGATCC	Cloning of Pro <i>MIR824</i>
R-promofull/ <i>Bam</i> HI	CCGGGATCCGTCGGAAGGAAAGCCGTGATGTGAGG	Cloning of Pro <i>MIR824</i>
F-promo-LTRE/ <i>Hind</i> III	CCGGGATCCCTACCCCTAACACTTATATTTTTGCCTTCCATAG	Cloning of Pro <i>MIR824</i> -LTRE
F-MON60/ <i>Xba</i> I	GCTCTAGAATGGGCAAGGGCGAGGAAC	Cloning of the GFP S <sub>65</sub> T
R-MON60/ <i>Sac</i> I	CGAGCTCTCACTTGTAGAGTTCATCCATGCCATGCG	Cloning of the GFP S <sub>65</sub> T
<b>ProAGL16 Vectors</b>		
F-AGL16/ <i>Bam</i> HI	GGATCCATGGGAAGGGGCAAGATCGCGATTAAG	Cloning of AGL16 ORF
R-AGL16HA/ <i>Bam</i> HI	GGATCCCTCAAGCGTAATCTGGAACATCGTATGGGTATGCAAT GAAGGAAAAATAGTTGAGTTGG	Cloning of AGL16 ORF
F-proAGL16/ <i>Xho</i> I	CCGCTCGAGAGAACAATTTGTCTTGGAAATTTAAATTTAACTA	Cloning ProAGL16
R-proAGL16/ <i>Xba</i> I	TGCTCTAGACTTGCCCTTCCAATTTCTGCTTCTATCA	Cloning ProAGL16
R-proAGL16ln2/ <i>Xba</i> I	GCTCTAGACGACGCTCCTTTTGCAGAA	Cloning ProAGL16 <sub>l2</sub>
<b>Probes cDNA</b>		
F-SCL6-III	GAATAATGCGGAAGCTGCTACGAG	Probe to detect <i>SCL6-III</i>
R-SCL6-III	AAACGTGATCTAACCCAAATGAAAAGC	Probe to detect <i>SCL6-III</i>
F1-AGL16	ATGGGAAGGGGCAAGATCGCGATTAAG	Probe to detect <i>AGL16</i>
R1-AGL16	TTATGCAATGAAGGAAAAATAGTTGAGTTGG	Probe to detect <i>AGL16</i>
<b>Probes oligos</b>		
miR824	TCCCTTCTCACAAATGGTCTA	Oligoprobe to detect miR824 sense
miR824*	TAGACCATTTGTGAGAAGGGA	Oligoprobe to detect miR824*
miR171a	GATATTGGCGCGGCTCAATCA	Oligoprobe to detect miR171 sense
miR426	CGTAAGGACAAATTTCCAAA	Oligoprobe to detect miR426 sense
miR156	GTGCTCACTCTTCTGTCA	Oligoprobe to detect miR156 sense
miR168	TTCCCGACCTGCACCAAGCGA	Oligoprobe to detect miR168 sense
miR165	GGGGATGAAGCCTGGTCCGA	Oligoprobe to detect miR165 sense
siR480(+)	TACGCTATGTTGGACTTAGAA	Oligoprobe to detect ta-siRNA sense
<b>RLM-RACE</b>		
RLMAGL16	AACATAAGTGTGTTGGCACACCG	Primer for RT specific for AGL16 3'
AGL16GSP	ATGCAATGAAGGAAAAATAGTTGAGTTGGATAGC	Primer specific for AGL16 CDS
GSP1_At1g05930	AATTGCCCAACTTAGCCGGC	Primer specific for At1g05930 CDS
GSP2_At1g05930	AAGACAGATGTCGTCGCCAGC	Primer specific for At1g05930 CDS
GSP3_At1g05930	TAGGATACTCCGCTCCTCAGGC	Primer specific for At1g05930 CDS
GSP1_At1g65370	AGTCCTAGAGTAGTAGACATGGCATG	Primer specific for At1g65370 CDS
GSP2_At1g65370	TACCCCTCGCTTTGGTGGCTG	Primer specific for At1g65370 CDS
GSP3_At1g65370	AAGCCCTTAGTTGTGCTCGCAC	Primer specific for At1g65370 CDS
GSP1_At1g65150	AGTCCCAGACTCTAGAGTAGTAGACC	Primer specific for At1g65150 CDS
GSP2_At1g65150	TGTTAGGTGATTGGATCCACGCG	Primer specific for At1g65150 CDS
GSP3_At1g65150	TGTCATCTGCCTCAGAGTCCCC	Primer specific for At1g65150 CDS
GSP1_At1g65050	ACTTTAGAGTAGTAGACATGGCATGG	Primer specific for At1g65050 CDS
GSP2_At1g65050	AGTCCCTCACGGTCCAAGTAAGC	Primer specific for At1g65050 CDS
GSP3_At1g65050	ATGCTGGGATAAATTGTCATCTGCC	Primer specific for At1g65050 CDS
GSP1_ANR1	TTGCCTTCAATCGCATTTGTTCTTCC	Primer specific for ANR1 CDS
GSP2_ANR1	TATGAGTTGAAGTTGCGGTGGTGC	Primer specific for ANR1 CDS
GSP3_ANR1	CTAGGAAAGTTGTAGCCCTAGTCTGA	Primer specific for ANR1 CDS
GSP1_AGL17	GTACTTTTCTCGACAATTCGAGGTT	Primer specific for AGL17 CDS
GSP2_AGL17	TCTACTAGCTCATGATGTCCAATCC	Primer specific for AGL17 CDS
GSP3_AGL17	AAGATGTCTTATAATGGGACTGCTCAGGC	Primer specific for AGL17 CDS
GSP1_AGL21	AGAGCTCCACATTTTCTTGATGAATCC	Primer specific for AGL21 CDS
GSP2_AGL21	ATCTGAGTGTGTGATTCATCATCCGC	Primer specific for AGL21 CDS
GSP3_AGL21	TATTCGTTTGCTCTTGGTGGAGTGC	Primer specific for AGL21 CDS
<b>qPCR</b>		
F-qPCRAGL16	ACCTCCACAAGAAAGTAAACCTAATGC	Real time PCR specific for AGL16
R-qPCRAGL16	TGGCTGAGCTGAAGATGGACATG	Real time PCR specific for AGL16
F-qPCRTIP41	AGAGTTGATGGTGTGCTTATGAGATTG	Real time PCR specific for <i>TIP41</i> -li
R-qPCRTIP41	TGGATACCTTTTCGACATAGAGAC	Real time PCR specific for <i>TIP41</i> -li

Table A.2 continued

<b>RT-PCR</b>		
F1-AGL16	ATGGGAAGGGGCAAGATCGCGATTAAG	RT-PCR specific for <i>AGL16</i>
R1-AGL16	TTATGCAATGAAGGAAAAATAGTTGAGTTGG	RT-PCR specific for <i>AGL16</i>
F2-AGL16	GCTTGCGATTCTCTGCGATGC	RT-PCR specific for <i>AGL16</i>
R2-AGL16	TTTCTGAACTGGTTTCTCCTTTGGC	RT-PCR specific for <i>AGL16</i>
F-SCL6-III	GAATAATGCGGAAGCTGCTACGAG	RT-PCR specific for <i>SCL6-III</i>
R-SCL6-III	AAACGTGATCTAACCCAAATTGAAAAGC	RT-PCR specific for <i>SCL6-III</i>
F- $\beta$ -TUBULIN	CGTGGATCACAGCAATACAGAGCC	RT-PCR specific for $\beta$ - <i>TUBULIN</i>
R- $\beta$ -TUBULIN	CCTCCTGCACCTTCCACTTCGTCTTC	RT-PCR specific for $\beta$ - <i>TUBULIN</i>
F-pri-miR824	TAATCATCACTGCTCTCTTCTCCAT	RT-PCR specific for pri-miR824
R-pri-miR824	AAACTCTTTTATTTTTATTTAGAGAGAAACCTACTT	RT-PCR specific for pri-miR824
F-At4g24415	TAATCATCACTGCTCTCTTCTCCATC	RT-PCR specific for At4g24415
R-At4g24415	AAACTCTTTTATTTTTATTTAGAGAGAAACCTACTTGTATA	RT-PCR specific for At4g24415
F1-At4g24410	AATCATCACTGCTCTCTTCTCCATC	RT-PCR specific for At4g24410
F2-At4g24410	ATTTCAATGGGATCTCGTGACGG	RT-PCR specific for At4g24410
R1-At4g24410	CTCAATACATGAGACAGGTCCACT	RT-PCR specific for At4g24410
<b>EMSA</b>		
CArg1s	TTTCCTAATTAGGACA	CArg box motif 1 AG binding
CArg1as	TGTCCTAATTAGGAAA	CArg box motif 1 AG binding
CArg2s & as	TTACTATATATAGTAA	CArg box motif 2 AGL15 binding
CArg3s & as	TTAGTATATATACTAA	CArg box motif 3 AGL15 binding mut
<b>T-DNA genotyping</b>		
F-AGL16geno	CCGAGAGGTGGGACTATGGTT	Genotyping of <i>agl16-1</i>
R-AGL16geno	TCTCCATGCATTTTCGGTTTT	Genotyping of <i>agl16-1</i>
F-M1geno	TTGCAGCAGTGACTTTTGTGGCC	Genotyping of <i>m1</i>
R-M1geno	TTTGTGTTCTTTGCAGACCTGA	Genotyping of <i>m1</i>
F-M2geno	AGCCAATGTATGATAAGACCAAA	Genotyping of <i>m2</i>
R-M2geno	ATCGGTTTCAGGGTGTCTCCG	Genotyping of <i>m2</i>
F-M3geno	TGATCCGTGTGGTCCTTCAA	Genotyping of <i>m3, m4</i>
R-M3geno	GTCGGAAAAAGCCGTGATGTG	Genotyping of <i>m3, m4</i>
F-RDR6geno	ATGGGGTCAGAGGAAATATGAA	Genotyping of <i>rdr6-15</i>
R-RDR6geno	TTGCACGTGTTGTCAAAGGATC	Genotyping of <i>rdr6-15</i>
LB1 Left Border	GCCTTTTCAGAAATGGATAAATAGCCTTGCTTCC	Genotyping of all SAIL T-DNA lines
pROK2 Left Border	GCGTGGACCGCTTGCTGCAACT	Genotyping of all SALK T-DNA lines

## C. Vector maps

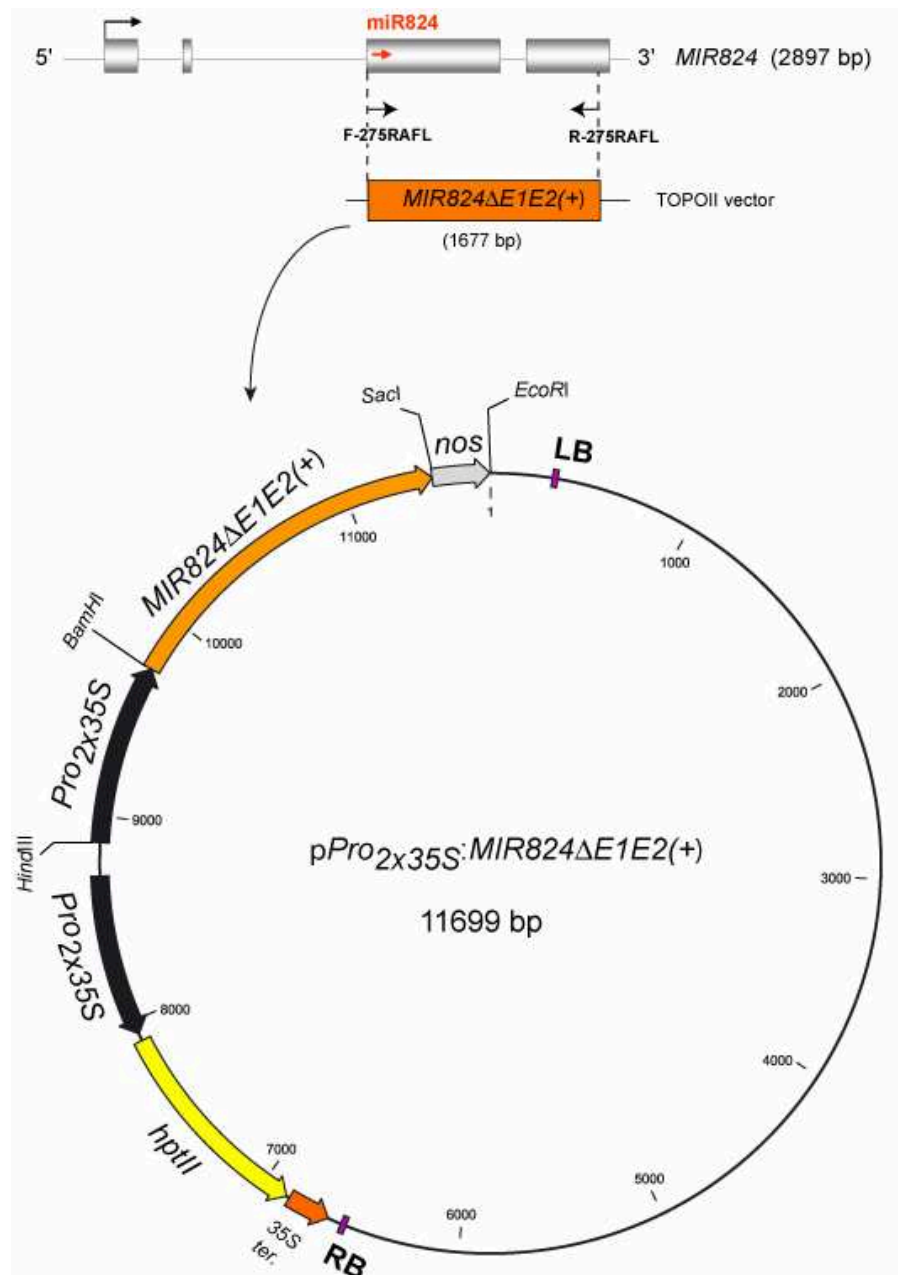


**Figure A.1: Vector map of  $pPro_{2x35S}:MIR824\Delta E1E2(+)$**  (Bacteria: Kan<sup>R</sup>, Plant: Hyg<sup>R</sup>) with relevant restriction sites indicated.

The third and a part of the fourth exon of *MIR824* were amplified using primers F-275RAFL and R-275RAFL (oligonucleotide primers Appendix Table A.2) and the 1677 bp PCR fragment cloned into TOPOII vector. The insert was subcloned in a modified 1300 pCambia binary vector downstream of the double 35S promoter using *Bam*HI/*Sac*I restriction sites.

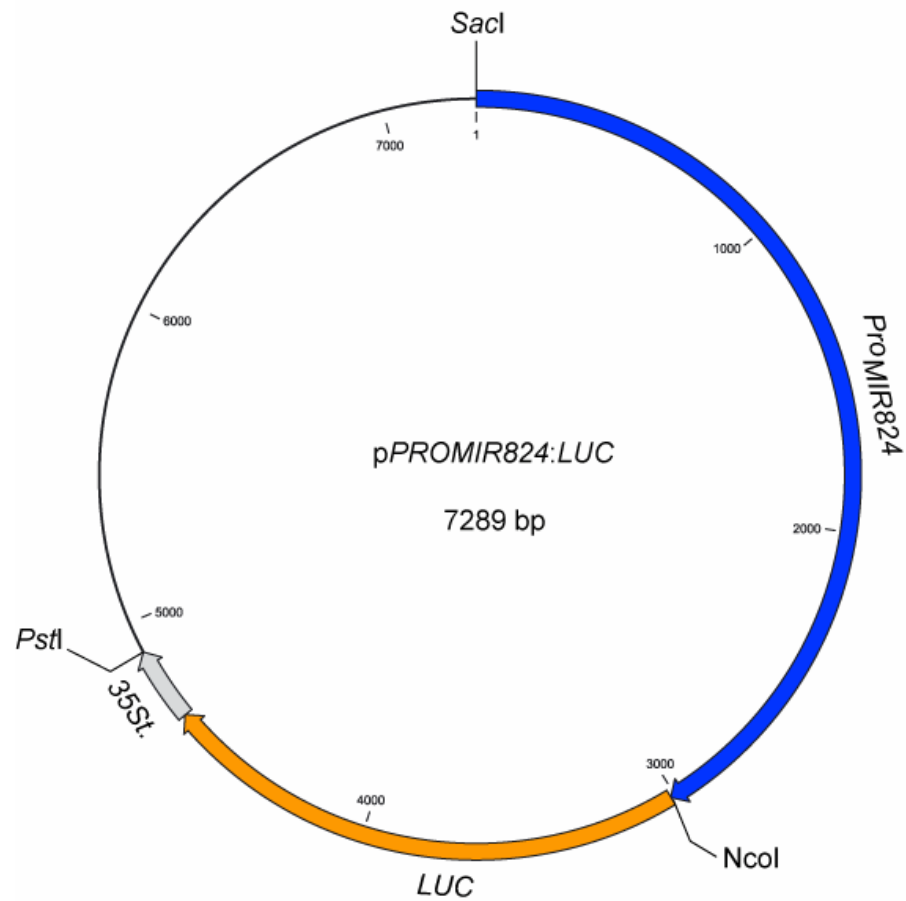


**Figure A.2: Vector map of pPro<sub>MIR824</sub>:Luc (Amp<sup>R</sup>) with relevant restriction sites indicated.**

Construction of this vector is described in Kutter *et al.* (2007) supplemental methods. The vector backbone is pLitmus 28 (Invitrogen).

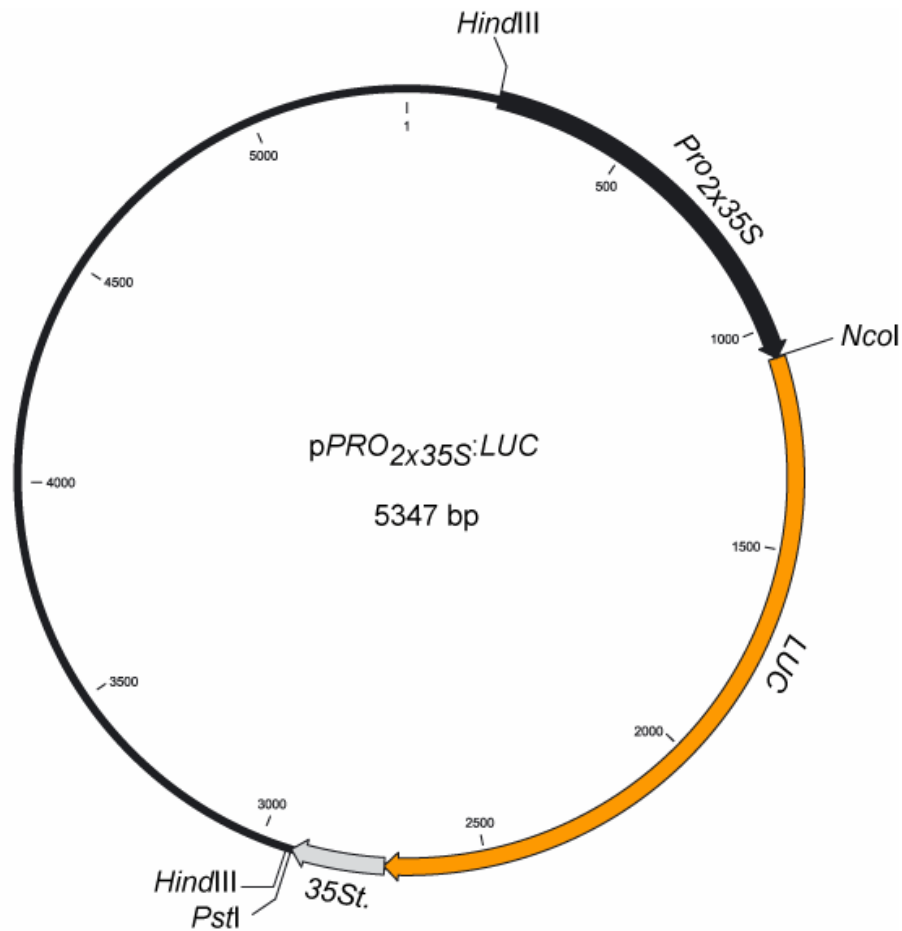


**Figure A.3: Vector map of pPro<sub>2x35S</sub>:Luc (Amp<sup>R</sup>) with relevant restriction sites indicated.**

The cassette containing the Pro<sub>2x35S</sub>:LUC and 35S terminator was excised from the plasmid pGN35Sluc<sup>+</sup> (Molinier *et al.*, 2004) and subcloned in pLitmus 28 (Invitrogen) as described in Kutter *et al.* (2007) supplemental methods.

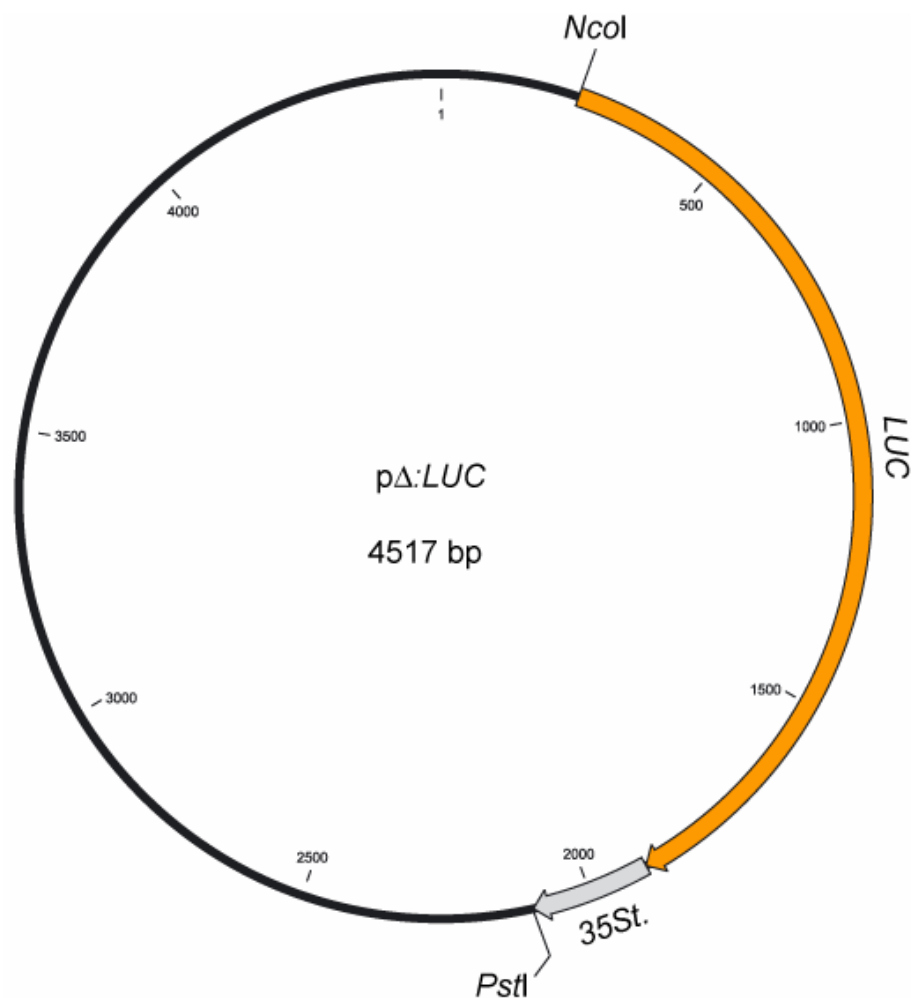


**Figure A.4: Vector map of pΔ:Luc (Amp<sup>R</sup>) with relevant restriction sites indicated.**

The cassette containing the promoterless *LUC* and 35S terminator was excised from the plasmid pGN35Sluc<sup>+</sup> (Molinier *et al.* 2004) and subcloned in pLitmus 28 (Invitrogen) as described in Kutter *et al.* (2007) supplemental methods.

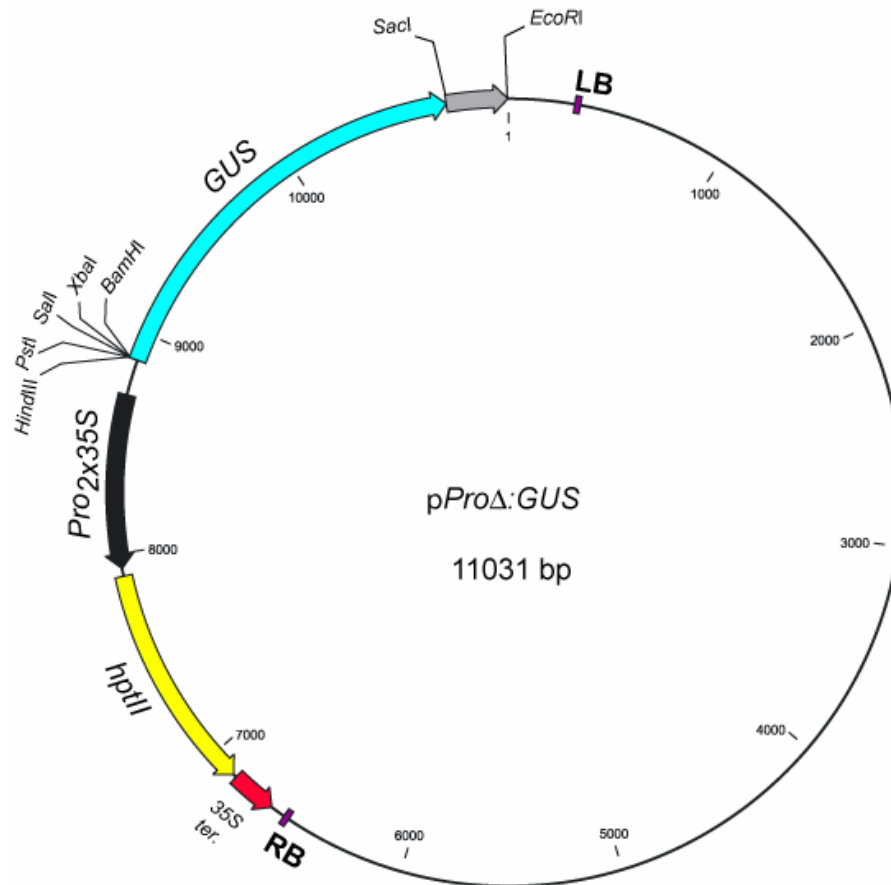


**Figure A.5: Vector map of pProΔ:GUS** (Bacteria: Kan<sup>R</sup>, Plant: Hyg<sup>R</sup>) with relevant restriction sites indicated.

A cassette containing a *GUS* gene and the nos terminator was excised from pBI121 (Clontech) plasmid using *Hind*III and *Eco*RI restriction sites and inserted in a pCambia 1300 binary vector using the same restriction sites.



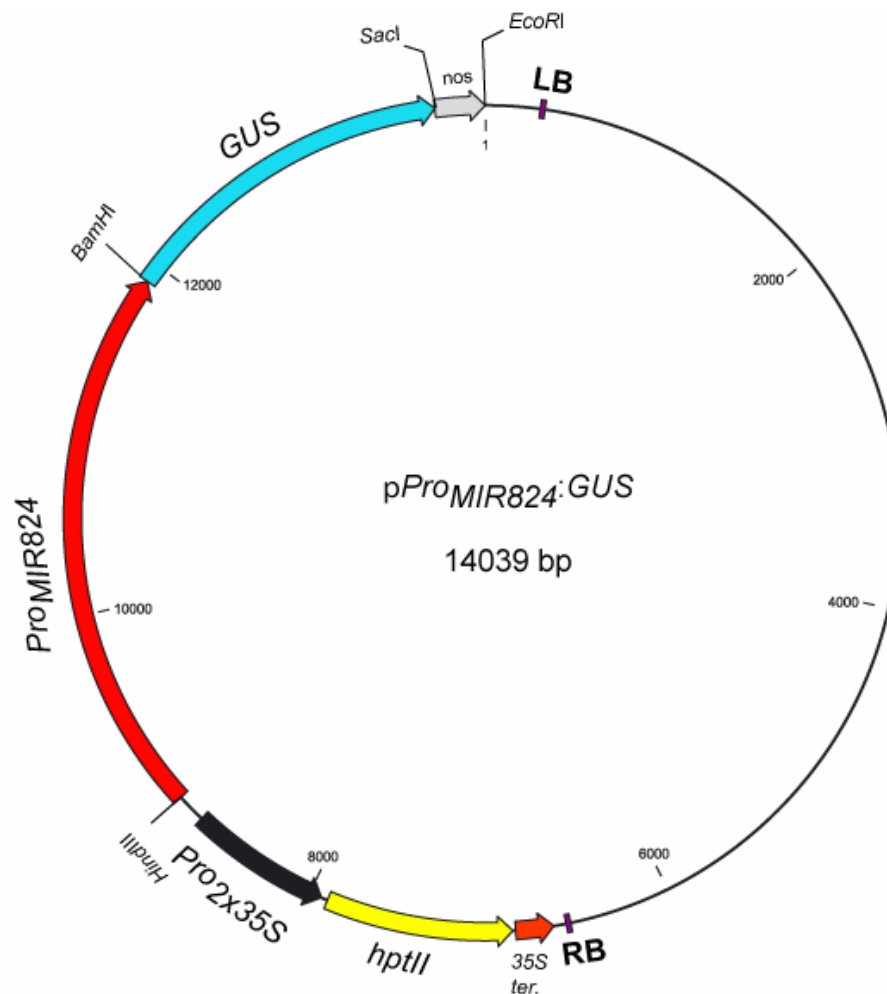


**Figure A.6: Vector map of *pPro<sub>MIR824</sub>:GUS*** (Bacteria: Kan<sup>R</sup>, Plant: Hyg<sup>R</sup>) with relevant restriction sites indicated.

The genomic region downstream of the 3'UTR of At4g24400 and upstream of *MIR824* (At4g24415) was amplified using primers F-promofull/*HindIII* and R-promofull/*BamHI* (oligonucleotide primers Appendix Table A.2) containing respectively a *HindIII* and a *BamHI* restriction site. The 2.9 kb PCR fragment was subcloned in the *pPro $\Delta$ :GUS* vector (Appendix Figure A.5) using the same restriction enzymes.

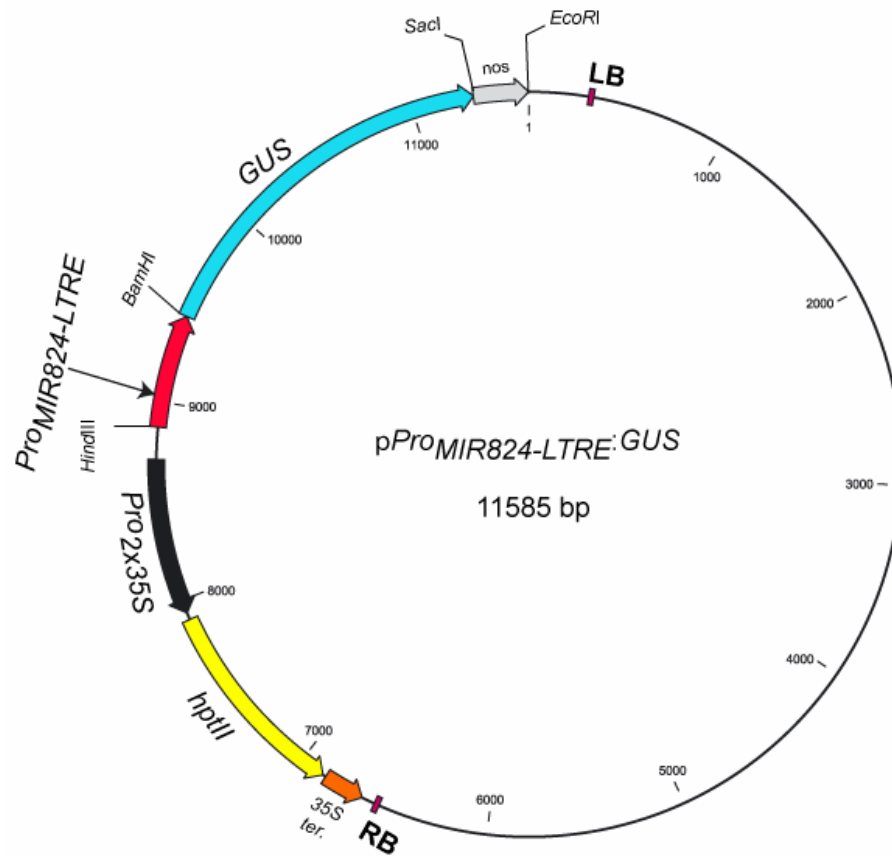


**Figure A.7: Vector map of pPro<sub>MIR824-LTRE</sub>:GUS** (Bacteria: Kan<sup>R</sup>, Plant: Hyg<sup>R</sup>) with relevant restriction sites indicated.

The genomic region upstream of *MIR824* (At4g24415) lacking the cold responsive *cis*-acting element (LTRE) was amplified using primers F-promo-LTRE/*Hind*III and R-promofull/*Bam*HI (oligonucleotide primers Appendix Table A.2) containing respectively a *Hind*III and a *Bam*HI restriction site. The 501 bp PCR fragment was subcloned in the pProΔ:GUS vector (Appendix Figure A.5) using the same restriction enzymes.

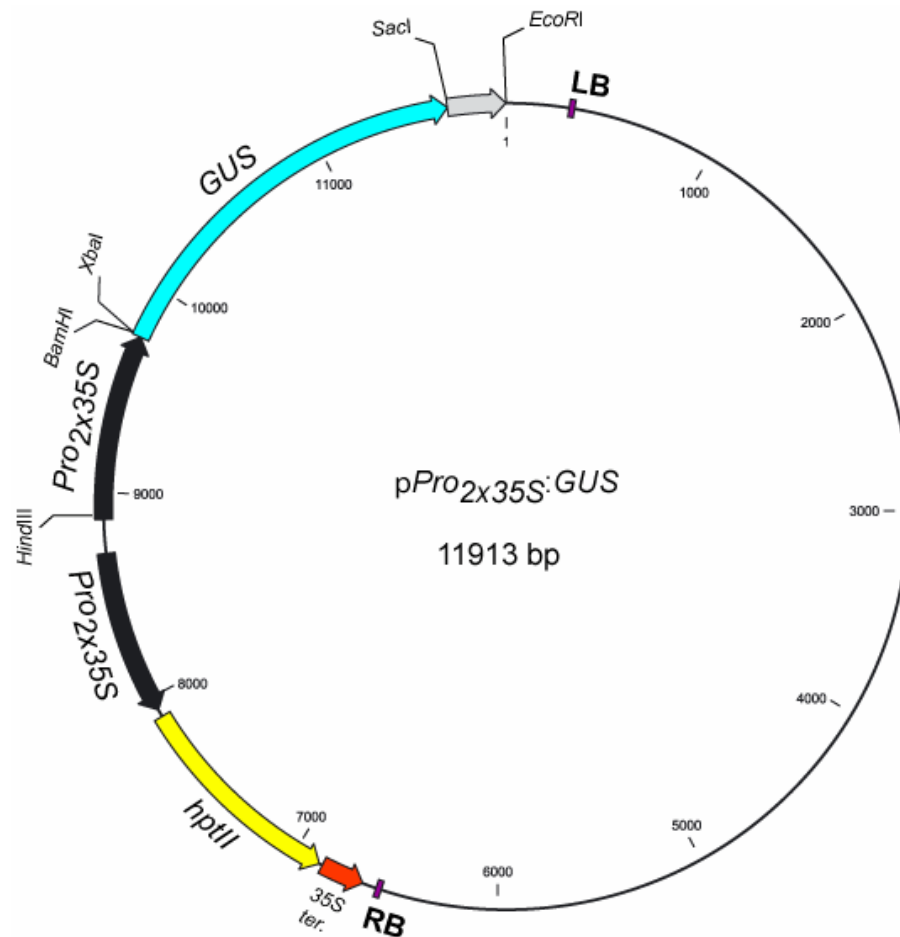


**Figure A.8: Vector map of pPro<sub>2x35S</sub>:GUS** (Bacteria: Kan<sup>R</sup>, Plant: Hyg<sup>R</sup>) with relevant restriction sites indicated.

The vector backbone is a 1300 pCambia binary vector in which the cassette containing a 2x35S:GUS and nos terminator from pBI121 (Clontech) was cloned using *HindIII*/*EcoRI* combination.

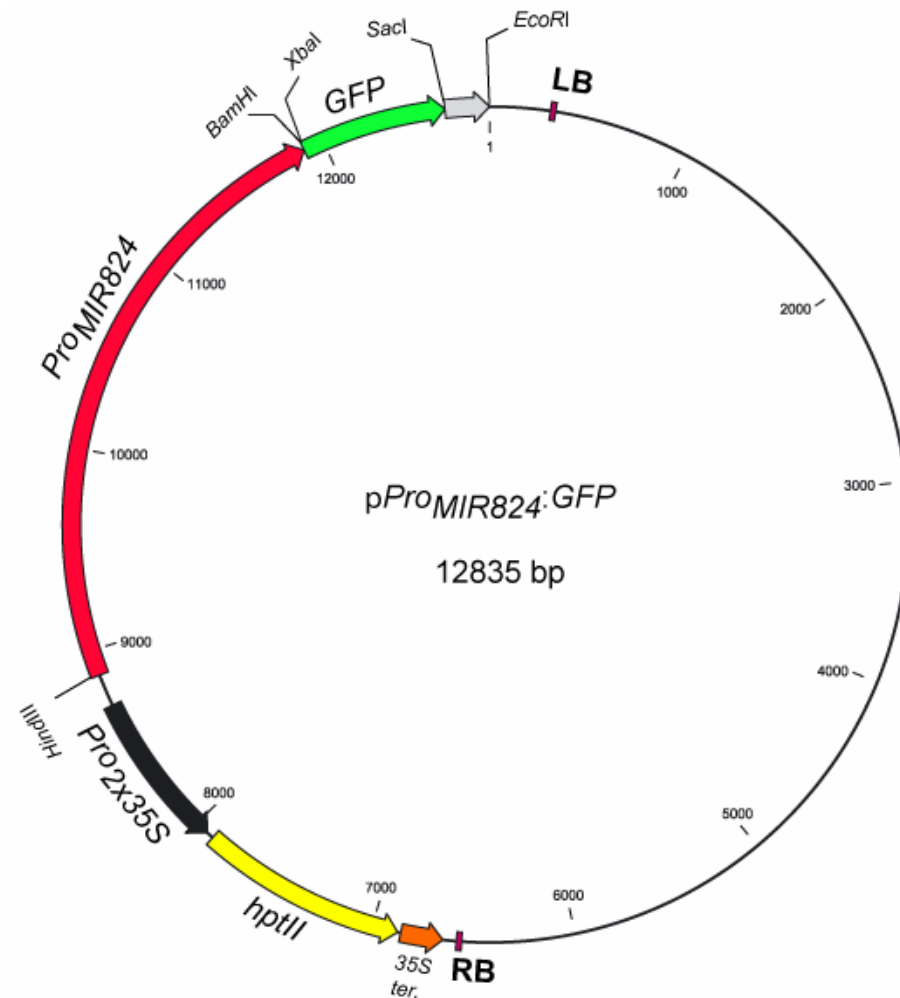


**Figure A.9: Vector map of pPro<sub>MIR824</sub>:GFP** Bacteria: Kan<sup>R</sup>, Plant: Hyg<sup>R</sup>) with relevant restriction sites indicated.

The genomic region downstream of the 3'UTR of At4g24400 and upstream of *MIR824* (At4g24415) was amplified using primers F-promofull/*HindIII* and R-promofull/*BamHI* (oligonucleotide primers Appendix Table A.2) containing respectively a *HindIII* and a *BamHI* restriction site. The 2.9 kb PCR fragment was subcloned in place of the double 35S in the pPro<sub>2x35S</sub>:*GUS* vector (Appendix Figure A.5) using the same restriction enzymes. The GFP was amplified from pMON30060 (Pang *et al.* 1996) using the primers F-MON60/*XbaI* and R-MON60/*SacI* and cloned in place of the *GUS* gene.

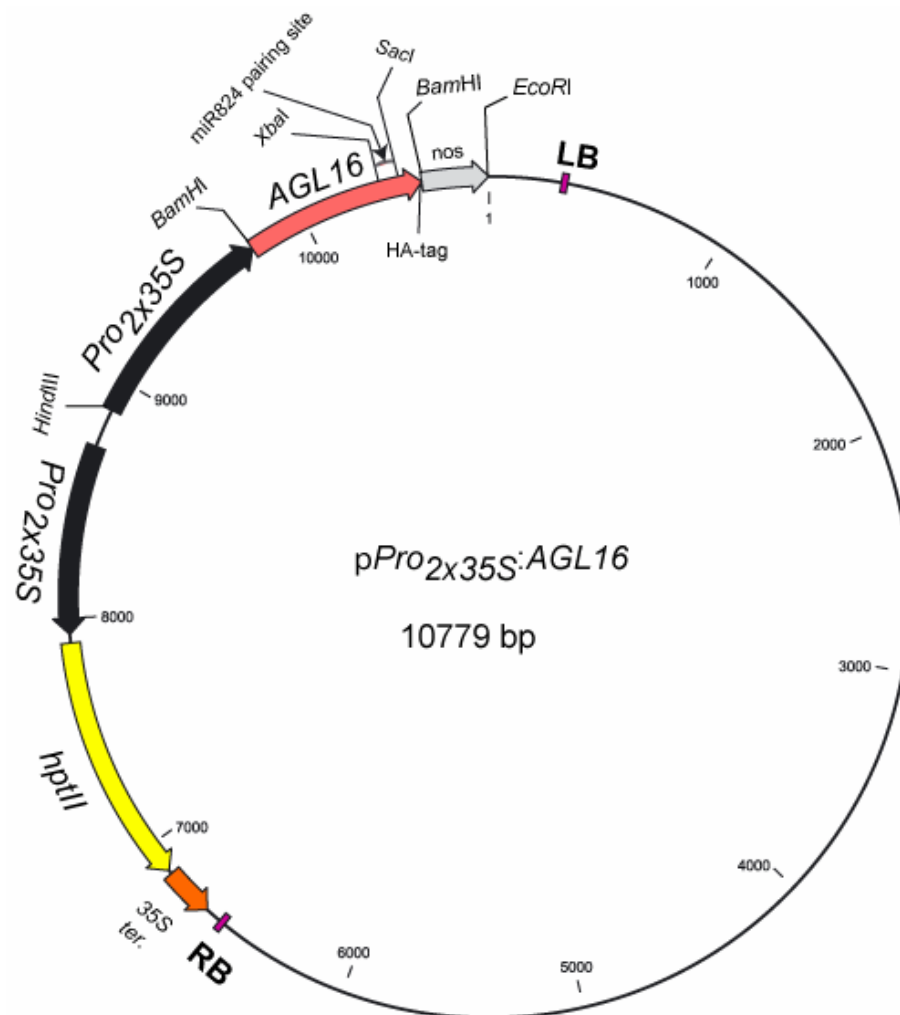


**Figure A.10: Vector map of pPro<sub>2x35S</sub>:AGL16** Bacteria: Kan<sup>R</sup>, Plant: Hyg<sup>R</sup>) with relevant restriction sites indicated.

The wild-type *AGL16* containing an HA-tag at the 3' end was cloned downstream of the double 35S promoter as a *Bam*HI/*Bam*HI fragment as described in details in Kutter *et al.* (2007), supplemental methods.

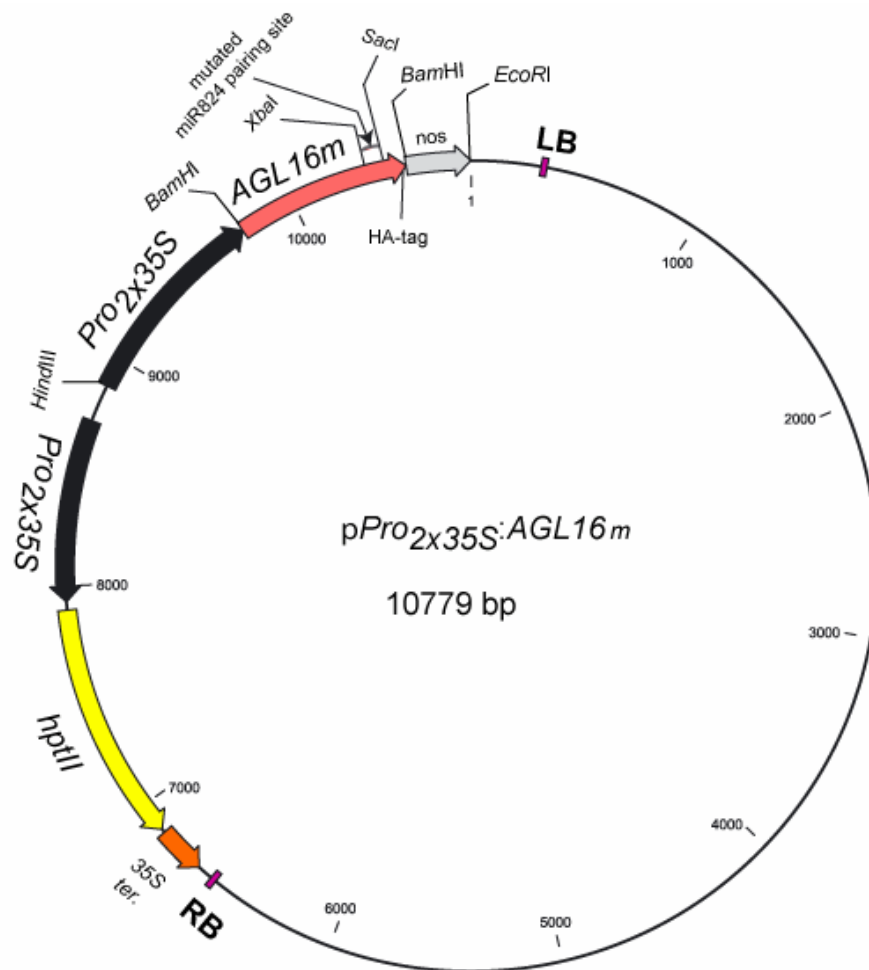


**Figure A.11: Vector map of pPro<sub>2x35S</sub>:AGL16m** (Bacteria: Kan<sup>R</sup>, Plant: Hyg<sup>R</sup>) with relevant restriction sites indicated.

The mutated *AGL16* containing an HA-tag at the 3' end was cloned downstream of the double 35S promoter as a *Bam*HI/*Bam*HI fragment as described in details in Kutter *et al.* (2007), supplemental methods.

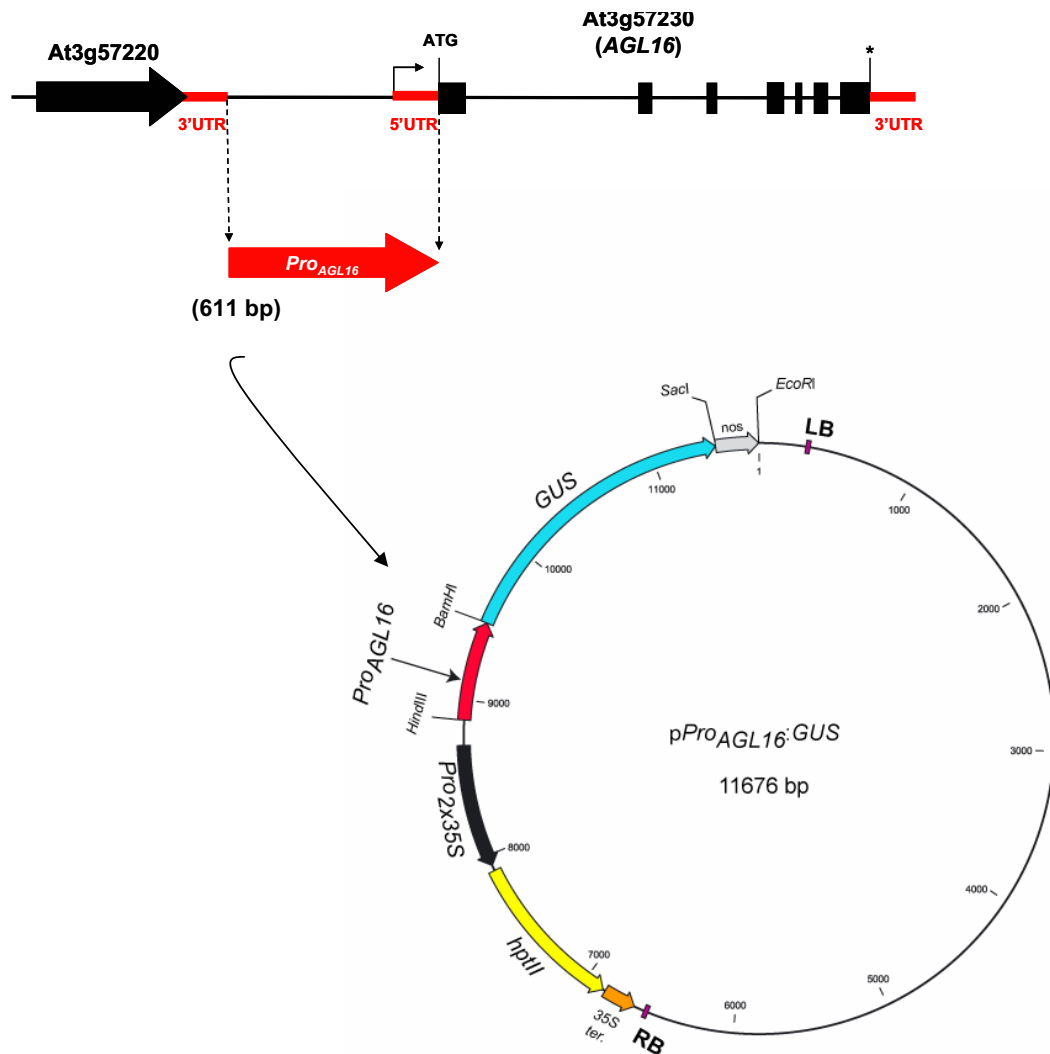


**Figure A.12: Vector map of *pProAGL16:GUS*** (Bacteria: Kan<sup>R</sup>, Plant: Hyg<sup>R</sup>) with relevant restriction sites indicated.

The genomic region downstream of the 3'UTR end of *At3g57220* and upstream of *AGL16* (*At3g57230*) was amplified using primers F-proAGL16/*XhoI* and R-proAGL16/*XbaI* containing respectively a *XhoI* and a *XbaI* restriction site. The 501 bp PCR fragment was subcloned in the *pProΔ:GUS* vector (Appendix Figure A.5) digested with *SacI* and *XbaI*.

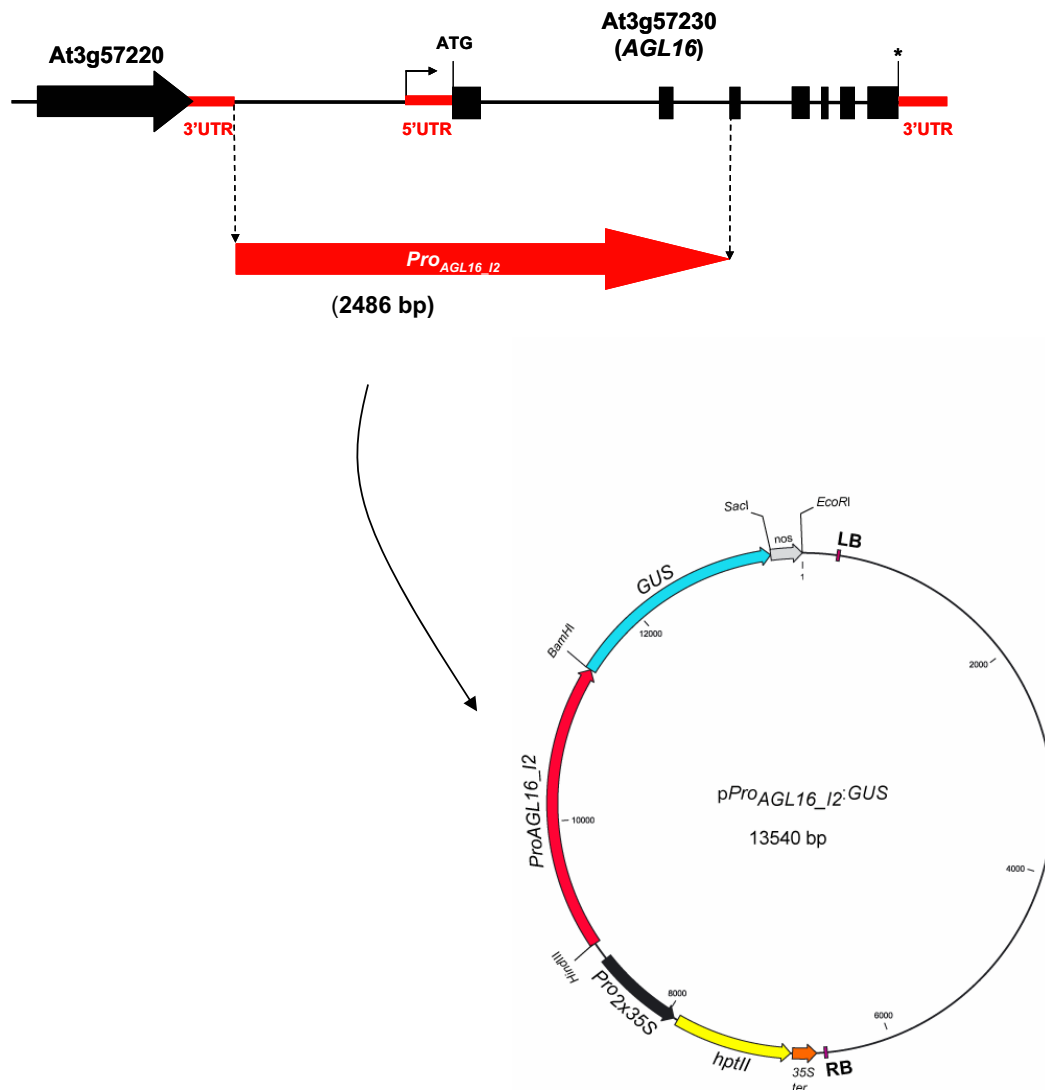


**Figure A.13: Vector map of pPro<sub>AGL16</sub>:GUS** (Bacteria: Kan<sup>R</sup>, Plant: Hyg<sup>R</sup>) with relevant restriction sites indicated.

The genomic region downstream of the 3'UTR end of At3g57220 and upstream of AGL16 (At3g57230) was amplified using primers F-proAGL16/*Xho*I and R-proAGL16In2/*Xba*I containing respectively a *Xho*I and a *Xba*I restriction site. The 501 bp PCR fragment was subcloned in the pProΔ:*GUS* vector (Appendix Figure A.5) digested with *Sac*II and *Xba*I.



## D. Characterization of mutant lines

**Table A.3.: Characterization of mutant lines.**

Note: mutants highlighted in grey were provided by other groups

Name	AGI	mutant	ecotype	mutation	number	reference
<b>RNA silencing mutants</b>						
AGO1	At1g48410	<i>ago1-3</i>	Col-0	EMS	Garlic_371_C09	Bohmert et al, 1998
		<i>ago1-x</i>	Col-0	T-DNA	N576191	
		<i>ago1-y</i>	Col-0	T-DNA	N617308	
		<i>ago1-z</i>	Col-0	T-DNA	N569180	
AGO2	At1g31280	<i>ago2-x</i>	Col-0	T-DNA	N508590	
		<i>ago2-y</i>	Col-0	T-DNA	N537548	
AGO3	At1g31290	<i>ago3-x</i>	Col-0	T-DNA	N501761	
		<i>ago3-y</i>	Col-0	T-DNA	N505335	
AGO4	At2g27040	<i>ago4</i>	Col-0	T-DNA	N571772	
AGO5	At2g27880	<i>ago5-x</i>	Col-0	T-DNA	N571808	
		<i>ago5-y</i>	Col-0	T-DNA	N563806	
AGO6	At2g32940	<i>ago6-x</i>	Col-0	T-DNA	N531553	
		<i>ago6-y</i>	Col-0	T-DNA	N522133	
AGO7	At1g69440	<i>ago7-1</i>	Col-0	T-DNA	N537458	Vazquez et al., 2004
		<i>ago7-x</i>	Col-0	T-DNA	N580533	
		<i>ago7-y</i>	Col-0	T-DNA	N586842	
AGO8	At5g21030	<i>ago8-x</i>	Col-0	T-DNA	N510860	
		<i>ago8-y</i>	Col-0	T-DNA	N614640	
AGO9	At5g21150	<i>ago9-x</i>	Col-0	T-DNA	N626176	
		<i>ago9-y</i>	Col-0	T-DNA	N627358	
AGO10	At5g43810	<i>ago10-y</i>	Col-0	T-DNA	N500457	
		<i>ago10-x</i>	Col-0	T-DNA	N500460	
HYL1	At1g09700	<i>hyl1-1</i>	No-0	Ds		Lu & Fedoroff, 2000
		<i>hyl1-2</i>	Col-0	T-DNA	N564863	Vazquez et al., 2004
HEN1	At4g20910	<i>hyl1-1</i>	Ler	EMS		Chen et al, 2002
		<i>hen1-5</i>	Col-0	T-DNA	N549197	Vazquez et al., 2004
SE	At2g27100	<i>se-1</i>	Col-0	T-DNA	N3257	Redei, 1965
		<i>se-3</i>	Col-0	T-DNA	N683196	Grigg et al, 2005
		<i>se-x</i>	Col-0	T-DNA	N550410	
		<i>se-y</i>	Col-0	T-DNA	N559424	
		<i>se-z</i>	Col-0	T-DNA	N338653	
DCL1	At1g01040	<i>dcl1-7</i> ( <i>sin1-1</i> )	gl-1	EMS		Golden et al., 2002; Schauer et al., 2002
		<i>dcl1-8</i> ( <i>sin1-2</i> )	gl-1	EMS		Golden et al., 2002; Schauer et al., 2003
		<i>dcl1-9</i>	Ler	EMS		Golden et al., 2002; Schauer et al., 2004
		<i>dcl1-x</i>	Col-0	T-DNA	Garlic_1293_D08	
DCL2	At3g03300	<i>dcl2-1</i>	Col-0	T-DNA	N564627	Xie et al., 2003
		<i>dcl2-2/</i> <i>dcl2-5</i>	Col-0	T-DNA	N623586	Kurihara and Watanabe, 2004; Akbergenov et al, 2006; Blevins et al., 2006
		<i>dcl2-3</i>	Col-0	T-DNA	N595069	Vazquez et al, 2004
		<i>dcl2-6</i>	Col-0	T-DNA	N516557	
DCL3	At3g43920	<i>dcl3-1</i>	Col-0	T-DNA	N505512	Xie et al., 2003
		<i>dcl3-2</i>	Col-0	T-DNA	Garlic_327_D02	Akbergenov et al, 2006; Blevins et al, 2006
DCL4		<i>dcl4-2</i>	Col-0	T-DNA	Garlic_510_A03	Xie et al, 2005; Blevins et al., 2006
RNase III	At3g20420	<i>dcl5-x</i>	Col-0	T-DNA	N567855	
RDR1	At1g14790	<i>rdr1-1</i>	Col-0	T-DNA	Garlic_672_F11	
		<i>rdr1-2</i>	Col-0	T-DNA	N507638	Vazquez et al, 2004

Table A.3 continued

RDR2	At4g11130	<i>rdr2-1</i>	Col-0	T-DNA	Garlic_1277_H08	Xie et al., 2004; Blevins et al., 2006
RDR6	At3g49500	<i>rdr6-15</i>	Col-0	T-DNA	Garlic_617_H07	Allen et al., 2004; Akbergrenov et al, 2006
SGS3	At5g23570	<i>sgs3-x</i>	Col-0	T-DNA	Garlic_436_D09	
		<i>sgs3-y</i>	Col-0	T-DNA	N501377	
SDE3	At1g05460	<i>sde3-x</i>	Col-0	T-DNA	Garlic_447_D01	
		<i>sde3-y</i>	Col-0	T-DNA	N503347	
		<i>sde3-4</i>	Col-0	T-DNA	N592019	Vazquez et al, 2004
HASTY	At3g05040	<i>hst-x</i>	Col-0	T-DNA	N579289	
		<i>hst15</i>	Col-0	T-DNA	N579290	Allen et al, 2005
XRN4	At1g54490	<i>xrn4-3</i>	Col-0	T-DNA	N514209	Gazzani et al., 2004
WEX	At4g13870	<i>wex-2</i>	Col-0	T-DNA	N503278	Vazquez et al, 2004
		<i>wex-3</i>	Col-0	T-DNA	N618757	
		<i>wex-4</i>	Col-0	T-DNA	Garlic_506_F09	
		<i>wex-5</i>	Col-0	T-DNA	Garlic_450_C02	
		<i>wex-6</i>	Col-0	EMS	tilling	
<b>miR824 locus mutants</b>						
m1	At4g24415	<i>m1</i>	Col-0	T-DNA	N500582	
m2	At4g24415	<i>m2</i>	Col-0	T-DNA	N507098	
m3	At4g24415	<i>m3</i>	Col-0	T-DNA	N542802	
m4	At4g24415	<i>m4</i>	Col-0	T-DNA	N599968	
m5	At4g24415	<i>m5</i>	Col-0	T-DNA	N638988	
m6	At4g24415	<i>m6</i>	Col-0	T-DNA	N638986	
<b>miR824 target</b>						
AGL16	At3g57230	<i>agl16-1</i>	Col-0	T-DNA	N604701	
		<i>agl16-w</i>	Col-0	T-DNA	N591008	
		<i>agl16-x</i>	Col-0	T-DNA	N604714	
		<i>agl16-y</i>	Col-0	T-DNA	N555648	
		<i>agl16-z</i>	Col-0	T-DNA	N634080	
<b>AGL16 clade members</b>						
AGL15	At5g13790	<i>agl15-x</i>	Col-0	T-DNA	N576234	
AGL17	At2g22630	<i>agl17-x</i>	Col-0	T-DNA	N551003	
AGL21	At4g37940	<i>agl21-x</i>	Col-0	T-DNA	N511370	
ANR1	At2g14210	<i>anr1-x</i>	Col-0	T-DNA	N549283	
		<i>anr1-y</i>	Col-0	T-DNA	N543618	
<b>other potential miR824 target mutants</b>						
At1g05930	At1g05930	<i>tm1-y</i>	Col-0	T-DNA	N563375	
		<i>tm1-z</i>	Col-0	T-DNA	N593929	
At1g65370	At1g65370	<i>tm2-y</i>	Col-0	T-DNA	N604078	
		<i>tm2-z</i>	Col-0	T-DNA	N544365	
At1g65150	At1g65150	<i>tm3-y</i>	Col-0	T-DNA	N535507	
		<i>tm3-z</i>	Col-0	T-DNA	N648395	
<b>stomatal mutants</b>						
YODA	At1g63700	<i>yda-1</i>	Col-0	EMS	N6392	Bergmann et al., 2003
		<i>yda-2</i>	Col-0	EMS	N6393	Bergmann et al., 2003
		<i>yda-x</i>	Col-0	T-DNA	N553981	
ER	At2g26330	<i>er-x</i>	Col-0	T-DNA	N326027	

Table A.3 continued

ERL1	At5g62230	<i>erl1-x</i>	Col-0	T-DNA	N519567	
		<i>erl1-y</i>	Col-0	T-DNA	N581669	
ERL2	At5g07180	<i>erl2-x</i>	Col-0	T-DNA	N326261	
		<i>erl2-y</i>	Col-0	T-DNA	N507643	
SDD1	At1g04110	<i>sdd1-x</i>	Col-0	T-DNA	N343957	
		<i>sdd1-y</i>	Col-0	T-DNA	N535559	
FLP	At5g33970	<i>flp-x</i>	Col-0	T-DNA	N533970	
FMA	At1g32585	<i>fma-x</i>	Col-0	T-DNA	N373701	
TMM	At1g80080	<i>tmm-x</i>	Col-4	T-DNA	N528664	
<b>candidates by profiling Col-0 vs. <i>dcl3-1</i></b>						
PAP25	At4g36350	<i>pap25-x</i>	Col-0	T-DNA	N525921	
		<i>pap25-y</i>	Col-0	T-DNA	N619551	
PAP5	At1g52940	<i>pap5-x</i>	Col-0	T-DNA	N544236	
		<i>pap5-y</i>	Col-0	T-DNA	N581481	
ROS1	At2g36490	<i>ros1-x</i>	Col-0	T-DNA	N545303	
		<i>ros1-y</i>	Col-0	T-DNA	N564264	
		<i>ros1-z</i>	Col-0	T-DNA	N510549	
<b>candidates by profiling Col-0 vs. <i>wex-1</i></b>						
ARF-GAP	At1g08680	<i>arf-x</i>	Col-0	T-DNA	N545055	
SNF2	At1g05120	<i>snf2-x</i>	Col-0	T-DNA	N630522	
LSD1-like	At4g21610	<i>lsd1-x</i>	Col-0	T-DNA	N552918	
3'5'EXO	At2g25910	<i>exo-x</i>	Col-0	T-DNA	N516153	
ENDONUCLEASE	At4g21600	<i>endo-x</i>	Col-0	T-DNA	N542421	
PPR	At4g19220	<i>ppr-x</i>	Col-0	T-DNA	N530976	
		<i>ppr-y</i>	Col-0	T-DNA	N530968	
RT-put	At4g04000	<i>rt1-x</i>	Col-0	T-DNA	N550715	
KINASE	At2g31880	<i>kin1-x</i>	Col-0	T-DNA	Garlic_623_D08	

## E. Publications

During the course of this work, the following articles have been published:

**Akbergenov, R., Si-Ammour, A., Blevins, T., Amin, I., Kutter, C., Vanderschuren, H., Zhang, P., Gruissem, W., Meins, F., Jr., Hohn, T., and Pooggin, M.M. (2006).**  
Molecular characterization of geminivirus-derived small RNAs in different plant species.  
Nucleic Acids Res. **34**: 462-471.

**Kutter, C., Schöb, H., Stadler, M., Meins, F. Jr., Si-Ammour, A. (2007).**  
A MicroRNA-Mediated Regulation of Stomatal Development in Arabidopsis.  
Plant Cell. *in print* (online available)

## F. Eidesstattliche Erklärung

Hiermit erkläre ich, dass ich die vorliegende Arbeit selbständig angefertigt habe und nur die von mir angegebenen Quellen und Hilfsmittel verwendet habe. Ich versichere ebenfalls, dass diese Arbeit an keiner anderen Einrichtung zur Begutachtung eingereicht wurde.

Basel, September 2007

Claudia Kutter

## G. Curriculum vitae

### Personal Information

Name	Claudia Kutter
Date of Birth	April 24 <sup>th</sup> , 1978
Nationality	German
Address	Maulbeerstrasse 66 4058 Basel Switzerland
Phone	work +41 61 697 6704
Email	claudia.kutter@fmi.ch

### Education

2003 - present	Friedrich Miescher Institute, Basel, Switzerland <b>Ph.D. student</b>
1996 - 2001	Martin-Luther-University Halle-Wittenberg, Faculty of Biology, Halle/Saale, Germany <b>Study of Biology</b> <b>Diplom</b> (Master of Science): 09/2001

### Research Experience

2003 - present	Friedrich Miescher Institute, Basel, Switzerland (Supervisor Prof. Dr. Frederick Meins, Jr.) <b>Ph.D. thesis:</b> "MicroRNA-Mediated Regulation of Stomatal Development in Arabidopsis"
2002 - 2003	Centro de Investigación Científica de Yucatán, Unidad de Biotecnología, Mérida, México (Supervisor Dr. Jorge M. Santamaría Fernández) <b>Research Assistant:</b> "Phytoremediation and Bioadsorption for the Sustainable Use of Water - Use of <i>Salvinia minima</i> BAKER for Phytoremediation of Lead and Arsenic"
2001 - 2002	Colegio de Postgraduado - Campus San Luis Potosí, Salinas de Hidalgo, México (Supervisor Dr. Adrián R. Quero Carillo) <b>Research Assistant:</b> " <i>Bouteloua curtipendula</i> MICHX. TORR. - Plant Breeding Project; Establishing and Characterization of the Ecotype Collection and Analysis of the Agamic Complex"
2000 - 2001	Leibniz Institute of Plant Biochemistry, Halle/Saale, Germany (Supervisor Prof. Claus Wasternack) <b>Diplom thesis</b> (Master of Science): "Functional Characterization of Allene Oxide Cyclase in <i>Lycopersicon esculentum</i> MILL."

---

## Publications

### Articles

**Kutter, C., H. Schöb, M. Stadler, F. Meins Jr., and A. Si-Ammour** (2007). A MicroRNA-mediated Regulation of Stomatal Development in Arabidopsis. *Plant Cell. in print* (online available)

**Akbergenov R., A. Si-Ammour, T. Blevins, I. Amin, C. Kutter, H. Vanderschuren, P. Zhang, W. Gruissem, F. Meins Jr, T. Hohn, and M.M. Pooggin** (2006). Molecular characterization of geminivirus-derived small RNAs in different plant species. *Nucleic Acids Res.* **34**(2), 462-71.

**Wasternack C., I. Stenzel, B. Hause, G. Hause, C. Kutter, H. Maucher, J. Neumerkel, I. Feussner, and O. Miersch O.** (2006). The wound response in tomato - role of jasmonic acid. *J Plant Physiol.* **3**, 297-306.

**Kutter C., T. Hoffmann, and J. M. Santamaría** (2004). Capacity of *Salvinia minima* BAKER to tolerate and accumulate As and Pb. *Engineering in Life Sciences* **4**, 61-65.

**Hause B., G. Hause, C. Kutter, O. Miersch, and C. Wasternack** (2003). Enzymes of jasmonate biosynthesis occur in tomato sieve elements. *Plant Cell Physiol.* **44**(6), 643-48.

### Book chapter

**Morales-Nieto, C. R., A. R. Quero-Carrillo, C. Kutter, T. Hoffmann, and L. Miranda-Jiménez** (2006). *Bouteloua curtipendula* (MICHX.) TORR. genetic resources potential for arid rangelands recovering in México. submitted as chapter for the book: *Desertificación, retos y oportunidades*.